

THE INTERACTION OF CD4 WITH THE ENDOCYTIC
PATHWAY DURING DOWN-REGULATION

~~The Mechanisms Involved In The~~
~~Down-Regulation Of CD4 And~~
~~Its Intracellular Trafficking.~~

by

Ian J. Parsons B.Sc.(Hons)

A Thesis submitted for the degree of
Doctor of Philosophy of the
University of London

1994

Laboratory for Molecular Cell Biology
And Department of Biology,
University College London,
London WC1E 6BT.

ProQuest Number: 10045506

All rights reserved

INFORMATION TO ALL USERS

The quality of this reproduction is dependent upon the quality of the copy submitted.

In the unlikely event that the author did not send a complete manuscript and there are missing pages, these will be noted. Also, if material had to be removed, a note will indicate the deletion.



ProQuest 10045506

Published by ProQuest LLC(2016). Copyright of the Dissertation is held by the Author.

All rights reserved.

This work is protected against unauthorized copying under Title 17, United States Code.
Microform Edition © ProQuest LLC.

ProQuest LLC
789 East Eisenhower Parkway
P.O. Box 1346
Ann Arbor, MI 48106-1346

ABSTRACT

CD4 expressed at the surface of lymphoid cells is down-regulated in response to antigenic stimulation. Down-regulation is believed to involve the activation of protein kinase C, and can be mimicked by phorbol esters, such as phorbol myristic acid (PMA), but the cellular mechanisms that result in clearance of CD4 from the cell surface are not understood. In this thesis I describe experiments which analyse phorbol ester-induced down-regulation in detail in HeLa cells that stably express CD4. I show that down-regulation is a multi-step process in which the kinetics and intracellular itinerary of CD4 are modulated. Specifically, I show that: (1) phorbol ester treatment, presumably through the phosphorylation of CD4, increases the association of CD4 with coated pits 3 fold; (2) the rate of CD4 endocytosis is increased 3 fold, and the intracellular pool of CD4 is doubled at equilibrium in the presence of phorbol ester. Fluid-phase internalization is not affected by PMA treatment; (3) in the absence of PMA CD4 is endocytosed into the transferrin receptor-containing early endosomal compartment, from where it can recycle to the plasma membrane. In the presence of phorbol ester however, CD4 is diverted from the early endosome-plasma membrane recycling pathway, to a compartment in the perinuclear region of the cell, that can be costained with antibodies to the cation independent mannose 6-phosphate receptor (CI-MPR); (4) inhibition of kinase and phosphatase activities, inhibits the internalization and recycling of CD4, respectively, suggesting that the constitutive endocytosis and recycling of CD4 in HeLa-CD4 cells, may involve cycles of phosphorylation and dephosphorylation.

CONTENTS

	Page
1. Introduction.	15
1.1 General Introduction.	15
1.2 The Structure Of CD4.	15
1.3 The Immunological Function Of CD4.	18
1.3.a The Role Of CD4 In T Cell Ontogeny.	19
1.3.b The Role Of CD4 During Negative Selection.	20
1.3.c The Role Of CD4 During Positive Selection.	21
1.3.d The Mechanism Of Thymocyte Maturation.	21
1.3.e The Role Of CD4 In T Cell Activation.	23
1.3.f The Ability Of CD4 To Function In Signal Transduction.	24
1.4 The Endocytic Pathway.	26
1.4.a Endocytosis.	26
1.4.b Clathrin-dependent and Clathrin- independent Endocytosis.	26
1.4.c Compartments In The Endocytic Pathway.	29
1.5 Entry Into The Endocytic Pathway.	33
1.5.a Endocytosis Signals.	33
1.5.b Structure Of An Endocytosis Signal.	35
1.5.c Other Endocytosis Signals.	36
1.5.d Entry Into The Endocytic Pathway From The <i>Trans</i>-Golgi Network.	37
1.5.e Lysosomal Targeting Signals.	38
1.5.f Modification Of Sorting Signals By Phosphorylation.	39
1.5.g Exclusion From The Endocytic Pathway.	4 1
1.6 The Role Of CD4 In HIV Infection.	42
1.7 Phorbol Esters.	43

1.7.a	Activation of Protein Kinase C.	43
1.7.b	Down-Regulation Of CD4 And Its Interaction With The Endocytic Pathway.	44
1.8	Aim Of Work Described In This Thesis.	46
2.	Materials and Methods	47
2.1	Cells Lines and Cell Culture.	47
2.2	Antibodies.	47
2.3	Q4120 Iodination.	48
2.4	Loading Of Protein A Sepharose Beads With Anti-CD4 (Hoxie 21).	49
2.5	Detection Of Cell Surface CD4 After PMA Treatment.	50
2.6	Detection Of Cell Surface CD4 After PMA Treatment In Hypertonic Medium.	51
2.7	Cell Surface CD4 Endocytosis Assay.	51
2.8	Fluid Phase Endocytosis Assays.	52
2.9	Electron Microscopic Localization Of CD4.	54
2.10	Immunofluorescence Endocytosis Assay.	54
2.11	Immunofluorescence.	55
2.12	Sodium Dodecyl Sulphate-Polyacrylamide Gel Electrophoresis.	56
2.13	Immunoblotting.	57

2.14	Cell Fractionation.	Page 57
2.15	Enzyme assays.	60
2.16	Bicinchoninic Acid Protein (BCA) Assay.	61
2.17	Cell Surface Iodination and PMA-Induced Down-Regulation.	61
2.18	Detection Of Cell Surface CD4 After PMA Treatment In The Presence of Staurosporine.	63
2.19	Detection Of Cell Surface CD4 And CD4^{cyt}- Following Treatment Of Cells With Staurosporine and Okadaic Acid.	63
2.20	Endocytosis Kinetics Of CD4 and CD4^{cyt}- In The Presence Of Staurosporine And Okadaic Acid.	64
2.21	Fluid Phase Endocytosis In HeLa-CD4 Cells In The Presence Of Staurosporine And Okadaic Acid.	65
2.21	Fluid Phase Endocytosis In HeLa-CD4 Cells In The Presence Of Staurosporine And CGP41/251.	65
3.	Results	67
3.1	Downregulation Of Cell Surface CD4 On Lymphocytic And Non-Lymphocytic Cells.	67
3.1.1	PMA Induces CD4 Down-regulation.	67
3.1.2	The Effect Of PMA On The Endocytosis Kinetics Of CD4.	73
3.1.3	The Specificity Of The Effect Of PMA On CD4 Endocytosis.	77
3.1.4	PMA Enhances CD4 Endocytosis Through Coated Pits.	80
3.1.5	The Signals Involved In The Endocytosis And Trafficking Of CD4.	87

	Page
3.1.5.1 Constitutive Endocytosis Of CD4 May Involve Phosphorylation Of The Cytoplasmic Domain.	87
3.1.5.2 The Kinetics Of Cell Surface CD4 Up-regulation In The Presence Of Stsp.	93
3.1.5.3 The Effect Of Stsp On The Fluid-Phase Endocytosis Of HRP in HeLa-CD4 Cells.	95
3.1.5.4 Phosphorylation Of The Cytoplasmic Domain Of CD4 May Be An Important Feature Of Its Intracellular Trafficking.	100
3.1.5.5 The Effect Of OKA On The Endocytosis Kinetics Of CD4.	101
3.1.5.6 The Effect Of OKA On The Fluid-Phase Endocytosis Of HRP In HeLa-CD4 Cells.	104
3.2 The Intracellular Sorting Of CD4 During PMA-Induced Modulation.	106
3.2.1 Characterization Of The Compartment Containing CD4 During PMA Induced-CD4 Down-Regulation.	109
3.2.1.1 Fractionation Studies.	109
3.2.1.2 Double Staining studies.	118
3.2.1.3 The Intracellular Fate Of CD4 During PMA-Induced Down-Regulation.	127
3.3 Comparison Of The HeLa-CD4 Model System With The T Cell Line, SupT1.	133
4. Discussion	141
4.1 PMA-Induced CD4 Endocytosis.	142
4.2 Phosphorylation Of The Cytoplasmic Domain Of CD4 May Be An Important Feature In The Constitutive Internalization And Intracellular Trafficking Of CD4.	144
4.3 PMA-Induced Endosomal Sorting Of CD4.	147

	Page
4.4 PMA-Induced Degradation Of CD4.	150
4.5 PMA-Induced Down-Regulation In Lymphoid Cells.	151
4.6 Future Work.	153
Acknowledgements	155
5. References.	156

LIST OF FIGURES

	Page
Figure 1. Diagrammatic representation of CD4.	17
Figure 2. Schematic diagram representing the course of T cell ontogeny.	20
Figure 3. Schematic diagram of the endocytic pathway.	30
Figure 4. Standard curves for the fluid-phase markers horseradish peroxidase, and lucifer yellow.	53
Figure 5. Horseradish peroxidase standard curve.	60
Figure 6. Bovine serum albumin (BSA) standard curve.	61
Figure 7. The effect of PMA on CD4 down-regulation in SupT1 cells.	68
Figure 8. The concentration dependence of PMA-induced CD4 down-regulation in HeLa-CD4 cells.	70
Figure 9. CD4 down-regulation time courses.	72
Figure 10. The acid stripping efficiencies at pH3.00 and pH2.00.	74
Figure 11. The effect of PMA on the endocytosis of CD4 in HeLa-CD4 cells.	75
Figure 12. TCA precipitation of the medium from the time points in the endocytosis assay.	76
Figure 13. The effect of PMA on fluid endocytosis in HeLa-CD4 cells.	79
Figure 14. The effect of hypertonic medium on CD4	82

down-regulation in HeLa-CD4 cells.

Page

Figure 15.	Electron microscopic localization of CD4 in HeLa-CD4 cells treated with PMA.	83
Figure 16.	Graphical representation of the tabulated data in Table 2.	85
Figure 17.	Inhibition of PMA-induced CD4 down-regulation by Staurosporine in HeLa-CD4 cells.	89
Figure 18.	The effect of Staurosporine the kinetics of CD4 endocytosis.	92
Figure 19.	The effect of Staurosporine on CD4 cell surface expression.	94
Figure 20.	The effect of Staurosporine on the fluid phase endocytosis of HRP in HeLa-CD4 cells.	97
Figure 21.	The effect of Staurosporine and a specific protein kinase C inhibitor (CGP 41/251) on the fluid phase endocytosis of HRP in HeLa-CD4 cells.	98
Figure 22.	Diagrammatic representation of a model for the phosphorylation of CD4 during constitutive endocytosis in HeLa-CD4 cells.	99
Figure 23.	The effect of Okadaic acid on CD4 cell surface expression.	101
Figure 24.	The effect of Okadaic acid on the kinetics of CD4 endocytosis.	103
Figure 25.	The effect of Okadaic acid on the fluid-phase endocytosis of HRP in HeLa-CD4 cells.	105
Figure 26.	The cellular distribution of CD4 in the presence	108

or absence of PMA.

	Page
Figure 27. Subcellular organelle recovery following homogenization of HeLa-CD4 cells.	111
Figure 28. Subcellular fractionation of HeLa-CD4 and HeLa-CD4 ^{cyt-} cells on 30% percoll gradients.	113
Figure 29. Subcellular fractionation of HeLa-CD4 cells on a 25-50% continuous sucrose gradient.	115
Figure 30. Subcellular fractionation of HeLa-CD4 cells on a D ₂ O sucrose step gradient.	117
Figure 31. Immunoblot for rab7 in fractions from the D ₂ O sucrose step gradient.	117
Figure 32. Costaining of internalized CD4 with the TfR or CI-MPR at 37°C or 18°C in HeLa-CD4 cells.	123
Figure 33. Costaining of 2C2 mab with lamp 1 and 2 in HeLa-CD4 cells.	124
Figure 34. Costaining of the CI-MPR with 2C2 in HeLa-CD4 cells.	125
Figure 35. Costaining of the CI-MPR with 23C in HeLa-CD4 cells.	125
Figure 36. Costaining of CD4 ^{cyt-} with the CI-MPR in HeLa-CD4 ^{cyt-} cells.	126
Figure 37. Fluid-phase endocytosis in the presence and absence of PMA.	126
Figure 38. CD4 in HeLa-CD4 cells is degraded in the continued presence of PMA.	128

	Page
Figure 39. CD4 ^{cyt-} in HeLa-CD4 ^{cyt-} cells is not degraded in the continued presence of PMA.	128
Figure 40. CD4 ^{S408A} in HeLa-CD4 ^{S408A} cells is degraded in the continued presence of PMA.	129
Figure 41. CD4 is degraded in the continued presence of PMA.	132
Figure 42. Costaining of internalized CD4 with the CI-MPR in the presence of PMA, and costaining of the CI-MPR and 2C2 in SupT1 cells.	134
Figure 43. Degradation of CD4 in SupT1 cells in the continued presence of PMA (immunofluorescence).	137
Figure 44. Degradation of CD4 in SupT1 cells in the continued presence of PMA (immunoblotting).	138
Figure 45. Quantitative immunoprecipitation of CD4 using anti-CD4 protein A sepharose beads.	139
Figure 46. Degradation of cell surface CD4 in SupT1 cells in the continued presence of PMA.	140

LIST OF TABLES

	Page
Table 1. List of receptors containing known tyrosine-based motifs important for receptor endocytosis.	34
Table 2. Effect of PMA on the distribution of gold-labelled CD4 on HeLa-CD4 cells.	84
Table 3. Effect of PMA on the proportion of coated plasma membrane in HeLa-CD4 cells.	86
Table 4. Endocytosis rates of wild type and mutant forms of CD4 in HeLa cells.	88

ABBREVIATIONS

APC	Antigen presenting cell.
ASGP-R	Asialoglycoprotein receptor.
BCA	Bicinchoninic acid.
BHK cells	Baby hamster kidney cells.
BM	Binding medium.
BSA	Bovine serum albumin.
CD4 ^{cyt-}	CD4 lacking the cytoplasmic domain.
CD4 ^{S408A}	CD4 with cytoplasmic serine 408 mutated to alanine.
CD-MPR	Cation dependent mannose 6-phosphate receptor.
CI-MPR	Cation independent mannose 6-phosphate receptor.
DAG	1,2-Diacylglycerol.
DMEM	Dulbecco's modified Eagle's medium.
EDTA	Ethylenediaminetetra acetic acid.
EGF-R	Epidermal growth factor receptor.
EM	Electron microscopy.
ER	Endoplasmic reticulum.
FCS	Foetal calf serum.
FITC	Fluorescein isothiocyanate.
h	Hour.
HA	Haemagglutinin.
HEPES	N-2-Hydroxyethylpiperazine-N'-2-ethanesulfonic acid.
HIV	Human immunodeficiency virus.
HRP	Horseradish peroxidase.
IP ₃	Inositol 1,4,5-triphosphate.
kD	Kilo Daltons.
lamp	Lysosomal-associated membrane protein.
LAP	Lysosomal acid phosphatase.
LDL-R	Low density lipoprotein receptor.
lgp	Lysosomal membrane glycoprotein.
LY	Lucifer yellow.
mab	Monoclonal antibody.

MHC	Major histocompatibility complex.
min	Minute.
MVB	Multivesicular body.
NMR	Nuclear magnetic resonance.
OKA	Okadaic acid.
PAGE	Polyacrylamide gel electrophoresis.
PBS	Phosphate buffered saline.
pIg-R	Poly-immunoglobulin receptor.
PLC	Phospholipase C.
PMA	Phorbol myristic acid.
PMSF	Phenylmethyl-sulfonyl fluoride.
PNS	Postnuclear supernatant.
RME	Receptor-mediated endocytosis.
SDS	Sodium dodecyl sulphate.
SHPP	N-succinimidyl-3-(4-hydroxyphenyl)-propionate.
Stsp	Staurosporine.
TBS	Tris buffered saline.
TCA	Trichloroacetic acid.
TCR	T cell receptor.
TEA	Triethanolamine.
TfR	Transferrin receptor.
TGN	<i>Trans</i> -Golgi network.
TRITC	Tetramethyl-rhodamine isothiocyanate.

1. INTRODUCTION

1.1 GENERAL INTRODUCTION.

The cell surface expression of the CD4 molecule on thymocytes (Reinherz *et al* 1979), and on major histocompatibility (MHC) class II restricted T lymphocytes (Maddon *et al* 1986), is crucial for the normal functioning of the immune system.

CD4, a member of the immunoglobulin supergene family, is a type I transmembrane glycoprotein whose cDNA was isolated and reported in 1985 (Maddon *et al* 1985). CD4 is a non-polymorphic protein that has a molecular mass of 55 kilo Daltons (kD), and consists of an extracellular (~370 amino acid residues), transmembrane (~22 amino acids) and cytoplasmic (38 amino acids) domain (Figure 1) (Maddon *et al* 1985; Clark *et al* 1987). There is a high degree of homology between species and unless otherwise stated it is human CD4 that is discussed below.

CD4 functions primarily at the cell surface in T cell ontogeny and activation. However, under certain physiological conditions the cell surface expression of CD4 is modulated. This down-regulation is thought to involve the interaction of CD4 with the endocytic pathway, although the mechanisms of modulation are not fully understood. CD4 also functions as the primary cellular receptor for the human immunodeficiency viruses (HIV-1 and HIV-2).

1.2 THE STRUCTURE OF CD4.

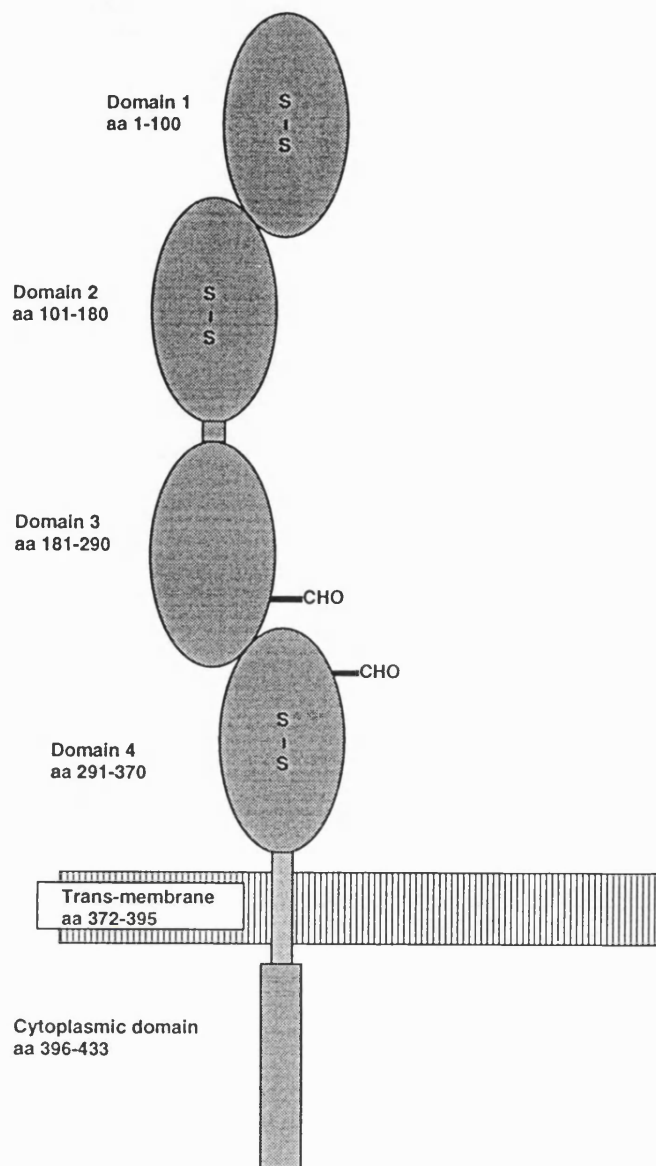
The extracellular domain of CD4 possesses four immunoglobulin-like domains whose crystal structures have been solved (Wang *et al* 1990; Ryu *et al* 1990; Brady *et al* 1993a; 1993b). Initially, the structure of the N-terminal portion, domains 1 and 2 (D1/D2), was determined (Wang *et al* 1990; Ryu *et al* 1990), and recently, the structure of domains 3 and 4 (D3/D4) of rat CD4 was solved (Brady *et al* 1993a; 1993b). Each domain contains antiparallel β barrels characteristic of an immunoglobulin fold, and, except for D3, an inter-sheet disulphide bond. D1 superimposes well onto the β -sheet framework of the variable domain of an immunoglobulin κ light chain, D2 resembles an immunoglobulin constant domain, and together they form a rigid rod-like shape.

When compared to D1/D2, D3/D4 is rotated by 30°, and both

domains 3 and 4 have one N-linked glycosylation site (asparagines 271 and 300, respectively). D3 is marginally broader than D2, possibly due to the absence of an intersheet disulphide bond (Brady *et al* 1993a; 1993b). The structure of D3/D4 is very similar to D1/D2, such that CD4 is believed to form an extended rod-like molecule approximately 125 Å in length. Between D2 and D3 there are five amino acid residues, the conformation of which is presently unknown. However, these five residues are believed to adopt a fully extended β sheet conformation, resulting in a short, flexible "hinge"-type region, that may be an essential feature of the biological functioning of CD4.

The CD4 extracellular domain is linked to the plasma membrane by a single 24 amino acid hydrophobic transmembrane domain, and is retained in the membrane by a putative stop transfer sequence of several basic amino acids that immediately follow the transmembrane region. The CD4 cytoplasmic domain consists of 38 amino acids that are highly conserved in the species sequenced to date (Figure 1, B).

A



B

CD4

human	:	R	C	R	H	R	R	D	A	E	R	M	S	Q	I	K	R	L	L	S	E	K	K	T	C	Q	C	P	H	R	F	Q	K	T	C	S	P	I	
macaque	:	R	C	R	H	R	R	D	A	E	R	M	S	Q	I	K	R	L	L	S	E	K	K	T	C	Q	C	P	H	R	F	Q	K	T	C	S	P	I	
chimpanze	:	R	C	R	H	R	R	D	A	Q	R	M	S	Q	I	K	R	L	L	S	E	K	K	T	C	Q	C	P	H	R	F	Q	K	T	C	S	P	I	
murine	:	R	C	R	H	Q	Q	R	D	A	A	P	M	S	Q	I	K	R	L	L	S	E	K	K	T	C	Q	C	P	H	R	M	Q	K	S	H	N	L	I
rat	:	R	C	R	H	Q	Q	R	D	A	A	P	M	S	Q	I	K	R	L	L	S	E	K	K	T	C	Q	C	S	H	R	M	Q	K	S	H	N	L	I
dog	:	K	C	W	R	R	R	R	D	A	E	R	M	S	Q	I	K	R	L	L	S	E	K	K	T	C	Q	C	S	H	R	I	Q	K	T	C	S	L	I
rabbit	:	K	C	R	H	R	R	D	A	Q	R	M	S	Q	I	K	R	L	L	S	E	K	K	T	C	Q	C	P	H	R	L	Q	K	T	Y	N	L	L	

Figure 1. Diagrammatic representation of CD4. **A:** The extracellular, transmembrane, and cytoplasmic domains. **B:** The amino acid sequence of the cytoplasmic domain of human, macaque, chimpanzee, mouse, rat, rabbit and dog CD4. (Boxed areas represent regions of complete homology.)

1.3 THE IMMUNOLOGICAL FUNCTION OF CD4.

CD4 is expressed on the surfaces of thymocytes and MHC class II restricted T cells, where it functions together with the T cell receptor/CD3 complex (TCR) in T cell ontogeny and activation.

Using cell adhesions assays and mutational analysis, domains 1 and 2 of CD4 have been demonstrated to interact with MHC class II molecules (Doyle and Strominger 1987; Gay *et al* 1987; Lamarre *et al* 1989; Fleury *et al* 1991), and the β_2 -domain of MHC class II (residues 134-143), has been identified as being crucial for the binding of CD4 (Konig *et al* 1992; Cammarota *et al* 1992). This is a non-polymorphic loop in a similar location to the CD8 binding site on class I MHC. The interaction between CD4 and class II MHC may simply function to increase the affinity of binding between the TCR and the same MHC class II molecules, indicating that CD4 plays a subsidiary role in T cell function, and has thus been termed an "accessory" molecule. However, evidence discussed below, suggests that CD4 physically associates with the TCR during activation, and as such, may contribute directly to signal transduction, due to its physical and functional association with the lymphocyte-specific protein tyrosine kinase, p56^{lck}, a member of the *src* gene family (Veillette *et al* 1988; Rudd *et al* 1988). Thus CD4 is more appropriately regarded as a "co-receptor".

In addition to its expression on the surface of thymocytes and MHC class II restricted T cells, CD4 is expressed on some cells of the macrophage/monocyte lineage (Stewart *et al* 1986), however its function in these cells is unclear. CD4 is also known to function as the primary cellular receptor for the human immunodeficiency viruses 1 and 2 (Maddon *et al* 1986; Sattentau and Weiss 1988). The HIV glycoprotein gp120, is believed to bind to domain 1 of CD4, with residues in the complementarity determining region (CDR) 2-like domain being important. However, the regions involved in gp120 and class II MHC binding, were shown to be distinct in antibody binding and mutational studies (Lamarre *et al* 1989; Fleury *et al* 1991).

The primary site of CD4 function appears to be at the cell surface, however, various physiological and experimental stimuli can induce its down-regulation (discussed below). The down-regulation of CD4 is presumed to occur by endocytosis. However,

the mechanisms by which CD4 is removed from the cell surface have yet to be elucidated in detail, and the exact intracellular fate of the down-regulated CD4 molecules has not been determined. These questions are addressed in this study.

1.3.a *The Role Of CD4 In T Cell Ontogeny.*

The mature T lymphocytes found in the peripheral blood and lymphoid tissues contribute to virtually all adaptive immune responses. These T cells, which have left the thymus (the major site for T cell development), must be tolerant to self antigens, but able to recognize foreign antigens in association with self-MHC proteins. There are two major subsets of T cells: The class II MHC restricted T cells, which are CD4 positive (CD4⁺), and the class I MHC restricted T cells, which are CD8 positive (CD8⁺). The CD4⁺ T cells generally have helper activities, secreting cytokines and promoting the differentiation of B lymphocytes and other haemopoietic cells following activation by antigen. On the other hand, CD8⁺ T cells primarily have cytotoxic activity, and upon recognition of antigen in association with class I MHC molecules, trigger apoptosis in the target cell.

The generation of the body's T cell repertoire occurs in the thymus by a mechanism that involves both positive and negative selection. Negative selection is responsible for the elimination or inactivation of those potentially harmful T cells which recognize self antigens bound to MHC molecules, whereas positive selection preferentially favours the differentiation of T cells that are capable of recognizing foreign antigens in association with MHC molecules (Figure 2).

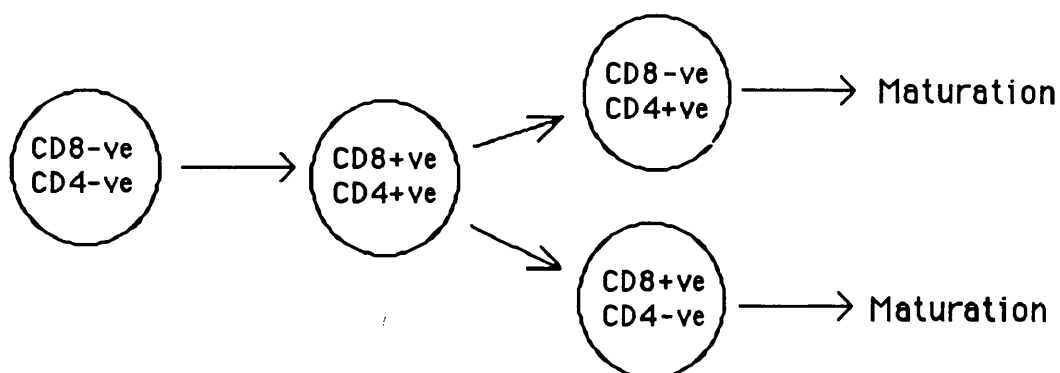


Figure 2. Schematic diagram representing the course of T cell ontogeny. A double negative CD4/CD8 thymocyte matures to a double positive CD4/CD8 thymocyte. The double positive cell matures to a single positive CD8⁺ or CD4⁺ cell depending on whether the TCR is class I or II restricted. Non-permissive combinations of TCR and CD4/CD8, and cells recognizing self antigens are eliminated and do not develop to mature T cells.

1.3.b *The Role Of CD4 During Negative Selection.*

The elimination of T cell clones expressing TCRs specific for self-antigens is crucial for the maintenance of tolerance. That CD4 is involved in negative selection was demonstrated by the *in vivo* treatment of specific mouse strains with anti-CD4 monoclonal antibodies (mabs). When neonatal mice expressing class II MHC autoreactive TCRs, were injected with sufficient anti-CD4 mabs, development of CD4⁺ T cells was blocked, possibly due to inhibition of positive selection. However, this treatment prevented the deletion of CD8⁺ T cells bearing the class II MHC autoreactive receptor (Fowlkes *et al* 1988; MacDonald *et al* 1988). These results suggested that negative selection of autoreactive TCRs requires recognition of class II MHC by both the TCR and CD4, and that it occurs at a CD4⁺/CD8⁺ double-positive precursor stage. Thus when recognition by CD4 is prevented by anti-CD4, negative selection fails and cells bearing the autoreactive TCR can mature into CD8⁺ T cells.

1.3.c *The Role Of CD4 During Positive Selection.*

The suggestion that CD4 is involved in positive selection came from studies on neonatal mice. When mice were injected with anti-MHC class II mabs (anti-Ia) from birth, it was found that the thymus and spleen of these animals were devoid of CD4⁺ class II restricted T cells. The development of CD8⁺ class I restricted T cells was not affected by this treatment, suggesting that the production of CD4⁺ class II specific T cells was dependent on interaction with functional MHC class II molecules on antigen presenting cells (APC) (Kruisbeek *et al* 1983 and 1985). The results indicated that there was a requirement for the TCR to interact with MHC, or MHC to interact with CD4, or both. The fact that TCR and MHC interact during selection was demonstrated in transgenic mice. Transgenic mice expressing a TCR specific for a fragment of pigeon cytochrome c in association with class II MHC (E^k), only developed mature CD4⁺CD8⁻ cells, when the MHC haplotype E^k was expressed, and the resulting population of peripheral T cells was almost exclusively CD4⁺ (Berg *et al* 1989; Kaye *et al* 1989). In addition to the indication that TCR and MHC class II interact during positive selection, these results also suggest a role for CD4 in selection. Further evidence for the role of CD4 in positive selection came from experiments on foetal thymi, and pregnant mice treated with anti-CD4 mabs (Zuniga-Pflucker *et al* 1989). Foetal thymi in organ culture, treated with intact anti-CD4 mab, or anti-CD4 Fab, failed to generate single-positive CD4 T cells. The development of double positive CD4⁺/CD8⁺ thymocytes, and CD8⁺ T cells was unaffected by either treatments. Similarly, pregnant mice injected with anti-CD4 mabs, gave birth to neonates that lacked CD4 single-positive cells in their thymi, and the development of double positive CD4⁺/CD8⁺ thymocytes was unaffected by this treatment. These results indicate both *in vitro* and *in vivo*, that CD4 functions in the selection events that generate single-positive CD4 T cells.

1.3.d *The Mechanism Of Thymocyte Maturation.*

Two mechanisms have been proposed to explain the selective maturation of T cells bearing a co-receptor appropriate to the specificity of the TCR: these are, (a) the instructive model (Robey

et al 1991; Borgulya *et al* 1991) and, (b) the selective/stochastic model (Janeway 1988; Davis *et al* 1993; Chan *et al* 1993).

The instructive model proposes that at a CD4⁺/CD8⁺ double-positive stage, the co-receptor together with the TCR on the thymocyte interact with the same MHC on thymic stromal cells. This interaction produces a specific signal that leads to down-regulation of the non-selected co-receptor. Therefore, CD4 interaction with a MHC class II specific receptor, signals the double-positive thymocyte to repress CD8.

The selective/stochastic model proposes that at the CD4⁺/CD8⁺ double-positive stage, either CD4 or CD8 expression is randomly down-regulated so that only useful combinations are selected for differentiation into mature T cells; i.e. a class II MHC restricted TCR with CD4, or a class I MHC restricted TCR with CD8. In general, non-permissive combinations, such as a thymocyte with a class I MHC restricted TCR with CD4 would not undergo positive selection.

In fact, recent experiments in transgenic mice have indicated that T cell ontogeny is a two step mechanism involving both mechanisms (Davis *et al* 1993; Chan *et al* 1993). The first step is a stochastic event, where MHC molecules bind to the TCR on double-positive CD4⁺CD8⁺ thymocytes, causing the random down-regulation of either CD4 or CD8. The second step is an instructive event, where the appropriate co-receptor (CD4 or CD8) must bind to the same MHC molecule with which the TCR is interacting. This permits thymocyte differentiation to the final stage, a single-positive T cell that is either CD4⁺, expressing a class II restricted TCR, or CD8⁺, expressing a class I restricted TCR. In addition, this differentiation to the final CD4⁺ T cell may not require the CD4-p56^{lck} interaction, as overexpression of CD4 lacking a cytoplasmic domain in transgenic mice (five to six fold above normal CD4 levels found in normal T cells), gives rise to a normal helper T cell population (Killeen and Littman 1993). Thus it appears that the primary role for CD4 during T cell ontogeny is in adhesion, stabilizing the interaction of the TCR with the MHC class II complexes.

1.3.e *The Role Of CD4 In T Cell Activation.*

Following selection and maturation in the thymus, CD4⁺ and CD8⁺ T cells are exported from this organ to the periphery, where they can function in immune responses. Mature peripheral CD4⁺ T cells generally have helper functions, and are involved in T cell activation. This function was shown in early studies which demonstrated that certain anti-CD4 antibodies, when prebound to peripheral blood leukocytes, could block stimulation by:

(i) antigen (Biddison *et al* 1983); (ii) anti-TCR/CD3 antibodies plus accessory cells bearing class II MHC molecules (Bank and Chess 1985); and, (iii) cross-linked anti-TCR/CD3 antibodies immobilized on Sepharose beads (Bank and Chess 1985). In addition, antibodies against CD4, inhibited the formation of MHC class II complexes between T cells and lymphoblastoid B cells (Biddison *et al* 1984). CD4 was subsequently shown to interact with MHC class II molecules through its extracellular domain (Doyle and Strominger 1987; Gay *et al* 1987; Lamarre *et al* 1989; Fleury *et al* 1991), and it was proposed that CD4 provides an "accessory function" increasing the avidity of a T cell for its antigen processing cell. However, evidence discussed below indicates that CD4 is not just an accessory molecule in T cell activation, but is a co-receptor with the TCR/CD3 complex, functioning as a signal transducing molecule.

When CD4 is cross-linked to the TCR using immobilized or prebound anti-CD4 and anti-TCR antibodies, T cell proliferation is of greater magnitude than that produced by anti-TCR antibodies alone (Eichmann *et al* 1987; Anderson *et al* 1987; Owens *et al* 1987), suggesting that CD4 and TCR are required to interact to produce an optimal signal to activate T cells. Other studies, which demonstrated intracellular calcium mobilization and interleukin (IL) 2-receptor expression, also found that antibody mediated cross-linking of TCR with CD4 enhanced T cell activation (Emmrich *et al* 1987; Ledbetter *et al* 1987). Anti-TCR and anti-CD4 heteroconjugates induced greater synthesis of inositol triphosphate (IP₃), than anti-TCR antibodies alone, and the heteroconjugates caused the down-regulation of both TCR complexes and CD4, during an 18 h incubation at 37°C (Ledbetter *et al* 1988). Fluorescence resonance energy transfer (FRET) has also indicated that CD4 is close to TCR during T cell activation (0-

100 Å), and that the FRET between CD4 and TCR is dependent on the cytoplasmic domain of CD4 (Mittler *et al* 1989).

These studies indicated that CD4, when in close proximity to the TCR, is actively involved in T cell stimulation. Indeed, when the distribution of CD4 was investigated in murine T cells interacting with a B hybridoma cell line, it was found to co-cluster with the TCR, indicating that both CD4 and the TCR are concentrated within the same region during antigen recognition (Kupfer *et al* 1987).

1.3.f The Ability Of CD4 To Function In Signal Transduction.

With the discovery that the cytoplasmic domain of CD4 associates with the lymphocyte-specific, *src*-related non-receptor tyrosine kinase, p56^{lck} (Rudd *et al* 1988; Veillette *et al* 1988), a mechanism for involvement of CD4 in T cell activation was provided.

The association of CD4 and p56^{lck} is dependent on the cytoplasmic domain of CD4 (Shaw *et al* 1989; Turner *et al* 1990; Veillette *et al* 1990). Specifically, a pair of cysteines at positions 420 and 422 in the cytoplasmic domain of CD4 (Figure 1, B) (Shaw *et al* 1990; Turner *et al* 1990); and a pair of cysteines at positions 20 and 23 in the unique N-terminal region of p56^{lck}, are essential for the association (Shaw *et al* 1989; 1990; Turner *et al* 1990). The pairs of cysteines in CD4 and p56^{lck} may co-ordinate a metal ion (Shaw *et al* 1990), and mutation of any of these cysteines to serine or alanine completely disrupts the physical and functional interaction between CD4 and p56^{lck} (Shaw *et al* 1990; Turner *et al* 1990).

The importance of the CD4-p56^{lck} interaction in T cell activation was demonstrated using CD4-deficient T cell hybridomas. Mutant forms of CD4 unable to interact with p56^{lck}, and expressed in class II MHC-restricted CD4-deficient hybridomas, were incapable of activating the cells when challenged with antigen. However, when wild type CD4 was transfected into the CD4-deficient hybridomas, it was able to interact with p56^{lck} and restore antigen-induced T cell activation (Glaichenhaus *et al* 1991). Similar results were obtained in a separate study where either CD4 or the CD8 α chain were expressed in class II MHC restricted hybridomas. When the hybridomas were activated using mouse L

cells expressing the antigen, in association with MHC class II specific for the TCR on the hybridomas, only the cells expressing wild type CD4 were activated, as assessed by the production of IL2. Hybridomas expressing CD8 α or CD4 molecules lacking a cytoplasmic domain, produced much lower levels of IL2 than the cells expressing wild type CD4 (Miceli *et al* 1991). Two separate studies demonstrated that cross-linking of CD4 on murine T cells induced the rapid tyrosine phosphorylation of p56^{lck} at the autophosphorylation (Tyr-394), and regulatory (Tyr-505) sites, suggesting that tyrosine phosphorylation events may be important in CD4-mediated signalling (Veillette *et al* 1989a; Luo and Sefton 1990). It was subsequently shown that this cross-linking of CD4 resulted in the rapid activation of the tyrosine-specific protein kinase activity of p56^{lck}, followed as soon as 1-2 minutes after cross-linking of CD4, by the phosphorylation, on tyrosine residues, of the ζ chain in the TCR/CD3 complex (Veillette *et al* 1989b). These results suggest that during T cell activation some of the tyrosine phosphorylation events may be mediated by signalling through CD4, and these phosphorylation events are dependent on the expression of functional p56^{lck} (Straus and Weiss 1992). Indeed, the juxtapositioning of CD4 and the TCR through binding the same MHC class II molecule, would bring p56^{lck} close to the ζ chain of the TCR/CD3 complex. Activation of p56^{lck} may be mediated by the tyrosine phosphatase, CD45, which has been demonstrated to dephosphorylate the p56^{lck} regulation site, Tyr-505 (Mustelin *et al* 1989; Ostergaard *et al* 1989; Sieh *et al* 1993). Activated p56^{lck} could then phosphorylate tyrosine residues in antigen recognition activation motifs on CD3 chains, thereby providing binding sites for the newly identified protein tyrosine kinase, p70^{zap}. P70^{zap} may then activate down-stream effector molecules in the signalling pathway leading to complete activation of the T cell (Weiss 1993).

From the studies discussed above it is clear that CD4 plays a crucial role during T cell activation. The CD4 extracellular domain interacts with MHC class II molecules on antigen presenting cells, and the cytoplasmic domain which is associated with p56^{lck}, permits CD4 to participate directly in signal transduction.

1.4 THE ENDOCYTIC PATHWAY.

As previously mentioned, CD4 is down-regulated under a variety of physiological and experimental conditions, e.g. exposure of T cells to specific antigen, cross-linking antibodies and phorbol esters (Acres *et al* 1986; Weyand *et al* 1987; Rivas *et al* 1988). The modulation of cell surface CD4 may function in facilitating the de-adhesion of the T cell and the APC following activation, and could de-sensitize the T cell to further stimuli. The mechanisms of this down-regulation are not completely understood, however, they are presumed to involve the interaction of CD4 with the endocytic pathway.

1.4.a ENDOCYTOSIS.

Endocytosis is a property of virtually all nucleated cells, and is responsible for the uptake of extracellular molecules and fluid. Endocytosis can occur by at least two mechanisms: (i) Phagocytosis, which is ligand-induced and is responsible for the uptake of large particles, and is not discussed further here; and (ii) Pinocytosis, which is a constitutive process that primarily occurs through the continual invagination of plasma membrane clathrin-coated pits to form coated vesicles. Pinocytosis is responsible for: (a) fluid phase endocytosis; (b) bulk membrane cycling; and (c) receptor-mediated endocytosis (RME), and accounts for the majority of the constitutive endocytic activity in several cell types (Watts and Marsh 1992). However, there is some suggestion that clathrin-independent endocytic mechanisms may exist in some cells (van Deurs *et al* 1989).

1.4.b *Clathrin-dependent and Clathrin-independent Endocytosis.*

The clathrin coat is composed of clathrin triskelions which are three-legged structures, consisting of three heavy chains (~190 kD) and three light chains (23-27 kD). These clathrin triskelions are the assembly units of a polygonal lattice found on the surface of coated pits and vesicles. Between this lattice and the lipid bilayer is an inner shell of protein, previously known as assembly protein, but now termed adaptor (AP) complexes. The clathrin on

coated pits and vesicles of the endocytic pathway, and from the *trans*-Golgi network (TGN) appear to be the same, however, the AP complexes are distinct.

The AP complexes are composed of two proteins ~100 kD each, and two smaller subunits, ~50 kD and ~20 kD respectively. The AP complexes from the plasma membrane are termed AP-2 (or HA-2) adaptors, and the 100 kD proteins of the HA-2 adaptors are known as α - and β -adaptin. The AP complexes from the TGN are termed AP-1 (or HA-1) adaptors, and the 100 kD proteins of the HA-1 adaptors are known as β' - and γ -adaptin (Robinson 1992; Schmid 1992).

The adaptor complexes are believed to be components of the cellular sorting machinery involved in endocytosis, recruiting different trafficking receptors to coated pits. Consistent with this theory, direct binding of adaptors to the cytoplasmic domains of membrane proteins has been demonstrated. Affinity purified HA-2 adaptors were found to bind to low density lipoprotein receptor (LDL-R) tail constructs, and this binding was inhibited by preincubating the adaptors with the cation-independent mannose 6-phosphate receptor (CI-MPR), polymeric immunoglobulin receptor (pIg-R), or a peptide corresponding to the cytoplasmic domain of influenza HA containing the tyrosine mutation involved in endocytosis (Pearse 1988). HA-1 adaptors did not bind to the column. Similarly, a peptide corresponding to the cytoplasmic domain of human lysosomal acid phosphatase (LAP) bound HA-2 adaptors, and HA-1 adaptors bound poorly (Sosa *et al* 1993). In contrast, peptides corresponding to the cytoplasmic domains of CI-MPR and cation-dependent mannose 6-phosphate receptor (CD-MPR) bound both HA-1 and HA-2 adaptors (Glickman *et al* 1989; Sosa *et al* 1993), and mutation of tyrosine 26 in the cytoplasmic domain of the CI-MPR to valine, abolished binding of HA-2 but not HA-1 adaptor complexes (Glickman *et al* 1989). Proteolytic cleavage of adaptor complexes has suggested that the amino terminal part of the adaptors are involved in binding to the peptide corresponding to the CD-MPR cytoplasmic domain (Sosa *et al* 1993).

HA-2 adaptor binding to the Epidermal growth factor receptor (EGF-R) has now been demonstrated *in vivo* (Sorkin and Carpenter 1993). Inhibition of normal clathrin-coated pit assembly by potassium depletion, did not prevent binding of HA-2 adaptors to

the cytoplasmic domain of EGF-Rs, thus suggesting that receptor-adaptor complex association occurs before clathrin-coated pits are fully assembled. In a similar manner to the experiments with CD-MPR, results from this study suggest that the amino terminal region of the HA-2 adaptors are involved in receptor binding.

Clathrin-coated pits occupy about 2% of the plasma membrane (Griffiths *et al* 1989; Pelchen-Matthews *et al* 1991) and pinch off at a rate of ~1% per min forming up to 1000 coated vesicles (average diameter ~100 nm) per min, accounting for most, if not all, of the membrane and fluid-phase endocytosis in the cells studied (e.g. in HeLa or baby hamster kidney (BHK) cells - Marsh and Helenius 1980). Acidification of the cytosol (inhibits endocytosis of clathrin-coated pits and vesicles), of BHK cells inhibited the majority of fluid-phase endocytosis (Davoust *et al* 1987), and hypertonic medium, which prevents normal coated pit assembly (Heuser and Anderson 1989), inhibited the down-regulation of CD4 in HeLa-CD4 cells (Pelchen-Matthews *et al* 1993). In addition, measurement in rat hepatocytes of the activation energies required for both fluid-phase and RME, indicated that they are essentially the same, suggesting that both these forms of endocytosis are mediated by the same vesicle population (Oka and Weigel 1989).

In contrast, a number of reports suggest that clathrin-independent endocytosis may make a significant contribution to a cell's constitutive endocytic activity. Both hypertonic medium and potassium depletion prevent normal coated pit assembly (Larkin *et al* 1983; Heuser and Anderson 1989; Hansen *et al* 1991), and have been employed to inhibit RME in a number of cells types (Daukas and Zigmond 1985; Madshus *et al* 1987; Hansen *et al* 1991; 1993; Oka *et al* 1989; Heuser and Anderson 1989; Pelchen-Matthews *et al* 1993). However, fluid-phase endocytosis of markers such as lucifer yellow, and [¹⁴C]-sucrose is only partially inhibited in some of these cells by these treatments (Oka *et al* 1989; Madshus *et al* 1987; Hansen *et al* 1991; Daukas and Zigmond 1985). Acidification of the cytoplasm has been shown to inhibit clathrin-coated pits from "pinching-off" from the plasma membrane (Heuser 1989), thereby blocking RME of transferrin and epidermal growth factor in cells such as Hep 2, HeLa, Vero and chicken fibroblasts (Sandvig *et al* 1987; Heuser 1989). However, this treatment had little effect on the fluid-phase

endocytosis of lucifer yellow (Sandvig *et al* 1987). In addition, anti-clathrin antibodies delivered into the cytosol of CV-1 cells inhibited RME and fluid-phase endocytosis by 40-50% (Doxsey *et al* 1987). The failure to completely inhibit fluid-phase uptake could reflect a technical problem of delivering sufficient antibody to all the target cells, or it could indicate the existence of clathrin-independent endocytic mechanisms.

The mechanism of clathrin-independent endocytosis is unclear, however, experiments with drugs such as cytochalasin D and colchicine which act on microfilaments and microtubules, respectively, have been shown to inhibit fluid-phase endocytosis, without affecting RME, suggesting that the cytoskeleton may be involved in some way (Sandvig and van Deurs 1990).

The experimental systems employed to demonstrate the existence of a clathrin-independent endocytic pathway can have significant effects on cell morphology and viability (A. Pelchen-Matthews unpublished), and at present no evidence exists to demonstrate that two endocytic pathways mediate the uptake of different plasma membrane components. The evidence for clathrin-dependent endocytosis suggests that this pathway is able to supply the total endocytic activity for a cell. However, a situation where a cell may require additional endocytic activity could occur after a period of stress, and the methods used to inhibit clathrin-dependent endocytosis may be sufficient to stimulate an alternative pathway. It should be noted at this point that the principle route of internalization in the HeLa cells used in this study on the mechanisms involved in CD4 down-regulation, is believed to be clathrin-mediated.

1.4.c Compartments In The Endocytic Pathway.

Clathrin-coated pits are responsible for mediating the delivery of components from the cell surface to the endocytic pathway. At least three distinct compartments have been identified along this pathway (Figure 3). These are the endosomes, which are subdivided into the "early" and "late" endosomes, and the lysosomes.

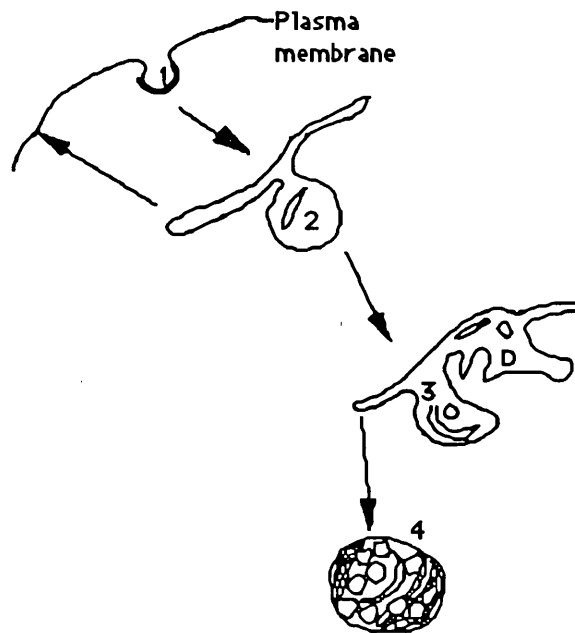


Figure 3. Schematic diagram of the endocytic pathway. 1, clathrin-coated pit; 2, early (peripheral) endosome; 3, late (perinuclear) endosome (pre-lysosome); 4, Lysosome.

The formation of clathrin-coated pits, followed by their invagination and budding from the plasma membrane to form a clathrin-coated vesicle, is an energy-dependent process (Schmid and Carter 1990). Following budding from the plasma membrane, the clathrin-coated vesicle is uncoated and subsequently fuses with the early endosome (Griffiths *et al* 1989). Early endosomes (sometimes referred to as the sorting endosome - Dunn and Maxfield 1992) are a distinct subpopulation of endosomes that appear to be located primarily in the peripheral cytoplasm of the cell (Gruenberg *et al* 1989), and can be labelled by short incubations (2-10 min) with fluid-phase markers (Griffiths *et al* 1989). They can also be labelled with antibodies to the small GTP-binding proteins rab 4 and rab 5 (van der Sluijs *et al* 1991; Chavrier *et al* 1990). It is thought that the rab proteins may regulate distinct vesicular transport events at the level of membrane targeting and/or fusion (Gorvel *et al* 1991; van der Sluijs *et al* 1992; Bucci *et al* 1992; Lombardi *et al* 1993). The early endosome is composed of a network of tubular and tubulovesicular structures, and in some cells they can form

extended networks (Marsh *et al* 1986; Griffiths *et al* 1989; Gruenberg *et al* 1989; Hopkins *et al* 1990; Tooze and Hollinshead 1991). The early endosome is responsible for the sorting of material internalized from the cell surface. A large proportion of the membrane and many receptors (e.g. Transferrin receptor (TfR) with bound apotransferrin, and LDL-R) are recycled to the plasma membrane from the tubular expansions, while other specific receptors (e.g. EGF-R and bound epidermal growth factor (EGF), or antigen cross-linked Fc receptors) remain in the vesicular part of the organelle, and are targeted to late endosomes and finally lysosomes where they are degraded. Other routes from the early endosome to structures for membrane recycling, transcytotic vesicles, synaptic vesicles, compartments for loading of MHC class II with antigen, or Golgi complex also exist in various cell types. The mechanisms through which sorting between these different compartments is controlled have yet to be identified. However the mildly acidic environment of pH 6-6.5, in the early endosome (Tycko and Maxfield 1982; Marsh *et al* 1983; Murphy *et al* 1984; Kielian *et al* 1986; Sipe and Murphy 1987; Schmid *et al* 1989), is a key factor in at least some of these endocytic sorting events.

A second population of endosomes distinct from the early endosomes (Schmid *et al* 1988), known as the late endosomes (or pre-lysosomal compartment), are generally located in the perinuclear region of the cell (Griffiths *et al* 1988; Gruenberg *et al* 1989), and are labelled by longer incubations (20-30 min) with fluid-phase markers (Griffiths *et al* 1989). They can also be labelled with antibodies to the small GTP-binding proteins rab 7 and rab 9 (Chavrier *et al* 1990; Lombardi *et al* 1993). They often contain a number of small internal vesicular profiles, which are thought to be involved in sorting to lysosomes. Late endosomes have a lower pH than the early endosomes, pH 5.5 or less (Tycko and Maxfield 1982; Roederer *et al* 1987; Kielian *et al* 1986; Schmid *et al* 1989), which is believed to be a crucial feature for some sorting events. Late endosomes receive material from the early endosomes and Golgi complex, and are also involved in sorting, delivering the endosomal content to lysosomes (e.g. ligated EGF-R), and recycling of CI-MPR to the Golgi complex (Kornfeld and Mellman 1989). Transport from the early to the late endosomes is microtubule dependent, as demonstrated by microtubule depolymerization using the drug nocodazole

(Gruenberg *et al* 1989; Bomsel *et al* 1990), and also depends on the presence of microtubule binding proteins, in particular the mechanochemical motors kinesin and cytoplasmic dynein (Bomsel *et al* 1990). Reduced temperature (16-20°C), has also been shown to inhibit transport of markers to late endosomes (Mueller and Hubbard 1986; Griffiths *et al* 1988). The late endosomes in some cells are characterized by their high content CI-MPR, and they can also be labelled with antibodies to the lysosomal membrane glycoprotein, lgp120 (Griffiths *et al* 1990).

The final station along the pathway is the lysosome, and this is where the bulk of the cellular acid hydrolase activity is located. The lysosomes have a lower pH than the late endosomes (pH 5 or below compared to pH 5.5) (Tycko and Maxfield 1982), are essentially devoid of the CI-MPR (Griffiths *et al* 1990), and are the major cellular site involved in biodegradation.

The mechanism(s) by which material is transported from the early endosomes to late endosomes and finally to lysosomes, remains a point of some debate (Griffiths and Gruenberg 1991; Murphy 1991). Helenius *et al* (1983) proposed two models. The first is known as the maturation model, and proposes that endocytic vesicles fuse with one another in the peripheral cytoplasm of the cell, to form the sorting endosome. This sorting endosome then gradually matures, showing an increase in the number of internal vesicular profiles as it moves to the perinuclear region of the cell (this structure is often referred to as a multivesicular body (MVB), with recycling vesicles continually budding off. Vesicles derived from the Golgi, containing newly synthesized lysosomal enzymes fuse with the maturing endosome gradually 'converting' it to a lysosome (Stoorvogel *et al* 1991; Dunn and Maxfield 1992; van Deurs *et al* 1993). The second theory proposes that early and late endosomes are pre-existing stable organelles, through which internalized receptors and their ligands pass. Endocytic vesicles from the plasma membrane fuse with the early endosome in the peripheral cytoplasm (Griffiths *et al* 1989), and 'carrier vesicles', which resemble the MVB (Gruenberg *et al* 1989), derived from the early endosomes, deliver their contents to the perinuclear late endosomes. Transport to lysosomes is also predicted to occur by a vesicle shuttle mechanism similar to that operating between the plasma membrane and endosomes.

1.5 ENTRY INTO THE ENDOCYTIC PATHWAY.

1.5.a *Endocytosis Signals.*

The initial indication as to the presence of internalization signals was proposed by Bretscher *et al* (1980) who showed that receptors cluster into coated pits. The first indication of their identity and location came from studies on naturally occurring endocytosis-defective mutant LDL-Rs, in patients with familial hypercholesterolaemia (Goldstein *et al* 1985; Davis *et al* 1986). One patient's LDL-Rs in particular (J.D.), had a single tyrosine to cysteine mutation, at position 807 in the cytoplasmic domain of the receptor (Davis *et al* 1986). This mutation caused the receptors to be less efficiently clustered into clathrin-coated pits compared to wild type receptors. It was later demonstrated that the first 22 amino acids (790-811) of the cytoplasmic domain of the LDL-R were sufficient for its rapid endocytosis. The tyrosine at position 807 was found to be a critical feature of the internalization signal, although, substitution with either phenylalanine, or tryptophan (aromatic amino acids), still permitted rapid LDL-R endocytosis. Subsequently internalization signals have been identified in a number of other receptors (Table 1).

For many of the receptors listed in Table 1, mutation of the tyrosine residue within the putative endocytosis signal, greatly reduced the internalization of that receptor.

Table 1. List of receptors containing known tyrosine-based motifs important for receptor endocytosis.

Receptor	Putative Internalization Signal	Reference
ASGP-R	TKE Y Q D LQHL	Fuhrer et al 1991
CD-MPR	PAA Y RG V GDD	Johnson et al 1990
CI-MPR	VS Y K Y SK V NK	Lobel et al 1989
HA Y543, F546	NGS LQYRI F	Canfield et al 1991
lamp-1	KRSHAG Y Q T I	Naim and Roth 1994
LAP	Q P P G Y RH V AD	Williams and Fukuda 1990
LDL-R	IN F DNP VY QK	Peters et al 1990
pIgR	ADLA Y SA F LL	Chen et al 1990
TfR	EP L S Y TR F SL	Breitfeld et al 1990
		Jing et al 1990
		Alvarez et al 1990
		Collawn et al 1990

The putative endocytosis signal is boxed, and the tyrosine residues which have been shown to be important for internalization are in boldface type. ASGP-R, asialoglycoprotein receptor; CD-MPR, cation-dependent mannose 6-phosphate receptor; CI-MPR, cation-independent mannose 6-phosphate receptor; HA Y543, F546, a mutant influenza haemagglutinin; LAP, lysosomal acid phosphatase; pIg-R, polymeric immunoglobulin receptor; the amino acid sequences are given in single letter code.

Collectively, the data published on the listed receptors in Table 1 indicate that a tyrosine residue is a common feature of the endocytosis signal, although aromatic residues, usually phenylalanine, can sometimes replace the tyrosine. However, site directed mutagenesis studies on a number of receptors such as LDL-R, TfR, CI-MPR, LAP and influenza virus haemagglutinin (HA), have demonstrated that while the tyrosine appears to be the most important residue, it is not the only functional amino acid within the endocytosis signal (Chen *et al* 1990; Collawn *et al* 1991; Canfield *et al* 1991; Lehmann *et al* 1992; Naim and Roth 1994). The internalization sequences of these proteins are now known,

and the data indicates that the signal usually contains 6 amino acids with a large hydrophobic amino acid in the last position, and an aromatic residue in position 1 or 3. The amino acids in positions 2, 4 and 5 tend to be polar and those often found in turns are common. The LDL-R is a type I transmembrane protein and when the human LDL-R internalization motif, FDNPVY, was transplanted into the TfR (a type II transmembrane protein), it was found to mediate transferrin uptake (Collawn *et al* 1991). Similarly, when the TfR endocytosis signal, YTRF, was transplanted into the type I transmembrane protein, CI-MPR, it was found to function as an efficient internalization signal (Jadot *et al* 1992). These results demonstrate that internalization signals are interchangeable between type I and II transmembrane proteins, and suggest that the orientation of the signal is not important.

1.5.b Structure Of An Endocytosis Signal.

Mutational analyses of endocytosis signals, such as that in the cytoplasmic domain of the LDL-R, have confirmed the importance of an aromatic residue within these motifs (Chen *et al* 1990).

Ktistakis *et al* (1990) first identified two major features of the tyrosine-based endocytosis signal: an excess of turn-promoting amino acids between the aromatic residue and plasma membrane, and a tendency for positively charged or polar residues at positions 1 and 2 C-terminal, and 1, 4, and 6 residues N-terminal to the aromatic residue. These data suggested that the tyrosine-based endocytosis signals may be an exposed loop containing an aromatic residue that is stabilized by hydrogen bonding.

Collawn *et al* (1990) searched the protein structure data bank for sequences corresponding to the internalization motif, YTRF, in the TfR, and found that the majority of sequences had protein backbone conformations very similar to a tight turn, as found in type 1 β turns, or at the ends of helices. In addition, a search for sequences similar to that of the LDL-R tetrapeptide endocytosis signal, NPVY, also found that these too showed a high tendency to adopt tight turn conformations. These findings lead to the prediction that a tight turn may be a common feature of internalization signals (Collawn *et al* 1990).

This idea gained further support from nuclear magnetic resonance (NMR) analysis of a peptide (CNPVYQKTT) containing

part of the LDL-R internalization signal (Bansal and Gierasch 1991). This peptide was found to adopt a tight turn conformation in solution, and that when either the asparagine or proline were mutated to alanine, this conformation was disrupted. The structure of the peptide revealed that the side chains of asparagine and tyrosine were in very close apposition, suggesting that interaction between these two side chains may stabilize the turn, possibly through hydrogen bonding.

A separate NMR study which analysed an 18 amino acid peptide, corresponding to the cytoplasmic domain of LAP, also supported the tight turn motif (Eberle *et al* 1991). The results from this study indicated that part of the peptide corresponding to residues QPPGY adopted a tight turn conformation in solution. In addition, the side chain of the glutamine is close to that of the hydroxyl group of the tyrosine, again suggesting that the turn may be stabilized through hydrogen bonding.

1.5.c Other Endocytosis Signals.

Experiments with the CD-MPR indicated that a tyrosine-based endocytosis motif is not the only functional internalization signal, and that in addition to the YRGV sequence, six residues, FPHLAF, also function as an endocytosis signal for this receptor (Johnson *et al* 1990). Both signals must be present for maximal receptor internalization. However, membrane proteins which lack a tyrosine-based internalization signal also undergo endocytosis. These include the CD3 γ chain (Letourneur and Klausner 1992), CD4 (Pelchen-Matthews *et al* 1989; 1991; 1992; 1993; Marsh *et al* 1990), the Fc receptor (FcRII-B2) (Miettinen *et al* 1989; 1992), and the adipocyte/skeletal muscle glucose transporter, GLUT4 (Corvera *et al* 1994).

When the cytoplasmic domain of CD3 γ was fused to the Tac antigen (IL-2 receptor α chain), some of the chimeric protein was delivered to the plasma membrane, whilst the majority of the protein was found in the lysosomes (Letourneur and Klausner 1992). The sequence which appeared to be mediating the delivery of this chimeric protein to lysosomes was DKQTLL, of which the di-leucine was shown to be specifically required. This signal, now termed a di-leucine motif, was also active as an

endocytosis signal, internalizing 90% of prebound iodinated anti-Tac antibody in 60 min (Letourneur and Klausner 1992).

Both CD4 and FcRII-B2 are endocytosed through coated pits (Pelchen-Matthews *et al* 1991; 1993; Miettinen *et al* 1989; 1992), and both possess a di-leucine within their cytoplasmic domains. The di-leucine in CD4 has been shown to be required for down-regulation (Shin *et al* 1991), and as this down-regulation appears to occur by endocytosis through coated pits (Section 3.1 Pelchen-Matthews *et al* 1993), it is possible that the di-leucine may function as an endocytosis signal.

1.5.d Entry Into The Endocytic Pathway From The Trans-Golgi Network.

In addition to sorting receptors and their ligands endocytosed from the plasma membrane, the endosomes are also responsible for sorting proteins delivered directly from the secretory pathway. The best documented pathway for the direct delivery of receptors from the secretory pathway to the endosomes is that used by the CI-MPR. Both the CI-MPR and CD-MPR, are primarily responsible for the direct delivery of newly synthesized lysosomal hydrolases from the secretory pathway to the endocytic pathway without appearing at the plasma membrane (Dahms *et al* 1989; Kornfeld and Mellman 1989; Ludwig *et al* 1991; Rijnboutt *et al* 1992). The CI-MPR is also responsible for the uptake and delivery to the endocytic pathway of extracellular lysosomal hydrolases.

In contrast to the lysosomal hydrolases, the delivery route of the lysosomal membrane glycoproteins (lgp's) from the TGN remains under question. In a similar manner to newly synthesized lysosomal hydrolases, transport of rat lgp120 from the TGN to lysosomes appears to occur via a direct intracellular route without appearing at the plasma membrane (Harter and Mellman 1992). However, newly synthesized lgp120 was detected at the plasma membrane when high levels of lgp120 were expressed. These results indicated that direct intracellular delivery of lgp120 from the TGN to the endocytic pathway was the major route. In contrast to these observations, studies on the human lysosomal membrane glycoprotein, lamp-1, have indicated that it is first transported from the TGN to the cell surface, from where it is

endocytosed into the endocytic pathway and is delivered to lysosomes (Williams and Fukuda 1990). This is a similar mechanism of delivery to lysosomes as that used by lysosomal acid phosphatase (Braun *et al* 1989), and LEP100 (Mathews *et al* 1992). Thus it appears as though lysosomal membrane glycoproteins are delivered to lysosomes either via the cell surface and entry into the endocytic pathway, or through the direct intracellular route similar to that taken by the CI-MPR.

1.5.e *Lysosomal Targeting Signals.*

As previously outlined above lysosomal membrane glycoproteins (lgp's) can reach the lysosomes either by an intracellular route or via the plasma membrane. The delivery of LAP and lamp-1 to lysosomes from the cell surface requires a tyrosine residue in the cytoplasmic domain, that comprises part of an endocytosis signal. Mutation of the tyrosine to another residue such as phenylalanine or alanine, resulted in an accumulation of LAP and lamp-1 at the plasma membrane (Peters *et al* 1990; Williams and Fukuda 1990), and mutation of the cytoplasmic domain tyrosine residue at position 8 in the rat lgp120 to cysteine, blocked delivery of lgp120 to lysosomes and led to increased lgp120 plasma membrane levels (Harter and Mellman 1992). In addition to the tyrosine in the cytoplasmic domain of rat lgp120, an adjacent glycine residue (position 7) also appears to be required for efficient lysosomal sorting. Similarly, mutation of glycine 412 to alanine in LAP, leads to increased expression of LAP at the cell surface (Lehmann *et al* 1992). These results indicate that the GY residues in the cytoplasmic domains of rat lgp120 and LAP form part of a lysosomal sorting signal, and that the tyrosine residue can also function in endocytosis. A number of different lgp's possess the GY motif in their cytoplasmic domains, but it has yet to be demonstrated that this motif functions as a lysosomal targeting signal for these other proteins.

Other lysosomal targeting signals which have been identified are the DKQTLL and YQPL sequences in the CD3 γ chain of the TCR (Letourneur and Klausner 1992). Both the YQPL and DKQTLL signals were individually sufficient to induce endocytosis and delivery of the Tac antigen to lysosomes. The targeting of lysosomal hydrolases to lysosomes is dependent on the CI- and

CD-MPRs, and in CI-MPR this targeting is dependent on the sequences LLHV and YSKV (Johnson and Kornfeld 1992). When these sequences were deleted from the cytoplasmic domain of CI-MPR, the targeting of Cathepsin D was completely inhibited. However, deletion of just the LLHV sequence increased the levels of CI-MPR reaching the plasma membrane, suggesting that the di-leucine might function in sorting CI-MPR from the TGN to the endocytic pathway. This di-leucine, although similar to that in the CD3 γ chain in terms of intracellular sorting, does not appear to function in CI-MPR endocytosis (Lobel *et al* 1989).

The relative importance of the leucine-based signal in the targeting of proteins to lysosomes has been suggested in studies with the type II lysosomal integral membrane protein, LIMP II (Vega *et al* 1991). The C-terminal cytoplasmic domain of this protein contains a leucine-isoleucine dipeptide at positions 475 and 476, respectively, that is critical for the targeting of LIMP II to lysosomes (Sandoval *et al* 1994). Time-course studies of the distribution of a series of point mutants indicated that the dipeptide signals LI, LL, LV, LA or II could target LIMP II to lysosomes to different extents. In addition, NMR analysis of an icosapeptide which corresponded to the cytoplasmic domain of LIMP II, revealed that in solution this peptide adopted either random coil conformations or transient configurations. In particular, the segment LIR adopted a conformation close to the values of an α helix, suggesting that the lysosomal targeting signal LI in LIMP II is within a domain that forms an extended configuration.

1.5.f Modification Of Sorting Signals By Phosphorylation.

CD4 on the surface of T cells undergoes very limited endocytosis due to its association with p56^{lck} (Pelchen-Matthews *et al* 1991; 1992). However, encounter with specific antigen, or treatment with phorbol ester causes the rapid and transient phosphorylation and down-regulation of CD4 (Acres *et al* 1986; Blue *et al* 1987; Hoxie *et al* 1988; Hurley *et al* 1989). Phorbol esters induce the dissociation of CD4 and p56^{lck} (Hurley *et al* 1989; Pelchen-Matthews *et al* 1993), probably as a consequence of phosphorylation of the cytoplasmic domain of CD4 (Hurley *et al* 1989), and this dissociation appears to precede the modulation of

CD4 (Sleckman *et al* 1992; Yoshida *et al* 1992). Down-regulation of CD4 in response to phorbol ester has recently been shown to occur by endocytosis through coated pits (Section 3.1; Pelchen-Matthews *et al* 1993), and it is likely that this internalization is due to protein kinase C (PKC)-mediated phosphorylation of the cytoplasmic domain of the molecule, as a mutant CD4 molecule (CD4^{S408A}) lacking a critical serine phosphorylation site, responds with a reduced and slower increase in CD4 endocytosis (A. Pelchen-Matthews unpublished).

Although the signals required for coated pit localization of CD4 have yet to be identified, the cytoplasmic domain contains a di-leucine sequence which is essential for down-regulation (Shin *et al* 1991). Other conserved amino acids which are required for phorbol ester-induced modulation include methionine 407 and isoleucine 410 (Shin *et al* 1991). The residues surrounding the serine 408 show a strong tendency to form an α helix, with the hydrophobic residues methionine 407, isoleucine 410, leucine 413, and leucine 414, arranged on the same side of the helix (Shin *et al* 1991). Phosphorylation of the cytoplasmic domain of CD4, in particular serine 408, might disrupt this structure creating or enhancing an endocytosis signal, which may involve the di-leucine sequence (a phosphoserine-dileucine signal).

Evidence for a phosphoserine-dileucine signal being involved in endocytosis has come from experiments with CD3 γ (Dietrich *et al* 1994). The cytoplasmic domain of this molecule contains a serine residue (S126), in a consensus PKC phosphorylation site, 4 amino acids N-terminal to a di-leucine motif (L131, L132). This di-leucine motif, in addition to the serine residue were shown to be required for PKC-mediated down-regulation, as demonstrated by their mutation to alanine and valine respectively. The di-leucine internalization signal appears to be active only when the serine residue is phosphorylated, i.e. it can be switched from an inactive to an active form by phosphorylation.

Another situation where phosphorylation may modulate sorting of a receptor has come from experiments with the CI-MPR. The targeting of Cathepsin D in a cell line deficient in CI-MPR but expressing cytoplasmic tail mutants of the receptor, was found to be dependent on a di-leucine sequence and a YSKV motif (Johnson and Kornfeld 1992). Targeting of the Cathepsin D was partially inhibited when the sequence LLHV, containing the di-leucine, was

deleted, suggesting that the di-leucine is an important feature for efficient sorting of the CI-MPR at the TGN. This di-leucine is adjacent to a consensus casein kinase II site (Chen *et al* 1993). In addition, serine residues 2421 and 2492 in the cytoplasmic domain of the CI-MPR become transiently phosphorylated at or near the time of exit of the receptor from the TGN (Meresse and Hoflack 1993). These phosphoserines are within a motif in the cytoplasmic domain of CI-MPR which may be important for the high affinity binding of the Golgi-specific adaptor proteins, HA-1 (Le Borgne *et al* 1993).

The polymeric immunoglobulin receptor (pIg-R) is responsible for the transport of immunoglobulin A and M across a variety of epithelia. Tyrosine 743 in the cytoplasmic domain of pIg-R (Table 1) is required for receptor endocytosis into the early endosomes from where it is normally recycled back to the basolateral membrane. Studies have indicated that serine phosphorylation may modulate the sorting of "empty" pIg-R. Phosphorylation of serine 664 in the cytoplasmic domain of pIg-R resulted in efficient transcytosis in a model-MDCK cell system. Mutation of the serine to alanine inhibited this transcytosis, but mutation to aspartic acid, which mimics the negative charge of the phosphate group, resulted in a receptor that was efficiently transcytosed (Casanova *et al* 1990). In the presence of IgA however, mutation of serine 664 to alanine did not inhibit transcytosis of the pIg-R (Hirt *et al* 1993).

The sorting signals outlined above indicate that motifs containing tyrosine and di-leucine can function as endocytosis signals, and that other motifs can be modulated by such mechanisms as phosphorylation. Taken together, these data suggest that there are two classes of signals: constitutive and regulated.

1.5.g Exclusion From The Endocytic Pathway.

Endocytosis signals have been shown to mediate efficient internalization of some receptors via clathrin-coated pits and vesicles. However, not all cell surface proteins cluster into clathrin-coated pits, as their primary function appears to be at the cell surface. These proteins may not possess the signals necessary to cluster into clathrin-coated pits, or they may be actively prevented from entering pits.

For instance, the murine FcRII-B1 isoform expressed on B lymphocytes, unlike the FcRII-B2 isoform on macrophages, is not efficiently endocytosed. The FcRII-B1 receptor contains a 47 amino acid insert that appears to prevent the FcRII-B1 receptor from entering clathrin-coated pits, possibly through an interaction with cytoskeletal elements (Miettinen *et al* 1989; 1992). In polarized MDCK cells, retention of Na⁺,K⁺-ATPase at the basolateral membrane is believed to be maintained by the interaction of Na⁺,K⁺-ATPase with the cytoskeleton, preventing it from entering the endocytic pathway (Hammerton *et al* 1991). Similarly, CD4 expressed in T cells does not undergo efficient endocytosis. The tyrosine kinase, p56^{lck}, interacts with the cytoplasmic domain of CD4, and has been shown to prevent CD4 from entering clathrin-coated pits (Pelchen-Matthews *et al* 1992). The mechanism of this inhibition of endocytosis is not clear, however, some evidence indicates that p56^{lck} may interact with components of the cortical cytoskeleton (Louie *et al* 1988), possibly through its *src*-homology domains, which are known to be involved in protein-protein interactions, and have been identified in a number of actin-binding proteins (Koch *et al* 1991). Thus, p56^{lck} may prevent CD4 endocytosis in T cells by anchoring it to the cytoskeleton. Other proteins which do not cluster in clathrin-coated pits and undergo very limited endocytosis, include CD8 (Reid *et al* manuscript in preparation), and glycosphosphatidylinositol (GPI)-anchored proteins (Lemansky *et al* 1990; Keller *et al* 1992; Schell *et al* 1992)

1.6 THE ROLE OF CD4 IN HIV INFECTION.

The human immunodeficiency virus (HIV-1) is a retrovirus belonging to the family Lentivirinae, and is believed to be the aetiological agent for acquired immunodeficiency syndrome (AIDS) (Barre-Sinoussi *et al* 1983; Gallo *et al* 1984). HIV-1 is an enveloped virus, possessing a protein capsid containing the viral genome, enclosed within a lipid and protein membrane. The membrane contains one predominant glycoprotein complex, gp41-gp120, which is encoded by the viral *env* gene. This glycoprotein is synthesized as a single precursor polypeptide, known as gp160, and is subsequently proteolytically cleaved to yield a heterodimer of gp41-gp120. CD4 acts as the cellular receptor for HIV

(Dalglish *et al* 1984; Klatzmann *et al* 1984; McDougal *et al* 1986; Maddon *et al* 1986; Clapham *et al* 1987), by providing the cell surface binding sites recognized by the viral gp120 glycoprotein (Clayton *et al* 1988; Berger *et al* 1988; Richardson *et al* 1988).

Enveloped viruses infect their host cells by membrane fusion. Fusion can occur either at the plasma membrane or in endosomes. Some enveloped viruses use the acidic environment within endosomes to drive the reactions which lead to membrane fusion and infection, e.g. Semliki Forest virus; Influenza virus (for a recent review see Marsh and Pelchen-Matthews 1993). Other enveloped viruses do not use acidic pH, e.g. Rous Sarcoma virus (Gilbert *et al* 1988); HIV (Stein *et al* 1987; McClure *et al* 1988). At the current time little is known about the mechanisms that regulate the fusion activity of these viruses or their sites of cellular penetration.

To date the bulk of evidence has suggested that HIV penetrates cells by direct fusion at the cell surface (Stein *et al* 1987; Bedinger *et al* 1988; Maddon *et al* 1988; McClure *et al* 1988). These conclusions are based primarily on experiments in which CD4 receptor molecules containing mutations which disrupt the cytoplasmic domain, can be shown to function in virus infection. However, it is now clear that these mutations, whilst able to block phorbol ester-induced down-regulation, do not completely block endocytosis (Pelchen-Matthews *et al* 1989; 1991; 1993; unpublished; Marsh *et al* 1990). Furthermore, it is apparent for these viruses that the infection mechanisms observed in culture may not fully reflect the entry mechanisms employed *in vivo*. Indeed a number of studies have implicated endocytosis in the mechanism of virus entry (Pauza and Price 1988; Grewe *et al* 1990).

1.7 PHORBOL ESTERS.

1.7.a Activation Of Protein Kinase C.

Protein kinase C (PKC) is activated by the receptor-mediated hydrolysis of inositol phospholipids by phospholipase C (PLC), it is responsible for the phosphorylation of a number of intracellular substrates and for relaying information, in the form of

extracellular signals, across the plasma membrane to regulate many Ca^{2+} -dependent events (reviewed by Nishizuka 1986).

The primary products of PLC hydrolysis of phosphatidylinositol 4,5-bisphosphate (PIP_2), are inositol 1,4,5-triphosphate (IP_3), and 1,2-diacylglycerol (DAG) (Imboden and Stobo 1985; Pantaleo *et al* 1987). These products act as secondary messengers. IP_3 is responsible for the release of Ca^{2+} from intracellular stores, whilst DAG is the physiological activator of PKC.

Phorbol esters, such as phorbol myristic acid (PMA), have a very similar structure to DAG and are capable of activating PKC both *in vitro* and *in vivo* (Castagna *et al* 1982). Phorbol esters have been shown to affect the normal cellular distribution and trafficking of a variety of receptors including TfR, EGF-R, ASGP-R and LDL-R, within certain cell types (McGraw *et al* 1988; Magun *et al* 1980; Fallon and Schwartz 1987; Maziere *et al* 1986), and have also been shown to activate the Na^+/H^+ exchange protein (Besterman *et al* 1985). Recently phorbol esters have been shown to stimulate transcytosis in MDCK cells (Cardone *et al* 1994), and constitutive secretion in rat basophilic leukaemia cells (De Matteis *et al* 1993).

In addition to these effects, phorbol esters have more general effects on cell architecture and membrane processes. In particular, phorbol esters induce dramatic changes in cell shape and membrane in fibroblasts and macrophages (Miyata *et al* 1988; Phaire-Washington *et al* 1980a). PMA affects the organization of microtubules and microfilaments in macrophages (Phaire-Washington *et al* 1980b), which may account for the changes in cell shape, and stimulation of fluid-phase uptake and delivery to lysosomes (Swanson *et al* 1985).

Therefore, with these potential effects in mind, interpretation of results when employing phorbol esters can be very difficult, and require the use of stringent control experiments. Despite these effects, phorbol esters have proved to be an extremely useful reagent in the study of T cell activation, and are known to cause the modulation of CD4.

1.7.b Down-Regulation Of CD4 And Its Interaction With The Endocytic Pathway.

CD4 is a very important immunological molecule, functioning in T cell ontogeny and activation, and as the major cellular receptor for

HIV. Until recently little information was available concerning its endocytic properties and intracellular trafficking. The cell surface expression of CD4 is correlated with activation of T cells, such that cell surface CD4 is modulated following exposure of T cells to specific antigen (Acres *et al* 1986; Weyand *et al* 1987; Rivas *et al* 1988), or to cross-linking antibodies the TCR/CD3 complex (Rivas *et al* 1988), or CD2 (Blue *et al* 1989). In addition, the HIV early protein, Nef (Aiken *et al* 1994), and cross-linking antibodies against CD4 (Ledbetter *et al* 1988; Cole *et al* 1989; Thuillier *et al* 1990), cause down-regulation of CD4. The down-regulation of CD4 observed in response to antigenic stimulation of T cells, can be mimicked by treatment of cells with phorbol esters (Acres *et al* 1986; Weyand *et al* 1987), which activate PKC (Nishizuka 1986), and cause the transient phosphorylation of the CD4 cytoplasmic domain (Acres *et al* 1986; Blue *et al* 1987; Hoxie *et al* 1988). The exact mechanism by which cell surface CD4 is down-regulated is not fully understood, but it is thought that it may occur by endocytosis (Hoxie *et al* 1986; 1988; Petersen *et al* 1992), following the dissociation of p56^{lck} (Pelchen-Matthews *et al* 1993), and there is some indication in the literature that CD4 is degraded following phorbol ester treatment (Baenziger *et al* 1991; Shin *et al* 1991; Petersen *et al* 1992; Ruegg *et al* 1992). Despite these reports, the interaction of CD4 with the endocytic pathway and its exact intracellular fate during down-regulation have not been determined.

Previous results on the endocytic properties of human CD4 expressed in non-lymphoid cells (HeLa-CD4 and NIH3T3-CD4) and monocytic cells (HL-60) have demonstrated that it is constitutively endocytosed into the early endosome and recycled to the cell surface (Pelchen-Matthews *et al* 1989; 1991; Marsh *et al* 1990). Internalization occurs through clathrin-coated pits and vesicles, and at steady state about 40% of the CD4 is found inside the cells. The rates of CD4 internalization in HeLa-CD4 and NIH3T3-CD4 cells (2-3% per min and 4% per min, respectively), are significantly faster than bulk-flow uptake of mutant CD4 molecules lacking a cytoplasmic domain (Pelchen-Matthews *et al* 1991). In contrast, CD4 expressed in lymphocytic cells is not endocytosed (Pelchen-Matthews *et al* 1991), due to its association with p56^{lck} which prevents its entry into clathrin-coated pits (Pelchen-Matthews *et al* 1992).

1.8 AIM OF WORK DESCRIBED IN THIS THESIS.

This thesis and recent published work from this study (Pelchen-Matthews *et al* 1993), has examined the mechanism of phorbol ester-induced CD4 down-regulation, and the interaction of CD4 with the endocytic pathway during its modulation.

Since p56^{lck} has a significant effect on the endocytic properties of CD4 (Pelchen-Matthews *et al* 1992), CD4-transfected non-lymphoid HeLa cells were used in this study. The results presented in this thesis demonstrate that human CD4, expressed in HeLa-CD4 cells is rapidly down-regulated from the cell surface on addition of phorbol ester, thus indicating that down-regulation is not dependent on the presence of p56^{lck}. The initial effect, which follows the addition of phorbol ester, is to increase the rate of CD4 endocytosis through clathrin-coated pits. Phorbol esters divert internalized CD4 from the recycling pathway, and deliver it to a perinuclear compartment in the cell that costains by immunofluorescence for the CI-MPR. Delivery of CD4 to lysosomes is not apparent, however, degradation studies, indicate that CD4 is degraded. In lymphocytic cells, where p56^{lck} is expressed, phorbol ester-induced CD4 down-regulation appears to occur by a similar mechanism, with CD4 being delivered to a compartment that costains for CI-MPR, followed by its degradation. In addition, inhibition of kinase and phosphatase activities, indicate that constitutive endocytosis and recycling of CD4 in HeLa-CD4 cells, may involve cycles of phosphorylation and dephosphorylation.

2. MATERIALS AND METHODS

2.1 *Cells Lines and Cell Culture.*

CD4 transfected HeLa cells lines, HeLa-CD4 (Maddon *et al* 1986) subcloned by limiting dilution, HeLa-CD4^{cyt-} (a CD4 mutant from which the major portion of the cytoplasmic domain has been deleted (amino acid 403 to 433) and HeLa-CD4^{S408A} (a CD4 mutant in which serine at position 408 has been mutated to alanine (Maddon *et al* 1988)), were grown in Dulbecco's modified Eagle's medium (DMEM), supplemented with 4% FCS, 100 U/ml penicillin, 0.1 mg/ml streptomycin and 1 mg/ml G418 (Gibco BRL, Scotland), and were used 2 days after subculture unless otherwise stated. The lymphocytic cell line, SupT1 (Smith *et al* 1984), was grown in RPMI 1640 medium supplemented with 10% FCS, 100 U/ml penicillin and 0.1 mg/ml streptomycin, and the cells used while growing exponentially.

2.2 *Antibodies.*

Q4120 (an anti-CD4 mab) was developed by Dr. Q. Sattentau (Healy *et al* 1990), and was provided by the Medical Research Council AIDS Directed Programme Reagents Programme. Q4120 was labelled with tetramethyl-rhodamine isothiocyanate (TRITC, Cambridge Bioscience) according to the manufacturer's instructions.

Leu3a (an anti-CD4 mab) was obtained from Becton Dickinson & Co..

Mouse anti-CD4 ascites, Hoxie 21, was kindly provided by Dr. J.A. Hoxie (University of Pennsylvania, PA). This anti-CD4 antibody did not compete effectively with Q4120 or Leu3a indicating that it recognized a different epitope to Q4120 and Leu3a (Annegret Pelchen-Matthews, unpublished).

Fluorescein-conjugated anti-transferrin receptor mab, L01.1, was obtained from Becton Dickinson & Co..

Rabbit polyclonal serum specific for the cation-independent mannose 6-phosphate receptor (CI-MPR) was kindly provided by

Dr. W.J. Brown (Cornell University, Ithaca, NY; Brown and Farquhar, 1987).

Rabbit polyclonal serum specific for lysosomal associated membrane protein (lamp) 1 and 2 was kindly provided by Dr. S. Carlsson (University of Umeå, Sweden).

The mab 2C2 was prepared from a "heavy" membrane fraction from Hep 2 cells isolated by Percoll density centrifugation. The Percoll was removed from the fraction, and the resulting membrane preparation was injected into mice. Antibody was obtained by saturated ammonium sulphate precipitation (Marsh *et al* manuscript in preparation).

Rat mab (23C) raised against the t complex polypeptide (Willison *et al* 1989) was used to visualize the Golgi apparatus.

Rabbit polyclonal anti-rab 7 was kindly provided by Dr. Marino Zerial (EMBO, Germany; Chavrier *et al* 1990).

Peroxidase-conjugated, and rhodamine- or fluorescein-labelled anti-rabbit, anti-rat and anti-mouse reagents were purchased from Pierce and Warriner.

Enhanced chemiluminescence (ECL) reagents for immunoblotting were purchased from Amersham International.

2.3 Q4120 Iodination.

Q4120 (46.4 μ g) was dialysed into 0.1 M disodium tetraborate buffer, pH 8.50, using 3 changes of buffer, and the protein concentration of the dialysed material determined using bicinchoninic acid (BCA) protein assay (see BCA assay). 125 I-Bolton and Hunter reagent (500 μ Ci - Amersham International) were evaporated under a steady stream of nitrogen until dry, and reacted with 28 μ l of Q4120 (46.4 μ g, 309.5 pmoles) in 0.1 M borate buffer. The mix was vortexed every 2 min for 20 min and terminated by adding 272 μ l 0.2 M glycine in 0.1 M borate buffer. 2 x 5 μ l were added to 495 μ l PBS/0.25% gelatin for TCA precipitation (the TCA aliquots), the remainder of the mixture was fractionated on a 10 DG column (BioRad laboratories, 10 ml resin) prewashed with elution buffer (PBS/0.25% gelatin and 0.02% azide). 25 x 0.5 ml fractions were collected, 3 μ l counted in a gamma counter (NE 1600) and the elution profile was plotted.

The protein peak was pooled, split into 100 µl aliquots and frozen at -20°C.

TCA precipitation: The TCA precipitation allowed accurate determination of the specific activity of the ^{125}I -Q4120. The radiolabelled proteins before they were fractionated, and the pooled antibody fraction were analysed for their TCA soluble and precipitable counts. 5 µl of the antibody fraction and 5 µl proteins before fractionation (the TCA aliquots), were TCA precipitated in PBS/1% gelatin containing 13% TCA for 90 min at 4°C. The samples were centrifuged at 300 g for 5 min at 4°C and collected each of the supernatants and TCA precipitates. The precipitates and supernatants were counted in the gamma counter together with 10 µl, in duplicate, of the pooled antibody peak and TCA aliquots.

2.4 Loading Of Protein A Sepharose Beads With Anti-CD4 (Hoxie 21).

0.25 g of protein A sepharose (CL4B - Sigma) were weighed out and washed with 3 changes of PBS to make 1 ml of swollen beads (1 ml of beads has a binding capacity of 5 mg human IgG). 1 ml of Hoxie 21 ascites (26.29 mg/ml) was adjusted to pH 9.00 and 3 M NaCl, and incubated with the beads for 2 h at room temperature with gentle mixing. The mixture was centrifuged at 1200 g for 5 min, the supernatant removed, and its protein concentration determined at 280 nm in a spectrophotometer (LKB Ultrospec IIE). The beads were washed twice with 10 volumes of 3 M NaCl/0.05 M $\text{Na}_2\text{B}_4\text{O}_7 \cdot 10\text{H}_2\text{O}$, and resuspended in 10 ml 3 M NaCl/0.2 M $\text{Na}_2\text{B}_4\text{O}_7 \cdot 10\text{H}_2\text{O}$ containing 20 mM dimethylpimelimidate (Pierce and Warriner) for 30 min at room temperature with gentle mixing. The mixture was centrifuged at 1200 g for 5 min, the supernatant removed and the beads were washed once with 0.2 M ethanolamine (pH 8.00). Incubated the beads in 0.2 M ethanolamine (pH 8.00) for 2 h at room temperature with gentle mixing. The beads were washed twice with PBS and stored in PBS/0.02% NaN_3 at 4°C. These anti-CD4 protein A sepharose beads were tested for quantitative precipitation of CD4. One 100 mm plate of HeLa-CD4 cells was washed with PBS and scraped into 10

ml PBS at 4°C. The cell suspension was centrifuged at 300 g for 5 min at 4°C and the cell pellet was resuspended in 200 µl Tris lysis buffer pH 8.00, containing 3% NP40, 150 mM NaCl, 2 mM EDTA and protease inhibitors (1 mM PMSF and 10 µg/ml each of chymostatin, leupeptin, antipain and pepstatin) for 15 min on ice. The detergent-insoluble material was removed by centrifuging at full speed (13 000 rpm) in a microfuge (Heraeus) for 20 min at 4°C. The supernatant was recovered, and 15 µl, 20 µl, and 25 µl of prewashed anti-CD4 beads were added to 50 µl aliquots of the HeLa-CD4 lysate for 1 h at 4°C with gentle mixing. The beads were washed 3 times with TBS/0.5% TX100 and once with TBS to reduced the detergent content of the samples. Each pellet of beads was resuspended into 50 µl non-reducing 1 x sample buffer. Added 5 µl of non-reducing, 5 x sample buffer to 20 µl aliquots of the supernatants after immunoprecipitation, and 20 µl of lysate before precipitation. All samples were and heated to 95°C for 5 min, then loaded onto 10% acrylamide gels which were run at 20 mA for approximately 1 h. The proteins were transferred to nitrocellulose for 30 min at 1 A and immunoblotted (see immunoblotting below) for CD4.

2.5 Detection Of Cell Surface CD4 After PMA Treatment.

Cells in 16 mm diameter tissue culture wells were washed twice with binding medium (BM: RPMI 1640 lacking bicarbonate, supplemented with 0.2% BSA, and 10 mM HEPES, pH 7.40) at 37°C, before incubation in BM in the presence of 100 ng/ml PMA (Sigma) for times up to 6 h. Cells were cooled quickly by washing twice with BM at 4°C and incubated with gentle shaking in BM containing 0.3 nM ¹²⁵I-Q4120 for 2 h at 4°C . Unbound antibody was removed by washing 3 times with BM and 2 washes with PBS at 4°C. The cells were harvested in 400 µl 0.2 M NaOH and the wells rinsed with 400 µl H₂O which was then pooled with the respective cell lysate. The lysates were counted in the gamma counter and the level of antibody bound for each time point determined as a proportion of the original amount of antibody bound at the cell surface before the addition of PMA.

2.6 Detection Of Cell Surface CD4 After PMA Treatment In Hypertonic Medium.

HeLa-CD4 cells grown for 3 days in 16 mm diameter wells were preincubated for 5 min at 4°C in the presence or absence of hypertonic medium (0.45 M sucrose in RPMI 1640 lacking bicarbonate, supplemented with 0.2% BSA, 20 mM MES, and 20 mM succinic acid, pH 5.70), and warmed in fresh medium, containing 100 ng/ml PMA in the presence or absence of 0.45 M sucrose at pH 5.7 for 1 h at 37°C. The cells were cooled by washing 3 x with BM, and the amount of CD4 remaining at the cell surface detected using 0.3 nM ¹²⁵I-Q4120 for 2 h at 4°C with shaking. Unbound ligand was removed with 4 changes of BM and 2 changes of PBS at 4°C, and the cells were harvested in 400 µl of 0.2 M NaOH. The wells were rinsed with 400 µl of H₂O which was pooled with the respective lysate and the samples were counted in the gamma counter.

2.7 Cell Surface CD4 Endocytosis Assay.

HeLa-CD4 cells in 16 mm diameter tissue culture wells were cooled on ice for 10 min before briefly washing twice with BM at 4°C. A saturating concentration (8 nM) of ¹²⁵I-Q4120 was added to the cells and they were incubated at 4°C for 2 h with gentle shaking. Unbound ligand was removed using 3 quick washes with cold BM and duplicate aliquots of cells warmed to 37°C in BM in the presence or absence of 100 ng/ml PMA for times up to 120 min. Cells were returned to ice and cooled rapidly by washing 3 times with cold BM. To determine the proportion of internalized ligand, one of the duplicate cell aliquots was treated with elution medium (RPMI 1640 lacking bicarbonate, supplemented with 0.2% BSA, and 10 mM MES, pH 2.00). The cells were washed twice in cold elution medium then incubated in cold elution medium for 2 x 3 min at 4°C. The other aliquot of cells was harvested directly. Cells were harvested in 400 µl 0.2 M NaOH and the wells rinsed with 400 µl H₂O which was then pooled with the respective cell lysate. The lysates were counted in the gamma counter, and the

proportion of acid resistant to total cell counts was calculated for each time point and plotted.

2.8 Fluid Phase Endocytosis Assays.

Cells grown in 30 mm diameter dishes were washed twice in warm BM. Two fluid phase markers were used, horseradish peroxidase (HRP, type II obtained from Sigma) and lucifer yellow (LY, obtained from Molecular Probes). Cells were warmed in the presence or absence of 100 ng/ml PMA in BM containing either 5 mg/ml HRP or 1 mg/ml LY for times up to 120 min at 37°C. Cells were cooled rapidly by washing 6 times with BM at 4°C followed by 4 times with PBS at 4°C. Cells were scraped into 1 ml of PBS at 4°C and centrifuged at 300 g for 5 min at 4°C in a Beckman GS-6R. Each cell pellet which had been incubated in the presence of HRP was resuspended at 4°C in 1 ml PBS containing 0.1% Triton X (TX)-100 and incubated on ice for 15 min. The cell pellets which had been incubated in LY were resuspended in 0.5 ml PBS containing 0.05% TX-100 at 4°C and incubated on ice for 15 min. The level of HRP associated with each cell lysate was assayed using o-dianisidine in a microtitre plate assay (see HRP assay). LY was assayed as follows: 0.35 ml of each lysate were made up to 1.6 ml with PBS/0.05% TX-100/0.1 mg/ml BSA, and LY standards, containing a known quantity of LY were made up in an identical manner. The LY was assayed in a specrometer at excitation 430 nm (bandwidth 10 nm), emission 540 nm (bandwidth 18 nm). The protein concentration of each cell lysate was determined using the BCA protein assay (see protein assay).

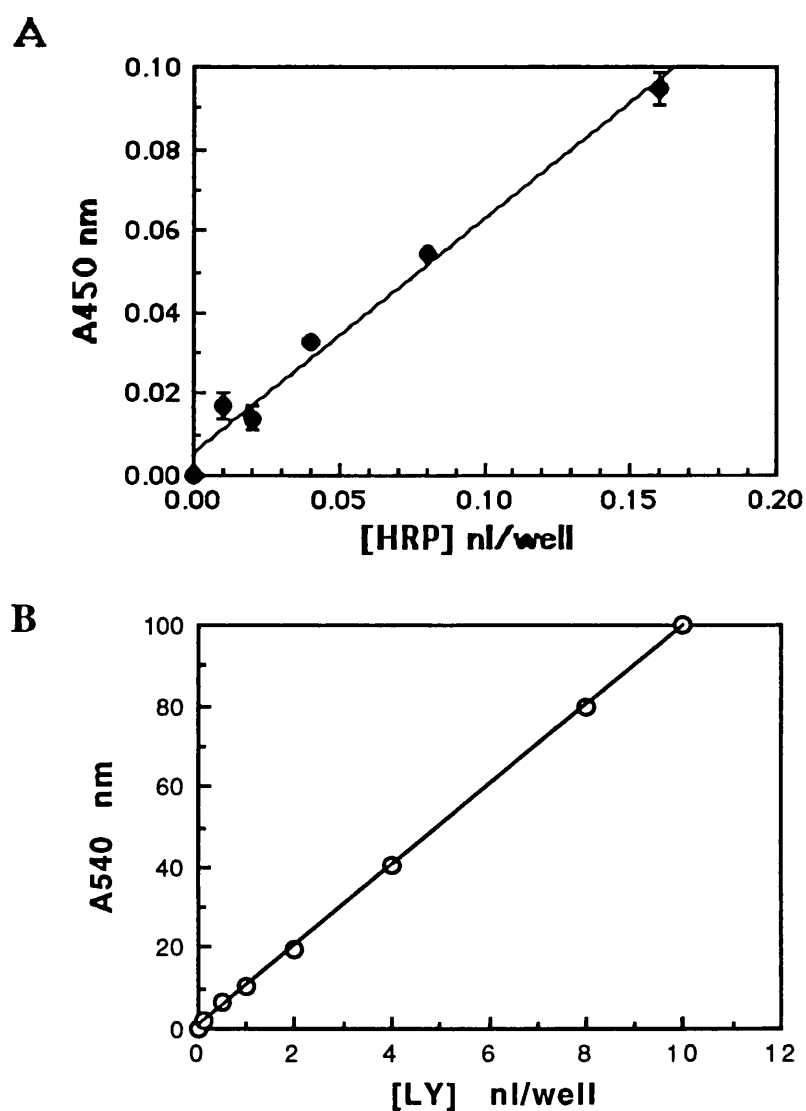


Figure 4. Standard curves for the fluid-phase markers horseradish peroxidase (A), and lucifer yellow (B). Standards were prepared from 5 mg/ml HRP or 1 mg/ml LY, and assayed at the same time as the test samples. HRP was quantitated at 450 nm, and LY quantitated at 540 nm.

2.9 Electron Microscopic Localization Of CD4.

HeLa-CD4 cells were seeded onto 22 mm² glass coverslips and grown for 2 days: Cells were cooled on ice for 10 min and washed 2 times with cold BM. Cells were labelled with 8 nM Leu3a in BM, for 2 h at 4°C with gentle mixing. Excess antibody was removed using 3 changes of cold BM (SupT1 cells were washed by centrifugation), and the cells labelled with 9 nm protein A-gold in BM for a further 2 h at 4°C with gentle mixing. After washing 3 times with cold BM the cells were either kept on ice or warmed to 37°C in the presence or absence of 100 ng/ml PMA. Cells were cooled by washing twice with cold BSA-free BM and fixed on ice for 30 min followed by 30 min at room temperature in 50 mM sodium cacodylate buffer pH 7.40 containing 2.5% glutaraldehyde. Post fixation was in 1% osmium tetroxide in 50 mM cacodylate buffer pH 7.40 for 1 h at 4°C in the dark. Cell pellets were dehydrated by sequential incubations in 70%, 90%, and 100% ethanol. The pellets were embedded in epon, baked overnight at 70°C, and thin sections were examined after staining with uranyl acetate and lead citrate. For quantitative analysis, the cells were examined systematically noting the position of every gold particle encountered.

Morphometric analysis of the 2 min time points in the presence and absence of PMA was carried out. 35 random images for each time point were taken at a magnification of x8000, and a transparent grid (dimensions 20 x 20 mm) was overlayed over each image. The number of plasma membrane and coated membrane intersects were counted (coated vesicles were only counted when they were close to the plasma membrane), and the proportion of coated membrane was calculated. The results were analysed by a student t test to determine whether there was a significant difference between the numbers obtained.

2.10 Immunofluorescence Endocytosis Assay.

Cells grown on 13 mm diameter glass coverslips were cooled on ice for 10 min and washed twice in BM at 4°C (SupT1 cells were

washed by centrifugation, spinning at 300 g for 5 min at 4°C between each wash). The cells were labelled with 8 nM Leu3a or rhodamine-conjugated Q4120 for 2 h at 4°C, washed 3 times with cold BM and incubated for various times at 37°C in BM in the presence or absence of 100 ng/ml PMA. After warming, the cells were cooled by washing 3 times with BM at 4°C and some cells were acid stripped at pH 3.00 as outlined above to remove any cell surface antibody. All cells were fixed in 3% paraformaldehyde in PBS for 15 min on ice followed by 15 min at room temperature and treated with 50 mM NH₄Cl in PBS. Some of the cells were permeabilized with 0.1% TX100 in PBS for 10 min at room temperature to reveal the intracellular antibody. Non-specific antibody binding sites were blocked in PBS/0.2% gelatin for 15 min at room temperature. The cells stained with Q4120-TRITC were counter stained with anti-TfR-FITC (L01.1, diluted 1:100, Becton and Dickinson & Co.). The Leu3a antibody was detected using rhodamine-labelled goat anti-mouse (Pierce and Warriner) diluted 1:2000 in PBS/0.2% gelatin. Cells on some coverslips were counter-stained with rabbit anti-cation-independent mannose 6-phosphate receptor (CI-MPR) diluted 1:200 in PBS/0.2% gelatin, followed by FITC-conjugated goat anti-rabbit (Pierce and Warriner) diluted 1:1000 in PBS/0.2% gelatin. SupT1 cells in 100 µl of PBS were added to poly-lysine coated 13 mm diameter coverslips for 30 min at room temperature to allow them to adhere to the glass. Coverslips were mounted in Moviol and observed using a confocal microscope (Bio-Rad MRC 600 model).

2.11 Immunofluorescence.

HeLa-CD4 cells grown on 13 mm diameter glass coverslips were washed twice with PBS. SupT1 cells growing exponentially in suspension were washed twice by centrifugation (300 g for 5 min - all subsequent washes were performed in an identical manner). Cells were fixed at -20°C in a 50:50 mixture of acetone and methanol for 1 min. Cells were washed 3 times with PBS, and non-specific antibody binding sites were blocked with PBS/0.2% gelatin. Cells were stained for 1 h at room temperature with 2C2

(1:5000), washed 3 times with PBS, and then co-stained with either lamp-1 (1:50 000) or lamp-2 (1:20 000), or CI-MPR (1:200). Cells were washed 3 times with PBS, 2C2 was visualized using rhodamine-labelled goat anti-mouse (1:2000), and lamp-1 and -2, and CI-MPR were detected using FITC-labelled goat anti-rabbit (1:1000). Cells were washed 3 times with PBS, and SupT1 cells in 100 μ l PBS were adhered poly-lysine coated 13 mm glass coverslips for 30 min at room temperature. Coverslips were mounted in moviol.

2.12 Sodium Dodecyl Sulphate-Polyacrylamide Gel Electrophoresis.

Discontinuous sodium dodecyl sulphate polyacrylamide gel electrophoresis (SDS-PAGE) was performed as per Laemmli (1970) on 10% acrylamide minigels (10 cm by 8 cm and 0.1 cm thick). Protein samples were diluted with sample buffer (final concentration of constituents: 0.0625 M Tris-HCl pH 6.8, 7.5% sucrose, 2% SDS, 0.005% bromophenol blue, and 10 mg/ml dithiothreitol for reducing conditions where appropriate), and broad range molecular weight markers were diluted into sample buffer as above (Bio-Rad or Sigma prestained standards or Rainbow coloured markers from Amersham International plc). All samples were heated to 95°C for 5 min and loaded onto 10% acrylamide minigels which were set up in a custom made apparatus containing running buffer (0.384 M glycine, 0.050 M Tris-HCl pH 8.8 and 0.1% SDS). Gels were run at 20 mA for approximately 1 h, and then stained for 1 h in Coomassie blue (stock solution: 44% Methanol, 11% Glacial Acetic Acid and 0.27 g/l Brilliant Blue R in H₂O); destaining was carried out for 45 min (stock solution: 7% Glacial Acetic Acid and 30% Methanol in H₂O) before being dried and if necessary set up for autoradiography in a light tight X-ray cassette. The molecular weights of proteins were estimated by calculating the distance migrated by each molecular weight marker as a proportion of the total electrophoresis distance (R_f value) and plotting this against the logarithm of its molecular weight.

2.13 Immunoblotting.

Cells grown in 100 mm diameter dishes were washed twice in PBS and harvested by scraping into PBS. SupT1 cells were harvested by centrifugation. The cells were centrifuged at 300 g for 5 min at 4°C and resuspended into 20 mM Tris-HCl lysis buffer, pH 8.0, containing 3% NP40, 20 mM Tris pH 8.0, 150 mM NaCl, 2 mM EDTA and protease inhibitors (1 mM PMSF and 10 µg/ml each of chymostatin, leupeptin, antipain and pepstatin) for 15 min on ice. The detergent insoluble material was removed by centrifuging at full speed (13 000 rpm) in a microfuge (Heraeus) for 20 min at 4°C. The supernatants were collected and the protein content in each lysate assayed using the BCA protein assay. The proteins were separated by non-reducing SDS-PAGE (as outlined above. Human CD4 immunoblotting requires non-reducing conditions), and transferred to a nitrocellulose membrane (Schleicher & Schuell) in Tris/Glycine buffer (20 mM Tris-Base, 150 mM Glycine and 20% Methanol) for 30 min at 1 A. The membrane was blocked in 10% dried skimmed milk powder (Marvel) in PBS containing 1% FCS and 0.1% Tween 20 (PMFT) overnight at 4°C with shaking, before the primary antibody was added for 1 h at room temperature (anti-CD4 mab was Q4120 used at 1.4 µg/ml diluted in PMFT). The membrane was washed 3 x 5 min with 0.1% Tween 20 in PBS (PBS-T) and incubated with the secondary antibody (anti-mouse-HRP used at 1:2500 in PMFT) for 1 h at room temperature. After extensive washing the HRP was developed using an enhanced chemiluminescence (ECL) detection system (Amersham International) as per the manufacturer's instructions.

2.14 Cell Fractionation.

Cells grown in 100 mm diameter dishes were cooled on ice for 10 min and washed twice in BM. The cells were labelled with 0.5 nM ¹²⁵I-Q4120 in BM for 2 h at 4°C with gentle shaking, and washed 3 times with BM at 4°C. Warm BM (37°C) plus or minus 100 ng/ml PMA was added to the cells for 1 or 2 h at 37°C, and in the last 5 min of this incubation the medium was replaced with fresh pre-warmed BM containing 5 mg/ml HRP in the presence or

absence of 100 ng/ml PMA. Cells were cooled quickly by washing twice with EM pH 3.00 at 4°C followed by 2 x 3 min in EM on ice, and reneutralized in BM by washing twice with BM and a 5 min incubation in BM on ice. The cells were washed twice with PBS at 4°C, gently scraped into 10 ml PBS and centrifuged at 300 g for 5 min at 4°C in a Beckman GS-6R. The cell pellet was washed once in 10 ml PBS at 4°C and the centrifugation step was repeated. Cells were gently resuspended into 1 ml homogenization buffer (10 mM Triethanolamine (TEA), 10 mM acetic acid, 1 mM EDTA, 0.25 M sucrose pH 7.40 - Harms *et al* 1980), and homogenized using 10 passes through a ball bearing homogenizer (Balch and Rothman 1985). with a clearance 15.1 µm. This routinely gave greater than 90% lysed cells with no visible nuclear damage, as assessed by light microscopy. The lysate was centrifuged at 1200 g for 10 min at 4°C, the supernatant collected, the pellet was washed in 1 ml homogenization buffer and was recentrifuged at 1200 g for 10 min at 4°C. The supernatants were pooled to give 2 ml of postnuclear supernatant (PNS) which was loaded onto one of 2 different gradient systems both of which are outlined below:

(i) 30% Percoll gradient - (modification of the gradient used by Marsh *et al* 1987). The PNS was made up to 9.671 ml with homogenization buffer and mixed with 3.215 ml isotonic percoll (made with 9 parts percoll and 1 part 10X homogenization buffer). This mixture was loaded into a 13.5 ml centrifuge tube containing a 0.614 ml 2.5 M sucrose cushion and the tube was heat sealed. The gradient was centrifuged at 20, 960 g for 30 min at 4°C in a near vertical rotor (NVT 65) in a Beckman ultracentrifuge, and fractionated from the bottom of the tube, collecting 10 drops per fraction.

(ii) 25-50% continuous sucrose gradient - (adapted from Brown and Farquhar 1987) 2 ml of PNS were loaded onto the top of a pre-formed 25-50% continuous sucrose gradient. This gradient was formed (in a 13.5 ml dome shaped centrifuge tube containing a 1 ml cushion of 10X homogenization buffer) using 5.1 ml 50% sucrose in homogenization buffer and 5.1 ml 25% sucrose in homogenization buffer using a gradient maker. The tube was heat sealed and the gradient centrifuged at 200, 000 g for 2 h 20 min

at 4°C in a near vertical rotor (NVT 65), and fractionated from the bottom of the tube, collecting 10 drops per fraction.

The fractions collected from the gradients were assayed for cpm per fraction (¹²⁵I-Q4120), β-Hexosaminidase and HRP activity (see enzyme assays), and density using a digital refractometer (ATAGO PR-1).

(iii) A third type of gradient (Gorvel *et al* 1991) was also tested to determine whether it could separate early and late endosomes. Cells (3 x 10⁸) grown in 100 mm diameter dishes were washed twice with BM at 37°C and labelled with 2 mg/ml HRP in BM for 10 min at 37°C. Cells were cooled quickly by washing 6 times with ice-cold BM followed by 4 washes with PBS at 4°C. The cells were carefully scraped into 10 ml ice-cold PBS and centrifuged at 300 g for 5 min at 4°C. The cell pellet was washed with 10 ml PBS at 4°C and the centrifugation repeated before the cells were resuspended into 0.5 ml homogenization buffer at 4°C. The cells were homogenized using 10 passes through the ball bearing homogenizer with a clearance of 15.1 μm, and centrifuged at 1200 g for 10 min at 4°C. The supernatant was collected; the pellet washed with 0.3 ml homogenization buffer, and re-centrifuged at 1200 g for 10 min at 4°C. The supernatants were pooled to make a 0.8 ml PNS. The PNS was adjusted to 40.6% sucrose using a 62% sucrose stock (final volume was 1.5 ml) and was loaded into an SW40 centrifuge tube. The PNS was overlaid with 2 steps of sucrose the first being 2 ml of 16% sucrose in D₂O (Deuterium oxide), and the second 2 ml of 10% sucrose in D₂O. Both sucrose steps contained 10 mM TEA and 10 mM acetic acid. These 2 sucrose steps were finally overlaid carefully with 0.5 ml homogenization buffer. The gradient was centrifuged at 154, 624 g in an SW40Ti rotor in a Beckman ultracentrifuge for 3 h 3 min at 4°C, and was fractionated from the bottom of the tube collecting 6 drops per fraction. β-Hexosaminidase and HRP activities in each fraction were assayed. Fractions were pooled in steps of 3 (i.e. fractions 1-3, 4-6 and so on) except fractions 16-20, which were all pooled. Non-reducing sample buffer was added to these pooled fractions, and they were separated on a 15% acrylamide gel. The proteins were transferred to nitrocellulose and immunoblotted for rab 7 (a late endosomal marker - Gorvel *et al* 1991).

2.15 Enzyme assays.

HRP assay: 40 μ l of each sample were pipetted in duplicate into a 96 well microtitre plate and 150 μ l of substrate (50 mM phosphate buffer pH 5.4, 0.08 mg/ml *o*-dianisidine (Sigma), 0.1% TX100 and 0.2% H_2O_2) added. The plate was incubated at room temperature until a brown colour developed and the assay was terminated by the addition of 10 μ l of 4% NaN_3 . The plate was read at 450 nm in a BioRad plate reader (Model 3550). The amount of HRP in each sample was determined by reference to an HRP standard curve which was incorporated into each assay.

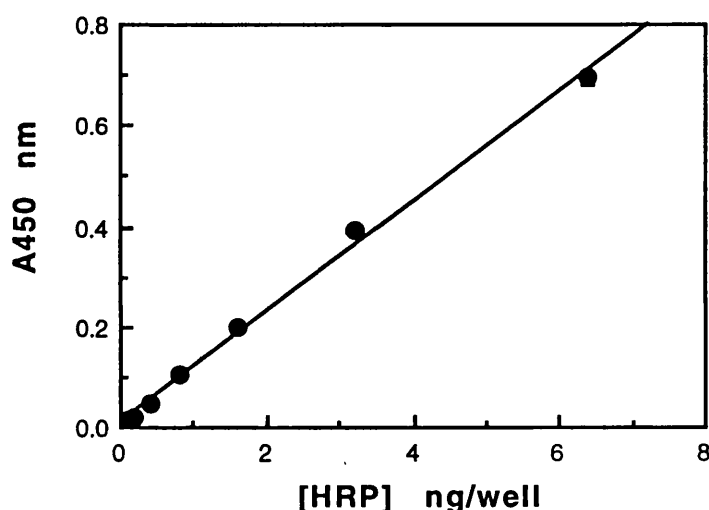


Figure 5. Horseradish peroxidase (HRP) standard curve. HRP standards were prepared from the 10 mg/ml HRP stock, and were assayed together with fractions from the gradients. HRP was quantitated at 450 nm.

β -Hexosaminidase assay: 20 μ l of each sample were pipetted in duplicate into a 96 well microtitre plate and 20 μ l of substrate (50 mM citrate buffer pH 4.8, 1.7 mg/ml *p*-nitrophenyl-N-acetyl- β -D-glucosaminide (Sigma) and 0.2% TX100) added. The plate was incubated at 37°C in the dark for 1 to 2 h before the addition of 200 μ l Glycine stop buffer (133 mM glycine, 83 mM Na_2CO_3 , 67 mM NaCl, pH 10.7) to produce a yellow colour. The plate was read at 405 nm in a BioRad plate reader (Model 3550).

2.16 Bicinchoninic Acid Protein (BCA) Assay.

10 μ l of each sample were pipetted in duplicate into a 96 well microtitre plate and 200 μ l of freshly prepared working reagent were added (50 parts reagent A and 1 part reagent B - Pierce and Warriner). The plate was incubated at 60°C for 30 to 60 min before cooling and reading at 562 nm in a BioRad plate reader (Model 3550). The amount of protein in each sample was determined by reference to a BSA standard curve which was incorporated into each assay.

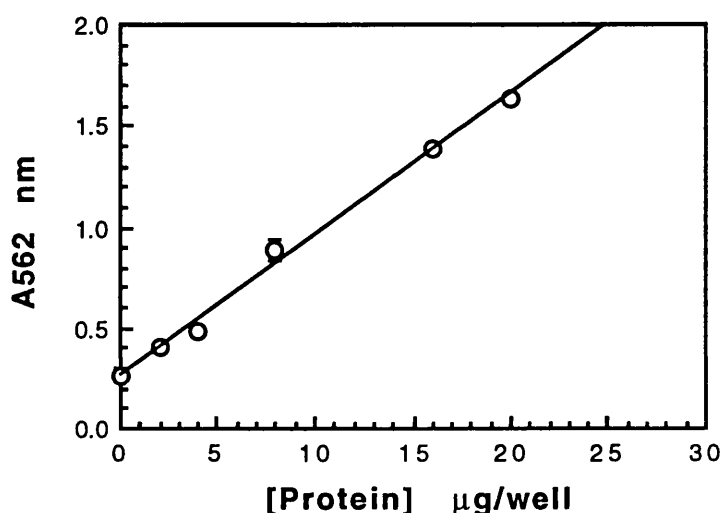


Figure 6. Bovine serum albumin (BSA) standard curve. A dilution series of a 2 mg/ml BSA standard was prepared and was assayed each time the BCA assay was used. The BSA standards were quantitated at 562 nm.

2.17 Cell Surface Iodination and PMA-Induced Down-Regulation.

This method was developed by Reid (1990 Ph.D. Thesis) and was a modification of the methods used by Bretscher and Lutter (1988) and Thompson *et al* (1987). SupT1 cells grown in suspension were washed twice in PBS by centrifugation (300 g for

5 min at 4°C). Cell pellets were resuspended into 50 µl 0.1 M Na₂HPO₄ and incubated on ice whilst the radiolabelling reagent was prepared.

Sulpho-SHPP was iodinated by the addition of 5 µg chloramine T to 80 mM sodium phosphate buffer, pH 7.0, containing 9.25 µg Sulpho-SHPP, 120 mM NaCl and 1.5 mCi ¹²⁵I in a final volume of 25 µl for 15 min on ice. The labelling reaction was terminated by the addition of 2 µl of 1 M sodium *p*-hydroxybenzoate containing 0.1 M NaI (this converts the unwanted reactive species into derivatives of hydroxybenzoate and destroys any excess chloramine T). The cells were resuspended into a fresh 50 µl aliquot of 0.1 M Na₂HPO₄ before being added to the ¹²⁵I-Sulpho-SHPP reagent for 20 min on ice. The cells were washed by centrifugation 3 times in PBS/10% FCS changing the centrifuge tube between each wash to try to reduce the amount of free ¹²⁵I. The cells were resuspended in BM up to 700 µl at 4°C, and 100 µl aliquots were warmed to 37°C in BM in the presence or absence of 100 ng/ml PMA for times up to 8 h. Cells were cooled with 9 ml cold BM, washed once with BM and twice with PBS at 4°C. The cells were lysed in 200 µl 20 mM Tris-HCl lysis buffer, pH 8.0, containing 3% NP40, 150 mM NaCl, 2 mM EDTA and protease inhibitors (1 mM PMSF and 10 µg/ml each of chymostatin, leupeptin, antipain and pepstatin) for 15 min on ice. The detergent insoluble material was removed by centrifuging at full speed (13 000 rpm) in a microfuge (Heraeus) for 20 min at 4°C. The supernatants were collected and centrifuged at 100, 000 g in a TLA 45 rotor in a Beckman tabletop ultracentrifuge for 30 min at 4°C. The supernatants were carefully collected and added to 25 µl prewashed protein A sepharose beads for 2 h at 4°C with gentle mixing. The samples were briefly centrifuged (20 sec in Heraeus microfuge) to pellet the protein A sepharose beads. The supernatants were carefully removed and the protein concentration in each lysate was determined using the BCA protein assay. Aliquots were removed from each lysate (containing equal amounts of protein) and added to 20 µl prewashed anti-CD4 conjugated protein A sepharose beads overnight at 4°C with gentle mixing. The beads were washed 3 times with TBS/0.5% TX100 and once with TBS to reduced the

detergent content of the samples. Each pellet of beads was resuspended into 1 x sample buffer containing 10 mg/ml dithiothreitol and heated to 95°C for 5 min. The samples were loaded onto 10% acrylamide gels which were run at 20 mA for approximately 1 h. The gels were stained, destained, dried and autoradiographed at -80°C.

2.18 Detection Of Cell Surface CD4 After PMA Treatment In The Presence of Staurosporine.

Cells grown for 3 days in 16 mm diameter wells were washed twice with BM, pH7.40, at 37°C. BM was added to the cells containing either no drugs, or a range of concentrations of Staurosporine (Stsp), 0.1 μ M, 0.5 μ M or 1.0 μ M at 37°C for 30 min. PMA was added to each of the wells except control wells (no drugs, or PMA only as the positive control) to a final concentration of 100 ng/ml for 1 hour at 37°C. All the cells were cooled quickly by washing twice with BM at 4°C, and were labelled with 0.3 nM 125 I-Q4120 for 2 hours at 4°C with shaking to detect the cell surface levels of CD4. Unbound ligand was removed with 4 changes of BM and 2 changes of PBS at 4°C, and the cells were harvested in 400 μ l of 0.2 M NaOH. The wells were rinsed with 400 μ l of H₂O which was pooled with the respective lysate and the samples were counted in the gamma counter.

2.19 Detection Of Cell Surface CD4 And CD4^{cyt} Following Treatment Of Cells With Staurosporine and Okadaic Acid.

(a) Staurosporine experiment

Cells grown for 2 days in 16 mm diameter wells were cooled on ice for 10 min and washed twice in BM pH7.40 at 4°C. The cells were pretreated with 0.5 μ M Staurosporine (Stsp) in BM for 30 min on ice, before replacing this medium with warm BM containing 0.5 μ M Stsp at 37 °C for 0, 5, 10, 30, and 60 min. The cells were rapidly cooled by washing three times with BM at 4°C, and the cell surface CD4 was detected by binding 0.49 nM 125 I-Q4120 in BM (0.5 ml per well) for 2 hours at 4°C with gentle

shaking. Unbound ligand was removed with 2 changes of BM and 2 changes of PBS at 4°C. The cells were checked under the light microscope to ensure that the Stsp had not had any gross effects on cell morphology before being harvested in 400 µl 0.2 M NaOH. Each well was rinsed with 400 µl H₂O which was then pooled with the respective lysate to yield a final volume of 800 µl. The lysates were counted in the gamma counter.

(b) Okadaic Acid experiment

Cells grown for 2 days in 16 mm diameter wells were washed twice with BM pH 7.40 at 37°C, and added 300 µl of BM at 37°C containing 1.25 µM okadaic acid (OKA) for 0, 20, and 60 min for the HeLa-CD4 cells and 0, 15, 30 and 60 min for the HeLa-CD4^{cyt}-cells. The 0 min time point in each cell line was incubated in BM at 37°C for 60 min in the absence of any drug. The cells were washed three times with BM at 4°C and cell surface CD4 was detected by adding 0.49 nM ¹²⁵I-Q4120 in BM (0.5 ml per well) for 2 hours at 4°C with gentle shaking. Unbound ligand was removed with 2 changes of BM and 2 changes of PBS at 4°C. The cells were checked under the light microscope to ensure that the OKA had not had any gross effects on cell morphology before being harvested in 400 µl 0.2 M NaOH. Each well was rinsed with 400 µl H₂O which was then pooled with the respective lysate to yield a final volume of 800 µl. The lysates were counted in the gamma counter.

2.20 Endocytosis Kinetics Of CD4 and CD4^{cyt}- In The Presence Of Staurosporine And Okadaic Acid.

Cells grown for 2 days in 16 mm diameter wells were cooled on ice for 10 min and washed twice with BM pH7.40 at 4°C. The cell surface CD4 was labelled with 0.3 nM ¹²⁵I-Q4120 in BM for 2 hours at 4°C with gentle shaking. In the last 30 min of this incubation time, cells for the Stsp experiment were pretreated with 0.5 µM Stsp; the medium for all subsequent washes for these particular cells contained 0.5 µM Stsp. Excess ligand was washed away with 3 changes of BM at 4°C, and BM was added at 37°C

containing either 1.25 μ M OKA, 0.5 μ M Stsp or no drug for 0, 5, 10, 20, 30 and 60 min with gentle shaking. The cells were cooled rapidly by washing twice with BM at 4°C, some of the cells were acid stripped by quickly washing twice with cold EM, pH3.00, followed by 2 x 3 min in EM at 4°C to reveal the acid resistant counts, and the remaining cells were washed twice with PBS at 4°C and harvested directly in 400 μ l 0.2 M NaOH. The acid stripped cells were washed twice in PBS at 4°C and harvested in 400 μ l 0.2 M NaOH. All wells were washed once with 400 μ l H₂O which was pooled with the respective lysate and the samples were counted in the gamma counter.

2.21 Fluid Phase Endocytosis In HeLa-CD4 Cells In The Presence Of Staurosporine And Okadaic Acid.

Cells grown for 2 days in 30 mm diameter tissue culture dishes were washed twice in BM, pH7.40, at 37°C. Cells for the Stsp assay were cooled on ice for 10 min and were pretreated with 0.5 μ M Stsp in BM at 4°C for 30 min. Added 0.55 ml of 5 mg/ml HRP in BM containing either 1.25 μ M OKA, 0.5 μ M Stsp or no drug per dish for, 0 (30 min on ice in BM containing 5 mg/ml HRP), 5, 10, 20, 40, 60 and 120 min at 37°C with gentle shaking (For the OKA assay the 120 min time point was omitted as toxic events on the cells by the OKA are noticeable after this time). The cells were washed six times with BM at 4°C followed by four times with PBS, also at 4°C. Each plate of cells was scraped in 1 ml of PBS at 4°C and centrifuged at 300 g for 5 min at 4°C. The subsequent cell pellets were each resuspended in 0.5 ml 0.1% TX100 in PBS to lyse the cells and incubated on ice for 15 min. The levels of HRP in the lysates were immediately assayed using o-dianisidine as a substrate (see section 2.15), and the cellular protein per lysate was quantified using the BCA protein assay.

2.21 Fluid Phase Endocytosis In HeLa-CD4 Cells In The Presence Of Staurosporine And CGP41/251.

Cells grown for 2 days in 30 mm diameter tissue culture dishes were cooled on ice for 10 min and washed twice in BM, pH7.40, at

4°C. Added BM at 4°C containing either 0.5 μ M Stsp, 0.5 μ M CGP 41/251 or no drug for 30 min with gentle shaking. The medium was replaced with 5mg/ml HRP in BM containing either 0.5 μ M Stsp, 0.5 μ M CGP 41/251 or no drug for 0 (30 min on ice in BM containing 5 mg/ml HRP), 5, 10, 20, 30 and 60 min at 37°C with gentle shaking. The cells were washed six times with BM at 4°C followed by four times with PBS, also at 4°C. Each plate of cells was scraped in 1 ml of PBS at 4°C and centrifuged at 300 g for 5 min at 4°C. The subsequent cell pellets were each resuspended in 0.5 ml 0.1% TX100 in PBS to lyse the cells and incubated on ice for 15 min. The levels of HRP in the lysates were immediately assayed using o-dianisidine as a substrate, and the cellular protein per lysate was quantified using the BCA protein assay.

3. RESULTS

3.1 DOWN-REGULATION OF CELL SURFACE CD4 OCCURS BY ENDOCYTOSIS THROUGH COATED PITS.

3.1.1 *PMA Induces CD4 Down-regulation.*

The control of cell surface CD4 is an important feature in T cell function, and under certain physiological conditions, the expression of CD4 at the plasma membrane is modulated. For example, CD4 is down-regulated from the cell surface of T cells following antigenic stimulation (Acres *et al* 1986; Weyand *et al* 1987; Rivas *et al* 1988). The modulation of CD4 in response to activation of T cells with specific antigen can be mimicked using phorbol esters (Acres *et al* 1986; Hoxie *et al* 1986; Clapham *et al* 1987; Wang *et al* 1987; Blue *et al* 1989; Moller *et al* 1990), which are known to activate protein kinase C (PKC; Castagna *et al* 1982). Figure 7 illustrates how cell surface CD4 levels are affected by phorbol myristic acid (PMA), on a T lymphoma-derived cell line, SupT1. Cell surface CD4 was reduced rapidly following the addition of PMA, with levels falling by 50% in 30 min and by >80% after 4-6 h (data kindly supplied by A. Pelchen-Matthews).

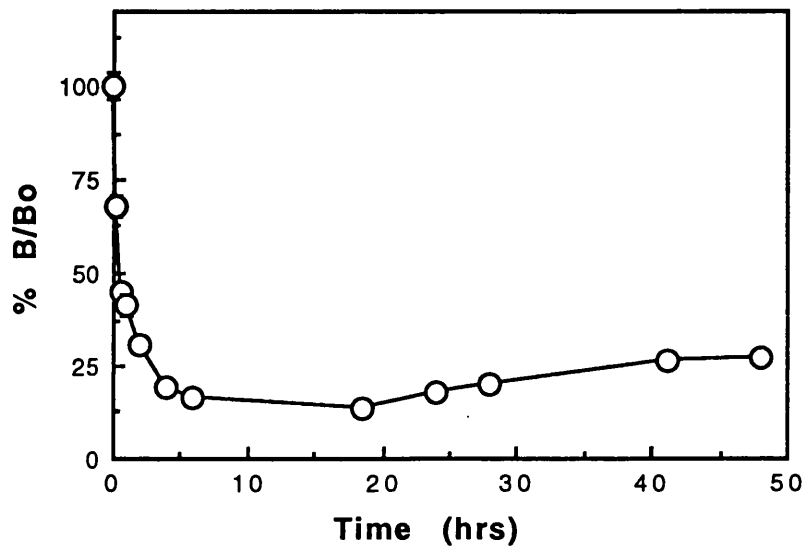


Figure 7. PMA-induced down-regulation of CD4 in SupT1 cells. Cells were treated with BM containing 100 ng/ml PMA for times up to 48 h at 37°C. After cooling the cells to 4°C, and washing, cell surface CD4 was determined using an iodinated anti-CD4 mab, Q4120, at sub-saturating concentrations (0.3nM). The plot shows binding of ^{125}I -Q4120 compared to untreated cells (B/Bo) after correction for cellular protein content.

The aim of this study is to establish the cellular mechanisms of CD4 down-regulation. In T cells and lymphoma/leukaemia derived T cell lines, such as SupT1, CD4 is associated with the lymphocyte specific *src*-related non-receptor tyrosine kinase, p56^{lck} (Rudd *et al* 1988; Veillette *et al* 1988). This interaction prevents CD4 endocytosis and restricts the molecule to the cell surface (Pelchen-Matthews *et al* 1992). Phorbol esters can modulate CD4 expression on p56^{lck}-negative CD4 expressing cells (Maddon *et al* 1988; Shin *et al* 1990; 1991; Pelchen-Matthews *et al* 1993), suggesting that in part at least, down-regulation is independent of p56^{lck}. To examine the mechanism of down-regulation in the absence of p56^{lck} non-lymphoid HeLa cells, stably transfected with the human CD4 cDNA were used (Maddon *et al* 1988).

Initially it was important to establish the concentration of PMA required for CD4 modulation. This was determined by treating HeLa-CD4 cells for 1 h with varying concentrations of PMA, then quantitating the level of cell surface CD4 using ¹²⁵I-Q4120 (Figure 8). Maximum down-regulation (~80%) was observed at a concentration of 100 ng/ml which is similar to that previously reported for peripheral blood lymphocytes (Bigby *et al* 1990; Moller *et al* 1990). Higher concentrations of PMA did not induce more CD4 down-regulation, and no modulation of CD4 was seen with 4 α -phorbol, a phorbol derivative, which does not activate PKC (Castagna *et al* 1982).

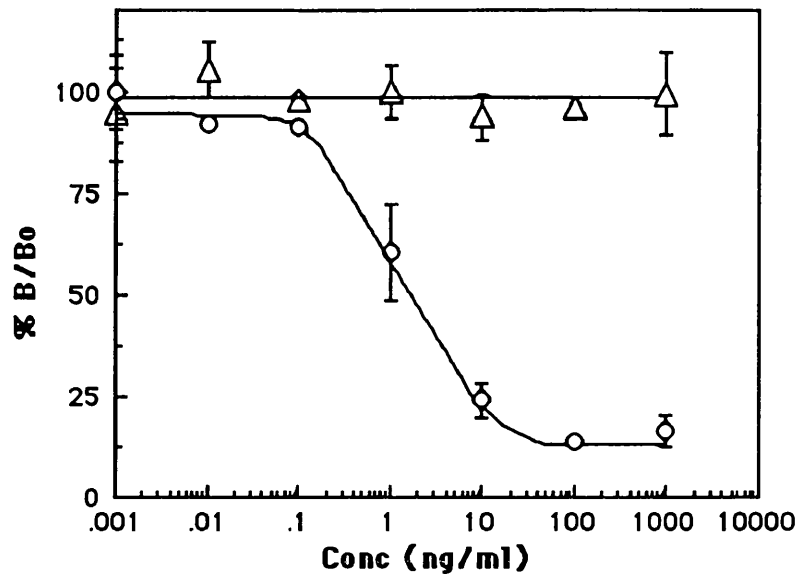


Figure 8. The concentration dependence of PMA-induced CD4 down-regulation in HeLa-CD4 cells. HeLa-CD4 cells grown in 16 mm wells were treated at 37°C in BM containing various concentrations of either PMA (open circles) or 4 α-phorbol (open triangles). After 1 h, the cells were cooled and the cell surface CD4 was quantitated using 0.3 nM ^{125}I -Q4120. The plot shows binding of ^{125}I -Q4120 compared to untreated cells (B/Bo) after correction for cell protein.

To determine the time course of down-regulation, HeLa-CD4 cells were exposed to 100 ng/ml PMA for times up to 6 h at 37°C, and, cell surface CD4 was detected using ¹²⁵I-Q4120. Nearly 75% of cell surface CD4 was rapidly lost within 30 min following the addition of PMA (Figure 9, A and B), and the levels of cell surface CD4 remained low (25-40% of that on non-PMA treated cells) for 3 h before beginning to recover. The recovery of cell surface CD4 may be due to down-regulation of protein kinase C (Collins *et al* 1982; Young *et al* 1987), and effects of PMA on CD4 transcription and translation (Neudorf *et al* 1991), as medium containing 100 ng/ml PMA removed from cells after 24 h treatment, can induce CD4 modulation when added to fresh HeLa-CD4 cells (A. Pelchen-Matthews, unpublished results). No down-regulation of CD4 was seen when the cells were held at 4°C in the presence of PMA, and modulation was slowed at 18°C but did reach the levels of down-regulation observed at 37°C (Figure 9, B).

Down-regulation was dependent on the presence of the CD4 cytoplasmic domain, as no modulation was observed in HeLa cells transfected with a mutant CD4 lacking the cytoplasmic domain (CD4^{cyt-}). In addition, little modulation was seen with a CD4 mutant in which the cytoplasmic serine residue 408 had been mutated to alanine (CD4^{S408A}). CD4^{S408A} cell surface levels decreased only 25% compared to control cells upon the addition of PMA (Figure 9, A).

These experiments demonstrate that phorbol esters rapidly modulate cell surface CD4 levels at a concentration of 100 ng/ml, and in keeping with published data, show that CD4 can be down-regulated from the plasma membrane of both non-lymphoid and lymphoid cells. This indicates that CD4 modulation is not T cell specific, nor does it require the presence of p56^{lck}.

As p56^{lck} interacts with CD4 and regulates the endocytic properties of CD4 (Pelchen-Matthews *et al* 1992), the HeLa cells stably expressing human CD4 were used to investigate the mechanisms of cell surface CD4 modulation following the addition of phorbol ester.

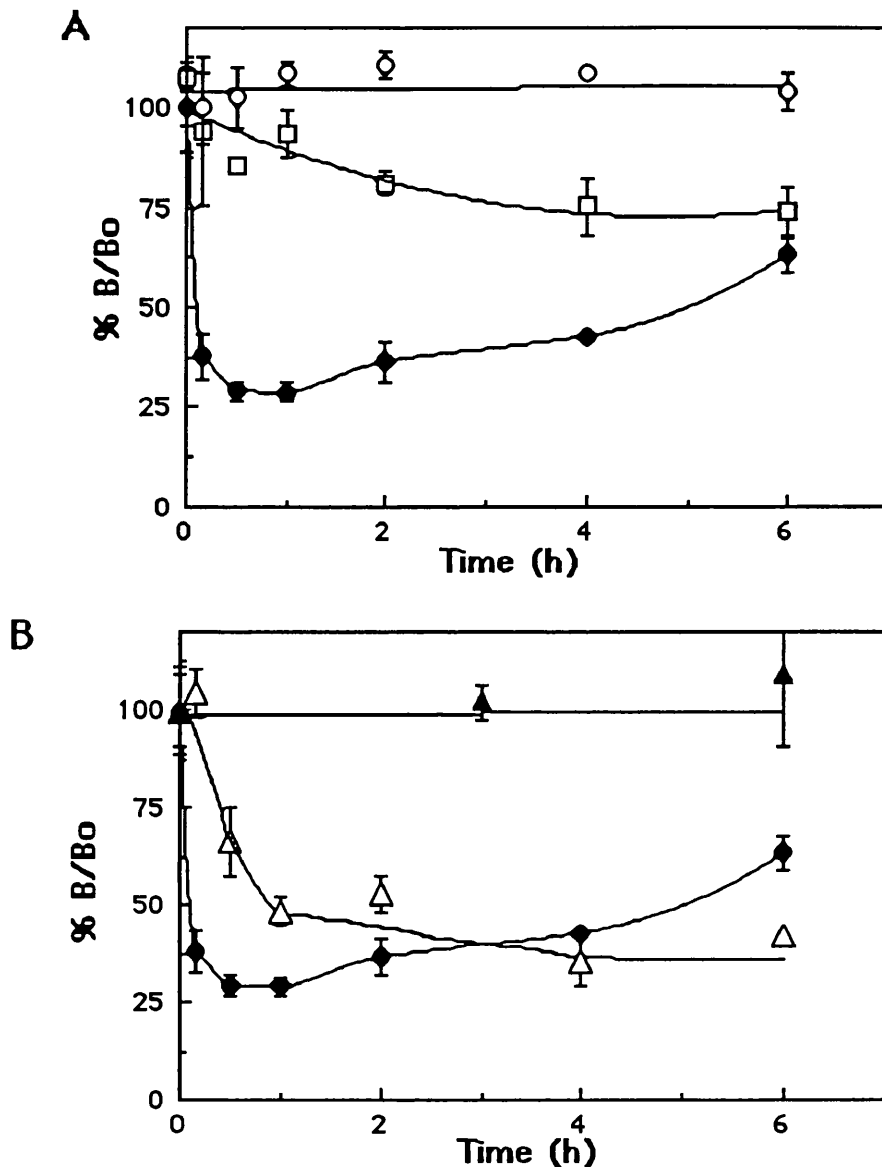


Figure 9. CD4 down-regulation time courses. HeLa-CD4 (filled circles), HeLa-CD4^{cyt} (open circles), and HeLa-CD4^{S408A} (open squares) cells were treated for various times with BM containing 100 ng/ml PMA at 37°C (A). HeLa-CD4 cells were treated with BM containing 100 ng/ml PMA at 0°C (filled triangles), 18°C (open triangles), or 37°C (filled circles) for various times (B). Following exposure to PMA the cells were cooled, and the levels of CD4 remaining at the cell surface detected using 0.3 nM ¹²⁵I-Q4120. The plots show binding of ¹²⁵I-Q4120 compared to untreated cells (B/Bo) after correction for cell protein.

3.1.2 *The Effect Of PMA On The Endocytosis Kinetics Of CD4.*

Results previously published from this laboratory demonstrate that CD4 expressed in HeLa and NIH3T3 cells, is constitutively endocytosed through coated pits, delivered to early endosomes and recycled to the plasma membrane (Pelchen-Matthews *et al* 1989; 1991; Marsh *et al* 1990). In order to determine how PMA affected this constitutive endocytosis, HeLa-CD4 cells were labelled at 4°C with ^{125}I -Q4120, washed, and warmed to 37°C for various times in the presence or absence of 100 ng/ml PMA (Figure 11).

The amount of endocytosed ^{125}I -Q4120/CD4 complexes were detected by acid stripping as outlined in the Materials and Methods (see Figure 10 for acid stripping efficiency). After a brief lag of 2 min, the rate of CD4 endocytosis increased 3 fold in the presence of PMA (from 2.4% per min to 8% per min). In addition, the intracellular steady state levels of CD4 at 60 min were doubled (from ~40-50% to ~80-90%) in the presence of PMA.

TCA precipitation of medium collected from the cells after incubation at 37°C warming, indicated that amount of TCA soluble ^{125}I (i.e. degraded ^{125}I -Q4120), only appeared to increase significantly in cells treated with PMA for 2 h (Figure 12). These longer incubation times may not reflect the fate of CD4 itself, as there could be dissociation of the ^{125}I -Q4120/CD4 complexes, especially in view of the fact that these complexes will have been trafficking through acidic organelles. These data demonstrate that PMA enhances the rate of CD4 endocytosis 3 fold, and doubles the amount of intracellular CD4 at steady state.

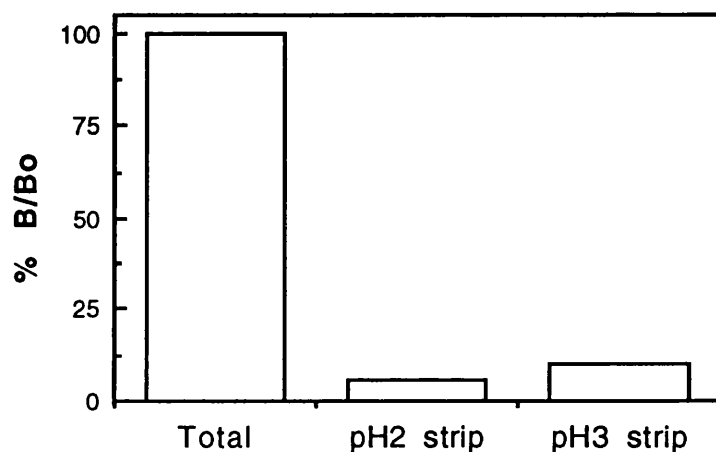


Figure 10. The acid stripping efficiencies at pH3.00 and pH2.00 at 4°C. HeLa-CD4 cells in 16 mm diameter wells were labelled with 0.3 nM ^{125}I -Q4120, then quickly washed twice with either pH2 or pH3 medium followed by 2 x 3 min in either stripping medium. The cells were harvested in 0.4 ml 0.2 M NaOH, the wells washed with 0.4 ml H₂O, and this wash was pooled with the respective lysate, and the lysates counted in the gamma counter. The plot shows binding of ^{125}I -Q4120 compared to untreated cells (B/Bo) after correction for cellular protein content.

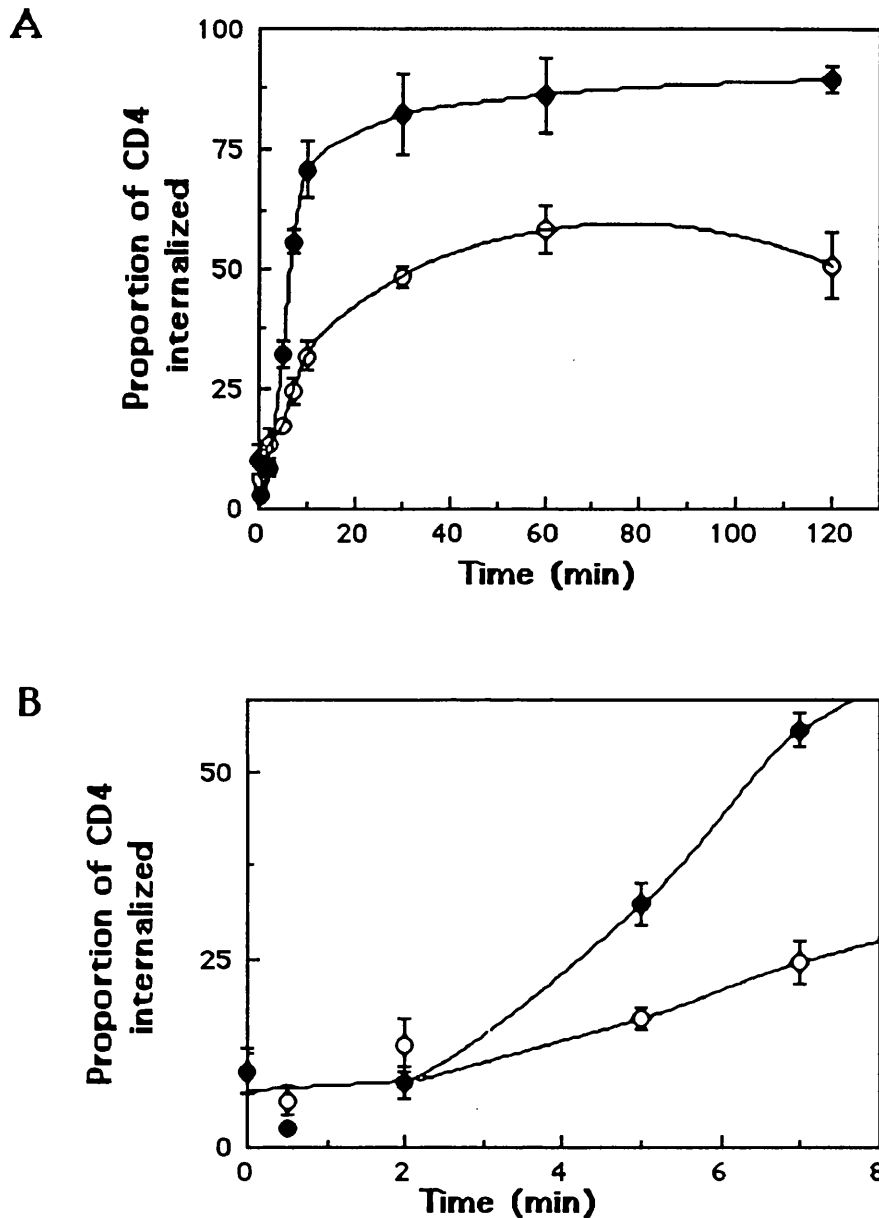


Figure 11. The effect of PMA on the endocytosis of CD4 in HeLa-CD4 cells. HeLa-CD4 cells were prelabelled with ^{125}I -Q4120 and treated for various times at 37°C in the presence (closed circles) or absence (open circles) of 100 ng/ml PMA. The plots show the ratios of acid resistant ^{125}I -Q4120 to the total cell-associated label. Panel B is an expansion of the initial portion of the graph in panel A.

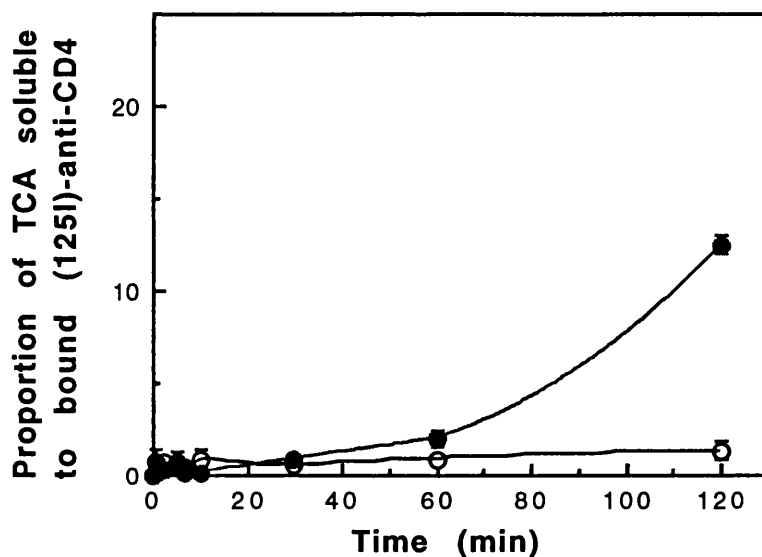


Figure 12. TCA precipitation of the medium from the time points in the endocytosis assay. The medium from the endocytosis assay was recovered after each incubation time, and TCA was added to a final concentration of 13% for 90 min at 4°C. Supernatants and precipitates were recovered and counted. The plot shows the proportion of TCA soluble counts to total amount of ^{125}I -anti-CD4 bound to the cells, in the presence (closed circles) or absence (open circles) of 100 ng/ml PMA.

3.1.3 *The Specificity Of The Effect Of PMA On CD4 Endocytosis.*

The enhanced uptake of CD4 in the presence of phorbol ester could be due to an increase in the association of CD4 with coated vesicles, or an increase in the number of vesicles. Vesicle formation at the cell surface can be measured either by bulk flow uptake of membrane components, or by the endocytosis of fluid-phase markers (Griffiths *et al* 1989; Pelchen-Matthews *et al* 1991). Previous work has demonstrated that the cytoplasmic domain of CD4 is required for phorbol ester-induced modulation (Bedinger *et al* 1988; Maddon *et al* 1988; Shin *et al* 1990; Figure 9), and published work from this laboratory has indicated that CD4^{cyt}-molecules are internalized by bulk flow transport through coated pits in HeLa and lymphoid cells (Pelchen-Matthews *et al* 1991). In order to determine whether PMA caused a general stimulation of bulk flow endocytosis in HeLa cells, as described in other cell systems, such as macrophages (Swanson *et al* 1985), the effect of PMA on internalization in HeLa cells was investigated. Results recently published from our laboratory indicate that PMA had no effect on the endocytosis rate of CD4^{cyt}-molecules (Pelchen-Matthews *et al* 1993).

Additional experiments, using fluid phase markers, horseradish peroxidase (HRP) and lucifer yellow (LY), were performed to determine whether PMA had any effect on vesicular trafficking in this system. HeLa-CD4 cells were incubated in either 5 mg/ml HRP or 1 mg/ml LY in the presence or absence of 100 ng/ml PMA for various times at 37°C. The cells were cooled, washed and cell lysates prepared for each time point. The levels of HRP, LY and cell protein were assayed for each lysate (Figure 13). With HRP the initial rate of fluid uptake was unaffected by phorbol ester (Figure 13, A). However, by 120 min the volume of accumulated intracellular marker was ~25% higher in PMA treated cells. Similar results were obtained with LY (Figure 13, B), however, the volume of fluid uptake appeared to be slightly less than that observed with HRP. This discrepancy may be due to the fact that HRP and LY levels were quantitated using two different types of assays.

The similar rates of fluid uptake in the presence and absence of PMA over the initial 30 min of the assays together with the finding that CD4^{cyt}- endocytosis is not affected by PMA (Pelchen-Matthews *et al* 1993), suggests that vesicle formation is unaffected by the addition of phorbol ester in these cells. However, the increase in fluid-phase marker after 120 min in the presence of PMA may be due to changes in the dimensions of the endosomal compartment

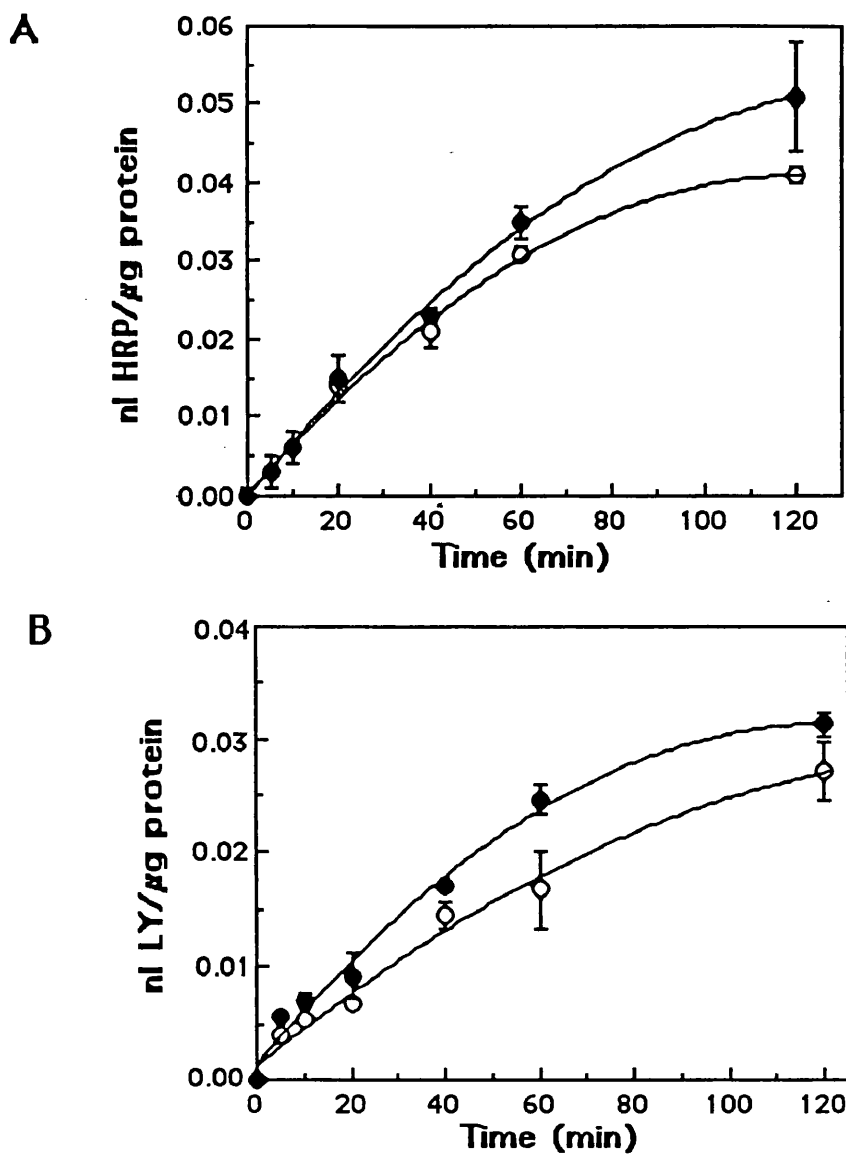


Figure 13. The effect of PMA on fluid endocytosis in HeLa-CD4 cells. Medium containing 5 mg/ml horseradish peroxidase (A), or 1 mg/ml lucifer yellow (B), was added to HeLa-CD4 cells in the presence (closed circles), or absence (open circles), of 100 ng/ml PMA for various times at 37°C. The volume of fluid uptake was determined by comparison with horseradish peroxidase or lucifer yellow standards after correction for cellular protein content.

3.1.4 PMA Enhances CD4 Endocytosis Through Coated Pits.

As previously mentioned, CD4 is constitutively endocytosed through coated pits in HeLa cells (Pelchen-Matthews *et al* 1991), suggesting that the cytoplasmic domain of CD4 possesses sequences which allow it to cluster within these specialized regions of the plasma membrane. The finding that PMA increases the rate of CD4 internalization without causing significant changes in endocytosis suggests that PMA increases the uptake of CD4 through coated pits. To address this issue two approaches were taken: (1) if uptake through the clathrin-coated pit pathway is inhibited, it would be possible to look to see whether PMA still causes CD4 modulation; and, (2) the association of CD4 with coated pits and vesicles in the presence of PMA can be directly analysed using gold immunolabelling electron microscopy.

Hypertonic medium has previously been used to inhibit the formation of clathrin-coated vesicles (Heuser and Anderson 1989). Medium containing 0.45 M sucrose and adjusted to pH 5.7 was used to inhibit endocytosis in the HeLa-CD4 cells (slight acidification of the medium improved the long term viability of the cells - Pelchen-Matthews and Marsh manuscript in preparation; Pelchen-Matthews *et al* 1993). Three day old HeLa-CD4 cells were preincubated in medium in the presence or absence of 0.45 M sucrose at pH 5.7 for 5 min at 37°C, before fresh medium was added, containing 100 ng/ml PMA in the presence or absence of 0.45 M sucrose at pH 5.7 for 1 h at 37°C. The levels of cell surface CD4 were detected using ¹²⁵I-Q4120 (Figure 14). Cells that were treated with PMA in the presence of the hypertonic medium at pH 5.7 showed only 10% down-regulation of the cell surface CD4, compared to the control cells treated with PMA alone which showed 70% modulation.

This experiment suggested that PMA-induced CD4 down-regulation involves uptake through clathrin-coated pits and vesicles. The second approach which was used to confirm this suggestion was gold immunolabelling electron microscopy.

To assess CD4 interaction with coated pits directly gold immunolabelling electron microscopy (EM) was used. HeLa-CD4

cells were labelled on ice with 8 nM Leu3a (an anti-CD4 mab) for 2 h, followed by 9 nm protein A-gold for 2 h at 4°C. A control for specific labelling was included, and this was cells labelled with medium for 2 h (no antibody), followed by the 9 nm protein A-gold for 2 h at 4°C. Previous control experiments have demonstrated that this particular gold probe had no effect on the endocytosis kinetics of CD4, as detected using ¹²⁵I-Leu3a (Pelchen-Matthews *et al* 1991; Marsh *et al* 1990; Marsh *et al* 1993). The cells, except for the 0 min time point which was immediately processed, were warmed to 37°C in the presence or absence of 100 ng/ml PMA, for short periods of time, quickly cooled and processed for EM (see Materials and Methods). Ultrathin sections were analysed under the EM, and for the quantitation, were systematically examined, noting the position of each gold particle encountered. In cells treated with PMA, gold particles were visualized at the plasma membrane, intracellularly and juxtaposed to coated regions of the plasma membrane (Figure 15).

Table 2 shows the distribution of gold in both PMA-treated and untreated cells. In the absence of PMA, 4.0-5.5% of the gold particles counted, were found to be within coated regions of the plasma membrane, in agreement with a previous study (Pelchen-Matthews *et al* 1991). However, in the presence of PMA, there was a transient increase in the amount of gold particles associated with coated pits and vesicles with increasing time, peaking at greater than 10% of all the gold counted. When these results were calculated as a proportion of the gold particles at the plasma membrane, the peak of gold associated with coated structures at 2 min was 12% (Figure 16). This peak represented about a 3 fold increase in CD4 associated with coated pits and vesicles, above the level of coated pit associated CD4 observed in untreated cells.

To ensure that PMA had not increased the number of coated pits or vesicles, the proportion of coated membrane to total plasma membrane was analysed in the presence and absence of PMA. This morphometric analysis indicated that there was no difference in the amount of coated membrane at 2 min in the presence of PMA, compared to control cells at the same time point (Table 3). A student t test of the proportion of coated membrane in the presence and absence of PMA from each image analysed indicated

that, the probability of the small difference in the proportions of coated plasma membrane in the presence and absence of PMA, being due to chance is greater than 0.5, which is not significant. Given the estimated life time of a coated pit at the cell surface (1-2 min - Anderson *et al* 1977; Marsh and Helenius 1980; Griffiths *et al* 1989), a 3 fold increase in the association of CD4 with coated pits can fully account for the enhanced CD4 endocytosis kinetics induced by PMA. Furthermore, the peak of coated pit-associated CD4 was observed to coincide with the onset of rapid PMA-induced internalization in the biochemical assay (Figure 11). Thus the lag phase in PMA-induced CD4 endocytosis may result from the time required to activate PKC, phosphorylate CD4, and recruit CD4 into coated pits.

This set of experiments demonstrate that CD4 down-regulation is not T cell specific and does not require the presence of p56^{lck}. In addition, they show that phorbol esters do not stimulate endocytosis in the HeLa cell system, but induce an increase in CD4 association with coated pits, enhancing its internalization kinetics, and doubling the intracellular pool at steady state.

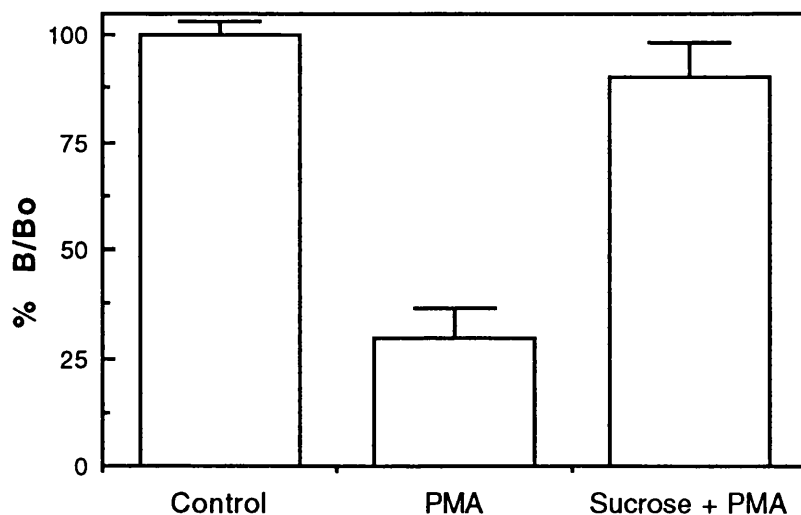


Figure 14. The effect of hypertonic medium on CD4 down-regulation in HeLa-CD4 cells. Cells were warmed at 37°C in medium in the presence or absence of PMA and hypertonic medium, and the levels of CD4 remaining at the cell surface were detected with ¹²⁵I-Q4120. The plot shows binding of ¹²⁵I-Q4120 compared to untreated cells (B/Bo) after correction for cell protein.

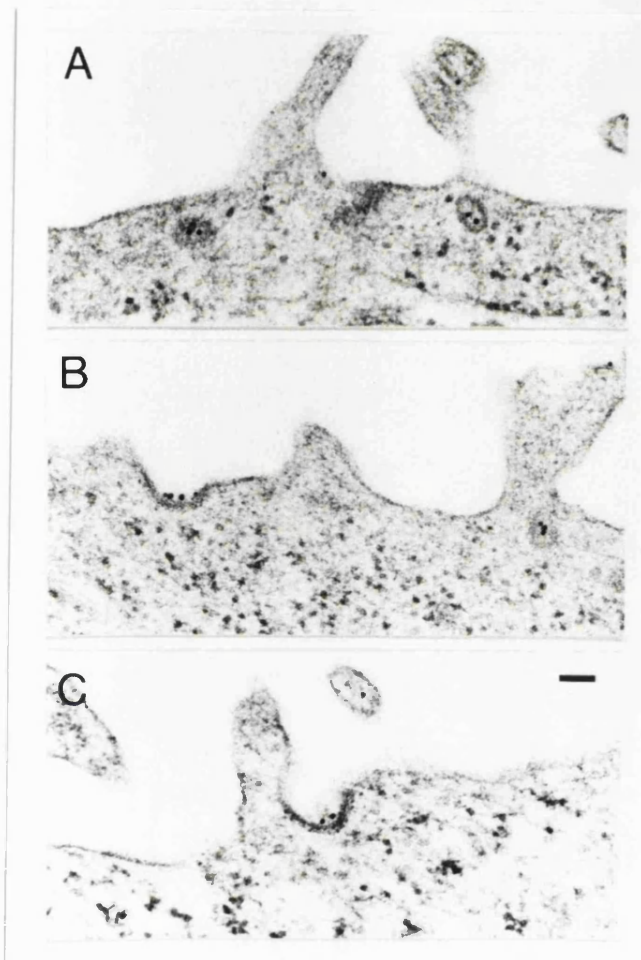


Figure 15. Electron microscopic localization of CD4 in HeLa-CD4 cells treated with PMA. HeLa-CD4 cells were labelled on ice with 8 nM Leu3a followed by 9 nm protein A-gold, washed and warmed to 37°C in the presence of 100 ng/ml PMA for 2 min (A and B), and 3 min (C). Gold particles can be seen associated with coated pits and profiles which maybe either pits or vesicles. Scale bar, 100 nm.

Table 2. Effect of PMA on the distribution of gold-labelled CD4 on HeLa-CD4 cells

Time at 37°C	Total no. of particles counted	Particles over non-coated plasma membrane		Particles over coated pits and vesicles*		Internalized Particles		Unclassified
		%		%		%		
A: Control								
0	511	475	(93.0)	21	(4.1)	0	(0.0)	15
1 min	349	310	(88.8)	18	(5.2)	18	(5.2)	3
2 min	346	314	(90.8)	18	(5.2)	10	(2.9)	4
3 min	416	330	(79.3)	23	(5.5)	56	(13.5)	7
4 min	316	252	(79.7)	8	(2.5)	48	(15.2)	8
B: + PMA								
1 min	378	325	(86.0)	27	(7.1)	25	(6.6)	1
2 min	329	253	(76.9)	34	(10.3)	29	(8.8)	13
3 min	372	275	(73.9)	33	(8.9)	52	(14.0)	12
4 min	289	185	(64.0)	15	(5.2)	82	(28.4)	7

Distributions of Leu3a/protein A-gold particles were analyzed as detailed in the text and in Pelchen-Matthews *et al* 1991.

* Only particles observed immediately juxtaposed to the clathrin coat were counted in this category.

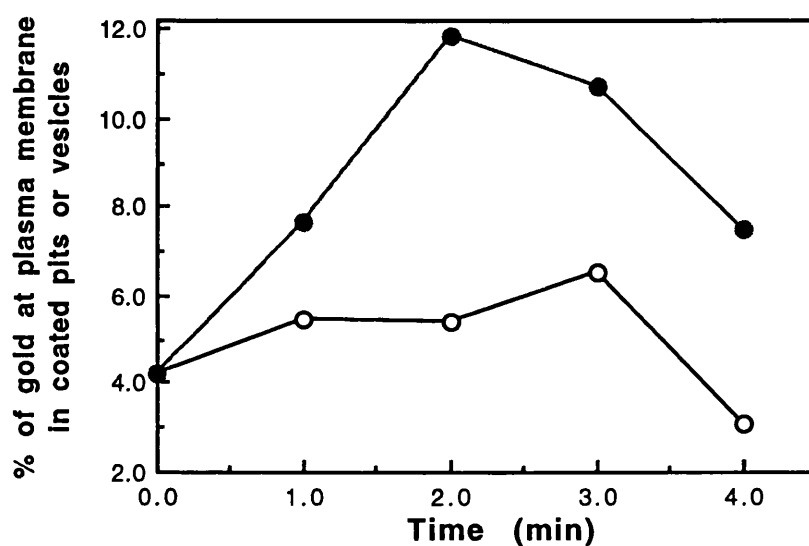


Figure 16. Graphical representation of the tabulated data in Table 2. The amount of gold in coated structures was plotted as a ratio of the total gold counted at the cell surface in the presence (closed circles) or absence (open circles) of 100 ng/ml PMA.

Table 3. Effect of PMA on the proportion of coated plasma membrane in HeLa-CD4 cells.

Time at 37°C	Total No. of intersects	Total No. of coated membrane intersects	Total No. of non-coated membrane intersects*	Proportion of coated plasma membrane (%)
A: Control 2 min	5999	104 ± 2	5895	1.73 ± 0.03
B: Plus PMA 2 min	7714	129 ± 3	7585	1.67 ± 0.04

*Coated vesicles were counted only when they were close to the plasma membrane

3.1.5 THE SIGNALS INVOLVED IN THE ENDOCYTOSIS AND TRAFFICKING OF CD4.

3.1.5.1 *Constitutive Endocytosis Of CD4 May Involve Phosphorylation Of The Cytoplasmic Domain.*

PMA, which activates protein kinase C (PKC) (Castagna *et al* 1982), causes CD4 down-regulation by endocytosis through coated pits (Section 3.1.4; Hoxie *et al* 1986; 1988; Petersen *et al* 1992; Pelchen-Matthews *et al* 1993), and transient phosphorylation of the cytoplasmic domain (Acres *et al* 1986; Blue *et al* 1987; Hoxie *et al* 1988; Shin *et al* 1990; 1991). Phosphorylation of serine residues in the cytoplasmic domain of CD4, in particular serine 408 has been demonstrated to occur following the addition of phorbol esters (Shin *et al* 1990; 1991). These data suggest that CD4 endocytosis may involve phosphorylation following the addition of phorbol ester.

In HeLa-CD4 cells, CD4 has been demonstrated to be endocytosed constitutively (Pelchen-Matthews *et al* 1989; 1991) in the absence of any PKC activators. Therefore, is phosphorylation of the cytoplasmic domain of CD4 required for its concentration into clathrin-coated pits and constitutive internalization? Evidence that phosphorylation of the cytoplasmic domain of CD4 may be required for constitutive endocytosis, comes from the observation that, when the serine at position 408 is mutated to alanine (CD4^{S408A}), the rate of CD4 endocytosis is reduced 3 fold, such that the uptake of this mutant CD4 is similar to that of CD4^{cyt}-molecules (Table 4) which are internalized by bulk flow (Pelchen-Matthews *et al* 1991).

To further investigate the role of phosphorylation in CD4 endocytosis experiments were performed using cells treated with staurosporine. Stsp is a membrane permeable alkaloid, that induces cell death by apoptosis in 24 h at a concentration of 1 μ M, however, the toxic effects of this drug can be seen within 6 h, following its addition to cells (Jacobson *et al* 1993).

PMA-induced CD4 modulation, was blocked by incubating HeLa-CD4 cells in the presence of the non-specific kinase inhibitor, staurosporine (Stsp; Meyer *et al* 1989). HeLa-CD4 cells were

treated with a range of Stsp concentrations, 0.1 μ M, 0.5 μ M or 1.0 μ M in BM for 30 min at 37°C before adding PMA to a final concentration of 100 ng/ml for 1 hour at 37°C. The cells were cooled by washing, and the amount of CD4 remaining at the cell surface detected using 125 I-Q4120 (Figure 17). Stsp completely inhibited PMA-induced CD4 down-regulation at a concentration of 0.1 μ M, indicating that phosphorylation of CD4 by kinase is required for modulation. Furthermore at higher concentrations of Stsp the level of cell surface CD4 was increased (~40% at 1.0 μ M Stsp). Given that the intracellular pool of cycling CD4 is approximately 40% of the total CD4 cycling pool in these cells, the up-regulation of CD4 at the higher concentrations of Stsp, could be explained by inhibition of CD4 endocytosis, while recycling is unaffected, i.e., the intracellular pool of CD4 is transferred to the cell surface.

Table 4. *Endocytosis rates of wild type and mutant forms of CD4 in HeLa cells. (CD4^{cyt-} and CD4^{S408A} data kindly supplied by Annegret Pelchen-Matthews.)*

CD4 Molecule	Endocytosis Rate (% per min)
wild type	2.55±0.30
CD4 ^{cyt-}	0.69±0.22
CD4 ^{S408A}	0.79±0.09

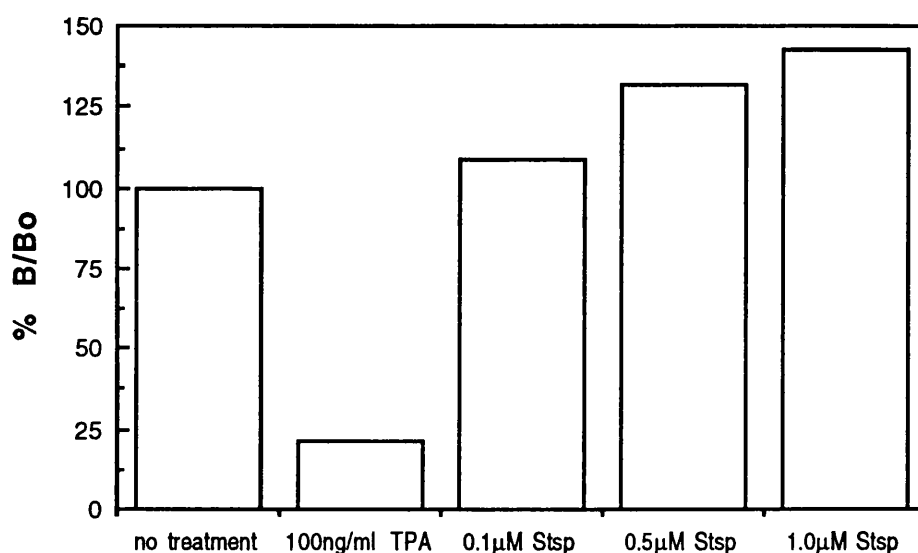


Figure 17. Inhibition of PMA-induced CD4 down-regulation by Staurosporine in HeLa-CD4 cells. Cells were pretreated in the presence or absence of a range of Stsp concentrations (0.1 μ M, 0.5 μ M, and 1.0 μ M) for 30 min at 37°C. PMA was then added to the cells, except control cells (no drugs, or PMA only as the positive control) to a final concentration of 100 ng/ml for 1 hour at 37°C. The levels of CD4 remaining at the cell surface were detected using 0.3 nM 125 I-Q4120. The plot shows binding of 125 I-Q4120 compared to untreated cells (B/Bo) after correction for cellular protein content.

The prediction that Stsp inhibits constitutive internalization of CD4 was tested in an endocytosis assay. With the toxic effects of Stsp in mind, Stsp was used at a concentration of 0.5 μ M, experiments had a duration of no more than 2.5 h in the presence of the drug, and cell morphology was monitored at the end of each experiment. A Stsp concentration of 0.5 μ M inhibits the activities of PKC (IC₅₀ 6 nM), protein kinase A (IC₅₀ 15 nM), phosphorylase kinase (IC₅₀ 3 nM), S6 kinase (IC₅₀ 5 nM), and the tyrosine-specific kinase of the epidermal growth factor receptor (IC₅₀ 2.5 nM - Meyer *et al* 1989).

HeLa-CD4 and HeLa-CD4^{cyt-} cells were cooled on ice, and labelled with ¹²⁵I-Q4120 for 2 h. In the final 30 min of this incubation time, Stsp was added to the test cells to a concentration of 0.5 μ M, and subsequent washes of these cells were performed with 0.5 μ M Stsp in the washing medium. The cells were warmed to 37°C in the presence or absence of 0.5 μ M Stsp for various times, cooled and either acid stripped as previously described, or harvested directly to allow determination of the proportion of acid resistant to total cell counts (Figure 18).

In the initial 10 min of the experiment, Stsp inhibited the internalization rate of CD4 3 fold (2% per min to 0.8% per min - Figure 18, A), such that the endocytosis kinetics of wild type CD4 were reduced to that of the CD4^{cyt-} molecules, and the intracellular pool of CD4 at 60 min was approximately 50% less in the presence of Stsp compared to control cells. In the initial 10 min of the endocytosis of CD4^{cyt-} molecules, Stsp did not appear to have a significant effect, however inhibition of internalization was apparent after 20 min. As CD4^{cyt-} molecules are endocytosed by bulk flow (Pelchen-Matthews *et al* 1991), this result suggests that Stsp inhibits vesicular trafficking from the cell surface. This is not entirely surprising given the fact that dynamin, a molecule that has been shown to be required for receptor-mediated endocytosis via coated pits, is regulated by phosphorylation (van der Bliek *et al* 1993; Herskovits *et al* 1993; Robinson *et al* 1993). However, the effects of Stsp on the internalization of intact CD4 are far more dramatic than those observed with the CD4^{cyt-} molecules.

These data suggest that Stsp significantly inhibits the endocytosis of CD4, implying that phosphorylation of the cytoplasmic domain of CD4 is involved in its constitutive internalization. Stsp did appear to have effects on vesicular trafficking from the plasma membrane (Figure 18, B), however these effects were not sufficient to account for the inhibition of CD4 internalization in the presence of the drug.

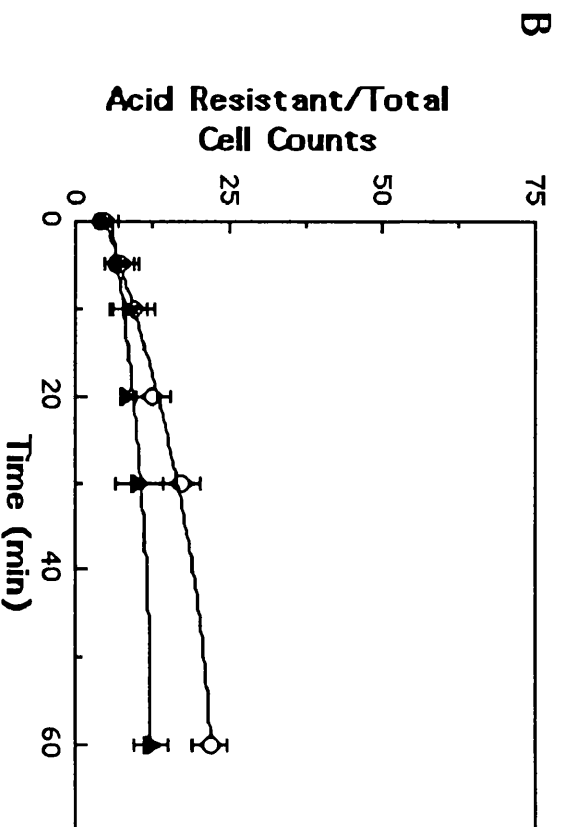
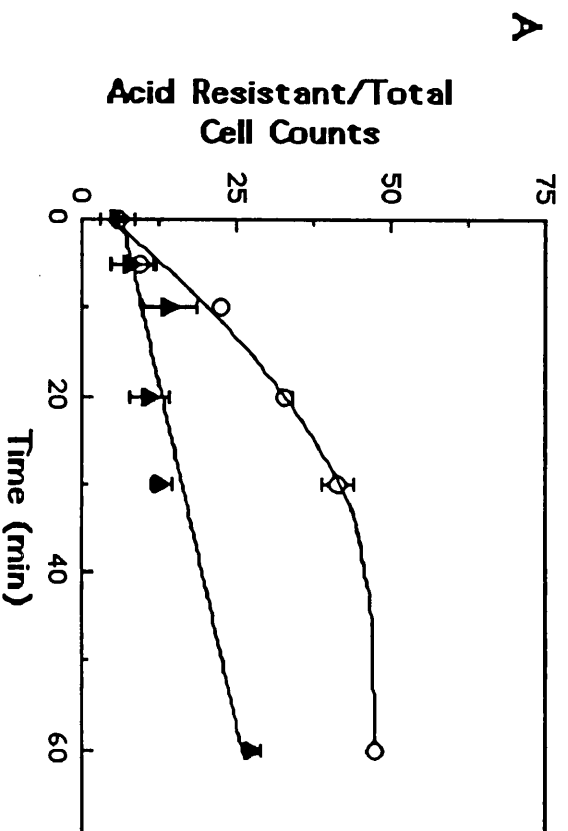


Figure 18. The effect of Staurosporine on the kinetics of CD4 endocytosis. HeLa-CD4 (A) and HeLa-CD4^{cyt-} (B) cells were labelled with ¹²⁵I-Q4120 on ice, and in the last 30 min of this incubation time, cells with 0.5 μ M Stp. The cells were warmed to 37°C for various times in the presence or absence of 0.5 μ M Stp (closed triangles), cooled and either acid stripped, or harvested directly. The plots show the ratios of acid resistant ¹²⁵I-Q4120 to the total cell associated label.

3.1.5.2 The Kinetics Of Cell Surface CD4 Up-Regulation In The Presence Of Stsp.

Stsp has been shown to inhibit the constitutive CD4 endocytosis (Figure 18), and PMA-induced CD4 down-regulation, leading to the up-regulation of cell surface CD4 (Figure 17). The kinetics of this up-regulation in the presence of Stsp was investigated in HeLa-CD4 and HeLa-CD4^{cyt-} cells.

Cells were pre-treated with Stsp at 4°C for 30 min, before warming to 37°C in the presence of 0.5 µM Stsp for various times. The cells were cooled by washing and the levels of cell surface CD4 detected using ¹²⁵I-Q4120.

Stsp caused up-regulation of CD4 at the cell surface, leading to the accumulation of some 40-50% more CD4 than untreated cells (Figure 19). This data could be interpreted as Stsp enhancing the recycling of CD4 to the cell surface. However, experiments on CD4 endocytosis in the presence and absence of Stsp, indicate that Stsp inhibits the endocytosis of CD4 (Figure 18, A), reducing its endocytosis kinetics to that of bulk flow uptake (0.8% per min). Stsp did not appear to affect the cell surface expression of the CD4^{cyt-} molecules, suggesting that the drug does not have a significant effect on vesicular trafficking in these cells.

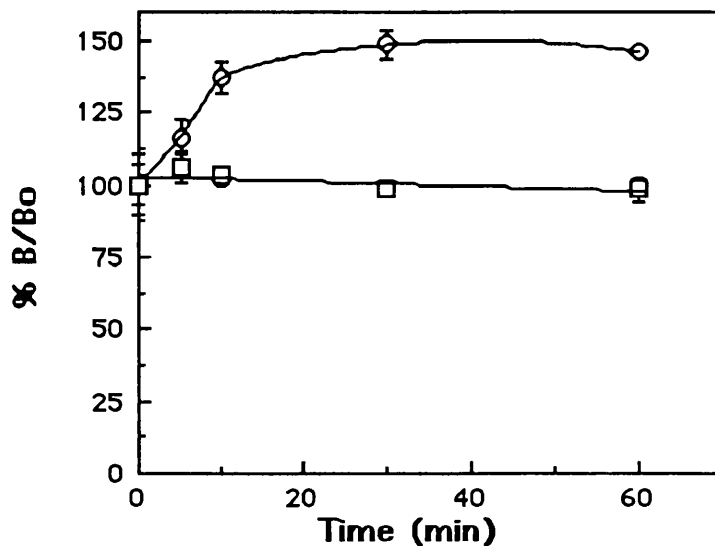


Figure 19. The effect of Staurosporine on CD4 cell surface expression. HeLa-CD4 (open circles) and HeLa-CD4^{cyt}- (open squares) cells were pre-treated with Stsp at 4°C for 30 min, before warming to 37°C in the presence of 0.5 μ M Stsp for various times. The cells were cooled, washed and the levels of cell surface CD4 detected using ¹²⁵I-Q4120. The plot shows binding of ¹²⁵I-Q4120 compared to untreated cells (B/Bo) after correction for cell protein.

3.1.5.3 *The Effect Of Stsp On The Fluid-Phase Endocytosis Of HRP in HeLa-CD4 Cells.*

Although the previous data suggests that Stsp affects the transport of CD4, it is possible that these effects may occur by the inhibition of coated vesicle formation, as suggested by the trafficking of the CD4^{cyt-} molecules (Figure 18, B). To determine whether Stsp had a significant effect on vesicular trafficking from the plasma membrane, the fluid-phase uptake of HRP in HeLa-CD4 cells was investigated in the presence of the drug.

HeLa-CD4 were pre-treated with 0.5 μ M Stsp for 30 min at 4°C, and subsequent washes of these cells were performed with 0.5 μ M Stsp in the washing medium. Control cells were pretreated with medium only for 30 min at 4°C. Cells were incubated in 5 mg/ml HRP in the presence or absence of 0.5 μ M Stsp for various times at 37°C. Cells were then cooled by washing, cell lysates were prepared, and the levels of HRP assayed (Figure 20).

Stsp appeared to inhibit the fluid-phase endocytosis rate about 1.5 fold compared to control cells in the initial 10 min. This result suggests that the reduced kinetics of constitutive CD4 endocytosis in the presence of Stsp may be due, at least in part, to an inhibition of vesicular trafficking from the plasma membrane. However, the inhibition of CD4 internalization in the presence of Stsp is 3 fold, which is approximately double that observed for fluid-phase uptake in the presence of the drug.

A second specific PKC inhibitor, CGP41 251 (Meyer *et al* 1989), was used to confirm the inhibition of fluid-phase internalization in the presence of Stsp. HeLa-CD4 cells were pretreated with 0.5 μ M Stsp, 0.5 μ M CGP41 251, or no drug 30 min at 4°C, then warmed to 37°C for various times in 5 mg/ml HRP either in the presence of 0.5 μ M Stsp, 0.5 μ M CGP41 251, or no drug. The cells were then cooled by washing, cell lysates prepared, and the levels of HRP assayed (Figure 21). The initial 20 min fluid-phase uptake of HRP was similar in the presence of Stsp and CGP41 251, however, CGP41 251 inhibited HRP uptake less than Stsp in longer incubation times, suggesting that kinases other than PKC are involved in vesicular trafficking in these cells.

These data indicate that the reduction of the kinetics of constitutive CD4 internalization in the presence of Stsp, is significantly greater than that observed for fluid-phase uptake and endocytosis of CD4^{cyt}- molecules (Figure 20 and Figure 18, B) in the presence of the kinase inhibitors tested. The fact that vesicular trafficking from the plasma membrane was affected by the kinase inhibitors was not surprising, as the activity of dynamin, a molecule involved in receptor-mediated endocytosis via coated pits, is regulated by phosphorylation (van der Blik *et al* 1993; Herskovits *et al* 1993; Robinson *et al* 1993). These data obtained with the kinase inhibitors, together with the reduced internalization kinetics of the CD4^{S408A} molecules implies that phosphorylation may be involved in the constitutive endocytosis of CD4.

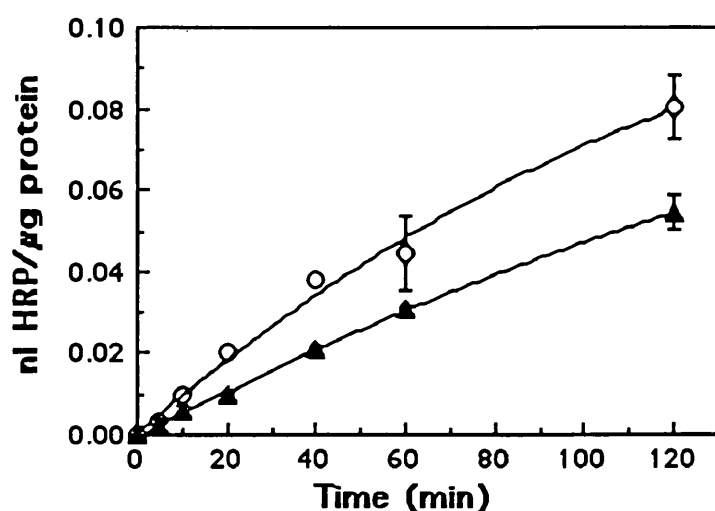


Figure 20. The effect of Staurosporine on the fluid phase endocytosis of HRP in HeLa-CD4 cells. Cells were pre-treated for 30 min at 4°C in the presence or absence of 0.5 μ M Stsp. Cells were incubated in 5 mg/ml HRP in the presence (closed triangles) or absence (open circles) of 0.5 μ M Stsp at 37°C for various times, cooled by washing, cell lysates prepared, and the levels of HRP assayed (as described in Materials and Methods).

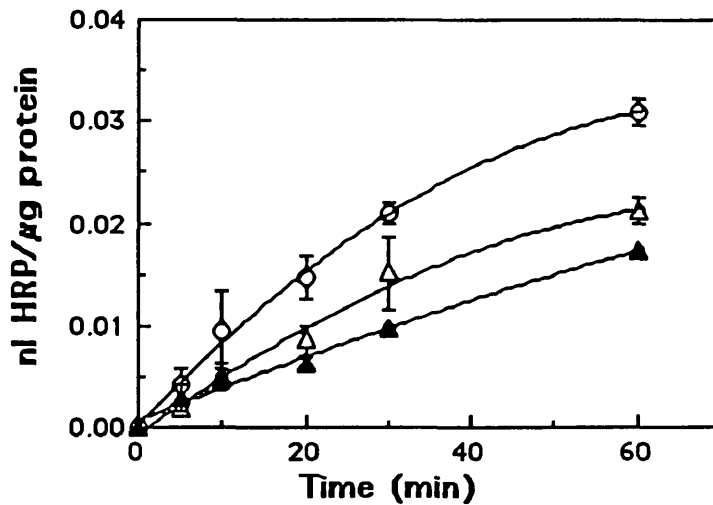


Figure 21. The effect of Staurosporine and a specific protein kinase C inhibitor (CGP41 251) on the fluid phase endocytosis of HRP in HeLa-CD4 cells. Cells were pre-treated with 0.5 μ M Stp or 0.5 μ M CGP41 251 for 30 min at 4°C, then incubated in 5 mg/ml HRP either in the presence of 0.5 μ M Stp (closed triangles), 0.5 μ M CGP 41/251 (open triangles), or no drug (open circles) at 37°C for various times. The cells were cooled by washing, cell lysates were prepared, and the levels of HRP assayed.

Based on the above observations, a model for the involvement of phosphorylation in the constitutive endocytosis of CD4 in HeLa-CD4 is proposed in Figure 22 (steps 1 to 2).

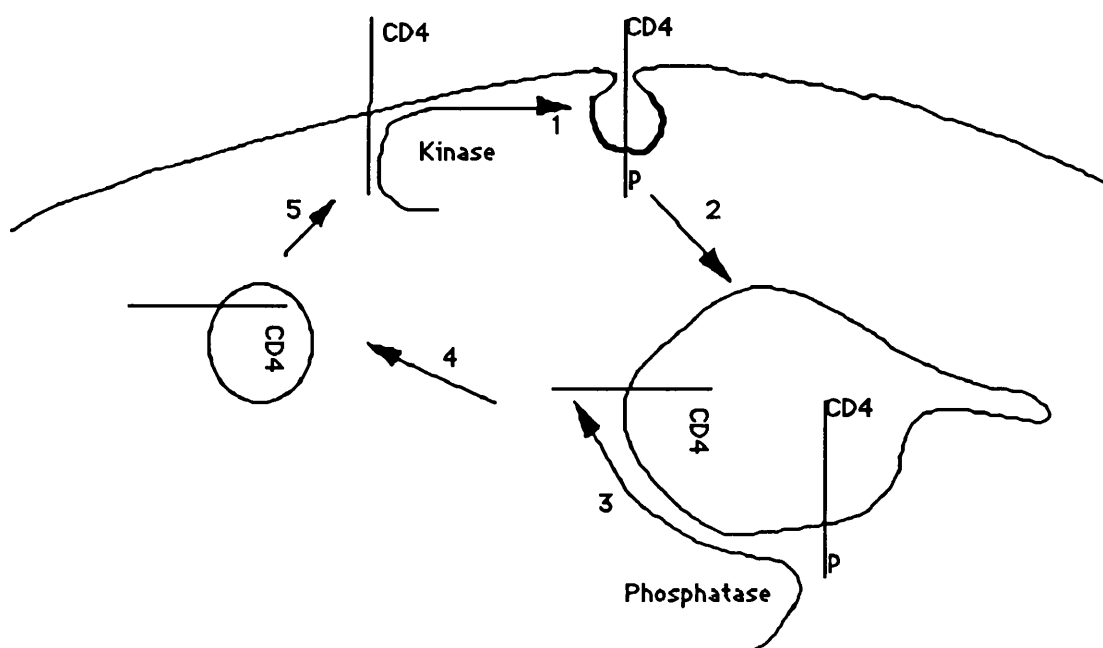


Figure 22. Diagrammatic representation of a model for the phosphorylation of CD4 during constitutive endocytosis in HeLa-CD4 cells. CD4 is phosphorylated by kinase at the plasma membrane (step 1) allowing it to cluster in clathrin-coated pits, internalize and be delivered to early endosomes (step 2). At some unknown stage, CD4 is dephosphorylated by phosphatase (step 3), allowing it to recycle to the plasma membrane (steps 4 and 5).

Mutant forms of CD4 which lack certain phosphorylation sites (CD4^{cyt-} and CD4^{S408A}), are taken into the cell by bulk flow (~0.8% per min); an endocytosis rate above bulk flow internalization is enhanced. Phorbol esters enhance CD4 uptake considerably; but enhanced CD4 endocytosis is seen in non-PMA treated cells, therefore suggesting that CD4 may undergo basal phosphorylation. In HeLa-CD4 cells, CD4 is constitutively recycled to the plasma membrane (Pelchen-Matthews *et al* 1989; Marsh *et al* 1990). However, when CD4 molecules are phosphorylated following the addition of phorbol esters (Acres *et al* 1986; Blue *et al* 1987; Hoxie *et al* 1988; Shin *et al* 1990), they are sorted to a compartment in the perinuclear region of the cells, and the recycling of CD4 is reduced (Figure 26; Pelchen-Matthews *et al* 1993). These data

suggest that for CD4 to recycle to the plasma membrane there may be a requirement to dephosphorylate its cytoplasmic domain (Figure 22, steps 3 to 5).

The possible role for phosphorylation in the constitutive endocytosis of CD4 was investigated using the non-specific kinase inhibitor Stsp. The role of dephosphorylation in the intracellular trafficking of CD4 proposed in the above model, can be tested by using an inhibitor of phosphatases. The tumour promoting, membrane permeable polyether fatty acid, okadaic acid (OKA), was used as the inhibitor of phosphatases (Cohen *et al* 1990). OKA was used at a concentration of 1.25 μ M, which is known to specifically inhibit both protein phosphatases (PP) 1 (IC_{50} ~10-15 nM), and PP2A (IC_{50} ~0.1 nM - Cohen *et al* 1990). Toxic effects of OKA were noticed after 120 min, when cells had begun to round up and detach from the substrate. Therefore, experiments in the presence of OKA were performed for only 60 min, after which time no visible changes in cell morphology were evident.

3.1.5.4 Phosphorylation Of The Cytoplasmic Domain Of CD4 May Be An Important Feature Of Its Intracellular Trafficking.

If steps 3 to 5 in the above model (Figure 22) are inhibited then CD4 would not recycle to the cell surface, and plasma membrane levels of CD4 would be down-regulated.

This was tested by incubating HeLa-CD4 and HeLa-CD4^{cyt-} cells in medium containing 1.25 μ M OKA for various times at 37°C (Figure 23). The cells were cooled, and the levels of cell surface CD4 were detected using ¹²⁵I-Q4120. The plasma membrane expression of CD4 was reduced by 30% in 20 min in the presence of OKA, and remained at this level for the next 40 min. No down-regulation of cell surface CD4^{cyt-} was observed in the first 20 min in the presence of OKA. The increase in the standard errors in both cell lines at 60 min may be due to toxic effects on the cells, however, no change in cell morphology was apparent after this time.

The down-regulation of cell surface CD4 could be due to a slight increase in the endocytosis rate of CD4, with no change in the

recycling rate. Alternatively, the results could be interpreted as a reduction in the recycling kinetics of CD4 with no change in the endocytosis rate.

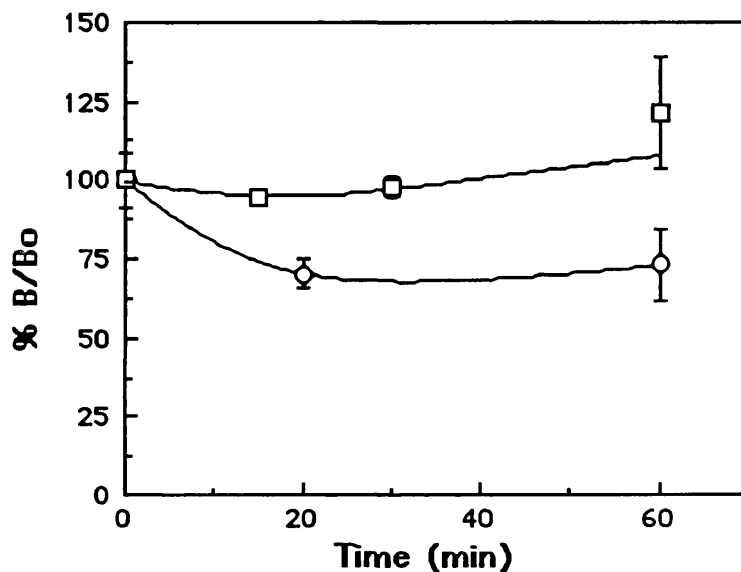


Figure 23. The effect of Okadaic acid on CD4 cell surface expression. HeLa-CD4 (open circles) and HeLa-CD4^{cyt}- (open squares) cells were treated with 1.25 μ M OKA at 37°C for various times. The cells were cooled, washed and the levels of cell surface CD4 were detected using ¹²⁵I-Q4120. The plot shows binding of ¹²⁵I-Q4120 compared to untreated cells (B/Bo) after correction for cellular protein content.

3.1.5.5 The Effect Of OKA On The Endocytosis Kinetics Of CD4.

The effect of OKA on the trafficking of CD4 was tested in an endocytosis assay. HeLa-CD4 and HeLa-CD4^{cyt}- cells were cooled on ice, and labelled with ¹²⁵I-Q4120 for 2 h, and warmed to 37°C

for various times in the presence or absence of 1.25 μ M OKA. The cells were cooled and were either acid stripped as described above, or harvested directly to allow determination of the acid resistant and total cell counts.

OKA did not appear to inhibit the endocytosis of CD4 (Figure 24). However, after 60 min in the presence of OKA the intracellular pool of CD4 was increased by about 20% suggesting that OKA inhibited the recycling of CD4 to the plasma membrane (Figure 24, A).

If dephosphorylation of the cytoplasmic domain is required for CD4 to recycle to the plasma membrane, then in the presence of OKA, CD4 may be delivered to the perinuclear region cell after 60 min, in a similar fashion to CD4 modulation in the presence of phorbol ester (Figure 26, G and H). When the distribution of CD4 was investigated by immunofluorescence in the presence of OKA, no change in the distribution was observed compared to control cells, i.e., the CD4 intracellular staining was similar to that after 60 min endocytosis (Figure 26, B). The reason no movement of anti-CD4/CD4 complexes to the perinuclear region of the cells was apparent, may be due to the fact that in interphase HeLa cells, intracellular transport is inhibited in the presence of OKA (Lucocq *et al* 1991), however, no effect on CD4 endocytosis was observed in the HeLa-CD4 cells.

OKA did not have a significant affect on the endocytosis rate or the size of the intracellular pool of CD4^{cyt-} (Figure 24, B), suggesting that OKA has no significant effect on vesicular trafficking from the plasma membrane, or recycling of CD4^{cyt-} molecules from endosomes to the cell surface in this cell type.

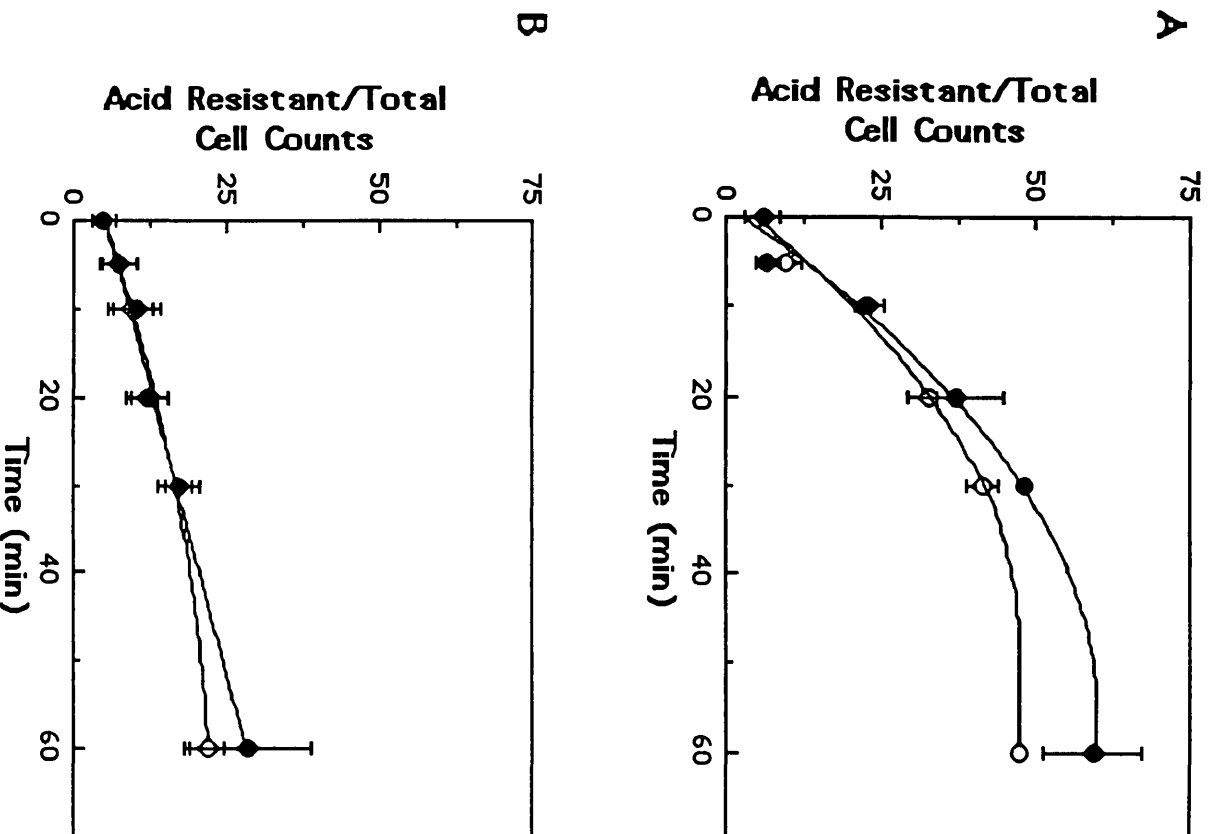


Figure 24. The effect Okadaic acid on the kinetics of CD4 endocytosis. HeLa-CD4 (A) and HeLa-CD4^{cyt-} (B) cells were labelled with ¹²⁵I-Q4120 on ice for 2h, and then were warmed to 37°C for various times in the presence (closed circles) or absence (open circles) of 1.25 μ M OKA. The cells were cooled and either acid stripped, or harvested directly. The plots show the ratios of acid resistant ¹²⁵I-Q4120 to the total cell associated label.

3.1.5.6 *The Effect of OKA On The Fluid-Phase Endocytosis Of HRP In HeLa-CD4 Cells.*

The data obtained on the CD4^{cyt-} molecules in the presence of OKA, suggested that OKA does not affect vesicular trafficking to and from the plasma membrane in these HeLa cells. This was further investigated using the fluid-phase marker HRP.

HeLa-CD4 cells were incubated in 5 mg/ml HRP in the presence or absence of 1.25 μ M OKA for various times at 37°C (Figure 25). The cells were then cooled by washing, cells lysates were prepared, and the levels of HRP were assayed. OKA did not appear to inhibit the fluid-phase uptake of HRP, again suggesting that vesicular trafficking to and from the cell surface is not affected by OKA in these cells.

Results from a separate study have indicated that OKA inhibits intracellular transport and fluid-phase endocytosis in interphase HeLa cells (Lucocq *et al* 1991), however the data presented here demonstrate that OKA has no affect on fluid-phase endocytosis and recycling in the HeLa-CD4 cells. It is likely that different phosphatases are involved in such fundamental cell properties in two different strains of HeLa cells, since the results are not directly comparable.

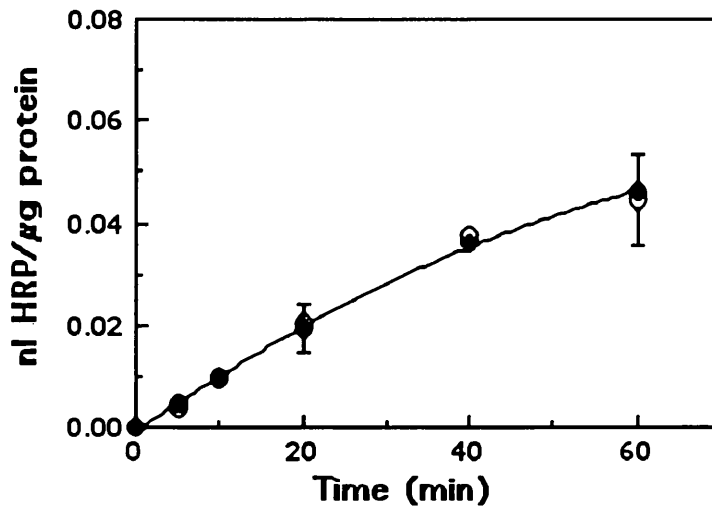


Figure 25. The effect of Okadaic acid on the fluid-phase endocytosis of HRP in HeLa-CD4 cells. Cells were incubated in 5 mg/ml HRP in the presence (closed circles) or absence (open circles) of 1.25 μ M OKA for various times at 37°C. The cells were cooled by washing, cell lysates were prepared, and the levels of HRP assayed (see Materials and Methods for HRP assay).

In HeLa-CD4, NIH3T3-CD4 and monocytes CD4 undergoes constitutive endocytosis (Pelchen-Matthews *et al* 1989; 1991; Marsh *et al* 1990). Using Stsp to inhibit kinase, the results indicate that the constitutive endocytosis of CD4 is inhibited, thus inferring that phosphorylation of the cytoplasmic domain of CD4 may play a role in the internalization of CD4. OKA, a protein phosphatase inhibitor, on the other hand, inhibited the recycling of CD4 leading to an increase in the CD4 intracellular pool, thus suggesting that phosphorylation of the cytoplasmic domain of CD4 is important for its intracellular sorting.

3.2 THE INTRACELLULAR SORTING OF CD4 DURING PMA-INDUCED MODULATION.

Computer models of CD4 cycling dynamics have indicated that an increase in endocytosis alone can account for down-regulation (Pelchen-Matthews *et al* 1993), yet, previous work has shown that, CD4 stably expressed in HeLa cells, is delivered to an intracellular compartment in the juxta-nuclear region, where it is thought to be degraded within 2 h (Shin *et al* 1991). However, little is known about the mechanism of transfer to the perinuclear region nor the nature of the perinuclear organelles.

To follow the intracellular redistribution of CD4 during PMA-induced modulation, HeLa-CD4 cells were labelled with Leu3a on ice and warmed to 37°C in the presence or absence of PMA. The cells were cooled rapidly, and either acid stripped to remove any cell surface ligand or fixed directly in paraformaldehyde. The cells were then either permeabilized to reveal intracellular CD4/anti-CD4 complexes, or stained intact to show cell surface CD4 only; the Leu3a was detected using rhodamine-labelled goat anti-mouse (Figure 26). After 1 h internalization at 37°C in the absence of PMA, CD4/anti-CD4 complexes were located in intracellular structures (possibly early endosomes) dispersed throughout the cytoplasm of the cells (Figure 26, B), and at the cell surface (Figure 26, A). At early time points (10 min) in the presence of PMA, the internalized CD4/anti-CD4 complexes showed a similar distribution to the intracellular staining in unstimulated cells (Figure 26, C). However, after longer incubations (30 min -1 h) cell surface CD4 became undetectable (Figure 26, E and F) and the internalized CD4/anti-CD4 complexes were located in perinuclear region (Figure 26, D, G and H), which after 1 h were seen in tight clusters in the juxta-nuclear region of the cells (Figure 26, G and H). These data suggested that in the presence of PMA CD4 was moving along the endocytic pathway, possibly to later endocytic organelles. In contrast, internalized CD4 in unstimulated cells showed a dispersed early endosomal staining pattern even after prolonged incubation at 37°C (Figure 26, B).

To characterize the compartment, or compartments, which contained CD4 during phorbol ester-induced down-regulation two techniques were used. The first was cell fractionation, and the second was double label indirect immunofluorescence.

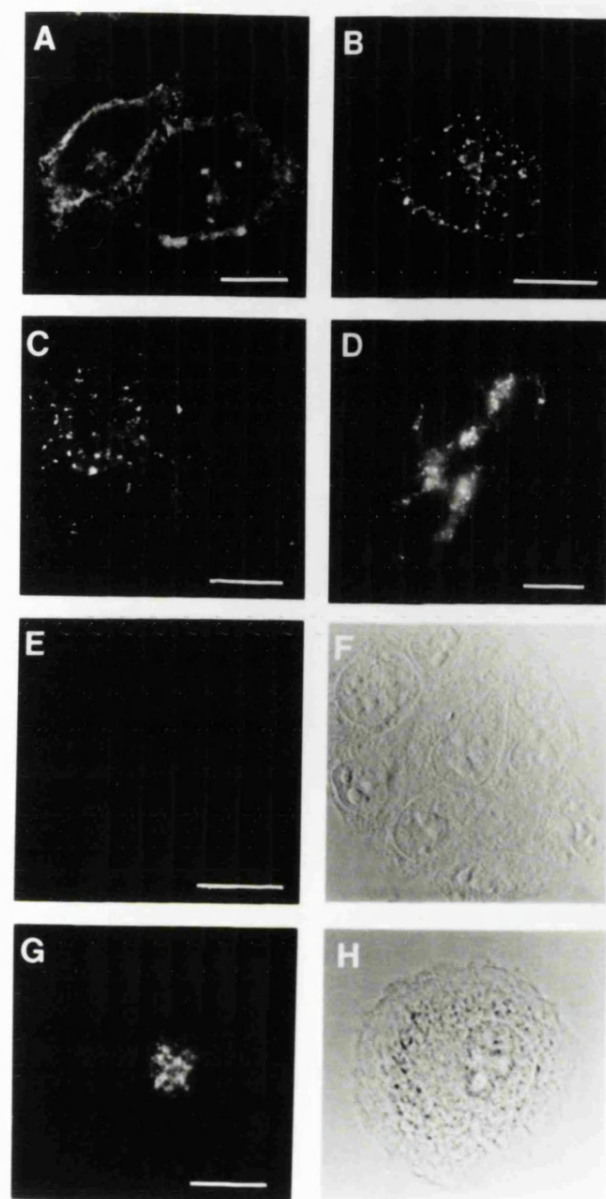


Figure 26. The cellular distribution of CD4 in the presence or absence of PMA. HeLa-CD4 cells were labelled with Leu3a on ice, and warmed to 37°C for 1 h in the absence of PMA (A and B), or 10 min (C), 30 min (D), and 1 h (E to H) in the presence of 100 ng/ml PMA. Cells were fixed and stained intact with anti-mouse rhodamine (A, E and F). Alternatively, cell surface antibody was removed by acid stripping, before fixing, permeabilizing to reveal intracellular antibody and staining with anti-mouse rhodamine (B, C, D, G and H). F and H are phase contrast views of E and G respectively. Scale bars, 10 μm .

3.2.1 Characterization Of The Compartment Containing CD4 During PMA Induced-CD4 Down-Regulation.

3.2.1.1 Fractionation Studies.

The immunofluorescence experiments (Figure 26) suggest that in the presence of PMA, CD4 is redistributed from the early endosomes to later endocytic organelles. To identify the compartments involved in trafficking of CD4 during PMA-induced down-regulation attempts were made to separate early endosomes, late endosomes and lysosomes, using centrifugation techniques and density media, which have previously been employed to separate endosomal compartments in rat liver cells (Mullock *et al* 1989), BHK cells (Marsh *et al* 1987; Gorvel *et al* 1991), and Madin-Darby bovine kidney (MDBK) cells (Park *et al* 1991) to mention a few examples.

Initial experiments were carried out to homogenize HeLa-CD4 cells in a ball bearing homogenizer (Balch and Rothman 1985). HeLa-CD4 cells were cooled on ice and washed with PBS at 4°C. The cells were scraped in PBS and resuspended in 1 ml homogenization buffer (TEA/sucrose pH7.40: 10 mM triethanolamine, 10 mM acetic acid, 1 mM EDTA and 0.25 M sucrose - Harms *et al* 1980). The cell suspension was homogenized in the ball bearing homogenizer with a clearance of 15.1 μm , using 10 passes, which resulted in 90% cell breakage with no significant nuclear damage. The cell homogenate was routinely checked under the light microscope.

It was next necessary to determine whether the intracellular organelles still remained intact after the lysis procedure. HeLa-CD4 cells were labelled with 5 mg/ml HRP at 37°C for 30 min, and cooled by washing with 10 x 10 ml of PBS at 4°C. The cells were scraped in PBS, resuspended in 1 ml homogenization buffer, and homogenized using 10 passes through the ball bearing homogenizer. An aliquot of the lysate was removed, and a post nuclear supernatant (PNS) was prepared by centrifuging the homogenate at 1200 g for 10 min at 4°C. To determine how much of the HRP was latent (i.e. within sealed subcellular compartments) the PNS was centrifuged at 106 000 g for 30 min

at 4°C. The resulting supernatant yielded the soluble material (probably released from organelles during the lysis procedure), and the pellet gave the latent material (i.e. within intact organelles). HRP and β -hexosaminidase (a lysosomal enzyme) activities were assayed according to the protocols described in the Materials and Methods section. Figure 27 shows the activities recovered in each fraction, and for both HRP (Figure 27, A) and β -hexosaminidase (Figure 27, B) approximately 60% of the activity was recovered in the latent fraction.

Having determined that majority of the endosomes remained intact during the homogenization procedure, it was then possible to fractionate the homogenate. Initially self forming Percoll gradients were used similar in principle to those described by Marsh *et al* (1987).

HeLa-CD4 and HeLa-CD4^{cyt}- cells were labelled with ¹²⁵I-Q4120 for 2 h at 4°C, warmed to 37°C in the presence of PMA for 2 h. In the final 5 min of the 2 h incubation, the HeLa-CD4 cells were labelled with 5 mg/ml HRP in the presence of PMA at 37°C, to label early endosomes. All the cells were cooled by washing, acid stripped to remove cell surface label, and the cell suspensions were homogenized as outlined above. Postnuclear supernatants were prepared and mixed with isotonic percoll to give 2 x 30% percoll mixtures. These mixtures were loaded into 2 separate gradient tubes which were sealed, and centrifuged for 30 min at 20, 960 g at 4°C. The gradients were fractionated from the base of the tubes collecting 10 drops per fraction, and were assayed for ¹²⁵I-Q4120, HRP and β -hexosaminidase activities (Figure 28). Calculation of recoveries indicated that of the ~50% of the cell associated activity loaded onto the gradients, 80% was recovered. The density of the fractions was measured using a digital refractometer, and the readings were converted to sucrose density in g/ml, by comparison to sucrose standards. ¹²⁵I-Q4120/CD4 complexes were observed to co-migrate with the ¹²⁵I-Q4120/CD4^{cyt}- molecules at the top of the gradients at a density of 1.040-1.055 g/ml (Figure 28).

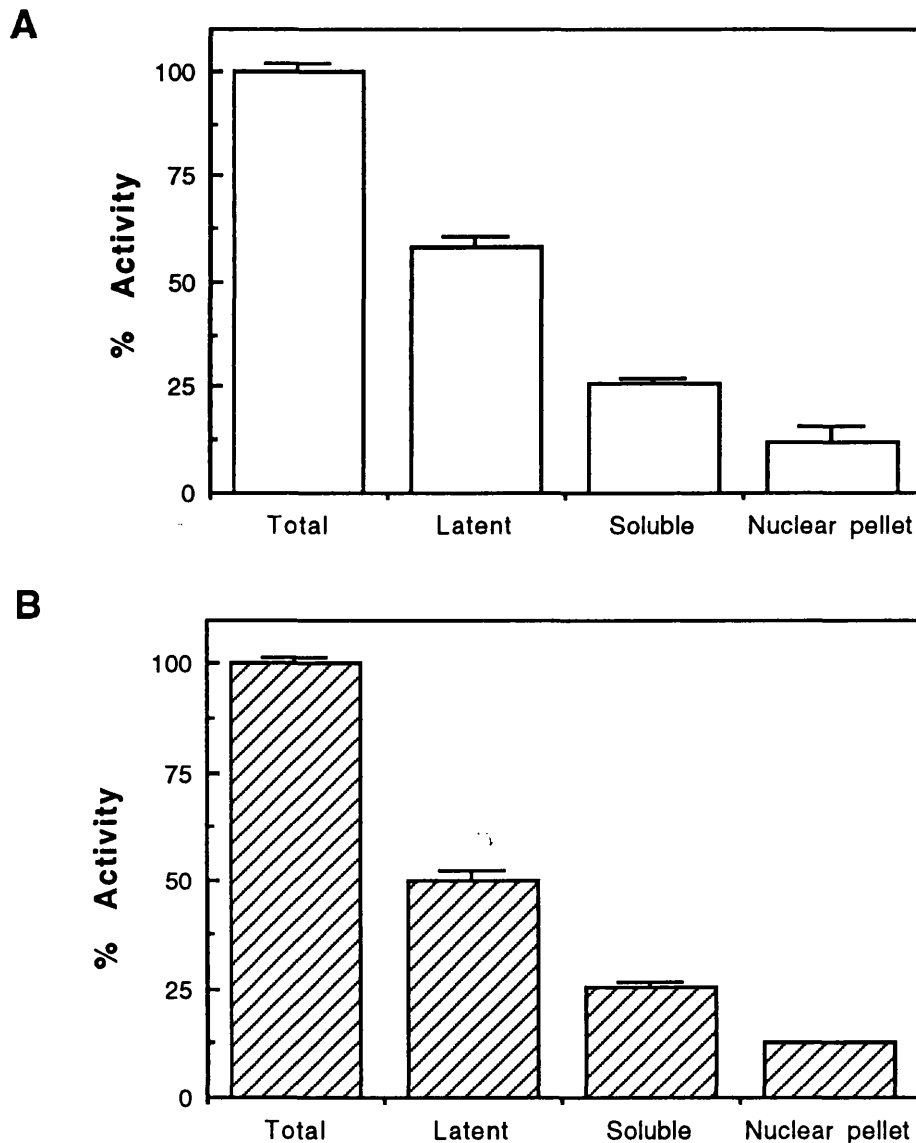


Figure 27. The proportion of HRP (A) and β -hexosaminidase (B) activities associated with subcellular organelles after homogenization of a HeLa-CD4 cell suspension. HeLa-CD4 cells were incubated with 5 mg/ml HRP at 37°C, cooled by washing and a cell suspension prepared. The suspension was homogenized in a ball bearing homogenizer, and a PNS prepared. The membranes in the PNS were removed using high speed centrifugation, and the HRP and β -hexosaminidase activities in the different fractions determined using the enzyme assays described in the Materials and Methods. The graphs shows the % activity in each fraction compared to the total activity in the PNS.

The markers HRP and β -hexosaminidase, which mark the early endosomes and lysosomes respectively, are clearly separated on the 30% Percoll gradient. The CD4 and CD4^{cyt-} co-migrated with HRP/early endosomal peak. The CD4^{cyt-} molecules are not down-regulated in response to phorbol esters (Figure 9), and by fluorescence, the intracellular cycling pool of CD4^{cyt-} is seen in a dispersed punctate staining pattern throughout the cytoplasm of the cell (Figure 36), resembling early endosomal staining. Thus the co-fractionation of CD4^{cyt-} and HRP supports the view that CD4^{cyt-} molecules are in the early endosome.

The compartment containing intact CD4, seen by fluorescence in the perinuclear region of the cell during PMA-induced down-regulation (Figure 26, G and H), did not appear to separate from the early endosomes in this gradient system. No significant level of ¹²⁵I-anti-CD4 was seen in the lysosome fraction for either CD4 or CD4^{cyt-}, suggesting that either the CD4-ligand complexes failed to reach the lysosomes or were rapidly degraded once they were delivered to these organelles. The apparent co-fractionation of CD4 and CD4^{cyt-} suggested that the CD4 was contained in early endosomes clustered in the perinuclear region of the cell, or that early and late endosomes fail to separate in this gradient system. Fluid-phase endocytosis experiments in cells treated with PMA for 2 h, indicate that LY is taken up into early endosomes dispersed throughout the cytoplasm of the cell during a 10 min incubation in the presence of PMA (Figure 37). This suggests that the fluid-phase HRP does not go to the same location as CD4 during down-regulation, and that the CD4 is not within early endosomes in the perinuclear region of the cell. These data imply that early and late endosomes are not separating in this gradient system.

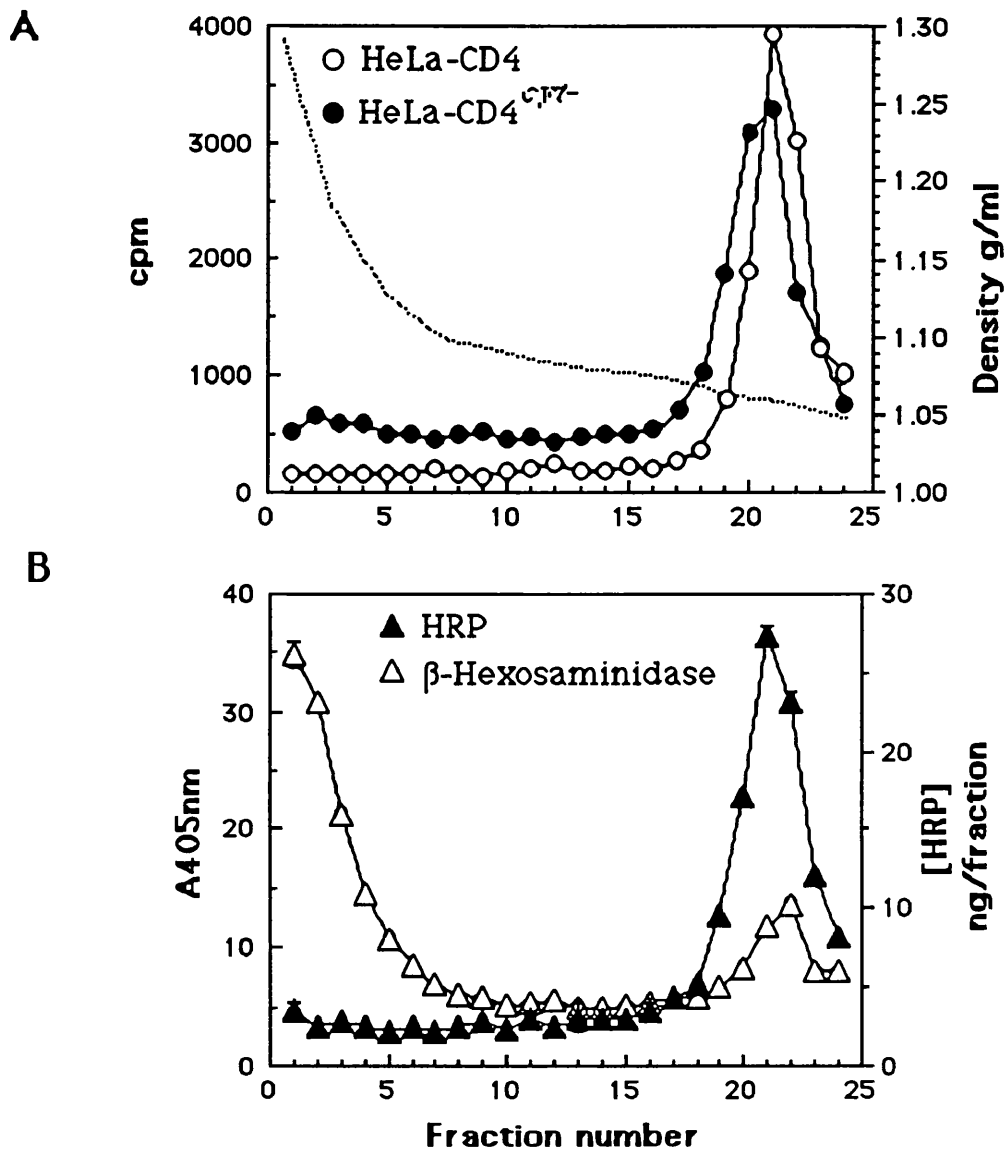


Figure 28. Subcellular fractionation of HeLa-CD4 and HeLa-CD4^{cyt-} cells on 30% Percoll gradients. Cells were labelled on ice with ¹²⁵I-Q4120, warmed to 37°C in the presence of 100 ng/ml PMA for 2 h, and in the final 5 min of this incubation, HRP was added to the HeLa-CD4 cells. Cells were cooled, acid stripped, PNS's were prepared for each cell line which were mixed with isotonic Percoll to a final concentration of 30%. The gradients were centrifuged, fractionated and analysed for their levels of ¹²⁵I-Q4120 (A), and in the HeLa-CD4 cells, their HRP (closed triangles) and β -hexosaminidase activities (open triangles) (B). The density profile of the 30% Percoll gradient is in panel A (dotted line).

Further gradient systems were used to try to separate the compartment containing CD4 during PMA-induced down-regulation. The first was a continuous sucrose gradient previously used to separate early and late endosomes from rat clone 9 hepatocytes, normal rat kidney and Chinese hamster ovary cells (Brown and Farquhar 1987).

HeLa-CD4 cells were labelled with ^{125}I -Q4120 for 2 h at 4°C, warmed to 37°C for 1 h in the presence of PMA. In the last 5 min of this incubation 5 mg/ml HRP was added in the presence of PMA to label the early endosomes. The cells were cooled by washing, acid stripped, homogenized as described above, and a PNS was prepared. Initially a 20-60% continuous sucrose gradient was tested, but it was found that the lysosomes and early endosomes did not show significant separation. This gradient was modified to a 25-50% continuous sucrose gradient. Cells were prepared exactly as described above and a PNS was loaded onto the pre-formed 25-50% continuous sucrose gradient. The gradient was centrifuged at 200,000 g for 2 h 20 min at 4°C. Ten drop fractions were collected from the bottom of the tube. The fractions were assayed for ^{125}I -Q4120, HRP, β -hexosaminidase activities and density. The distribution of HRP activity and ^{125}I -Q4120/CD4 complexes overlapped and peaked at fraction 17 (Figure 29), however, the ^{125}I -Q4120/CD4 complexes were distributed over a wider range of densities compared to the HRP containing early endosomes (1.105-1.155 g/ml for the ^{125}I -Q4120/CD4 complexes, compared to, 1.105-1.130 g/ml for the HRP activity). There was some overlap of the ^{125}I -Q4120/CD4 complexes with the lysosomal enzyme, β -hexosaminidase (density 1.135-1.190 g/ml), but the majority of the ^{125}I -Q4120 activity co-migrated with early endosomes. This gradient system, like the Percoll gradients, did not separate the compartment containing CD4 during down-regulation, from the early endosomes.

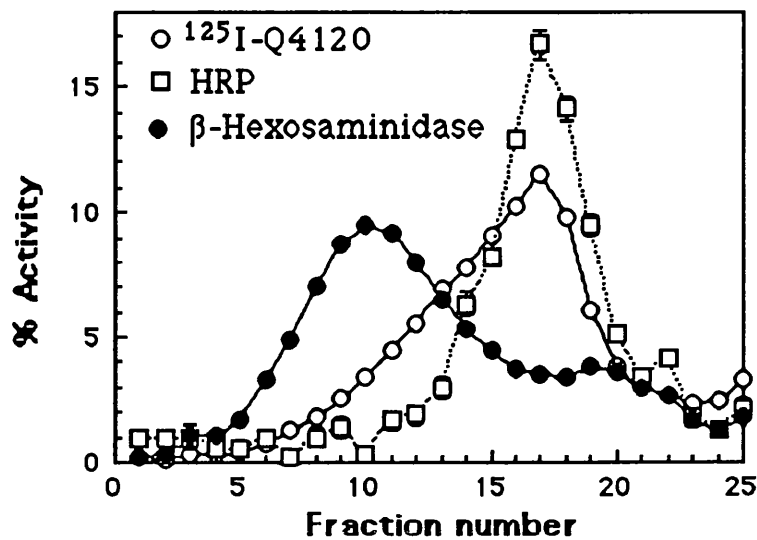
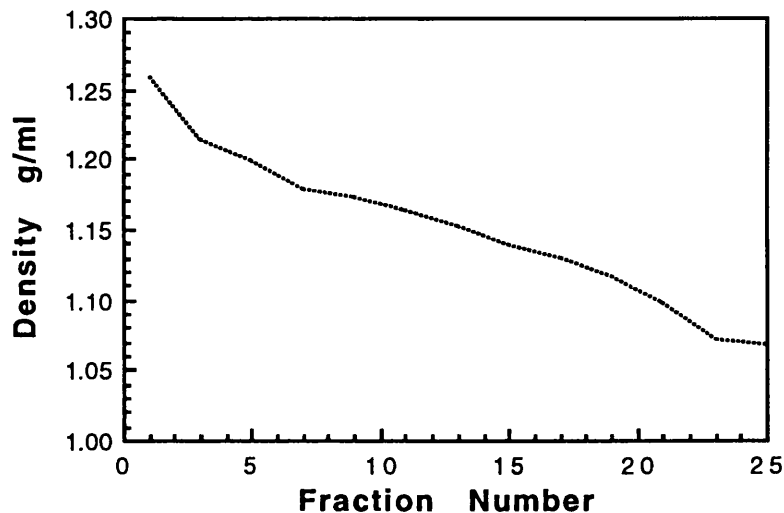
A**B**

Figure 29. Subcellular fractionation of HeLa-CD4 cells on a 25-50% continuous sucrose gradient. Cells were labelled with ^{125}I -Q4120 on ice, and warmed to 37°C for 1 h in the presence of 100 ng/ml PMA. In the final 5 min of this incubation, HRP was added to a concentration of 5 mg/ml in the presence of PMA. The cells were cooled, acid stripped and homogenized as described in the text. A PNS was prepared and was loaded onto the sucrose gradient which was centrifuged, and then fractionated. Fractions were analysed for their levels of ^{125}I -Q4120 (open circles), HRP (open squares) and β -hexosaminidase (closed circles) activities (A), plotted as a proportion of the activity loaded on the gradient. The sucrose density of the gradient is shown in panel B.

The third gradient system used was a sucrose step gradient made up in deuterium oxide (D₂O), which has been previously used to separate early and late endosomes in BHK cells (Gorvel *et al* 1991).

HeLa-CD4 cells were labelled with 2 mg/ml HRP for 10 min at 37°C, cooled by washing, and homogenized as outlined above. A PNS was prepared, and was adjusted to 40.6% sucrose using a 62% sucrose stock solution. This mixture was loaded into the bottom of a SW40 centrifuge tube, and overlaid with 16% sucrose in D₂O followed by a 10% sucrose step in D₂O. These two steps were finally overlaid with homogenization buffer, to give a 6 ml gradient. The gradient was centrifuged at 154, 624 g for 3 h 3 min at 4°C. The gradient was fractionated from the bottom of the tube collecting 6 drops per fraction, and the HRP and β -hexosaminidase activities were assayed. HRP and β -hexosaminidase activities were observed to co-migrate in fractions 1-6 (Figure 30), although some HRP was in fractions 10-12, separate from any β -hexosaminidase. This suggested that the majority of early endosomes were not separating from the lysosomes.

To determine whether late endocytic organelles were separating from the early endosomes and lysosomes the fractions were immunoblotted for rab7 - a late endosomal marker (Gorvel *et al.* 1991). Fractions were pooled in steps of 3 (i.e. 1-3, 4-6 and so on), except fractions 16 to 20, which were all pooled. Sample buffer was added to these pooled fractions, which were then separated on a 15% acrylamide gel, the proteins transferred to nitrocellulose and immunoblotted for rab7. The majority of the rab7 was located in fractions 4 to 6 (Figure 31), suggesting that late endosomes were co-migrating with the lysosomes and the majority of early endosomes in this gradient system.

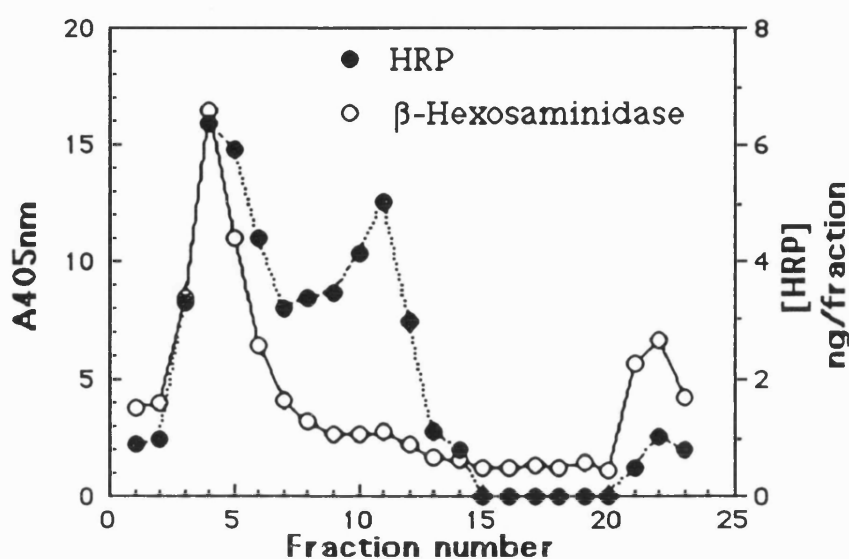


Figure 30. Subcellular fractionation of HeLa-CD4 cells on a D₂O sucrose step gradient. Cells were labelled with 2 mg/ml HRP at 37°C for 10 min, cooled by washing, and homogenized as outlined in the text. A PNS was prepared, and was adjusted to 40.6% sucrose using a 62% sucrose stock solution. This mixture was overlaid with 2 sucrose steps in D₂O, 16% and 10%, both containing 10 mM TEA and 10 mM acetic acid, and finally homogenization buffer. The 6 ml gradient was centrifuged, fractionated, and the HRP (closed circles) and β-hexosaminidase (open circles) activities were assayed.



Figure 31. Immunoblot for rab7 in fractions from the D₂O sucrose step gradient. Fractions from the D₂O sucrose step gradient were pooled in steps of 3 (i.e. 1-3, 4-6 and so on) except fractions 16-20 which were all pooled, non-reducing sample buffer was added, and the pooled fractions were separated on a 15% acrylamide gel. The proteins were transferred to nitrocellulose and immunoblotted for rab7.

From the immunofluorescence experiments (Figure 26) it is evident that the distribution of internalized anti-CD4 is changed in the presence of PMA. However, the nature of the compartment is not clear. Data from the Percoll gradient system suggests that the compartment is not lysosomal, however, the gradient systems used were unable to distinguish early and late endosomes. The indication that no significant portion of ^{125}I -anti-CD4 was seen in lysosomes even after 2 h in the presence of PMA, by no means proves that CD4 (and/or anti-CD4) is not reaching lysosomal compartments. On the contrary, CD4-ligand complexes could be delivered to lysosomes where they may be rapidly degraded so that no lysosomal pool can be detected. Indeed, a number of reports in the literature have suggested that CD4 is delivered to lysosomes following the addition of phorbol esters, where it is rapidly degraded (Baenziger *et al* 1991; Shin *et al* 1991; Petersen *et al* 1992; Ruegg *et al* 1992). Alternatively, endosomal compartments in some cell types are known to have acid proteolytic activity (Ludwig *et al* 1991; Casciola-Rosen and Hubbard 1991; Diment *et al* 1988; Roederer *et al* 1987), therefore, it is conceivable that CD4 is degraded in pre-lysosomal organelles.

3.2.1.2 Double Staining Studies.

The second approach which was used to try to characterize the juxta-nuclear compartment in which CD4 is seen 1 h after PMA treatment was costaining of different markers with CD4 by immunofluorescence. In unstimulated cells, CD4 is located at the cell surface, and intracellularly is found dispersed throughout the cytoplasm of the cell (Figure 26, A and B). Shortly after the addition of PMA, internalized CD4-anti-CD4 complexes were observed in a similar distribution to unstimulated cells. Longer incubations in the presence of PMA (1 h) caused a redistribution of the internalized CD4-anti-CD4 complexes to the perinuclear region of the cell (Figure 26, G and H), possibly later endocytic compartments. The transferrin receptor (TfR) and cation-independent mannose 6-phosphate receptor (CI-MPR) were used as markers for the early and late endosomes respectively (Griffiths *et al* 1988; 1990), lysosomal-associated membrane

proteins (lamp) 1 and 2 were used as markers for the lysosomes (Fukuda 1991), and β' -COP as a marker for the Golgi apparatus (Harrison-Lavoie *et al* 1993).

HeLa-CD4 cells were labelled with Q4120-TRITC for 2 h at 4°C, washed and warmed to 37°C for various times in the presence and absence of PMA. The cells were cooled, acid stripped, fixed, permeabilized and counter-stained with anti-TfR-FITC. The mouse mab anti-CD4 conjugate was used, as the anti-transferrin receptor conjugate was also a mouse mab. The use of these direct conjugates for immunofluorescence had the advantage that no second anti-mouse reagents were required, thereby minimizing the potential hazards of cross reacting antibodies.

In the absence of PMA internalized CD4-anti-CD4 complexes were observed to costain with antibodies to the TfR (Figure 32, A and B), suggesting that CD4 was within early endosomes. CD4-anti-CD4 complexes were also seen to costain with antibodies to the TfR 10 min after PMA treatment (Figure 32, C and D), indicating that during down-regulation, CD4 is endocytosed first into the early endosome. However, longer incubations in the presence of PMA induced an altered distribution of CD4-anti-CD4 complexes, such that the complexes are redistributed to the juxta-nuclear region of the cell, possibly to later endocytic organelles. This was investigated using costaining of CD4 with antibodies to the CI-MPR. When cells were prelabelled with Leu3a (anti-CD4 mab), warmed to 37°C in the presence of PMA for 1 h, processed and counter-stained with anti-CI-MPR antibodies (Leu3a was visualized using rhodamine-labelled goat anti-mouse, and CI-MPR was visualized using FITC-labelled goat anti-rabbit), the juxta-nuclear CD4 staining, was observed to significantly costain with antibodies to the CI-MPR (Figure 32, E and F). Delivery of CD4 to this compartment that can be costained with antibodies to the CI-MPR, was inhibited at 18°C in the presence of PMA for 1 h (Figure 32, G and H), so that the CD4 staining pattern was similar to unstimulated cells (Figure 32, A and B), suggesting that CD4 was still localized to early endosomes. In unstimulated cells, there was no significant costaining of CD4 and CI-MPR, with CD4 remaining in a dispersed punctate staining pattern throughout the cytoplasm of the cells (Figure 32, I and J). The distribution CI-MPR in the

HeLa-CD4 cells did not appear to be significantly affected by phorbol esters (compare Figure 32, D and H). However, by immunofluorescence it is difficult to conclude that the distribution of CI-MPR is not affected by PMA, since in the absence and presence of phorbol ester, the protein shows a very similar staining pattern. This problem could be resolved by using gold immunolabelling electron microscopy.

The costaining of CI-MPR with lysosomal markers such as lamp 1 and 2, could not be investigated directly, as all these antibodies were raised in rabbits. Therefore, costaining of 2C2 (mab prepared in house) with the lamp antibodies was first demonstrated. HeLa-CD4 cells were washed and fixed in a 50:50 mixture of acetone and methanol at -20°C , and stained with 2C2. Cells were counter-stained with either lamp 1 or 2. 2C2 was visualized with rhodamine-labelled goat anti-mouse, and the lamp antibodies were detected using FITC-labelled goat anti-rabbit (Figure 33). Extensive costaining of 2C2 was observed with both lamp 1 and 2, indicating that the antigen recognized by 2C2 is largely located in lysosomes.

The costaining of 2C2 with CI-MPR was now investigated, by fixing HeLa-CD4 cells in a 50:50 mixture of acetone and methanol at -20°C , and staining with antibodies to the CI-MPR followed by 2C2. CI-MPR, and 2C2 were visualized using FITC-labelled goat anti-rabbit and rhodamine-labelled goat anti-mouse respectively (Figure 34). The majority of CI-MPR and 2C2 did not costain, however, some costaining of 2C2 and CI-MPR was observed, but this could be lysosomal antigens *en route* to the lysosomes, through late endocytic compartments. In addition, CI-MPR did not significantly costain with a marker for the Golgi apparatus (Figure 35).

Previously published data has indicated in some cell types (normal rat kidney cells), the CI-MPR is concentrated in late endosomes (Griffiths *et al* 1988; 1990), whilst in other cell types (Chinese hamster ovary cells and rat clone 9 hepatocytes) it is distributed over the Golgi apparatus (Brown and Farquhar 1984; 1987). The distribution of the CI-MPR in the HeLa cells used in this study has not been extensively studied. However, the immunofluorescence data has indicated that the majority of the

CI-MPR in the HeLa-CD4 cells is not located within the Golgi apparatus (Figure 35), lysosomes (Figure 33 and 34), or early endosomes (Figure 32, A and B, and I and J), thus suggesting that the CI-MPR may be localized to later endocytic organelles. Fluid-phase endocytosis of a marker such as rhodamine-conjugated BSA, would help to resolve whether the CI-MPR is within endocytic organelles. It should be also noted at this point that costaining by immunofluorescence, does not necessarily mean that the proteins are within the same membrane-bound organelles, and this type of data, should ideally be supported by co-localization of the proteins at the electron microscopy level. However, due to unforeseen circumstances it was very difficult to perform this type of study.

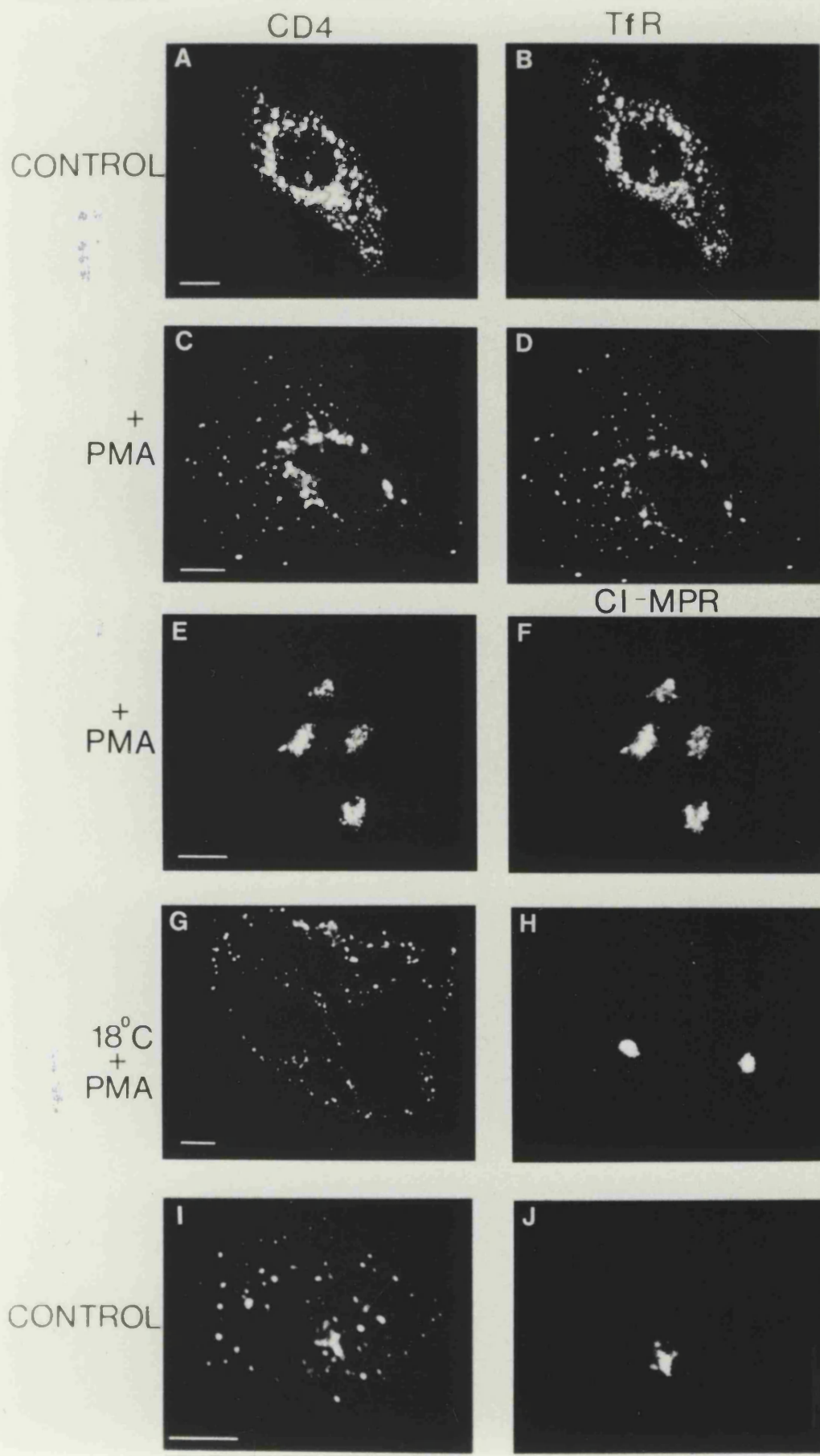
Taken together these experiments suggest that during phorbol ester-induced CD4 down-regulation, CD4 is diverted from the normal recycling pathway, and is delivered to a compartment in the perinuclear region of the cell that can be costained with antibodies to the CI-MPR, possibly late endocytic organelles. However, the CI-MPR in HeLa-CD4 cells has not been demonstrated to concentrate in late endosomes, as in other cell types (Griffiths *et al* 1988; 1990).

One question which arises is: is it the CD4 molecules which are redistributed to this perinuclear compartment, or are the early endosomes relocating to the perinuclear region? The strongest data which indicates that it is CD4 redistributed to the perinuclear organelles, comes from the CD4^{cyt}- molecules, which are not down-regulated in response to the addition of phorbol esters (Figure 9). When the HeLa-CD4^{cyt}- cells were prelabelled with Leu3a, warmed to 37°C in the presence of PMA for 1 h, cooled, acid stripped, fixed, permeabilized and counter-stained with antibodies to the CI-MPR, the cycling pool of CD4^{cyt}- remained in a dispersed punctate staining pattern (Figure 36), similar to that observed in unstimulated HeLa-CD4 (Figure 32, A), and there was no significant costaining with the CI-MPR. In addition, fluid-phase endocytosis assays in HeLa-CD4 treated with PMA for 2 h, demonstrates that LY in the presence of PMA, is internalized into early endosomes dispersed throughout the cytoplasm of the cell (Figure 37, A), in a similar fashion to untreated cells (Figure 37, B). Longer incubations in the presence of PMA, show that LY is

delivered to the juxta-nuclear region of the cell, but also has a dispersed punctate staining pattern over the cell, similar to unstimulated cells (Figure 37, C and D), suggesting that early endosomes are not redistributed the the perinuclear region of the cell. These observations suggest that phorbol esters do not cause early endosomes to relocate to the perinuclear region of the cell, but induce the redistribution of CD4.

Therefore, in addition to phorbol esters increasing the association of CD4 with coated pits, they cause CD4 to be diverted from the recycling pathway, to a compartment in the juxtannuclear region of the cell that can be costained with antibodies to the CI-MPR.

Figure 32. Costaining of internalized CD4 with the TfR or CI-MPR at 37°C or 18°C in HeLa-CD4 cells. Cells were labelled with Q4120-TRITC (A to D), or Leu3a (E to J) at 4°C, then either incubated at 37°C (A to F, and, I and J) or 18°C (G and H), for 10 min (C and D) or 1 h in the presence (C to H), or absence (A, B, I, and J) of 100 ng/ml PMA. The cells were fixed, permeabilized and internalized Leu3a was detected using anti-mouse rhodamine. In the absence of PMA at 37°C, CD4-containing vesicles (A) could be costained with FITC-labelled anti-TfR mab (B), but little or no costaining of CD4 (I) was observed with the CI-MPR (J). In the presence of PMA at 37°C, CD4 (C) costained with the TfR (D) after 10 min internalization, but after 1 h CD4 (E) costained with the CI-MPR (F). At 18°C costaining of CD4 (G) with the CI-MPR (H) was not evident. Optical sections were about 3 μm (A and B), or 1 μm (C to J) thick. Scale bars, A, B, E and F, 25 μm ; C, D, G and J, 10 μm .



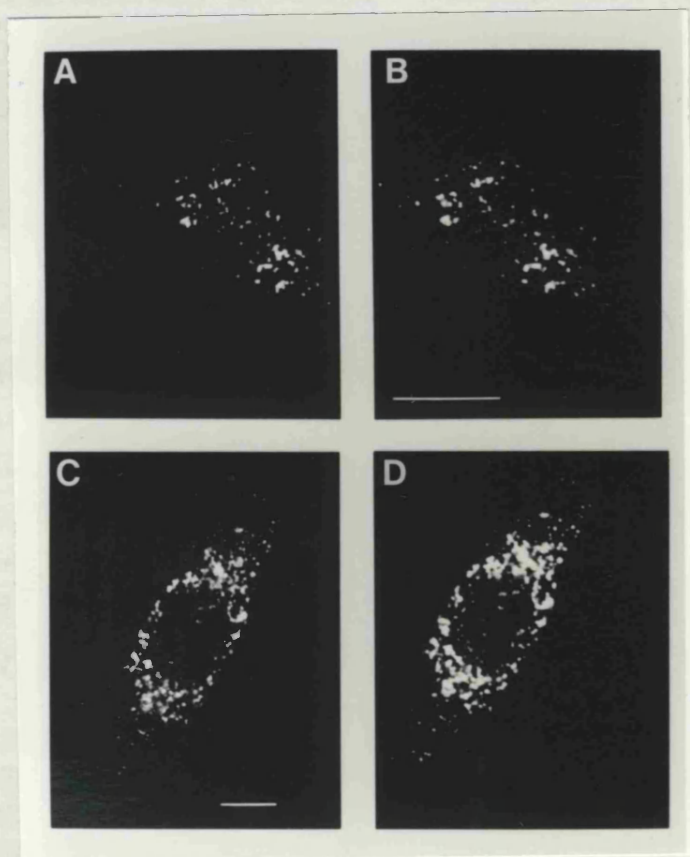


Figure 33. Costaining of 2C2 mab with lamp 1 and 2 in HeLa-CD4 cells. Cells were fixed in a 50:50 mixture of acetone and methanol at -20°C , and stained with 2C2 mab. 2C2 which was visualised with anti-mouse rhodamine, costained with both lamp 1 (A) and lamp 2 (C). The lamp antibodies were detected with anti-rabbit FITC. Optical sections $1\text{ }\mu\text{m}$ thick. Scale bars $10\text{ }\mu\text{m}$.

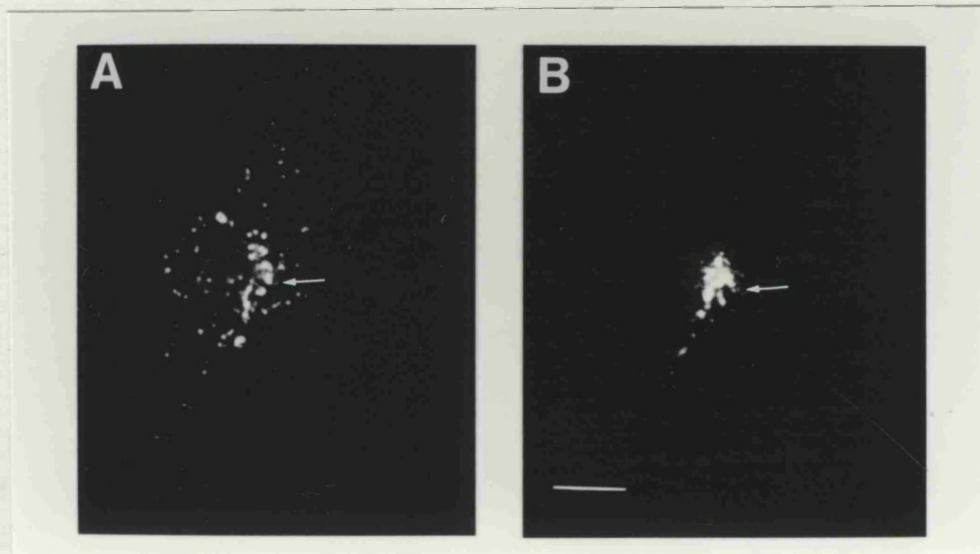


Figure 34. Costaining of the CI-MPR with 2C2 in HeLa-CD4 cells. Cells were fixed in a 50:50 mixture of acetone and methanol at -20°C , and stained with 2C2 mab and antibodies to the CI-MPR. 2C2 was detected using anti-mouse rhodamine, and the anti-CI-MPR antibodies were visualized using anti-rabbit FITC. Some costaining of the CI-MPR (B) and 2C2 (A) was observed (Arrows), but the majority of the CI-MPR did not costain with 2C2. Optical section $1\ \mu\text{m}$ thick. Scale bar $10\ \mu\text{m}$.

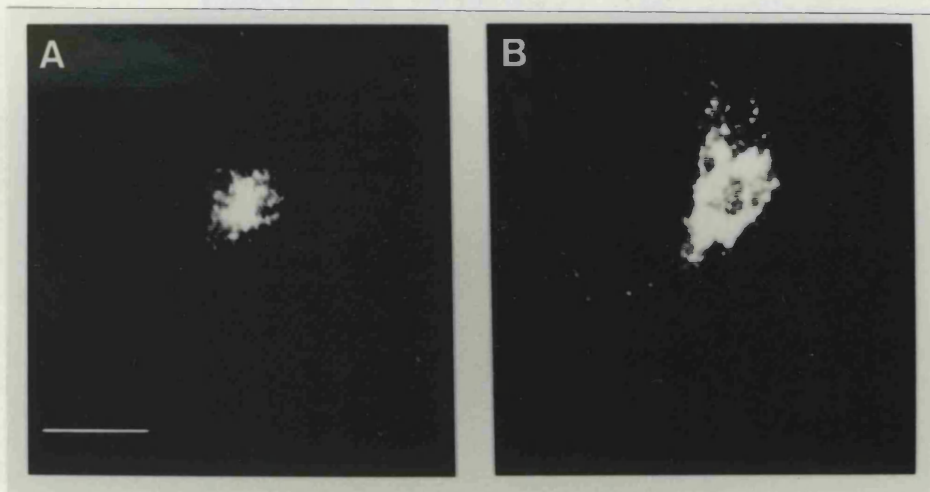


Figure 35. Costaining of the CI-MPR with 23C in HeLa-CD4 cells. Cells were fixed in 3% paraformaldehyde, permeabilized and stained with the antibody to the CI-MPR (A), followed by anti-rabbit FITC. No significant costaining of 23C (B) with CI-MPR was observed, (23C was visualized using anti-rat rhodamine). Optical section $2\ \mu\text{m}$ thick. Scale bar $25\ \mu\text{m}$.

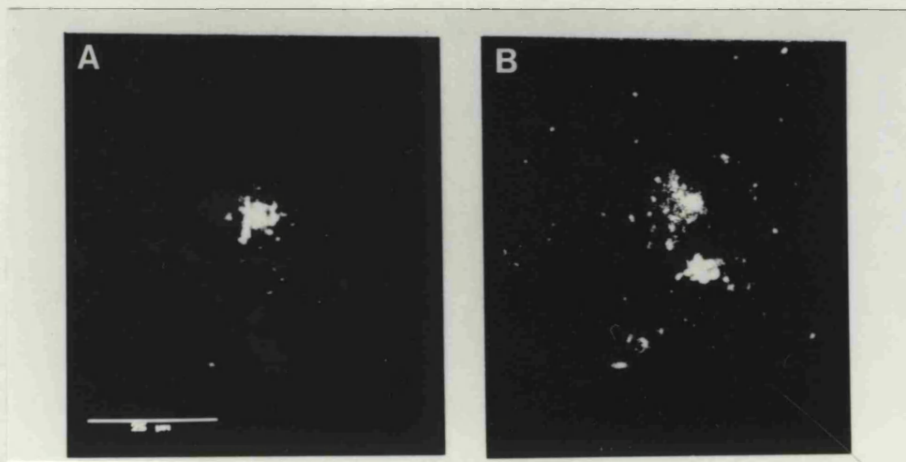


Figure 36. Costaining of CD4^{cyt-} with the CI-MPR in HeLa-CD4^{cyt-} cells. Cells were prelabelled with Leu3a (B), and warmed to 37°C for 1 h in the presence of 100 ng/ml PMA. The cells were fixed, permeabilized to reveal intracellular Leu3a which was detected using anti-mouse rhodamine, and subsequently counter-stained with antibodies to the CI-MPR (A). Optical section 1 μ m thick. Scale bar 25 μ m.

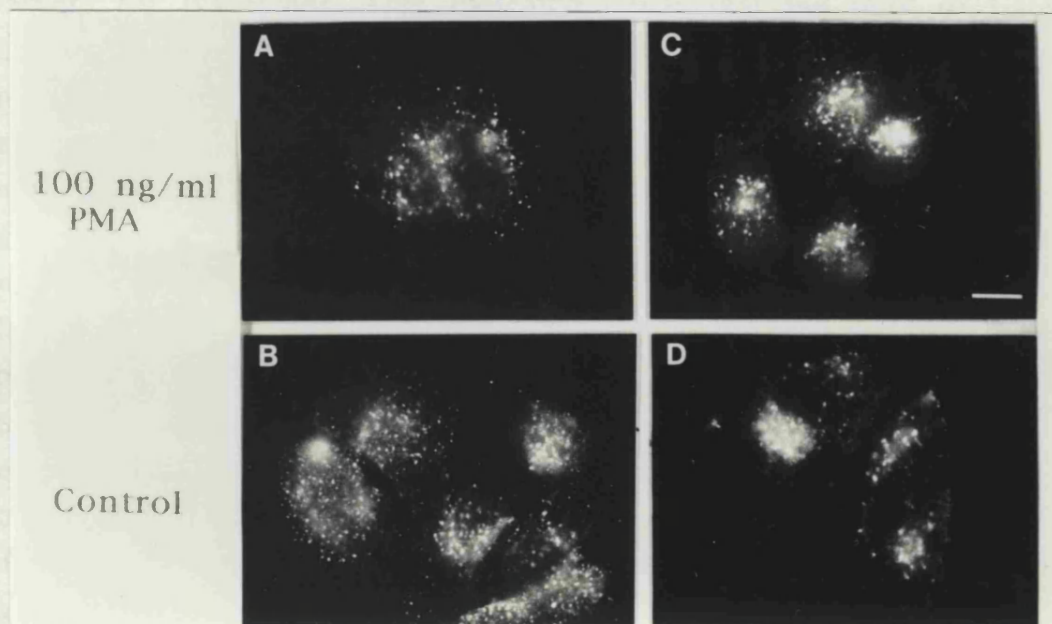


Figure 37. Fluid-phase endocytosis in the presence and absence of PMA. HeLa-CD4 cells on glass coverslips were incubated at 37°C in the presence (A and C) or absence (B and D) of 100 ng/ml PMA for 2 h, then 1 mg/ml LY was added to the cells in the continued presence (A and C) or absence (B and D) of 100 ng/ml PMA for 10 min (A and B), and 40 min (C and D). Cells were washed, fixed in 3% paraformaldehyde/0.02% glutaraldehyde, washed and mounted in moviol. Scale bar 10 μ m.

3.2.1.3 *The Intracellular Fate Of CD4 During PMA-Induced Down-Regulation.*

The data presented above indicate that CD4 is delivered to a perinuclear compartment that can be costained with antibodies to the CI-MPR during phorbol ester-induced down-regulation (Figure 32, E and F), and does not appear to reach lysosomes as judged by cell fractionation and immunofluorescence. As previously mentioned, there are a number of reports in the literature which suggest that CD4 is delivered to lysosomes following the addition of phorbol esters where it is rapidly degraded (Baenziger *et al* 1991; Shin *et al* 1991; Petersen *et al* 1992; Ruegg *et al* 1992). However, in this model system where CD4 is stably expressed in HeLa cells, CD4 does not appear to show extensive costaining with markers for lysosomes. This indicated either that the bulk of CD4 does not reach lysosomes or, if it does, it is rapidly degraded. In an attempt to determine whether phorbol esters induce the degradation of CD4, HeLa-CD4, HeLa-CD4^{cyt-} and HeLa-CD4^{S408A} were treated with PMA at 37°C for up to 8 h before fixing, permeabilizing and probing with Leu3a and rhodamine-labelled goat anti-mouse. Loss of fluorescent signal in the HeLa-CD4 cells after 4 h in the continued presence of PMA was evident, however, complete loss of the signal did not occur (Figure 38). It should be noted that this data suggests that the total cellular CD4 appears to behave in a morphologically similar manner to the cell surface pool of CD4.

No loss of fluorescence was evident in the HeLa-CD4^{cyt-} cells even after 8 h PMA treatment, and there was no obvious redistribution of CD4 (Figure 39), confirming that the cytoplasmic domain of CD4 is required for phorbol ester-induced down-regulation.

CD4^{S408A}, did show some loss of fluorescent signal (Figure 40), however, the loss of fluorescence did not appear to be as rapid as that observed with the HeLa-CD4 cells.

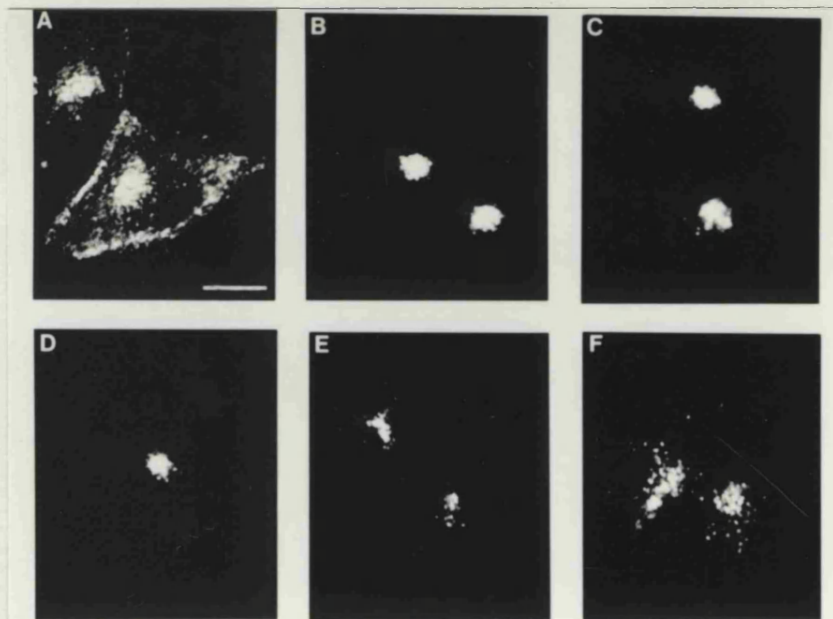


Figure 38. CD4 in HeLa-CD4 cells is degraded in the continued presence of PMA. HeLa-CD4 cells were incubated in the presence of 100 ng/ml PMA at 37°C for 0 (A), 1 (B), 2 (C), 4 (D), 6 (E), and 8 (F) h. Cells were cooled, fixed in paraformaldehyde, and permeabilized. CD4 was detected using 8 nM Leu3a followed by anti-mouse rhodamine. Images were taken under identical conditions.

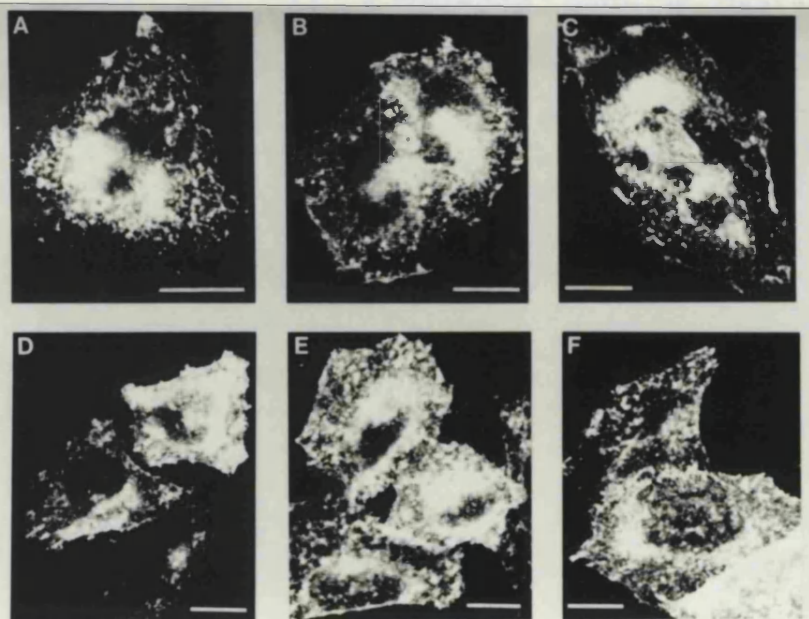


Figure 39. CD4^{cyt} in HeLa-CD4^{cyt} cells is not degraded in the continued presence of PMA. HeLa-CD4^{cyt} cells were incubated in the presence of 100 ng/ml PMA at 37°C for 0 (A), 1 (B), 2 (C), 4 (D), 6 (E), and 8 (F) h. Cells were cooled, fixed in paraformaldehyde, and permeabilized. CD4 was detected using 8 nM Leu3a followed by anti-mouse rhodamine. Images were taken under identical conditions.

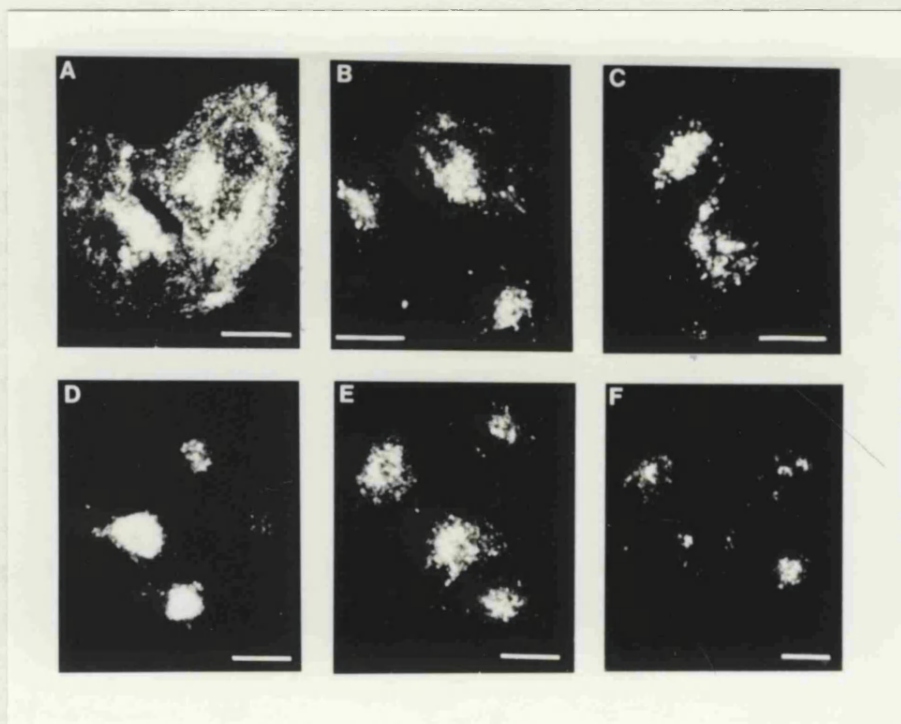


Figure 40. CD4^{S408A} in HeLa-CD4^{S408A} cells is degraded in the continued presence of PMA. HeLa-CD4^{S408A} cells were incubated in the presence of 100 ng/ml PMA at 37°C for 0 (A), 1 (B), 2 (C), 4 (D), 6 (E), and 8 (F) h. Cells were cooled, fixed in paraformaldehyde, and permeabilized. CD4 was detected using 8 nM Leu3a followed by anti-mouse rhodamine. Images were taken under identical conditions.

To measure degradation qualitatively each cell line (HeLa-CD4, HeLa-CD4^{cyt-} and HeLa-CD4^{S408A}) was treated with PMA for up to 8 h at 37°C, cell lysates for each time point were prepared, and the protein concentration per lysate was determined. Equal amounts of cell protein for each cell line were separated on non-reducing 10% SDS gels, transferred to nitrocellulose and immunoblotted for CD4. In HeLa-CD4 cells, CD4 was observed to be degraded, with a half time of 2 h 40 min in the continued presence of PMA (Figure 41, A and D). In contrast, CD4 in the HeLa-CD4^{cyt-} cell line showed very little or no degradation in the presence of PMA (Figure 41, B and D). The mutant form of CD4 where the serine at position 408 had been mutated to alanine, was degraded, but with slower kinetics than the wild type CD4; half time of degradation for CD4^{S408A} was approximately 5 h compared to 2 h 40 min for wild type CD4 (Figure 41, C and D). This suggests that serine 408 is an important feature in the cytoplasmic domain of CD4 involved the intracellular trafficking of the molecule.

This very qualitative set of experiments suggest that phorbol esters increase the rate of degradation of CD4. Degradation studies by Shin *et al* (1991) have suggested that CD4 is degraded with a $t_{1/2}$ of about 45 min in HeLa cells, which is approximately 3 and a half times faster than the $t_{1/2}$ calculated here. The discrepancy may be due to the way the experiments were performed. Shin *et al* (1991) metabolically labelled CD4, treated the cells with PMA, and immunoprecipitated CD4. This type of experiment is more quantitative than the qualitative immunoblotting experiments, provided that the CD4 is quantitatively immunoprecipitated. The $t_{1/2}$ of CD4 degradation obtained by Shin *et al* (1991) was from whole cell CD4, rather than the cell surface CD4 pool. The same is true for the immunoblotting experiments. Therefore, the $t_{1/2}$ of CD4 degradation obtained by both these methods may not reflect the degradation kinetics of cell surface CD4 in the presence of phorbol ester. Radiolabelling of the cell surface CD4, followed by PMA treatment and immunoprecipitation of CD4, would allow an accurate estimation of the degradation kinetics of cell surface CD4. Indeed, the one quantitative study on the degradation of cell

surface CD4 in the presence of phorbol ester, has suggested that ~90% is degraded in 8 h in human T cells (Ruegg *et al* 1992). However, the kinetics of CD4 degradation in T cells may be affected by the association of p56^{lck}, which must first dissociate from CD4, before CD4 can be down-regulated (Sleckman *et al* 1992; Yoshida *et al* 1992; Pelchen-Matthews *et al* 1993).

Phorbol esters, such as PMA activate protein kinase C (Castagna *et al* 1982), causing the transient phosphorylation and modulation of cell surface CD4 (Acres *et al* 1986; Blue *et al* 1987; Hoxie *et al* 1988; Maddon *et al* 1988; Shin *et al* 1990; 1991). The results presented here demonstrate that CD4 down-regulation is a rapid process, that can occur in the absence of p56^{lck}, and results in: (1) an increased association of CD4 with coated pits and vesicles; (2) a doubling of the CD4 intracellular pool at steady state; (3) altered endosomal sorting, so that CD4 in non-lymphoid cells is sorting from the recycling pathway, to a perinuclear compartment that can be costained with antibodies against the CI-MPR; and, (4) increased CD4 degradation. Although little costaining of CD4 and lysosomal markers was found, CD4 appeared to be degraded, with a half time of 2 h 40 min. Taken together, these results show that phorbol esters have multiple effects on the internalization and intracellular sorting of CD4, and indicate that phosphorylation of CD4 is likely to play some role in the interaction of CD4 with the endocytic pathway (See Section 3.1.5).

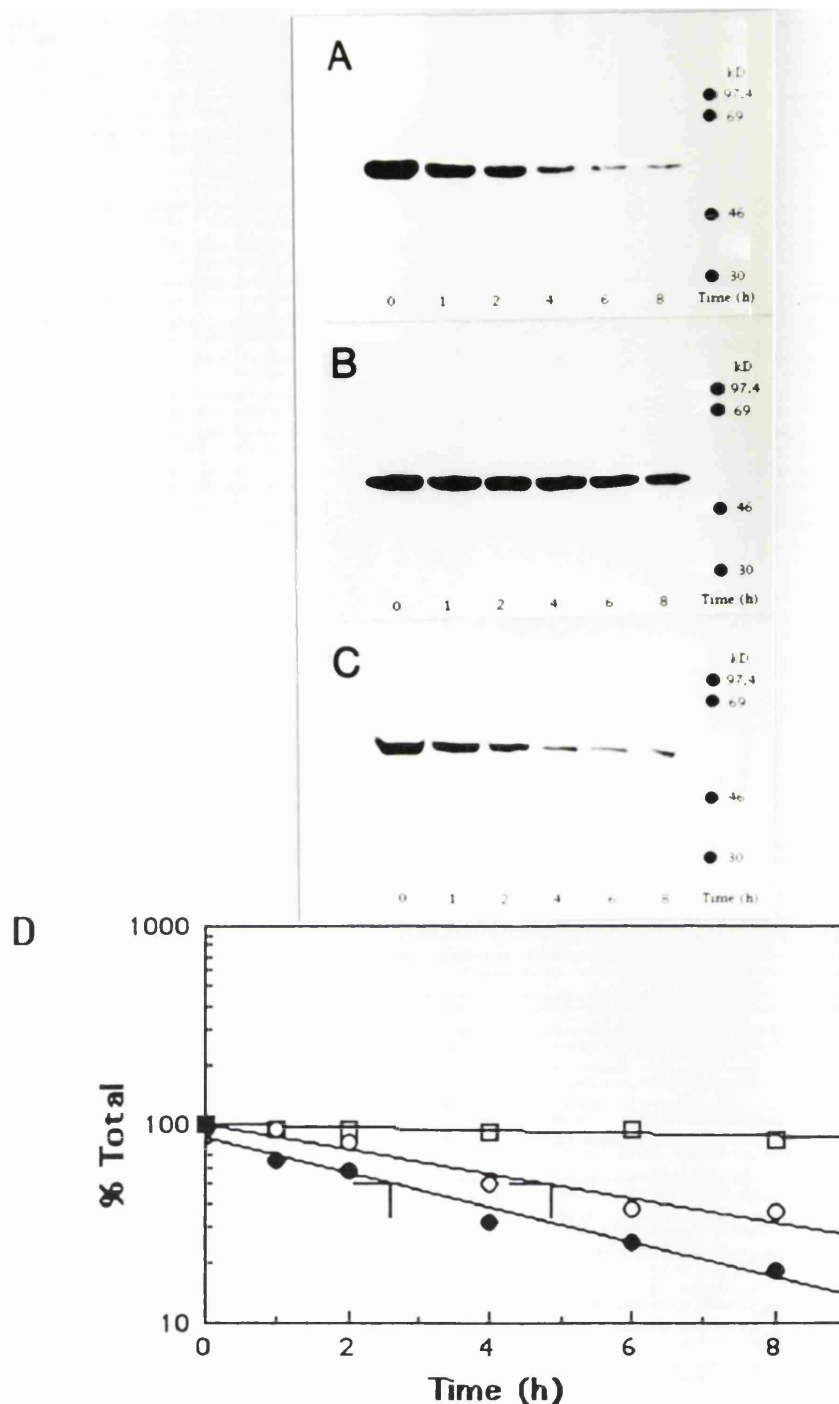


Figure 41. CD4 is degraded in the continued presence of PMA. HeLa-CD4 (A), HeLa-CD4^{cyt-/-} (B), and HeLa-CD4^{S408A} (C) were incubated in the presence of 100 ng/ml PMA at 37°C for various times. Cells were cooled, washed, lysed and analysed by non-reducing SDS-PAGE and CD4 immunoblotting. The immunoblots were quantified (D) by analysis of a digitized image in the program Optilab. HeLa-CD4, closed circles; HeLa-CD4^{cyt-/-}, open squares; HeLa-CD4^{S408A}, open circles.

3.3 COMPARISON OF THE HELA-CD4 MODEL SYSTEM WITH THE T CELL LINE, SUPT1.

As previously indicated, CD4 on the surface of SupT1 cells is rapidly modulated in response to the addition of phorbol esters (Figure 7), and cell surface CD4 levels remain low for about 48 h. In the absence of phorbol esters, CD4 on the surface of SupT1 cells is endocytosed very slowly (Pelchen-Matthews *et al* 1991). The low rate of CD4 internalization is due to its interaction with p56^{lck} (Pelchen-Matthews *et al* 1992), which inhibits CD4 from interacting with the endocytic pathway. However, upon the addition of phorbol esters, p56^{lck} dissociates from CD4 with a half time of 1-2 min (Pelchen -Matthews *et al* 1993), and CD4 endocytosis is increased more than 20 fold, from 0.2% per min to 4.2% per min.

Membrane trafficking has not been studied in detail in T cells, therefore the intracellular targeting of CD4 during phorbol ester-induced down-regulation was investigated in the T lymphoma-derived cell line, SupT1.

To determine whether CD4 on SupT1 cells is delivered to compartments that labelled for CI-MPR, as found in the HeLa-CD4 model system, SupT1 cells were prelabelled with Leu3a at 4°C, and warmed to 37°C in the presence of PMA for 1 h. The cells were cooled, acid stripped, fixed and permeabilized, and counter stained with antibodies to the CI-MPR. The Leu3a and CI-MPR were visualized using rhodamine-conjugated goat anti-mouse and FITC-conjugated goat anti-rabbit, respectively. The intracellular punctate CD4 staining that was observed, costained with antibodies to the CI-MPR (Figure 42), a result similar to that in the HeLa-CD4 model system. The CI-MPR in SupT1 cells did not significantly costain with the 2C2 mab, suggesting that the majority of CI-MPR is not localized to lysosomes (Figure 42, C and D).

Therefore, these data suggest that CD4 in lymphoid cells is delivered to a compartment that can be costained for the CI-MPR, and does not appear to reach lysosomes in a 1 h incubation in the presence of PMA, or if it does it is rapidly degraded.

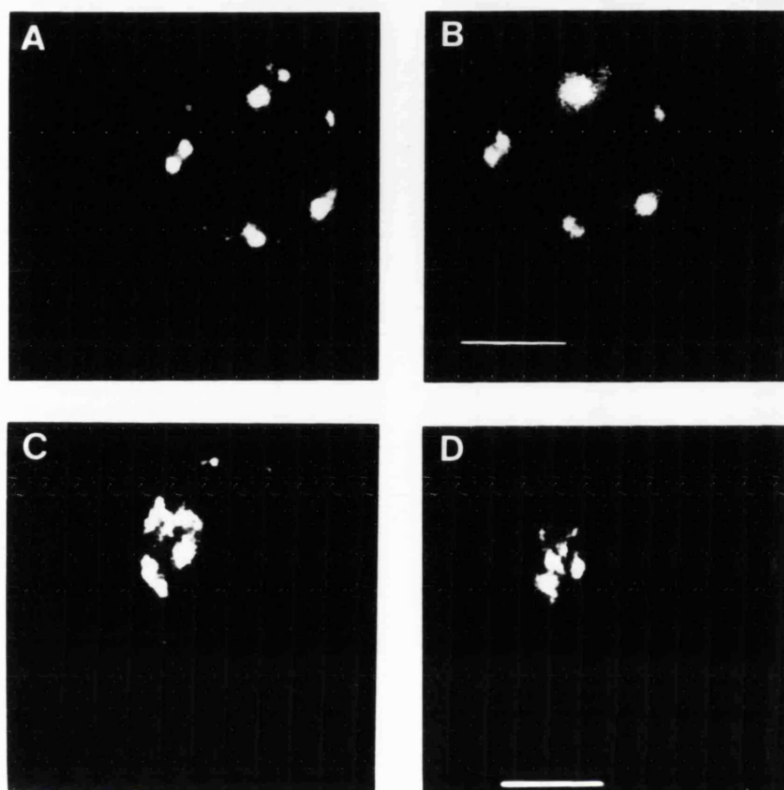


Figure 42. Costaining of internalized CD4 with the CI-MPR in the presence of PMA, and costaining of the CI-MPR with a lysosomal marker, 2C2, in SupT1 cells. SupT1 cells, growing exponentially, were labelled with 8 nM Leu3a (A), and warmed to 37°C in the presence of 100 ng/ml PMA. Cells were cooled, washed, fixed, and permeabilized to reveal intracellular Leu3a, which was visualized using anti-mouse rhodamine. Cells were counter-stained with anti-CI-MPR followed by anti-rabbit FITC, and CD4 containing vesicles were observed to costain with the CI-MPR (B). SupT1 cells were fixed in a 50:50 mixture of acetone and methanol at -20°C, and stained with the 2C2 mab and antibodies to the CI-MPR. 2C2 was visualized with anti-mouse-rhodamine (C), and the anti-CI-MPR antibodies were detected using anti-rabbit-FITC. Optical section 1 μm thick. Scale bar 5 μm .

To determine whether the CD4 was degraded in the continued presence of phorbol esters, cells were incubated in the presence of PMA for up to 8 h at 37°C. The cells were cooled, fixed, permeabilized and stained with Leu3a and rhodamine-conjugated goat anti-mouse. Initially the bulk of the CD4 was at the cell surface (Figure 43, A), but after 1 h PMA treatment punctate intracellular CD4 staining was observed. The fluorescent signal was seen to diminish the longer the incubation time in the presence of PMA, suggesting that the CD4 was being degraded (Figure 43). A similar experiment was carried out, only instead of analysing the CD4 by immunofluorescence, immunoblotting was used to try to quantitate this degradation. SupT1 cells were warmed to 37°C in the presence of PMA up to 8 h, cooled and cell lysates prepared for each time point. The protein level per lysate was determined using the BCA protein assay. Lysates containing equal amounts of cellular protein, were separated on non-reducing 10% SDS gels, the proteins were transferred to nitrocellulose, and immunoblotted for CD4 (Figure 44, A). The half life of CD4 in the continued presence of PMA was 3 h 20 min (Figure 44, B), which was slightly greater than that found for wild type CD4 in the HeLa-CD4 cells.

The turnover of cell surface CD4 (virtually the total cellular CD4) was analysed using a cell surface iodination assay, a method developed by Reid (1990 Ph.D. thesis), which was a modification of the methods used by Bretscher and Lutter (1988); Thompson *et al* (1987). Briefly, the labelling reagent was prepared by iodinating sulpho-SHPP for 15 min at 4°C, and was then added to cells in 0.1 M Na₂HPO₄ for 20 min on ice. The cells were washed with PBS/10% FCS, before being divided into seven equal aliquots and warmed to 37°C in the presence or absence of PMA for up to 8 h. The cells were cooled and cell lysates were prepared for each time point. The lysates were precleared by centrifuging at 100,000 g, and then by adding protein A sepharose beads at 4°C for 2 h. Immunoprecipitation of CD4 was carried out at 4°C with anti-CD4-conjugated protein A sepharose beads (immunoprecipitation was performed on lysates containing equal amounts of cellular protein. Protein levels were determined using the BCA protein assay after the preclearing steps). The anti-CD4 protein A

sepharose beads quantitatively precipitated CD4 from cell lysates (Figure 45). The washed precipitates were eluted from the beads using reducing SDS sample buffer, and separated on 10% SDS gels. The gels were dried and exposed to X-ray film (Figure 46). Cell surface CD4 was seen to be degraded with half time of about 3 h in the continued presence of PMA, a similar result found in the immunoblotting experiment. However, in the absence of PMA very little degradation of CD4 was observed, with only 25% of the cell surface pool being degraded in 8 h. The half time of degradation of cell surface CD4 on SupT1 cells in the absence of phorbol ester was ~20 h, thus indicating that PMA dramatically increases that rate of CD4 degradation in these cells.

The results obtained with SupT1 cells are similar to those previously published on human T cells, where ~90% of the cell surface CD4 was degraded in 8 h in the presence of phorbol ester (Ruegg *et al* 1992). Unfortunately, a half time for the degradation of cell surface CD4 was not published in the study on the T cells. The results in SupT1 cells suggest that 85% of the cell surface CD4 is degraded in 8 h (Figure 46, B). Although the fluorescence experiments suggested that CD4 was not reaching lysosomes after 1 h in the presence of PMA, it is possible that CD4 may be degraded in pre-lysosomal organelles, as in some cell types endosomal compartments are known to have acid proteolytic activity (Ludwig *et al* 1991; Casciola-Rosen and Hubbard 1991; Diment *et al* 1988; Roederer *et al* 1987).

Thus, in SupT1 cells, as in HeLa-CD4 cells, cell surface CD4 is down-regulated in response to the addition of phorbol esters, and is delivered to a compartment that can be counter-stained with antibodies for the CI-MPR. Significantly, CD4 in both the SupT1 and HeLa cells is degraded with similar kinetics in the continued presence of phorbol ester, suggesting that transport through the endocytic pathway may be similar in the two cell types.

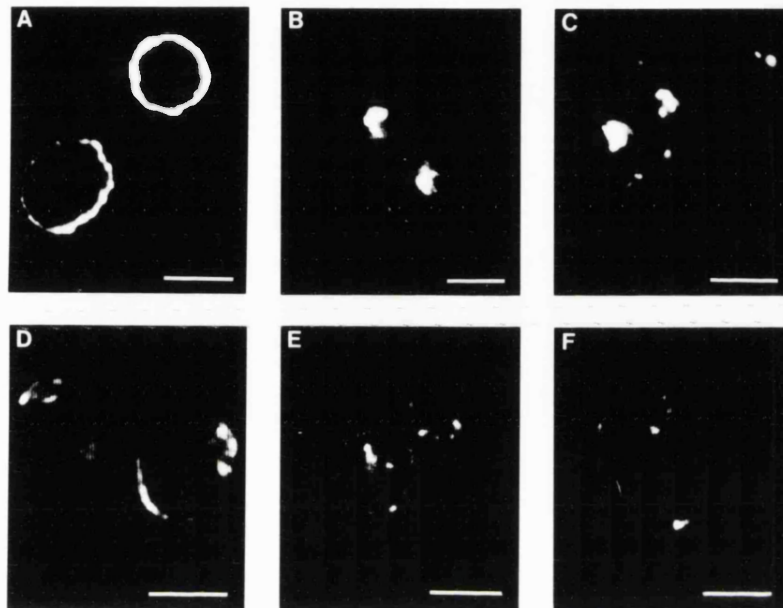
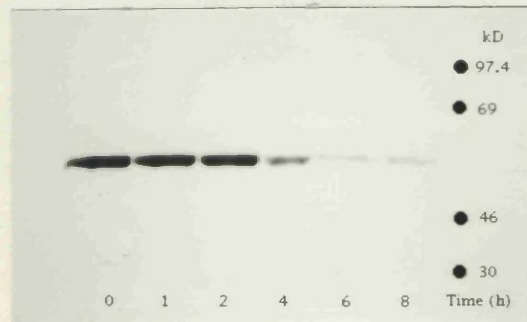


Figure 43. Degradation of CD4 in SupT1 cells in the continued presence of PMA. SupT1 cells, growing exponentially, were warmed to 37°C in the presence of 100 ng/ml PMA for 0 (A), 1 (B), 2 (C), 4 (D), 6 (E), and 8 (F) h. Cells were cooled, washed, fixed, and permeabilized. CD4 was detected using 8 nM Leu3a, followed by anti-mouse rhodamine. Scale bars 5 mm. Images were taken under identical conditions.

A



B

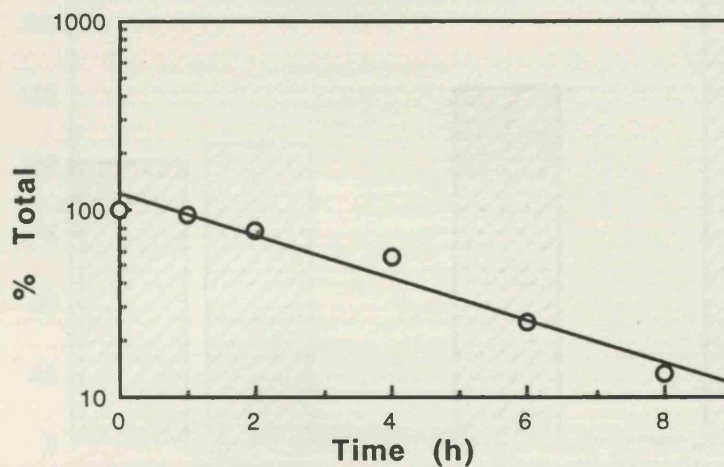
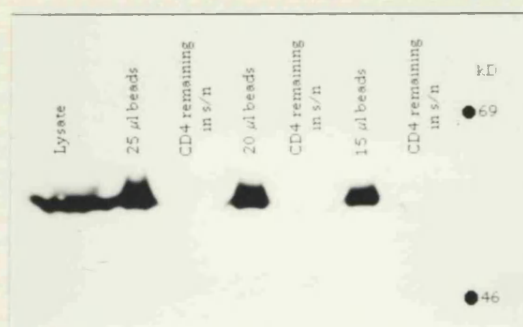


Figure 44. Degradation of CD4 in SupT1 cells in the continued presence of PMA. SupT1 cells, growing exponentially, were warmed to 37°C in the presence of 100 ng/ml PMA for various times. Cells were cooled, washed, and lysates prepared, which were analysed by non-reducing SDS-PAGE and CD4 immunoblotting (A). The immunoblots were quantified (B) by analysis of a digitized image in the program Optilab.

A



B

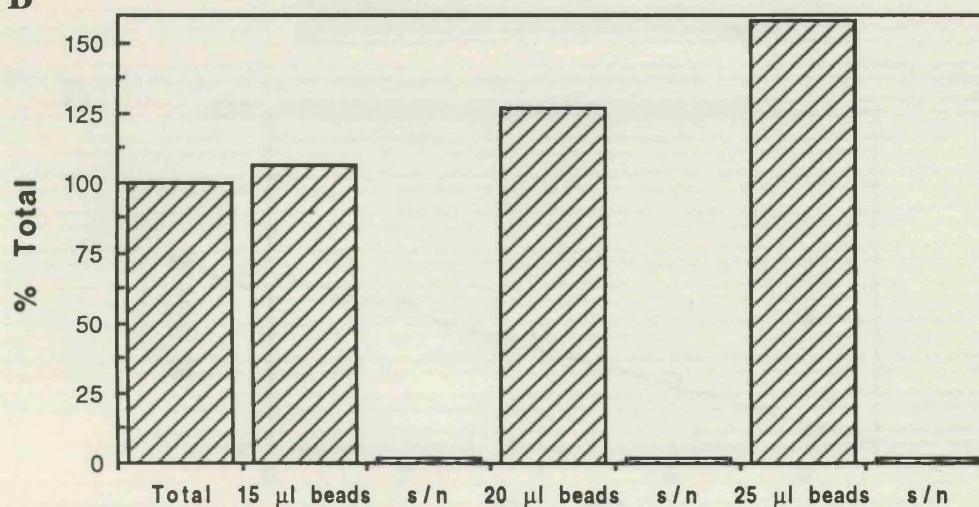


Figure 45. Quantitative immunoprecipitation of CD4 using anti-CD4 protein A sepharose beads. From one 100 mm plate of HeLa-CD4 cells a lysate was prepared in 200 μ l Tris lysis buffer pH8 (see Materials and Methods). Detergent-insoluble material was removed by centrifugation (13 000 rpm in a Heraeus microfuge at 4°C for 20 min), and the supernatant was recovered. To 50 μ l aliquots of the supernatant, 15 μ l, 20 μ l, and 25 μ l of prewashed anti-CD4 protein A sepharose beads were added for 1 h at 4°C with gentle mixing. The supernatants were recovered, and the beads washed, and samples were analysed by non-reducing SDS-PAGE and CD4 immunoblotting (A). The immunoblots were quantified (B) by analysis of a digitized image in the program Optilab. The increase in signal with increasing volume of beads used, may be due to some protein eluting from the beads, and reacting with anti-mouse-HRP reagent.

A



B

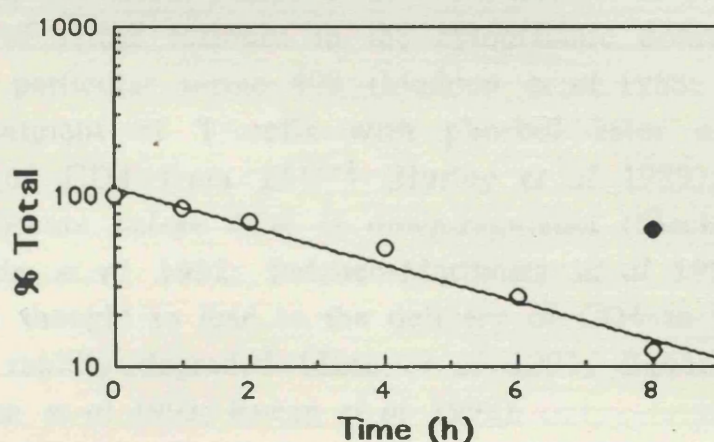


Figure 46. Degradation of cell surface CD4 in SupT1 cells in the presence (open circles) or absence (closed circles) of PMA. SupT1 cells, growing exponentially, were surface iodinated using ^{125}I -sulfo-SHPP, warmed to 37°C in the presence or absence of 100 ng/ml PMA for various times. Cells were cooled, washed and cell lysates prepared. Lysates were immunoprecipitated using 20 μl prewashed anti-CD4 protein A sepharose beads overnight at 4°C . The beads were resuspended in 20 μl reducing 1 x sample buffer, washed and analysed by SDS-PAGE. The gels were stained, destained, dried, and autoradiographed at -80°C (A). The autoradiographs were quantified (B) by analysis of a digitized image in the program Optilab.

4. DISCUSSION

Stimulation of T cells by antigen in association with MHC class II, or by cross-linking antibodies, leads to the modulation of cell surface CD4, suggesting that the control of cell surface CD4 is important for T cell function and physiology. The down-regulation of CD4 that follows T cell activation, can be mimicked by treating cells with phorbol ester, and permits biochemical and morphological analysis of the mechanisms that control cell surface CD4 expression. CD4 modulation is believed to occur by endocytosis (Hoxie *et al* 1986; 1988; Petersen *et al* 1992), and involves phosphorylation (Acres *et al* 1986; Blue *et al* 1987; Hoxie *et al* 1988) of serine residues in the cytoplasmic domain of the molecule, in particular serine 408 (Maddon *et al* 1988; Shin *et al* 1990). Treatment of T cells with phorbol ester causes the dissociation of CD4 from p56^{lck} (Hurley *et al* 1989), and this dissociation occurs before CD4 is down-regulated (Sleckman *et al* 1992; Yoshida *et al* 1992; Pelchen-Matthews *et al* 1993). CD4 modulation is thought to lead to the delivery of CD4 to lysosomes, where it is rapidly degraded (Shin *et al* 1991; Baenziger *et al* 1991; Petersen *et al* 1992; Ruegg *et al* 1992).

This thesis has examined the cellular mechanisms of phorbol ester-induced CD4 modulation, and the interaction of CD4 with the endocytic pathway during these processes. The results indicate that down-regulation involves rapid removal of CD4 from the cell surface, by endocytosis, which occurs through coated pits, and involves a PMA-induced increase in the rate of CD4 uptake. There is no stimulation of coated vesicle formation, but an increase in association of CD4 with existing coated pits. This implies the presence of an endocytosis signal activated by phosphorylation in the cytoplasmic domain of CD4. In the absence of phorbol ester CD4 is internalized through coated pits and is delivered to the early endosome, from where it is recycled to the cell surface. However, in the presence of PMA CD4 is diverted away from this recycling pathway, and is delivered to a compartment in the perinuclear region of the cell that can be costained with antibodies to the cation independent mannose 6-phosphate receptor. Qualitative studies have suggested that CD4 is degraded in the

continued presence of PMA. In addition, the constitutive endocytosis and recycling of CD4 in HeLa-CD4 cells may involve cycles of phosphorylation and dephosphorylation, as indicated by inhibition of kinase and phosphatase activities.

4.1 PMA-Induced CD4 Endocytosis.

CD4 expressed in non-lymphoid cells such as HeLa-CD4 and NIH3T3-CD4 cells, is constitutively endocytosed through coated pits and vesicles (2-4% per min - Pelchen-Matthews *et al* 1989; 1991; Marsh *et al* 1990). After 2 min following the addition of PMA, there is a 3 fold increase in the rate of CD4 internalization (Figure 11). In some cells, such as macrophages, phorbol ester has been shown to enhance the uptake of fluid phase markers (Swanson *et al* 1985). However, control experiments indicate that PMA does not affect the initial uptake of horseradish peroxidase (HRP) or lucifer yellow (LY) in these cells (Figure 13), nor does it appear to modulate the endocytosis and cycling properties of mutant CD4 molecules lacking a cytoplasmic domain which is endocytosed by bulk flow (Pelchen-Matthews *et al* 1991; 1993). These results suggest that the enhanced endocytosis of CD4 induced by PMA is not due to a general stimulation of vesicular trafficking from the plasma membrane, but must be due to an increased association of CD4 with endocytic coated pits. This was investigated using hypertonic medium, which inhibits normal coated pit assembly (Hansen *et al* 1991), and electron microscopy. Hypertonic medium almost completely inhibited PMA-induced CD4 down-regulation (Figure 14), thus suggesting that down-regulation occurs via coated pits and vesicles. Observations at the electron microscope level confirmed this. When the distribution of anti-CD4/protein A-gold complexes was quantitated, it was found that 2 min following the addition of PMA, there was approximately a 3 fold increase in the amount of gold particles associated with coated pits and vesicles (Figure 16 and Table 2). This increase can account for the enhanced CD4 endocytosis kinetics observed in the presence of PMA in the biochemical assay (Figure 11). Interestingly, the increased association of CD4 with coated pits is seen just before the enhanced endocytosis of CD4

(the lag shown in the inset in Figure 11). During this 2 min time period anti-CD4 located in coated pits at the plasma membrane is still accessible to the acid stripping procedure in the biochemical assay, therefore account for this lag period. This lag period observed in PMA-induced CD4 endocytosis may result from the time required to activate PKC, phosphorylate CD4 and recruit CD4 to coated pits.

The ability of a receptor, such as TfR or LDL-R, to cluster into coated pits, is dependent on the presence of an endocytosis signal within the cytoplasmic domain. For a number of receptors, a tyrosine-based motif has been identified, which functions as an internalization signal (Section 1.5.a). These endocytosis signals frequently contain a tyrosine residue within short sequences (~6 amino acids) and show a tendency to form a tight turn (discussed in Section 1.5.b), and mutation of amino acids which disrupt the turn, destroy these internalization signals.

The cytoplasmic domain of CD4 does not possess a tyrosine-based endocytosis signal, and there is only one aromatic amino acid (Phe426), which is near the C-terminus. This region of the cytoplasmic domain is dispensable for down-regulation (Shin *et al* 1991), and is therefore unlikely to contain any structural features important for CD4 internalization. A di-leucine in the cytoplasmic domain of CD4 (Leu413 and Leu414), as well as hydrophobic residues methionine 407 and isoleucine 410, however, have been shown to be required for phorbol ester-induced down-regulation (Shin *et al* 1991).

A di-leucine motif (Leu131 and Leu132) has been shown to function as an endocytosis and lysosomal targeting signal in the CD3 γ chain (Letourneur and Klausner 1992), and a recently published study has indicated that the di-leucine signal requires a nearby serine residue (Ser126), within a PKC consensus sequence, which when phosphorylated appears to activate the endocytosis of the CD3 γ chain (Dietrich *et al* 1994). This implies that the endocytosis signal on CD3 γ can be switched from an inactive to a functional state by phosphorylation.

The di-leucine in the cytoplasmic domain of CD4 is essential for down-regulation (Shin *et al* 1991), and is also located between two serine residues (Ser408 and Ser415) which are

phosphorylated following the addition of phorbol ester (Acres *et al* 1986; Hoxie *et al* 1988; Shin *et al* 1990). The importance of phosphorylation on these serine residues is demonstrated by the impairment of endocytosis and down-regulation of the CD4^{S408A} mutant (Table 4 and Figure 9), however, modulation of this mutant can be restored when the alanine at position 404 is mutated serine (Ser404 is phosphorylated in this mutant - Shin *et al* 1991).

These data imply that a phosphoserine-dileucine signal may mediate the recruitment of CD4 into coated pits, however, the mechanism of this interaction is still not clear. The residues surrounding Ser408 show a strong tendency to form an α helix, with Met407, Ile410, Leu413 and Leu414 arranged on the same side of the helix (Shin *et al* 1991). The role of phosphorylation in coated vesicle-mediated internalization has been controversial (Trowbridge *et al* 1993). However, phosphorylation of the cytoplasmic domain of CD4, particularly Ser408, might alter the disposition of the sequences involved in endocytosis, thereby creating or enhancing an internalization signal.

The results presented in this thesis indicate that PMA directly increases the association of CD4 with coated pits and vesicles and therefore the rate of CD4 endocytosis, thus implying that this may be one situation where phosphorylation of a serine residue close to a di-leucine creates or enhances an internalization signal.

4.2 Phosphorylation Of The Cytoplasmic Domain Of CD4 May Be An Important Feature In The Constitutive Internalization And Intracellular Trafficking Of CD4.

It is clear that PMA enhances CD4 endocytosis in HeLa-CD4 cells. Down-regulation of CD4 has now been demonstrated to occur by endocytosis via coated pits and vesicles (Figure 16 and Table 2; Pelchen-Matthews *et al* 1993), and addition of phorbol ester to cells causes the rapid and transient phosphorylation of CD4 (Acres *et al* 1986; Blue *et al* 1987; Hoxie *et al* 1988) particularly at serine 408 (Shin *et al* 1990). In HeLa-CD4 cells, CD4 is constitutively internalized through coated pits in the absence of any PKC activators (Pelchen-Matthews *et al* 1989; 1991;), however, there

are no studies which indicate that phosphorylation of the cytoplasmic domain of CD4 is required for its constitutive internalization. Two pieces of data suggest that phosphorylation of the CD4 cytoplasmic domain may also be required for this constitutive CD4 uptake. Firstly, when serine 408 is mutated to alanine the endocytosis rate of CD4 is reduced 3 fold (Table 4), and secondly, the non-specific kinase inhibitor, Stsp, blocks PMA-induced down-regulation of CD4 (Figure 17). A concentration of 0.1 μ M Stsp completely inhibited PMA-induced CD4 down-regulation, indicating that phosphorylation of the cytoplasmic domain of CD4 by kinase is required for modulation. In addition, at higher concentrations of Stsp the cell surface pool of CD4 was increased to ~140% compared to control cells. The intracellular pool of cycling CD4 is about 40% of the total CD4 cycling pool in the HeLa-CD4 cells, and given that the up-regulation of CD4 in the presence of higher concentrations of Stsp is ~40%, these data could be explained by an inhibition of CD4 endocytosis, while recycling is unaffected. Alternatively, higher concentrations of Stsp could stimulate recycling of CD4. These effects on the cycling of CD4 could both individually result in the transfer of the intracellular CD4 cycling pool to the cell surface.

The effect of Stsp on the constitutive endocytosis of CD4 was tested directly in an internalization assay (Figure 18). In the initial 10 min of the assay Stsp inhibited CD4 endocytosis 3 fold (from 2% per min to 0.8% per min), such that CD4 internalization was reduced to that of the CD4^{cyt-} molecules, which are endocytosed by bulk flow (Pelchen-Matthews *et al* 1991). These data suggest that the intracellular cycling pool of CD4 is transferred to the cell surface as a result of Stsp inhibiting the internalization of CD4, and this relocation of CD4 occurs in about 30 min in the presence of Stsp (Figure 19).

The initial internalization of the CD4^{cyt-} molecules (first 10 min of the assay) did not appear to be significantly affected by Stsp (Figure 18, B), however longer incubations in the presence of Stsp resulted in a reduction of the intracellular pool of CD4^{cyt-} molecules. These data suggest that Stsp inhibits the vesicular trafficking from the plasma membrane, which is not surprising in view of the fact that dynamin, a molecule that has been shown to

be required for receptor-mediated endocytosis via coated pits, is regulated by phosphorylation (van der Blik *et al* 1993; Herskovits *et al* 1993; Robinson *et al* 1993). The inhibition of vesicular trafficking from the cell surface was investigated further in a fluid-phase internalization assay (Figure 20). Stsp appeared to inhibit the fluid-phase uptake of HRP 1.5 fold compared to untreated cells in the initial 10 min of the assay. A specific PKC inhibitor (CGP41, 251) gave a similar result to Stsp (Figure 21). These data suggest that the reduced kinetics of constitutive CD4 internalization in the presence of Stsp may at least be in part due to an inhibition of vesicular trafficking from the cell surface. However, the reduced constitutive endocytosis of CD4 in the presence of Stsp is far more dramatic than the observed inhibition of fluid-phase and CD4^{cyt-} uptake. This implies that phosphorylation may be involved in the constitutive internalization of CD4.

Based on these observations in the presence of Stsp, a model for the involvement of phosphorylation in the constitutive endocytosis of CD4 in the HeLa-CD4 cells was proposed (Figure 22). Mutant forms of CD4 which lack phosphorylation sites (CD4^{cyt-} and CD4^{S408A}) are endocytosed by bulk flow; an internalization rate above bulk flow uptake (0.8% per min) is enhanced. Phorbol esters enhanced the internalization of CD4 considerably; but the constitutive endocytosis is also significantly higher than bulk flow uptake, therefore suggesting that CD4 may undergo basal phosphorylation. In HeLa-CD4 cells, CD4 is constitutively recycled to the plasma membrane (Pelchen-Matthews *et al* 1989; Marsh *et al* 1990). However, when CD4 molecules are phosphorylated following the addition of phorbol esters (Acres *et al* 1986; Blue *et al* 1987; Hoxie *et al* 1988; Shin *et al* 1990), they are sorted to a compartment in the perinuclear region of the cells, and the recycling of CD4 is reduced (Figure 26; Pelchen-Matthews *et al* 1993). These data suggest that for CD4 to recycle to the plasma membrane there may be a requirement to dephosphorylate its cytoplasmic domain (Figure 22, steps 3 to 5).

Based on the data obtained with Stsp, the model proposes that, CD4 is phosphorylated at the plasma membrane, presumably by PKC, (Figure 22, step 1), allowing it to cluster in coated pits, and be

internalized and delivered to early endosomes (step 2). At some unknown stage, CD4 may be dephosphorylated by phosphatase (step 3), therefore allowing it to recycle back to the plasma membrane (steps 4 and 5).

The possible role of dephosphorylation in the intracellular trafficking of CD4 proposed in the model was tested by using the phosphatase inhibitor OKA (Cohen *et al* 1990).

In contrast to the observations with Stsp, OKA caused an accumulation of intracellular CD4 (Figure 23), suggesting either that OKA was stimulating the constitutive endocytosis of CD4 or inhibiting its recycling from the intracellular pool. This was tested in an endocytosis assay (Figure 24). OKA did not appear to affect the constitutive internalization of CD4, however, after 60 min in the presence of the drug, the intracellular cycling pool of CD4 was increased by about 20%, suggesting that OKA inhibits the recycling of CD4 to the plasma membrane, possibly by preventing dephosphorylation of the cytoplasmic domain. OKA did not appear to significantly affect the trafficking of the CD4^{cyt}-molecules (Figure 24, B), implying that OKA does not affect the vesicular trafficking from the cell surface, or recycling to the plasma membrane. Fluid-phase uptake was also unaffected in the presence of OKA (Figure 25), further suggesting that vesicular trafficking in these HeLa-CD4 cells is not inhibited by OKA. In a separate study in interphase HeLa cells, OKA inhibited intracellular transport and fluid-phase uptake (Lucocq *et al* 1991). The discrepancy between these two studies may be due to the fact that different phosphatases may be involved in such fundamental cell properties in these different strains of HeLa cells.

The data obtained on the cycling of CD4 in the presence of OKA imply that phosphorylation of the cytoplasmic domain of CD4 is an important feature involved in its intracellular trafficking.

4.3 PMA-Induced Endosomal Sorting Of CD4.

Mathematical modelling of PMA-induced down-regulation indicates that as a result of increasing the endocytosis kinetics of CD4, PMA may alter the steady state distribution of CD4 between the plasma membrane and the endosomal compartment (Pelchen-

Matthews *et al* 1993). However, a number of different studies have indicated that phorbol ester-induced CD4 down-regulation results in the degradation of CD4 (Shin *et al* 1991; Baenziger *et al* 1991; Petersen *et al* 1992; Ruegg *et al* 1992). These studies suggest that CD4 degradation occurs in lysosomes, however, this has yet to be demonstrated.

Immunofluorescence microscopy demonstrated directly that PMA induced redistribution of CD4-anti-CD4 mab complexes, diverting them from the recycling pathway towards a compartment in the perinuclear region of the cell, possibly later endocytic compartments (Figure 26). This altered endosomal sorting was presumed to occur in early endosomes, where segregation of membrane components destined for lysosomes, from those destined to recycle has been demonstrated. In the absence of PMA, internalized CD4-anti-CD4 mab complexes were located in vesicular organelles throughout the cytoplasm, similar to an early endosomal staining pattern (Figure 32, A and B). However, in the presence of PMA, the majority of the internalized CD4-anti-CD4 mab complexes were seen clustered in the perinuclear region of the cell.

In an attempt to characterize the perinuclear compartment containing CD4 during PMA-induced down-regulation, subcellular fractionation studies were undertaken. The immunofluorescence experiments suggested that CD4 may be directed from early endosomes to late endosomal or lysosomal compartments in the presence of PMA. By separating the different compartments of the endocytic pathway, this altered endosomal sorting could be directly investigated. Three different gradient systems were used to analyse the distribution of early and late endosomes and lysosomes in HeLa-CD4 cells. These data suggested that CD4 was delivered to a subcellular compartment that co-migrated with the early endosomes. It was not possible to characterize this compartment as no convincing separation of early and late endosomes was demonstrated (immunoblotting of subcellular fractions suggested that the CI-MPR and rab 7 were co-migrating with early endosomes). However, the fractionation studies did indicate that the bulk of CD4-anti-CD4 mab complexes were not delivered to lysosomal compartments (Figure 28).

One method which could potentially be used to separate the early and late endosomes in the HeLa-CD4 cells is "density shifting". The distribution of the early endosomes on the gradient systems is known, therefore, the early endosomes could be "shifted" from this region of the gradient by using for example, an anti-TfR antibody complexed with colloidal gold, or conjugated with HRP, leaving the distribution of the late endosomes unchanged. If CD4 is delivered to late endocytic compartments, its location on these gradients ought to remain unchanged, and markers such as the CI-MPR and rab 7 should co-migrate with the CD4.

Another approach used to characterize the interaction of CD4 with endocytic pathway during down-regulation was double label indirect immunofluorescence microscopy. In unstimulated cells, the internalized CD4-anti-CD4 mab complexes found in vesicular organelles throughout the cytoplasm, were seen to costain with a mab to the TfR, indicating that CD4 is endocytosed from the plasma membrane and delivered to the early endosomes (Figure 32, A and B). In contrast, in the presence of PMA, the perinuclear compartment containing CD4 could be costained with antibodies to the CI-MPR (Figure 32, E and F), suggesting that CD4 may be delivered to components of the late endosome compartment. These data suggest that, in the presence of PMA, CD4 internalized into the early endosomes is diverted from the constitutive recycling pathway to the late endosome/lysosome pathway. However, costaining by immunofluorescence does not necessarily mean that the two proteins are within the same membrane-bound organelles. Immunofluorescence costaining should ideally be supported by co-localization of the two proteins by gold immunolabelling electron microscopy.

Thus, in addition to the effects on endocytosis, PMA-induced phosphorylation of CD4 may also generate a late endosomal or lysosomal targeting signal. The nature of this signal is not clear, however, in the absence of PMA, non-phosphorylated CD4 molecules are recycled to the plasma membrane suggesting that this signal can be "switched on" by phosphorylation, and it may involve or overlap with the di-leucine sequence involved in endocytosis. Truncation and mutation experiments indicate that

down-regulation of CD4 requires the membrane proximal half of the cytoplasmic domain, in particular the di-leucine sequence (Shin *et al* 1991). For both the CI-MPR and CD-MPR, a phosphorylation site is close to a di-leucine sequence which has been implicated in sorting to the endocytic pathway (Johnson and Kornfeld 1992; Meresse and Hoflack 1993; Chen *et al* 1993). However, this kinase site has very different specificity to that in CD4. PKC is responsible for phosphorylating the cytoplasmic domain of CD4, and in the cytoplasmic domains of CI- and CD-MPR, the di-leucine motif is close to a casein kinase II site, and at least in the cytoplasmic domain of the CI-MPR, the di-leucine does not appear to function as an endocytosis signal (Lobel *et al* 1989), suggesting that there may be subtle differences in the signals.

4.4 PMA-Induced Degradation Of CD4.

The costaining studies indicated that CD4 did not accumulate in lysosomal compartments in the presence of PMA (Figure 33 and 34). However, a number of studies have indicated that in the presence of phorbol ester, CD4 is degraded (Shin *et al* 1991; Baenziger *et al* 1991; Petersen *et al* 1992; Ruegg *et al* 1992). Fluorescence experiments indicated that after prolonged periods (4-8 h) in the presence of PMA, CD4 is degraded (Figure 38), and this is dependent on the cytoplasmic domain of the molecule (Figure 39). Immunoblotting of whole cell lysates was used in an attempt to quantify this degradation. CD4 was degraded with a half time of 2 h 40 min, whilst CD4^{cyt-} molecules were not degraded (Figure 41). Mutation of serine 408 to alanine decreased the efficiency of down-regulation (Figure 9), and also slowed the rate of degradation, so that the half time approximately doubled from 2 h 40 min to about 5 h (Figure 41, D). These results are in agreement with those of previous studies (Shin *et al* 1991; Baenziger *et al* 1991; Petersen *et al* 1992; Ruegg *et al* 1992), indicating that in the continued presence of PMA, CD4 is degraded. In addition, the results indicate that serine 408 is required in the efficient sorting of CD4 to the compartment in the perinuclear region of the HeLa cells, but it is not the only feature

in the CD4 cytoplasmic domain involved in altered endosomal sorting.

Lysosomal proteases have been found within the endosomes of normal rat kidney cells, rat hepatocytes, Swiss 3T3 cells and macrophages (Ludwig *et al* 1991; Casciola-Rosen and Hubbard 1991; Roederer *et al* 1987; Diment *et al* 1988). Experiments using mannosylated bovine serum albumin, showed that trichloroacetic acid-soluble degradation products began to appear after 6 min of internalization at 37°C (Diment and Stahl 1985), due to the presence of membrane-associated Cathepsin D in the endosomes of rabbit alveolar macrophages (Diment *et al* 1988). In Swiss 3T3 cells, the degradation of a fluorogenic substrate of Cathepsin B occurred after 3 min endocytosis at 37°C, and was still detected at 17°C (Roederer *et al* 1987). Similar results were obtained in rat hepatocytes (Casciola-Rosen and Hubbard 1991). Therefore, it appears that in some cell types lysosomal hydrolases are potentially active in endosomes. This could be of importance for the rapid inactivation of some biologically active molecules. For example, insulin is rapidly degraded ($t_{1/2}$) following its internalization in rat liver cells (Doherty *et al* 1990). It is likely however, that for some substrates this endosomal degradation does not go to completion, as only low concentrations of lysosomal hydrolases are located within endosomes (Ludwig *et al* 1991).

The immunofluorescence and fractionation studies failed to detect any anti-CD4-CD4 complexes costaining or co-migrating with lysosomes. However, it is clear that CD4 is being degraded in the continued presence of PMA. Whether this degradation can be attributed to the presence of active lysosomal hydrolases in the endosomes of HeLa-CD4 cells, remains to be determined.

4.5 PMA-Induced Down-Regulation In Lymphoid Cells.

In lymphoid cells the T cell specific tyrosine kinase, p56^{lck}, prevents CD4 from interacting with coated pits (Pelchen-Matthews *et al* 1992). However, the addition of phorbol ester causes CD4 and p56^{lck} to dissociate from one another (Hurley *et al* 1989). This dissociation occurs with a half time of 1-2 min (Pelchen-Matthews *et al* 1993), and occurs before CD4 is down-regulated

(Sleckman *et al* 1992; Yoshida *et al* 1992). It is possible that phorbol ester-induced serine phosphorylation of the cytoplasmic domain of CD4 may disrupt the CD4-p56^{lck} interaction. Following the dissociation of CD4 from p56^{lck}, CD4 is down-regulated from the cell surface (Figure 7). The endocytosis kinetics of CD4 increase more than 20 fold in the lymphocytic cell line, SupT1 (from 0.2% per min to 4.2% per min) following the addition of phorbol ester (Pelchen-Matthews *et al* 1993). Double labelling immunofluorescence microscopy in SupT1 cells, indicate that CD4 is down-regulated to a compartment that could be costained with antibodies to the CI-MPR (Figure 42, A and B), and does not appear to reach lysosomes (Figure 42, C and D), in a similar manner to CD4 modulation in the HeLa-CD4 cells. In addition, prolonged incubations in the continued presence of PMA resulted in the degradation of CD4 (Figure 43), which, when quantified by immunoblotting, indicated that the half time of CD4 degradation was 3 h 20 min (Figure 44). This result was further confirmed using a cell surface iodination assay followed by incubation in medium containing PMA. Quantitative immunoprecipitation of CD4 (Figure 45) demonstrated that the half time of CD4 degradation was 3 h (Figure 46).

The results obtained with the lymphocytic cell line SupT1, indicate that following the addition of phorbol ester, CD4 is down-regulated from the cell surface, delivered to a compartment that can be costained with antibodies to the CI-MPR, and is degraded with a half time of 3 h. This short study on CD4 down-regulation in lymphoid cells, where it is naturally expressed, suggests that on the HeLa cells CD4 appears to behave in a similar manner, and is not dependent on the presence of p56^{lck}.

The results in this thesis demonstrate that phorbol ester directly increase the association of CD4 with coated pits and vesicles, and thereby enhance the endocytosis kinetics of CD4 in HeLa-CD4 cells. Phorbol ester induces the altered endosomal sorting of internalized CD4 from the constitutive recycling pathway to a degradative pathway, such that CD4 is delivered to a perinuclear compartment that costains for the CI-MPR. CD4 then appears to

be degraded in the continued presence of phorbol ester with a half time of 2 h 40 min. A similar situation was found in lymphoid cells where CD4 is naturally expressed, and is associated with p56^{lck}. Following the addition of phorbol ester to SupT1 cells, CD4 is down-regulation from the cell surface, delivered to a compartment that can be costained for the CI-MPR, and in the continued presence of PMA is degraded with a half time of 3 h. In addition, inhibition of kinase and phosphatase activities indicate that the constitutive endocytosis and recycling of CD4 in HeLa-CD4 cells may involve cycles of phosphorylation and dephosphorylation.

4.6 Future Work.

Additional characterization of the compartment containing CD4 during phorbol ester-induced down-regulation is required. Costaining CD4 during down-regulation with a fluid-phase marker such as rhodamine-conjugated bovine serum albumin, will establish whether CD4 is within later endocytic organelles. Inhibition of lysosomal proteases during down-regulation may allow the identification of CD4 within lysosomes, by costaining CD4 with the mab, 2C2, and gold immunolabelling electron microscopy could be used to further characterize the organelle which CD4 appears to be delivered to in the presence of PMA. The colocalization of CD4 with CI-MPR and lysosomal markers following the addition of phorbol ester, could be investigated using this technique, thereby determining whether CD4 is delivered to late endosomes and or lysosomes, and it would also establish the morphology of this perinuclear compartment.

Having found that PMA enhances CD4 endocytosis through coated pits and vesicles, and causes its altered endosomal sorting, it is now important to determine which amino acids are essential for CD4 endocytosis and intracellular sorting. This could be achieved by creating a series of truncation mutants and by sequential point mutations in the cytoplasmic domain of CD4, similar to the experiments which identified the internalization signals of LDL-R, TfR, CI-MPR and LAP, and the intracellular sorting signals of the CI-MPR (Chen *et al* 1990; Collawn *et al* 1991;

Canfield *et al* 1991; Lehmann *et al* 1992; Chen *et al* 1993). Endocytosis assays will identify how the mutations affect the internalization of the CD4 mutant molecules, and immunofluorescence assays will allow rapid screening of the mutants, to establish the sequences involved in altered endosomal sorting in the presence of phorbol ester, and whether they are distinct from the endocytosis signal.

Other important questions which need to be addressed are the nature of the cellular machinery involved in the sorting of CD4, and how it is sorted in the endosomes. An association of HA-2 adaptor complexes with the cytoplasmic domain of CD4 would suggest that these complexes are part of the sorting machinery involved in recruiting CD4 molecules into clathrin-coated pits. Immunoprecipitation of CD4 followed by immunoblotting for HA-2 adaptor complexes could be used to approach this question. Fractionation techniques could also be employed to determine whether any proteins interact with the cytoplasmic domain of CD4 in endosomal compartments, and characterization of these proteins would determine whether they are part of any sorting machinery in the endosomes. The series of CD4 mutants created for the identification of the endocytosis signal could be used to determine which sequences in the cytoplasmic domain are required for sorting. Once these sequences have been identified, any structural determinants required for sorting could be investigated using NMR, in a similar manner to the studies on the internalization signals of LAP and LDL-R (Eberle *et al* 1991; Bansal and Gierasch 1991).

The indication that phosphorylation of the cytoplasmic domain of CD4 may be involved in the constitutive endocytosis and intracellular sorting of CD4 in HeLa cells, could also be tested more thoroughly, by making CD4 mutants with point mutations at the phosphorylation sites. These mutants could then be analysed for their intracellular trafficking by immunofluorescence endocytosis assays, and their phosphorylation states at the plasma membrane, and within endosomes, by subcellular fractionation, immunoprecipitation from fractions followed by *in vitro* kinase assays on the resulting precipitates.

ACKNOWLEDGEMENTS

I would like to thank the members of the Marsh laboratory past and present, in particular Annegret Pelchen-Matthews and Pamela Reid for their help throughout my time in the laboratory.

I would also like to thank my supervisor Dr. Mark Marsh for his help and guidance through this study. A special thanks must go to Sandra Pinkstone, whose has constantly supported and encouraged me throughout the study , and without her, I may never have completed this thesis.

5. REFERENCES

- Acres, B.R., Conlon, P.J., Mochizuki, D.Y., and Gallis, B., 1986. Rapid phosphorylation of the T4 antigen on cloned helper T cells induced by phorbol myristate acetate or antigen. *J. Biol. Chem.* **261**:16210-16214.
- Aiken, C., Konner, J., Landau, N.R., Lenburg, M.E., and Trono, D., 1994. Nef induces CD4 endocytosis: requirement for a critical dileucine motif in the membrane-proximal CD4 cytoplasmic domain. *Cell* **76**:853-864.
- Alvarez, E., Girones, N., and Davis, R.J., 1990. A point mutation in the cytoplasmic domain of the transferrin receptor inhibits endocytosis. *Biochem. J.* **267**:31-35.
- Anderson, P., Blue, M-L., Morimoto, C., and Schlossman, S.F., 1987. Cross-linking of T3 (CD3) with T4 (CD4) enhances the proliferation of resting T lymphocytes. *J. Immunol.* **139**:678-682.
- Anderson, R.G.W., Brown, M.S., and Goldstein, J.L., 1977. Role of the coated endocytic vesicle in the uptake of receptor-bound low density lipoprotein in human fibroblasts. *Cell* **10**:351-364.
- Baenziger, J.W., Okamoto, A., Hall, E., Verma, S., and Davis, C.G., 1991. The cytoplasmic tail of CD4 targets chimeric molecules to a degradative pathway. *New Biologist* **3**:1233-1241.
- Balch, W.E., and Rothman, J.E., 1985. Characterization of protein transport between successive compartments of the Golgi apparatus: asymmetric properties of donor and acceptor activities in a cell-free system. *Arch. Biochem. Biophys.* **240**:413-425.
- Bank, I., and Chess, L., 1985. Perturbation of the T4 molecule transmits a negative signal to T cells. *J. Exp. Med.* **162**:1294-1303.

Bansal, A., and Gierasch, L.M., 1991. The NPXY internalization signal of the LDL receptor adopts a reverse-turn conformation. *Cell* **67**:1195-1201.

Barre-Sinoussi, F., Chermann, J.C., Rey, F., Nugeyre, M.T., Charmaret, S., Gruest, J., Dauguet, C., Axler-Blin, C., Vezinet-Brun, F., Rouzioux, C., Rozenbaum, W., and Montagnier, L., 1983. Isolation of a T-lymphotropic retrovirus from a patient at risk for acquired immune deficiency syndrome (AIDS). *Science* **220**:868-871.

Bedinger, P., Moriarty, A., von Borstel II, R.C., Donovan, N.J., Steimer, K.S., Littman, D.R., 1988. Internalization of the human immunodeficiency virus does not require the cytoplasmic domain of CD4. *Nature* **334**:162-165.

Berg, L.J., Pullen, A.M., Fazekas de St. Groth, B., Mathis, D., Benoist, C., and Davis, M.M., 1989. Antigen/MHC-specific T cells are preferentially exported from the thymus in the presence of their MHC ligand. *Cell* **58**:1035-1046.

Berger, E.A., Fuerst, T.R., and Moss, B., 1988. A soluble recombinant polypeptide comprises the amino-terminal half of the extracellular region of the CD4 molecule contains an active binding site for human immunodeficiency virus. *Proc. Natl. Acad. Sci. USA* **85**:2357-2361.

Besterman, J.M., May Jr., W.S., LeVine III, H., Cragoe Jr., E.J., and Cuatrecasas, P., 1985. Amiloride inhibits phorbol ester-stimulated Na⁺/H⁺ exchange and protein kinase C. *J. Biol. Chem.* **260**:1155-1159.

Biddison, W.E., Rao, P.E., Talle M.A., Goldstein, G., and Shaw, S., 1983. Possible involvement of the T4 molecule in T cell recognition of class II HLA antigens: evidence from studies of proliferative responses to SB antigens. *J. Immunol.* **131**:152-157.

Biddison , W.E., Rao, P.E., Talle M.A., Goldstein, G., and Shaw, S., 1984. Possible involvement of the T4 molecule in T cell recognition of class II HLA antigens. *J. Exp. Med.* **159**:783-797.

Bigby, M., Wang, P., Fierro, J.F., and Sy, M-S., 1990. Phorbol myristate acetate-induced down-modulation of CD4 is dependent on calmodulin and intracellular calcium. *J. Immunol.* **144**:3111-3116.

Blue, M-L., Hafler, D.A., Craig, K.A., Levine, H., Schlossman, S.F., 1987. Phosphorylation of CD4 and CD8 molecules following T cell triggering. *J. Immunol.* **139**:3949-3954.

Blue, M-L., Daley, J.F., Levine, H., Branton, K.R., and Schlossman, S.F., 1989. Regulation of CD4 and CD8 surface expression on human thymocyte subpopulations by triggering through CD2 and CD3-T cell receptor. *J. Immunol.* **142**:374-380.

Bomsel, M., Parton, R., Kuznetsov, S.A., Schroer, T.A., and Gruenberg, J., 1990. Microtubule- and motor-dependent fusion in vitro between apical and basolateral endocytic vesicles from MDCK cells. *Cell* **62**:719-731.

Borgulya, P., Kishi, H., Muller, U., Kirberg, J., and von Boehmer, H., 1991. Development of the CD4 and CD8 lineage of T cells: instruction versus selection. *EMBO J.* **10**:913-918.

Brady, R.L., Dodson, E.J., Dodson, G.G., Lange, G., Davis, S.J., Williams, A.F., and Barclay, A.N., 1993a. Crystal structure of domains 3 and 4 of rat CD4: relation to the NH₂-terminal domains. *Science* **260**:979-983.

Brady, R.L., Lange, G., and Barclay, A.N., 1993b. Structural studies of CD4: crystal structure of domains 3 and 4 and their implication for the overall receptor structure. *Biochem. Soc. Trans.* **21**:958-963.

Braun, M., Waheed, A., and von Figura, K., 1989. Lysosomal acid phosphatase is transported to lysosomes via the cell surface. *EMBO J.* **8**:3633-3640.

Breitfeld, P.P., Casanova, J.E., McKinnon, W.C., and Mostov, K.E., 1990. Deletions in the cytoplasmic domain of the polymeric immunoglobulin receptor differentially affect endocytic rate and postendocytic traffic. *J. Biol. Chem.* **265**:13750-13757.

Bretscher, M.S., and Lutter, R., 1988. A new method for detecting endocytosed proteins. *EMBO J.* **7**:4087-4092.

Bretscher, M.S., Thomson, J.N., and Pearse, B.M.F., 1980. Coated pits act as molecular filters. *Proc. Natl. Acad. Sci. USA* **77**:4156-4159.

Brown, W.J., and Farquhar, M.G., 1984. The mannose-6-phosphate receptor for lysosomal enzymes is concentrated in *cis* Golgi cisternae. *Cell* **36**:295-307.

Brown, W.J., and Farquhar, M.G., 1987. The distribution of 215-kilodalton mannose 6-phosphate receptors with *cis* (heavy) and *trans* (light) Golgi subfractions varies in different cell types. *Proc. Natl. Acad. Sci. USA* **84**:9001-9005.

Bucci, C., Parton, R.G., Mather, I.H., Stunnenberg, H., Simons, K., Hoflack, B. and Zerial, M., 1992. The small GTPase rab 5 functions as a regulatory factor in the early endocytic pathway. *Cell* **70**:715-728.

Cammarota, G., Scheirle, A., Takacs, B., Doran, D.M., Knorr, R., Bannwarth, W., Guardiola, J., and Sinigaglia, F., 1992. Identification of a CD4 binding site on the β_2 domain of HLA-ADR molecules. *Nature* 799-801.

Canfield, W.M., Johnson, K.F., Ye, R.D., Gregory, W., and Kornfeld, S., 1991. Localization of the signal for rapid internalization of the bovine cation-independent mannose 6-phosphate/insulin-like

growth factor-II receptor to amino acids 24-29 of the cytoplasmic tail. *J. Biol. Chem.* **266**:5682-5688.

Cardone, M.H., Smith, B.L., Song, W., Mochly-Rosen, D., and Mostov, K.E., 1994. Phorbol myristate acetate-mediated stimulation of transcytosis and apical recycling in MDCK cells. *J. Cell Biol.* **124**:717-727.

Casanova, J.E., Breitfeld, P.P., Ross, S.A., and Mostov, K.E., 1990. Phosphorylation of the polymeric immunoglobulin receptor required for its efficient transcytosis. *Science* **248**:742-745.

Casciola-Rosen, L.A.F., and Hubbard, A.L., 1991. Hydrolases in intracellular compartments of rat liver cells. Evidence for selective activation and/or delivery. *J. Biol. Chem.* **266**:4341-4347.

Castagna, M., Takai, Y., Karibuchi, K., Sano, K., Kikkawa, U., and Nishizuka, Y., 1982. Direct activation of calcium-activated, phospholipid-dependent protein kinase by tumor-promoting phorbol esters. *J. Biol. Chem.* **257**:7847-7851.

Chan, S.H., Cosgrove, D., Waltzinger, C., Benoist, C., and Mathis, D., 1993. Another view of the selective model of thymocyte selection. *Cell* **73**:225-236.

Chavrier, P., Parton, R.G., Hauri, H.P., Simons, K., and Zerial, M., 1990. Localization of low molecular weight GTP binding proteins to exocytic and endocytic compartments. *Cell* **62**:317-329.

Chen, H.J., Remmler, J., Delaney, J.C., Messner, D.J., and Lobel, P., 1993. Mutational analysis of the cation-independent mannose 6-phosphate/insulin-like growth factor II receptor. A consensus casein kinase II site followed by 2 leucines near the carboxyl terminus is important for intracellular targeting of lysosomal enzymes. *J. Biol. Chem.* **268**:22338-22346.

Chen, W-J., Goldstein, J.L., and Brown, M.S., 1990. NPXY, a sequence often found in cytoplasmic tails, is required for coated pit-mediated internalization of the low density lipoprotein receptor. *J. Biol. Chem.* **265**:3116-3123.

Clapham, P.R., Weiss, R.A., Dalglish, A.G., Exley, M., Whitby, D., and Hogg, N., 1987. Human immunodeficiency virus infection of monocytic and T-lymphocytic cells: receptor modulation and differentiation induced by phorbol esters. *Virology* **158**:44-51.

Clark, S.J., Jefferies, W.A., Barclay, A.N., Gagnon, J., and Williams A.F., 1987. Peptide and nucleotide sequences of rat CD4 (W3/25) antigen: evidence for derivation from a structure with four immunoglobulin-related domains. *Proc. Natl. Acad. Sci. USA* **84**:1649-1653.

Clayton, L.K., Hussey, R.E., Steinbrich, R., Ramachandran, H., Husain, Y., and Reinherz, E.L., 1988. Substitution of murine for human CD4 residues identifies amino acids critical for HIV-gp120 binding. *Nature* **335**:363-366.

Cohen, P., Holmes, C.F.B., and Tsukitani, Y., 1990. Okadaic acid: a new probe for the study of cellular regulation. *Trends Biol. Chem.* **15**:98-102.

Cole, J.A., McCarthy, S.A., Rees, M.A., Sharrow, S.O., and Singer, A., 1989. Cell surface coregulation of CD4 and T cell receptor by anti-CD4 monoclonal antibody. *J. Immunol.* **143**:397-402.

Collawn, J.F., Stangel, M., Kuhn, L.A., Esekogwu, V., Jing, S., Trowbridge, I.S., and Tainer, J.A., 1990. Transferrin receptor internalization sequence YXRF implicates a tight turn as the structural recognition motif for endocytosis. *Cell* **63**:1061-1072.

Collawn, J.F., Kuhn, L.A., Liu, L-F.S., Tainer, J.A., and Trowbridge, I.S., 1991. Transferrin LDL and mannose-6-phosphate receptor internalization signals promote high-efficiency endocytosis of the transferrin receptor. *EMBO J.* **10**:3247-3253.

Collins, M.K.L., and Rozengurt, E., 1982. Binding of phorbol esters to high affinity sites on murine fibroblastic cells elicits a mitogenic response. *J. Cell Physiol.* **112**:42-50.

Corvera, S., Chawla, A., Chakrabarti, R., Joly, M., Buxton, J., and Czech, M.P., 1994. A double leucine within the GLUT4 glucose transporter COOH-terminal domain functions as an endocytosis signal. *J. Cell Biol.* **126**:979-989.

Dahms, N.M., Lobel, P., and Kornfeld, S., 1989. Mannose 6-phosphate receptors and lysosomal enzyme targeting. *J. Biol. Chem.* **264**:12115-12118.

Dalglish, A.G., Beverley, P.C.L., Clapham, P.R., Crawford, D.H., Greaves, M.F., and Weiss, R.A., 1984. The CD4 (T4) antigen is an essential component of the receptor for the AIDS retrovirus. *Nature* **312**:763-767.

Daukas, G., and Zigmond, S.H., 1985. Inhibition of receptor-mediated but not fluid-phase endocytosis in polymorphonuclear leukocytes. *J. Cell Biol.* **101**:1673-1679.

Davis, C.B., Killeen, N., Crooks, M.E.C., Raulet, D., and Littman, D.R., 1993. Evidence for a stochastic mechanism in the differentiation of mature subsets of T lymphocytes. *Cell* **73**:237-247.

Davis, C.G., Lehrman, M.A., Russell, D.W., Anderson, R.G.W., Brown, M.S., and Goldstein, J.L., 1986. The J.D. mutation in familial hypercholesterolemia: amino acid substitution in cytoplasmic domain impedes internalization of LDL receptors. *Cell* **45**:15-24.

Davoust, J., Gruenberg, J., and Howell, K.E., 1987. Two threshold values of low pH block endocytosis at different stages. *EMBO J.* **6**:3601-3609.

De Matteis, M.A., Santini, G., Kahn, R.A., Di Tulio, G., and Luini, A., 1993. Receptor and protein kinase C-mediated regulation of ARF binding to the Golgi complex. *Nature* **364**:818-821.

Dietrich, J., Hou, X., Wegener, A-M.K., and Geisler, C., 1994. CD3 γ contains a phosphoserine-dependent di-leucine motif involved in down-regulation of the T cell receptor. *EMBO J.* **13**:2156-2166.

Diment, S., and Stahl, P., 1985. Macrophage endosomes contain proteases which degrade endocytosed protein ligands. *J. Biol. Chem.* **260**:15311-15317.

Diment, S., Leech, M.S., and Stahl, P.D., 1988. Cathepsin D is membrane-associated in macrophage endosomes. *J. Biol. Chem.* **263**:6901-6907.

Doherty II, J-J., Kay, D.G., Lai, W.H., Posner, B.I., and Bergeron, J.J.M., 1990. Selective degradation of insulin within rat liver endosomes. *J. Cell Biol.* **110**:35-42.

Doxsey, S.J., Brodsky, F.M., Blank, G.S., and Helenius, A., 1987. Inhibition of endocytosis by anti-clathrin antibodies. *Cell* **50**:453-463.

Doyle, C., and Strominger, J.L., 1987. Interaction between CD4 and class II MHC molecules mediates cell adhesion. *Nature* **330**:256-259.

Dunn, K.W., and Maxfield, F.R., 1992. Delivery of ligands from sorting endosomes to late endosomes occurs by maturation of sorting endosomes. *J. Cell Biol.* **117**:301-310.

Eberle, W., Sander, C., Klaus, W., Schmidt, B., von Figura, K., Peters, C., 1991. The essential tyrosine of the internalization signal in lysosomal acid phosphatase is part of a β turn. *Cell* **67**:1203-1209.

Eichmann, K., Jonsson, J-I., Falk, I., and Emmrich, F., 1987. Effective activation of resting mouse T lymphocytes by cross-linking submitogenic concentrations of the T cell antigen receptor with either Lyt-2 or L3T4. *Eur. J. Immunol.* 17:643-650.

Emmrich, F., Kanz, L., and Eichmann, K., 1987. Cross-linking of the T cell receptor complex with the subset-specific differentiation antigen stimulates interleukin 2 receptor expression in human CD4 and CD8 T cells. *Eur. J. Immunol.* 17:529-534.

Fallon, R.J., and Schwartz, A.L., 1987. Mechanism of the phorbol ester-mediated redistribution of Asialoglycoprotein receptor: selective effects on receptor recycling pathways in Hep G2 cells. *Mol. Pharm.* 32:348-355.

Fleury, S., Lamarre, D., Meloche, S., Ryu, S-E., Cantin, C., Hendrickson, W.A., and Sekaly, R-P., 1991. Mutational analysis of the interaction between CD4 and class II MHC: class II antigens contact CD4 on a surface opposite the gp120-binding site. *Cell* 66:1037-1049.

Fowlkes, B.J., Schwartz, R.H., and Pardoll, D.M., 1988. Deletion of self-reactive thymocytes occurs at a CD4⁺8⁺ precursor stage. *Nature* 334:620-623.

Fuhrer, C., Geffen, I., and Spiess, M., 1991. Endocytosis of the ASGP receptor H1 is reduced by mutation of tyrosine-5 but still occurs via coated pits. *J. Cell Biol.* 114:423-431.

Fukuda, M., 1991. Lysosomal membrane glycoproteins. Structure, biosynthesis, and intracellular trafficking. *J. Biol. Chem.* 266:21327-21330.

Gallo, R.C., Salahuddin, S.Z., Popovic, M., Shearer, G.M., Kaplan, M., Haynes, B.F., Palker, T.J., Redfield, R., Oleske, J., Safai, B., White, G., Foster, P., and Markham, P.D., 1984. Frequent detection and isolation of cytopathic retroviruses (HTLV-III) from patient with AIDS and at risk for AIDS. *Science* 224:500-503.

Gay, D., Maddon, P., Sekaly, R., Talle, M.A., Godfrey, M., Long, E., Goldstein, G., Chess, L., Axel, R., Kappler, J., and Marrack, P., 1987. Functional interaction between human T-cell protein CD4 and the major histocompatibility complex HLA-DR antigen. *Nature* **328**:626-629.

Gilbert, J.M., Mason, D., and White, J.M., 1988. Fusion of Rous Sarcoma virus with host cells does not require exposure to low pH. *J. Virol.* **64**:5106-5113.

Glaichenhaus, N., Shastri, N., Littman, D.R., and Turner, J.M., 1991. Requirement for association of p56^{lck} with CD4 in antigen-specific signal transduction in T cells. *Cell* **64**:511-520.

Glickman, J.N., Conibear, E., and Pearse, B.M.F., 1989. Specificity of binding of clathrin adaptors to signals on the mannose-6-phosphate/insulin-like growth factor-II receptor. *EMBO J.* **8**:1041-1047.

Goldstein, J.L., Brown, M.S., Anderson, R.G.W., Russell, D.W., and Schneider, W.J., 1985. Receptor-mediated endocytosis: concepts from the LDL receptor system. *Ann. Rev. Cell Biol.* **1**:1-39.

Gorvel, J-P., Chavrier, P., Zerial, M., Gruenberg, J., 1991. rab 5 controls early endosome fusion in vitro. *Cell* **64**:915-925.

Grewe, C., Beck, A., and Gelderblom, H.R., 1990. HIV: early virus-cell interactions. *J. Acq. Imm. Defic. Synd.* **3**:965-974.

Griffiths, G., and Gruenberg, J., 1991. The arguments for pre-existing early and late endosomes. *Trends Cell Biol.* **1**:5-9.

Griffiths, G., Hoflack, B., Simons, K., Mellman, I., and Kornfeld, S., 1988. The mannose 6-phosphate receptor and the biogenesis of lysosomes. *Cell* **52**:329-341.

Griffiths, G., Back, R., and Marsh, M., 1989. A quantitative analysis of the endocytic pathway in baby hamster kidney cells. *J. Cell Biol.* **109**:2703-2720.

Griffiths, G., Matteoni, R., Back, R., and Hoflack, B., 1990. Characterization of the cation-independent mannose 6-phosphate receptor-enriched prelysosomal compartment in NRK cells. *J. Cell Sci.* **95**:441-461.

Gruenberg, J., Griffiths, G., and Howell, K.E., 1989. Characterization of the early endosome and putative endocytic carrier vesicles in vivo and with an assay of vesicle fusion in vitro. *J. Cell Biol.* **108**:1301-1316.

Hammerton, R.W., Krzeminski, K.A., Mays, R.W., Ryan, T.A., Wollner, D.A., and Nelson, W.J., 1991. Mechanism for regulating cell surface distribution of Na⁺,K⁺-ATPase in polarized epithelial cells. *Science* **254**:847-850.

Hansen, S.H., Sandvig, K., and van Deurs, B., 1991. The preendosomal compartment comprises distinct coated and noncoated endocytic vesicles populations. *J. Cell Biol.* **113**:731-741.

Harms, E., Kern, H., and Schneider, J.A., 1980. Human lysosomes can be purified from diploid skin fibroblasts by free flow electrophoresis. *Proc. Natl. Acad. Sci. USA* **77**:6139-6143.

Harrison-Lavoie, K.J., Lewis, V.A., Hynes, G.M., Collison, K.S., Nutland, E., and Willison, K.R., 1993. A 102 kDa subunit of a Golgi-associated particle has homolgy to β subunits or trimeric G proteins. *EMBO J.* **12**:2847-2853.

Harter, C., and Mellman, I., 1992. Transport of the lysosomal membrane glycoprotein lgp120 (lgp-A) to lysosomes does not require appearance on the plasma membrane. *J. Cell Biol.* **117**:311-325.

Healey, D., Dianda, L., Moore, J.P., McDougal, J.S., Moore, M.J., Estess, P., Buck, D., Kwong, P.D., Beverley, P.C.L., and Sattentau, Q.J., 1990. Novel anti-CD4 monoclonal antibodies separate human immunodeficiency virus infection and fusion of CD4⁺ cells from virus binding. *J. Exp. Med.* **172**:1233-1242.

Helenius, A., Mellman, I., Wall, D., and Hubbard, A., 1983. Endosomes. *Trends Biochem. Sci.* **8**:245-250.

Herskovits, J.S., Burgess, C.C., Obar, R.A., and Vallee, R.B., 1993. Effects of mutant rat dynamin on endocytosis. *J. Cell Biol.* **122**:565-578.

Heuser, J., 1989. Effects of cytoplasmic acidification on clathrin lattice morphology. *J. Cell. Biol.* **108**:401-411.

Heuser, J.E., and Anderson, R.G.W., 1989. Hypertonic media inhibit receptor-mediated endocytosis by blocking clathrin-coated pit formation. *J. Cell Biol.* **108**:389-400

Hirt, R.P., Hughes, G.J., Frutiger, S., Michetti, P., Perregaux, C., Poulain-Godefroy, O., Jeanguenat, N., Neutra, M.R., and Kraehenbuhl, J-P., 1993. Transcytosis of the polymeric Ig receptor requires phosphorylation of serine 664 in the absence but not the presence of dimeric IgA. *Cell* **74**:245-255.

Hopkins, C.R., Gibson, A., Shipman, M., and Miller, K., 1990. Movement of internalized ligand-receptor complexes along a continuous endosomal reticulum. *Nature* **346**:335-339.

Hoxie, J.A., Matthews, D.M., Callahan, K.J., Cassel, D.L., and Cooper, R.A., 1986. Transient modulation and internalization of T4 antigen induced by phorbol esters. *J. Immunol.* **137**:1194-1201.

Hoxie, J.A., Rackowski, J.L., Haggarty, B.S., and Gaulton, G.N., 1988. T4 endocytosis and phosphorylation induced by phorbol esters but not by mitogen or HIV infection. *J. Immunol.* **140**:786-795.

Hurley, T.R., Luo, K., and Sefton, B.M., 1989. Activators of protein kinase C induce dissociation of CD4, but not CD8, from p56^{lck}. *Science* **245**:407-409.

Imboden, J.B., and Stobo J.D., 1985. Transmembrane signalling by the T cell antigen receptor. Perturbation of the T3-antigen receptor complex generates inositolphosphates and releases calcium ions from intracellular stores. *J. Exp. Med.* **161**:446-456.

Jacobson, M.D., Burne, J.F., King, M.P., Miyashita, T., Reed, J.C., and Raff, M.C., 1993. Bcl-2 blocks apoptosis in cells lacking mitochondrial DNA. *Nature* **361**:365-368.

Jadot, M., Canfield, W.M., Gregory, W., and Kornfeld, S., 1992. Characterization of the signal for rapid internalization of the bovine mannose 6-phosphate/insulin-like growth factor-II receptor. *J. Biol. Chem.* **267**:11069-11077.

Janeway, Jr. C.A., 1988. Accessories or coreceptors? *Nature* **335**:208-210.

Jing, S., Spencer, T., Miller, K., Hopkins, C., and Trowbridge, I.S., 1990. Role of the human transferrin receptor cytoplasmic domain in endocytosis: localization of a specific sequence for internalization. *J. Cell Biol.* **110**:283-294.

Johnson, K.F., Chan, W., and Kornfeld, S., 1990. Cation-dependent mannose 6-phosphate receptor contains two internalization signals in its cytoplasmic domain. *Proc. Natl. Acad. Sci. USA* **87**:10010-10014.

Johnson, K.F., and Kornfeld, S., 1992. The cytoplasmic tail of the mannose 6-phosphate/insulin-like growth factor-II receptor has two signals for lysosomal enzyme sorting in the Golgi. *J. Cell Biol.* **119**:249-257.

Kaye, J., Hsu, M-L., Sauron, M-E., Jameson, S.C., Gascoigne, N.R.J., Hedrick, S.M., 1989. Selective development of CD4⁺ T cells in

transgenic mice expressing a class II MHC-restricted antigen receptor. *Nature* **341**:746-749.

Keller, G-A., Siegel, M.W., and Caras, I.W., 1992. Endocytosis of glycopospholipid-anchored and transmembrane forms of CD4 by different endocytic pathways. *EMBO J.* **11**:863-874.

Kielian, M.C., Marsh, M., and Helenius, A., 1986. Kinetics of endosome acidification detected by mutant and wild-type Semliki Forest virus. *EMBO J.* **5**:3103-3109.

Killeen, N., and Littman, D.R., 1993. Helper T-cell development in the absence of CD4-p56^{lck} association. *Nature* **364**:729-732.

Klatzmann, D., Champagne, E., Chamarret, S., Gruet, J., Guetard, D., Hercend, T., Gluckman, J-C., and Montagnier, L., 1984. T-lymphocyte T4 molecule behaves as the receptor for human retrovirus LAV. *Nature* **312**:767-768.

Koch, C.A., Anderson, D., Moran, M.F., Ellis, C., and Pawson, T., 1991. SH2 and SH3 domains: elements that control interactions of the cytoplasmic signaling proteins. *Science* **252**:228-674.

Konig, R., Huang, L-Y., and Germain, R.N., 1992. MHC class II interaction with CD4 mediated by a region analogous to the MHC class I binding site for CD8. *Nature* **356**:796-798.

Kornfeld, S., and Mellman, I., 1989. The biogenesis of lysosomes. *Annu. Rev. Cell Biol.* **5**:483-525.

Kruisbeek, A.M., Fultz, M.J., Sharrow, S.O., Singer, A., and Mond, J.J., 1983. Early development of the T cell repertoire. *In vivo* treatment of neonatal mice with anti-Ia antibodies interferes with differentiation of I-restricted but not K/D-restricted T cells. *J Exp. Med.* **157**:1932-1946.

Kruisbeek, A.M., Fowlkes B.J., Bridges, S.A., Mond, J.J., and Longo D.L., 1985. Lack of development of the L3T4⁺ subset in anti-Ia-

treated neonatal mice correlates with absence of thymic Ia bearing APC function. *J. Exp. Med.* **161**:1029-1047.

Ktistakis, N.T., Thomas, D., and Roth, M.G., 1990. Characteristics of the tyrosine recognition signal for internalization of transmembrane surface glycoproteins. *J. Cell Biol.* **111**:1393-1407.

Kupfer, A., Singer, S.J., Janeway, Jr., C.A., and Swain, S.L., 1987. Coclustering of CD4 (L3T4) molecule with the T-cell receptor is induced by specific direct interaction of helper T cells and antigen-presenting cells. *Proc. Natl. Acad. Sci. USA* **84**:5888-5892.

Laemmli, U.K., 1970. Cleavage of structural proteins during the assembly of the capsid of bacteriophage T4. *Nature* **227**:680-685.

Lamarre, D., Capon, D.J., Karp, D.R., Gregory, T., Long, E.O., and Sekaly, R-P., 1989. Class II MHC molecules and the HIV gp120 envelope protein interact with functionally distinct regions of the CD4 molecule. *EMBO J.* **8**:3271-3277.

Larkin, J.M., Brown, M.S., Goldstein, J.L., and Anderson, R.G.W., 1983. Depletion of intracellular potassium arrests coated pit formation and receptor-mediated endocytosis in fibroblasts. *Cell* **33**:273-285.

Le Borgne, R., Schmidt, A., Mauxion, F., Griffiths, G., and Hoflack, B., 1993. Binding of AP-1 Golgi adaptors to membranes requires phosphorylated cytoplasmic domains of the mannose 6-phosphate/insulin-like growth factor II receptor. *J. Biol. Chem.* **268**:22552-22556.

Ledbetter, J.A., June, C.H., Grosmaire, L.S., Rabinovitch, P.S., 1987. Crosslinking of surface antigens causes mobilization of intracellular ionized calcium in T lymphocytes. *Proc. Natl. Acad. Sci. USA* **84**:1384-1388.

Ledbetter, J.A., June, C.H., Rabinovitch, P.S., Grosmaire, L.S., Tsu, T.T., Imboden, J.B., 1988. Signal transduction through CD4 receptors: stimulatory vs. inhibitory activity is regulated by CD4 proximity to the CD3/T cell receptor. *Eur. J. Immunol.* **18**:525-532.

Lehmann, L.E., Eberle, W., Krull, S., Prill, V., Schmidt, B., Sander, C., von Figura, K., and Peters, C., 1992. The internalization signal in the cytoplasmic tail of lysosomal acid phosphatase consists of the hexapeptide PGYRHV. *EMBO J.* **11**:4391-4399.

Lemansky, P., Fatemi, S.H., Gorican, B., Meyale, S., Rossero, R., and Tartakoff, A.M., 1990. Dynamics and longevity of the glycolipid-anchored membrane protein, Thy-1. *J. Cell Biol.* **110**:1525-1531.

Letourneur, F., and Klausner, R.D., 1992. A novel di-leucine motif and a tyrosine-based motif independently mediate lysosomal targeting and endocytosis of CD3 chains. *Cell* **69**:1143-1157.

Lobel, P., Fujimoto, K., Ye, R.D., Griffiths, G., and Kornfeld, S., 1989. Mutations in the cytoplasmic domain of the 275 kd mannose 6-phosphate receptor differentially alter lysosomal enzyme sorting and endocytosis. *Cell* **57**:787-796.

Lombardi, D., Soldati, T., Riederer, M.A., Goda, Y., Zerial, M., and Pfeffer, S.R., 1993. Rab 9 functions in transport between late endosomes and the *trans* Golgi network. *EMBO J.* **12**:677-682.

Louie, R.R., King, C.S., Macauley, A., Marth, J.D., Perlmutter, R.M., Eckhart, W., and Cooper, J.A., 1988. p56^{lck} protein-tyrosine kinase is cytoskeletal and does not bind to polyomavirus middle T antigen. *J. Virology* **62**:4673-4679.

Lucocq, J., Warren, G., and Pryde, J., 1991. Okadaic acid induces Golgi apparatus fragmentation and arrest of intracellular transport. *J. Cell Science* **100**:753-759.

Ludwig, T., Griffiths, G., and Hoflack, B., 1991. Distribution of newly synthesized lysosomal enzymes in the endocytic pathway of normal rat kidney cells. *J. Cell Biol.* **115**:1561-1572.

Luo, K., and Sefton, B.M., 1990. Cross-linking of T-cell surface molecules CD4 and CD8 stimulates phosphorylation of the *lck* tyrosine protein kinase at the autophosphorylation site. *Mol. Cell. Biol.* **10**:5305-5313.

MacDonald, H.R., Hengartner, H., and Pedrazzini, T., 1988. Intrathymic deletion of self-reactive cells prevented by neonatal anti-CD4 antibody treatment. *Nature* **335**:174-176.

Maddon, P.J., Littman, D.R., Godfrey, M., Maddon, D.E., Chess, L., and Axel, R., 1985. The isolation and nucleotide sequence of a cDNA encoding the T cell surface protein T4: a new member of the immunoglobulin gene family. *Cell* **42**:93-104.

Maddon, P.J., Dalgleish, A.G., McDougal, J.S., Clapham, P.R., Weiss, R.A., and Axel, R., 1986. The T4 gene encodes the AIDS virus receptor and is expressed in the immune system and the brain. *Cell* **47**:333-348.

Maddon, P.J., McDougal, J.S., Clapham, P.R., Dalgleish, A.G., Jamal, S., Weiss, R.A., and Axel, R., 1988. HIV infection does not require endocytosis of its receptor, CD4. *Cell* **54**:865-874.

Madhus, I.H., Sandvig, K., Olsnes, S., and van Deurs, B., 1987. Effect of reduced endocytosis induced by hypotonic shock and potassium depletion on the infection of Hep 2 cells by picornaviruses. *J. Cell. Phys.* **131**:14-22.

Magun, B.E., Matrisian, L.M., and Bowden, G.T., 1980. Epidermal growth factor. Ability of tumour promoter to alter its degradation, receptor affinity and receptor number. *J. Biol. Chem.* **255**:6373-6381.

Marsh, M., and Helenius, A., 1980. Adsorptive endocytosis of Semliki Forest virus. *J. Mol. Biol.* **142**:439-454.

Marsh, M., and Pelchen-Matthews, A., 1993. Entry of animal viruses into cells. *Rev. Med. Virol.* **3**:173-185.

Marsh, M., Bolzau, E., Helenius, A., 1983. Penetration of Semliki Forest Virus from acidic prelysosomal vacuoles. *Cell* **32**:931-940.

Marsh, M., Griffiths, G., Dean, E., Mellman, I., and Helenius, A., 1986. Three dimensional structure of endosomes in BHK-21 cells. *Proc. Natl. Acad. Sci. USA* **83**:2899-2903.

Marsh, M., Parsons, I.J., Reid, P., and Pelchen-Matthews, A., 1993. Charting endocytic membrane traffic pathways. *Biochem. Soc. Trans.* **21**:703-706.

Marsh, M., Schmid, S., Kern, H., Harms, E., Male, P., Mellman, I., Helenius, A., 1987. Rapid analytical and preparative isolation of functional endosomes by free flow electrophoresis. *J. Cell Biol.* **104**:875-886.

Marsh, M., Armes, J.E., and Pelchen-Matthews, A., 1990. Endocytosis and recycling of CD4. *Biochem. Soc. Trans.* **18**:139-144.

Mathews, P.M., Martinie, J.B., and Fambrough, D.M., 1992. The pathway and targeting signal for delivery of the integral membrane glycoprotein LEP100 to lysosomes. *J. Cell Biol.* **118**:1027-1040.

Maziere, J.C., Maziere, C., Mora, L., Auclair, M., Goldstein, S., and Polonovski, J., 1986. Phorbol esters inhibit low density lipoprotein processing by cultured human fibroblasts. *F.E.B.S.* **195**:135-139.

McClure, M.O., Marsh, M., and Weiss, R.A., 1988. Human immunodeficiency virus infection of CD4-bearing cells occurs by a pH-independent mechanism. *EMBO J.* **7**:513-518.

McDougal, J.S., Kennedy, M.S., Sligh, J.M. Cort, S.P., Mawle, A., and Nicholson, K.A., 1986. Binding of HTLV-III/LAV to T4⁺ T cells by a complex of the 110 K viral protein and the T4 molecule. *Science* **231**:382-385.

McGraw, T.E., Dunn, K.W., and Maxfield, F.R., 1988. Phorbol ester treatment increases the exocytic rate of the transferrin receptor recycling pathway independent of serine-24-phosphorylation. *J. Cell Biol.* **106**:1061-1066.

Meresse, S., and Hofflack, B., 1993. Phosphorylation of the cation-independent mannose 6-phosphate receptor is closely associated with its exit from the *trans*-Golgi network. *J. Cell Biol.* **120**:67-75.

Meyer, T., Regenass, U., Fabbro, D., Alter, E., Rosel, J., Muller, M., Caravatti, G., and Matter, A., 1989. A derivative of staurosporine (CGP 41 251) shows selectivity for protein kinase C inhibition and *in vitro* anti-proliferative as well as *in vivo* anti-tumor activity. *Int. J. Cancer* **43**:851-856.

Miceli, M.C., von Hoegen, P., and Parnes, J.R., 1991. Adhesion versus coreceptor function of CD4 and CD8: role of the cytoplasmic tail in coreceptor activity. *Proc. Natl. Acad. Sci. USA* **88**:2623-2627.

Miettinen, H.M., Rose, J.K., and Mellman, I., 1989. Fc receptor isoforms exhibit distinct abilities for coated pit localization as a result of cytoplasmic domain heterogeneity. *Cell* **58**:317-327.

Miettinen, H.M., Matter, K., Hunziker, W., Rose, J.K., and Mellman, I., 1992. Fc receptor endocytosis is controlled by a cytoplasmic domain determinant that actively prevents coated pit localization. *J. Cell Biol.* **116**:875-888.

Mittler, R.S., Goldman, S.J., Spitalny, G.L., and Burakoff, S.J., 1989. T-cell receptor-CD4 physical association in a murine T-cell

hybridoma: induction by antigen receptor ligation. *Proc. Natl. Acad. Sci. USA* **86**:8531-8535.

Miyata, Y., Nishida, E., and Sakai, H., 1988. Growth factor- and phorbol ester-induced changes in cell morphology analyzed by digital image processing. *Exp. Cell Res.* **175**:286-297.

Moller, B.K., Andresen, B.S., Christensen, E.I., and Petersen, C.M., 1990. Surface membrane CD4 turnover in phorbol ester stimulated T-lymphocytes. *Fed. Euro. Biochem. Soc.* **276**:59-62.

Mueller, S.C., and Hubbard, A.L., 1986. Receptor-mediated endocytosis of asialoglycoproteins by rat hepatocytes: receptor-positive and receptor-negative endosomes. *J. Cell Biol.* **102**:932-942.

Mullock, B.M., Branch, W.J., van Schaik, M., Gilbert, L.K., and Luzio, J.P., 1989. Reconstitution of an endosome-lysosome interaction in a cell-free system. *J. Cell Biol.* **108**:2093-2099.

Murphy, R.F., 1991. Maturation models for endosome and lysosome biogenesis. *Trends Cell Biol.* **1**:77-82.

Mustelin, T., Coggeshall, K.M., and Atman, A., 1989. Rapid activation of the T-cell tyrosine protein kinase pp56^{lck} by the CD45 phosphotyrosine phosphatase. *Proc. Natl. Acad. Sci. USA* **86**:6302-6306.

Naim, H.Y., and Roth, M.G., 1994. Characteristics of the internalization signal in the Y543 Influenza virus hemagglutinin suggests a model for a recognition of internalization signals containing tyrosine. *J. Biol. Chem.* **269**:3928-3933.

Nishizuka, Y., 1986. Studies and perspectives of protein kinase C. *Science* **233**:305-312.

Neudorf, S., Jones, M., Parker, S., Papes, R., and Lattier, D., 1991. Phorbol esters down-regulate transcription and translation of the CD4 gene. *J. Immunol.* **146**:2836-2840

Oka, J.A., and Weigel, P.H., 1989. The pathways for fluid phase and receptor mediated endocytosis in rat hepatocytes are different but thermodynamically equivalent. *Biochem. Biophys. Res. Comm.* **159**:488-494.

Oka, J.A., Christensen, M.D., and Weigel, P.H., 1989. Hyperosmolarity inhibits galactosyl receptor-mediated but not fluid phase endocytosis in isolated rat hepatocytes. *J. Biol. Chem.* **264**:12016-12024.

Ostergaard, H.L., Shackelford, D.A., Hurley, T.R., Johnson, P., Hyman, R., Sefton, B.M., and Trowbridge, I.S., 1989. Expression of CD45 alters phosphorylation of the *lck*-encoded tyrosine protein kinase in murine lymphoma T-cell lines. *Proc. Natl. Acad. Sci. USA* **86**:8959-8963.

Owens, T., Fazekas de St. Groth, B., Miller, J.F.A.P., 1987. Coaggregation of the T-cell receptor with CD4 and other T-cell surface molecules enhances T-cell activation. *Proc. Natl. Acad. Sci. USA* **84**:9209-9213.

Pantaleo, G., Olive, D., Poggi, A., Kozumbo, W.J., and Moretta, A., 1987. Transmembrane signalling via the T11-dependent pathway of human T cell activation. Evidence for the involvement of 1,2-diacylglycerol and inositol phosphates. *Eur. J. Immunol.* **17**:55-60.

Park, J.E., Lopez, J.M., Cluett, E.B., and Brown, W.J., 1991. Identification of a membrane glycoprotein found primarily in the prelysosomal endosome compartment. *J. Cell Biol.* **112**:245-255.

Pauza, C.D., and Price, T.M., 1988. Human immunodeficiency virus infection of T cells and monocytes proceeds via receptor-mediated endocytosis. *J. Cell Biol.* **107**:959-968.

Pearse, B.M.F., 1988. Receptors compete for adaptors found in plasma membrane coated pits. *EMBO J.* 7:3331-3336.

Pelchen-Matthews, A., Armes, J.E., and Marsh, M. 1989. Internalization and recycling of CD4 transfected into HeLa and NIH3T3 cells. *EMBO J.* 8:3641-3649.

Pelchen-Matthews, A., Armes, J.E., Griffiths, G., and Marsh, M. 1991. Differential endocytosis of CD4 in lymphocytic and nonlymphocytic cells. *J. Exp. Med.* 173:575-587.

Pelchen-Matthews, A., Boulet, I., Littman, D.R., Fagard, R., Marsh, M., 1992. The protein kinase p56^{lck} inhibits CD4 endocytosis by preventing entry of CD4 into coated pits. *J. Cell Biol.* 117:279-290.

Pelchen-Matthews, A., Parsons, I.J., and Marsh, M. 1993. Phorbol ester-induced downregulation of CD4 is a multistep process involving dissociation from p56^{lck}, increased association with clathrin-coated pits, and altered endosomal sorting. *J. Exp. Med.* 178:1209-1222.

Peters, C., Braun, M., Weber, B., Wendland, M., Schmidt, B., Pohlmann, R., Waheed, A., and von Figura, K., 1990. Targeting of a lysosomal membrane protein: a tyrosine-containing endocytosis signal in the cytoplasmic tail of lysosomal acid phosphatase is necessary and sufficient for targeting to lysosomes. *EMBO J.* 9:3497-3506.

Petersen, C.M., Christensen, E.I., Andresen, B.S., and Moller, B.K., 1992. Internalization, lysosomal degradation and new synthesis of surface membrane CD4 on phorbol ester-activated T-lymphocytes and U-937 cells. *Exp. Cell Res.* 201:160-173.

Phaire-Washington, L., Wang, E., and Silversten, C., 1980a. Phorbol myristate acetate stimulates pinocytosis and membrane spreading in mouse peritoneal macrophages. *J. Cell Biol.* 86:634-640.

Phaire-Washington, L., Silversten, C., and Wang, E., 1980b. Phorbol myristate acetate stimulates microtubule and 10 nm filament extension and lysosome redistribution in mouse macrophages. *J. Cell Biol.* **86**:641-655.

Reid, P.A., 1990. The use of novel probes for radioiodination to study the endocytic pathway in human cell lines. Ph.D. Thesis, University of Dundee.

Reinherz, E.L., Kung, P.C., Goldstein, G., and Schlossman, S.F., 1979. Further characterization of the human inducer T cell subset defined by monoclonal antibody. *J. Immunol.* **123**:2894-2896.

Richardson, N.E., Brown, N.R., Hussey, R.E., Vaid, A., Matthews, T.J., Bolognes, D.P., and Reinherz, E.L., 1988. Binding site for human immunodeficiency virus coat protein gp120 is located in the NH₂-terminal region of T4 (CD4) and requires the intact variable-region-like domain. *Proc. Natl. Acad. Sci. USA* **85**:6102-6106.

Rijnboutt, S., Stoorvogel, W., Geuze, H.J., Strous, G.J., 1992. Identification of subcellular compartments involved in biosynthetic processing of cathepsin D. *J. Biol. Chem.* **267**:15665-15672.

Rivas, A., Takada, S., Koide, J., Sonderstrup-McDevitt, G., and Engleman, E.G., 1988. CD4 molecules are associated with the antigen receptor complex on activated but not resting T cells. *J. Immunol.* **140**:2912-2918.

Robey, E.A., Fowlkes, B.J., Gordon, J.W., Kloussis, D., von Boehmer, H., Ramsdell, F., and Axel, R., 1991. Thymic selection in CD8 transgenic mice supports an instructive model for commitment to a CD4 or CD8 lineage. *Cell* **64**:99-107.

Robinson, M.S., 1992. Adaptins. *Trends Cell Biol.* **2**:293-297.

Robinson, P.J., Sontag, J-M., Liu, J-P., Fykse, E.M., Slaughter, C., McMahon, H., and Sudhof, T.C., 1993. Dynamin GTPase regulated

by protein kinase C phosphorylation in nerve terminals. *Nature* **365**:163-166.

Roederer, M., Bowser, R., and Murphy, R.F., 1987. Kinetics and temperature dependence of exposure of endocytosed material to proteolytic enzymes and low pH: evidence for a maturation model for the formation of lysosomes. *J. Cell. Phys.* **131**:200-209.

Rudd, C.E., Trevillyan, J.M., Dasgupta, J.D., Wong, L.L., and Schillossman, S.F., 1988. The CD4 receptor is complexed in detergent lysates to a protein-tyrosine kinase (pp58) from human T lymphocytes. *Proc. Natl. Acad. Sci. USA* **85**:5190-5194.

Ruegg, C.L., Rajasekar, S., Stein, B.S., and Engleman, E.G., 1992. Degradation of CD4 following phorbol-induced internalization in human T lymphocytes. Evidence for distinct endocytic routing of CD4 and CD3. *J. Biol. Chem.* **267**:18837-18843.

Ryu, S-E., Kwong, P.D., Truneh, A., Porter, T.G., Arthos, J., Rosenberg, M., Dai, X., Xuong, N-H., Axel, R., Sweet, R.W., and Hendrickson, W.A., 1990. Crystal structure of an HIV-binding recombinant fragment of human CD4. *Nature* **348**:419-426.

Sandoval, I.V., Arredondo, J., Alcalde, J., Noriega, A.G., Vandekerckhove, J., Jimenez, M.A., and Rico, M., 1994. The residues Leu(Ile)⁴⁷⁵-Ile(Leu, Val, Ala)⁴⁷⁶, contained in the extended carboxyl cytoplasmic tail, are critical for targeting of the resident lysosomal membrane protein LIMP II to lysosomes. *J. Biol. Chem.* **269**:6622-6631.

Sandvig, K., and van Deurs, B., 1990. Selective modulation of the endocytic uptake of ricin and fluid phase markers without alteration in transferrin endocytosis. *J. Biol. Chem.* **265**:6382-6388.

Sandvig, K., Olsnes, S., Petersen, O.W., and van Deurs, B., 1987. Acidification of the cytosol inhibits endocytosis from coated pits. *J. Cell Biol.* **105**:679-689.

Sattentau, Q.J., and Weiss, R.A., 1988. The CD4 antigen: physiological ligand and HIV receptor. *Cell* **52**:631-633.

Schell, M.J., Maurice, M., Stieger, B., and Hubbard, A.L., 1992. 5' nucleotidase is sorted to the apical domain of hepatocytes via an indirect route. *J. Cell Biol.* **119**:1173-1182.

Schmid, S.L., 1992. The mechanism of receptor-mediated endocytosis: more questions than answers. *BioEssays* **14**:589-596.

Schmid, S.L., Fuchs, R., Male, P., and Mellman, I., 1988. Two distinct subpopulations of endosomes involved in membrane recycling and transport to lysosomes. *Cell* **52**:73-83.

Schmid, S.L., Fuchs, R., Kielian, M., Helenius, A., and Mellman, I., 1989. Acidification of endosome subpopulations in wild-type chinese hamster ovary cells and temperature-sensitive acidification-defective mutants. *J. Cell Biol.* **108**:1291-1300.

Schmid, S.L., and Carter, L.L., 1990. ATP is required for receptor-mediated endocytosis in intact cells. *J. Cell Biol.* **111**:2307-2318.

Shaw, A.S., Amrein, K.E., Hammond, C., Stern, D.F., Sefton, B.M., and Rose, J.K., 1989. The *lck* tyrosine protein kinase interacts with the cytoplasmic tail of the CD4 glycoprotein through its unique amin-terminal domain. *Cell* **59**:627-636.

Shaw, A.S., Chalupny, J., Whitney, J.A., Hammond, C., Amrein, K.E., Kavathas, P., Sefton, B.M., and Rose, J.K., 1990. Short related sequences in the cytoplasmic domains of CD4 and CD8 mediate binding to the amino-terminal domain of the p56^{lck} tyrosine protein kinase. *Mol. Cell. Biol.* **10**:1853-1862.

Shin, J., Doyle, C., Yang, Z., Kappes, D., Strominger, J.L., 1990. Structural features of the cytoplasmic region of CD4 required for internalization. *EMBO J.* **9**:425-434.

Shin, J., Dunbrack Jr., R.L., Lee, S., and Strominger, J.L., 1991. Phosphorylation-dependent down-regulation of CD4 requires a specific structure within the cytoplasmic domain of CD4. *J. Biol. Chem.* **266**:10658-10665.

Sieh, M., Bolen, J.B., and Weiss, A., 1993. CD45 specifically modulates binding of lck to a phosphopeptide encompassing the negative regulatory tyrosine of lck. *EMBO J.* **12**:315-321.

Sipe, D.M., and Murphy, R.F., 1987. High-resolution kinetics of transferrin acidification in BALB/c 3T3 cells: exposure to pH 6 followed by temperature-sensitive alkalization during recycling. *Proc. Natl. Acad. Sci. USA* **84**:7119-7123.

Sleckman, B.P., Shin, J., Igras, V.E., Collins, T.L., Strominger, J.L., and Burakoff, S.J., 1992. Disruption of the CD4-p56^{lck} complex is required for rapid internalization of CD4. *Proc. Natl. Acad. Sci. USA* **89**:7566-7570.

Smith, S.D., Shatsky, M., Cohen, P.S., Warnke, R., Link, M.P., and Glader, B.E., 1984. Monoclonal antibody and enzymatic profiles of human malignant T-lymphoid cells and derived cell lines. *Cancer Res.* **44**:5657-5661.

Sorkin, A., and Carpenter, G., 1993. Interaction of activated EGF receptors with coated pit adaptins. *Science* **261**:612-615.

Sosa, M.A., Schmidt, B., von Figura, K., Hille-Rehfeld, A., 1993. *In vitro* binding of plasma membrane-coated vesicle adaptors to the cytoplasmic domain of Lysosomal Acid Phosphatase. *J. Biol. Chem.* **268**:12537-12543.

Stein, B.S., Gowda, S.D., Lifson, J.D., Penhallow, R.C., Bensch, K.G., and Engleman, E.G., 1987. pH-independent HIV entry into CD4-positive T cells via virus envelope fusion to the plasma membrane. *Cell* **49**:659-668.

Stewart, S.J., Fujimoto, J., and Levy, R., 1986. Human T lymphocytes and monocytes bear the same Leu-3(T4) antigen. *J Immunol.* **136**:3773-

Stoorvogel, W., Strous, G.J., Geuze, H.J., Oorschot, V., and Schwartz, A.L., 1991. Late endosomes derive from early endosomes by maturation. *Cell* **65**:417-427.

Straus, D.B., and Weiss, A., 1992. Genetic evidence for the involvement of the lck tyrosine kinase in signal transduction through the T cell antigen receptor. *Cell* **70**:585-593.

Swanson, J.A., Yirinec, B.D., and Silverstein, S.C., 1985. Phorbol esters and horseradish peroxidase stimulate pinocytosis and redirect the flow of pinocytosed fluid in macrophages. *J. Cell Biol.* **100**:851-859.

Thompson, J.A., Lau, A.L., and Cunningham, D.D., 1987. Selective radiolabelling of cell surface proteins to a high specific activity. *Biochem.* **26**:743-750.

Thuillier, L., Selz, F., Metezeau, P., and Perignon, J-L., 1990. The activation of protein kinase C is not necessary for the monoclonal antibody-induced modulation of CD3 and CD4 antigens. *Eur. J. Immunol.* **20**:1197-1200.

Tooze, J., and Hollinshead, M., 1991. Tubular early endosomal networks in AtT20 and other cells. *J. Cell Biol.* **115**:635-653.

Trowbridge, I.S., Collawn, J.F., and Hopkins, C.R., 1993. Signal-dependent membrane protein trafficking in the endocytic pathway. *Ann. Rev. Cell Biol.* **9**:129-161.

Turner, J.M., Brodsky, M.H., Irving, B.A., Levin, S.D., Perlmutter, R.M., and Littman, D.R., 1990. Interaction of the unique N-terminal region of tyrosine kinase p56^{lck} with cytoplasmic domains of CD4 and CD8 is mediated by cysteine motifs. *Cell* **60**:755-765.

Tycko, B., and Maxfield, F.R., 1982. Rapid acidification of endocytic vesicles containing α_2 -macroglobulin. *Cell* **28**:643-651.

van der Blik, A.M., Redelmeier, T.E., Damke, H., Tisdale, E.J., Meyerowitz, E.M., and Schmid, S.L., 1993. Mutations in human dynamin block an intermediate stage in coated vesicle formation. *J. Cell Biol.* **122**:553-563.

van der Sluijs, P., Hull, M., Zahraoui, A., Tavitian, A., Goud, B., and Mellman, I., 1991. The small GTP binding protein rab 4 is associated with early endosomes. *Proc. Natl. Acad. Sci. USA* **88**:6313-6317.

van der Sluijs, P., Hull, M., Webster, P., Male, P., Goud, B., and Mellman, I., 1992. The small GTP-binding protein rab 4 controls an early sorting event on the endocytic pathway. *Cell* **70**:729-740.

van Deurs, B., Petersen, O.W., Olsnes, S., and Sandvig, K., 1989. The ways of endocytosis. *Int. Rev. Cytol.* **117**:131-177.

van Deurs, B., Holm, P.K., Kayser, L., Sandvig, K., and Hansen, S.H., 1993. Multivesicular bodies in Hep-2 cells are maturing endosomes. *Eur. J. Cell Biol.* **61**:208-224.

Vega, M.A., Rodriguez, F., Segui, B., Cales, C., Alcalde, J., and Sandoval, I.V., 1991. Targeting of lysosomal integral membrane protein LIMP II. The tyrosine-lacking carboxyl cytoplasmic tail of LIMP II is sufficient for direct targeting to lysosomes. *J. Biol. Chem.* **266**:16269-16272.

Veillette, A., Bookman, M.A., Horak, E.M., and Bolen, J.B., 1988. The CD4 and CD8 T cell surface antigens are associated with the internal membrane tyrosine-protein kinase p56^{lck}. *Cell* **55**:301-308.

Veillette, A, Bolen, J.B., and Bookman, M.A., 1989a. Alterations in tyrosine protein phosphorylation induced by antibody-mediated cross-linking of the CD4 receptor of T lymphocytes. *Mol. Cell. Biol.* **9**:4441-4446.

Veillette, A, Bookman, M.A., Horak, E.M., Samelson, L.E., and Bolen, J.B., 1989b. Signal transduction through the CD4 receptor involves the activation of the internal membrane tyrosine-protein kinase p56^{lck}. *Nature* **338**:257-259.

Veillette, A., Sleckman, B.P., Ratnofsky, S., Bolen, J.B., and Burakoff, S.J., 1990. The cytoplasmic domain of CD4 is required for stable association with the lymphocyte-specific tyrosine protein kinase p56^{lck}. *Eur. J. Immunol.* **20**:1397-1400.

Wang, P.T.H., Bigby, M., and Sy, M-S., 1987. Selective down modulation of L3T4 molecules on murine thymocytes by the tumor promoter, phorbol 12-myristate 13-acetate. *J. Immunol.* **139**:2157-2165.

Wang, J., Yan, Y., Garrett, T.P.J., Liu, J., Rodgers, D.W., Garlick, R.L., Tarr, G.E., Husain, Y., Reinherz, E.L., and Harrison, S.C., 1990. Atomic structure of a fragment of human CD4 containing two immunoglobulin-like domains. *Nature* **348**:411-418.

Watts, C., and Marsh, M., 1992. Endocytosis: what goes in and how? *J. Cell Science* **103**:1-8.

Weyand, C.M., Goronzy, J., and Fathman, C.G., 1987. Modulation of CD4 by antigenic activation. *J. Immunol.* **138**:1351-1354.

Weiss, A., 1993. T cell antigen receptor signal transduction: a tale of tails and cytoplasmic protein-tyrosine kinases. *Cell* **73**:209-212.

Williams, M.A., and Fukuda, M., 1990. Accumulation of membrane glycoproteins in lysosomes requires a tyrosine at a particular position in the cytoplasmic tail. *J. Cell Biol.* **111**:955-966.

Willison, K., Lewis, V., Zukerman, S., Cordell, J., Dean, C., Miller, K., Lyon, M.F., and Marsh, M., 1989. The *t* complex polypeptide 1 (TCP-1) is associated with the cytoplasmic aspect of Golgi membranes. *Cell* **57**:621-632.

Yoshida, H., Koga, Y., Nakamura, K., Kimura, G., and Nomoto, K., 1992. A lymphocyte-specific protein tyrosine kinase, p56^{lck}, regulates the PMA-induced internalization of CD4. *Biochim. Biophys. Acta* **1137**:321-330.

Young, S., Parker, P.J., Ullrich, A., and Stabel, S., 1987. Down-regulation of protein kinase C is due to an increased rate of degradation. *Biochem. J.* **244**:775-779.

Zuniga-Pflucker, J.C., McCarthy, S.A., Weston, M., Longo, D.L., Singer, A., and Kruisbeek, A.M., 1989. Role of CD4 in thymocyte selection and maturation. *J. Exp. Med.* **169**:2085-2096.

Phorbol Ester-induced Downregulation of CD4 is a Multistep Process Involving Dissociation from p56^{lck}, Increased Association with Clathrin-coated Pits, and Altered Endosomal Sorting

By Annegret Pelchen-Matthews, Ian J. Parsons, and Mark Marsh

From the Medical Research Council Laboratory for Molecular Cell Biology and Department of Biology, University College London, London WC1E 6BT, England

Summary

The phorbol ester phorbol myristate acetate (PMA) induces a rapid downregulation of CD4 from the surface of T cells and lymphocytic cell lines, as well as from CD4-transfected nonlymphoid cells. Here we have studied the mechanisms of this phorbol ester-induced CD4 modulation. Using HeLa-CD4 or NIH-3T3-CD4 cells, in which the endocytosis of CD4 is not influenced by the protein tyrosine kinase p56^{lck}, we show that PMA enhanced the uptake of CD4, increasing the rate of CD4 endocytosis three to five-fold, and doubling the proportion of CD4 found inside the cells. Trafficking of a CD4 mutant lacking the major portion of the cytoplasmic domain, as well as fluid phase endocytosis were not affected by PMA treatment. Studies in which clathrin-coated pits were disrupted through the use of hypertonic media indicated that both the constitutive and PMA-induced CD4 uptake occurred through coated vesicles. Electron microscopy demonstrated directly that PMA increases the association of CD4 with coated pits. Immunofluorescent staining of internalized CD4 showed that PMA also diverted CD4 from the early endosome-plasma membrane recycling pathway to a mannose 6-phosphate receptor-containing late endosomal compartment. In lymphoid or p56^{lck}-expressing transfected cells, these effects were preceded by the PMA-induced dissociation of CD4 and p56^{lck}, which released CD4 and made possible increased endocytosis and altered intracellular trafficking. Together these results indicate that phorbol esters have multiple effects on the normal endocytosis and trafficking of CD4, and suggest that phosphorylation may influence the interaction of CD4 with coated pits.

CD4 is a type I integral cell surface glycoprotein that is expressed primarily on thymocytes and MHC class II-restricted peripheral T cells (1, 2). The molecule is a member of the Ig supergene family and appears to function in T lymphocyte ontogeny (3) and in the activation of mature CD4⁺ T cells (4). In addition, CD4 acts as the primary receptor for the HIVs (5). The ectodomain of CD4 contains sites that can interact with nonpolymorphic regions of the MHC class II antigens and also bind to the gp120 component of the HIV envelope glycoproteins (6, 7). In addition, the cytoplasmic domain of CD4 interacts with a lymphocyte-specific *src*-related protein tyrosine kinase, p56^{lck} (8), and CD4 may therefore also function in signal transduction.

Although the primary site of CD4 function appears to be at the cell surface, it is known that various physiological and experimental stimuli can induce its downregulation. Indeed, loss of cell surface CD4 could be involved in the generation of CD4⁺CD8⁺ thymocytes, and the downregulation of CD4 on peripheral T cells may contribute to the induction of anergy and tolerance. Exposure of specific T cells to an

appropriate antigen (9–11), or to cross-linking Abs against CD4 (12, 13), the CD3-TCR complex (11), or CD2 (14) can induce a reduction in cell surface CD4 expression. In addition, cell surface CD4 levels can be modulated during HIV infection (15), after treatment with a soluble form of HIV gp120 (16, 17) or after exposure to gangliosides (18, 19). The modulation of CD4 that occurs during antigen encounter can be mimicked by treating cells with phorbol esters (9, 10). These activators of protein kinase C have been shown to cause transient phosphorylation of the CD4 cytoplasmic domain (9, 20, 21), which may then induce CD4 downmodulation by endocytosis (21–23). However, the mechanisms by which CD4 is cleared from the cell surface have not been elucidated in detail, and, although it appears that internalized CD4 is degraded after phorbol ester stimulation (23–26), the exact fate of the downregulated CD4 molecules has not been determined.

We have previously demonstrated that on transfected nonlymphoid (HeLa-CD4 or NIH-3T3-CD4) and monocytic cell lines (HL-60 and U937), CD4 is constitutively internalized

and recycled to the cell surface (27–29). Internalization occurs through coated pits and coated vesicles and, at steady state, ~40% of the CD4 is found inside the cells. In contrast, the CD4 expressed in lymphoid cell lines is not internalized (28), but is restricted to the cell surface through its interaction with p56^{lck} (30). In the present study, we have examined the mechanisms of phorbol ester-induced CD4 modulation. Since p56^{lck} clearly has a significant influence on the endocytic trafficking of CD4 (30), we have used CD4-transfected non-lymphoid cells for these experiments. We demonstrate that human CD4 expressed on HeLa-CD4 or NIH-3T3-CD4 cells can be downregulated by phorbol ester, and that this modulation is not dependent on the presence of p56^{lck}. The initial effect of phorbol ester is to increase the rate of CD4 endocytosis through coated pits. Furthermore, the level of CD4 recycling observed in the presence of phorbol esters is reduced as CD4 is diverted from the recycling pathway between early endosomes and the plasma membrane to a mannose 6-phosphate receptor-containing late endosomal compartment in the endocytic pathway. In lymphoid or p56^{lck}-expressing transfected cells, phorbol ester-induced CD4 downregulation appears to occur by a similar mechanism. However, the enhanced CD4 endocytosis is only possible after the rapid dissociation of CD4 from p56^{lck}.

Materials and Methods

Materials. Horseradish peroxidase (HRP)¹ type II and PMA were purchased from Sigma Chemical Co. Ltd. (Poole, Dorset, UK). A stock solution of PMA (2 mg/ml in ethanol) was stored at –20°C. The anti-CD4 mAb Leu3a was obtained from Becton Dickinson & Co. (Mountain View, CA), and Fab' fragments were prepared as described (27). The Q4120 Ab, developed by Dr. Quentin Sattentau (Centre d'Immunologie de Marseille-Luminy, INSERM-CNRS, Marseille, France) (31) was provided by the Medical Research Council AIDS Directed Programme Reagents Programme (South Mimms, Potters Bar, Herts, UK). Abs or Fab' fragments were radioiodinated as described (27, 28). Q4120 was labeled with tetramethyl-rhodamine isothiocyanate (TRITC; Cambridge Bio-Science, Cambridge, UK) according to the manufacturer's instructions, whereas the fluorescein-conjugated mAb to the transferrin receptor (TfR), L01.1, was purchased from Becton Dickinson & Co. A rabbit polyclonal serum specific for the cation independent mannose 6-phosphate receptor (CI-MPR) was kindly provided by Dr. W. J. Brown (Cornell University, Ithaca, NY) and has been previously characterized (32). The rabbit antiserum to p56^{lck}, anti-p56^{lck} (KERP), raised against a peptide covering residues 478–509 of murine p56^{lck}, has been described (30). A second antiserum, anti-p56^{lck} (RNGS), was raised against a peptide covering residues 39–64 of murine p56^{lck} starting with the sequence N'-RNGS (prepared by Dr. Torben Saermark, University of Copenhagen, Copenhagen, Denmark, for the European Community Concerted Action programme), and was affinity purified using the peptide

immobilized on Reactigel (Pierce and Warriner, Chester, UK). Peroxidase-conjugated, and rhodamine- or fluorescein-labeled anti-rabbit and anti-mouse reagents were purchased from Pierce and Warriner.

Cells and Cell Culture. Adherent HeLa and NIH-3T3 cell lines transfected with the cDNAs of human CD4 or mutant CD4^{ΔCT}, as well as M22, an NIH-3T3-CD4 cell line which has been super-transfected with the murine *lck* cDNA, were cultured as described (28, 30) and used 3 d after subculture unless otherwise indicated. CD4^{ΔCT} is a CD4 mutant from which the major portion of the cytoplasmic domain (comprising amino acids 403–433) has been deleted (33). The lymphocytic cell line SupT1 was grown in RPMI 1640 medium supplemented with 10% FCS, 100 U/ml of penicillin, and 0.1 mg/ml streptomycin and was used when growing exponentially.

Ab Binding and Endocytosis Assays. To determine levels of CD4 remaining on the cell surface after phorbol ester treatment, cells were cooled by washing twice in ice-cold binding medium (BM; RPMI 1640 lacking bicarbonate, supplemented with 0.2% BSA, and 10 mM Hepes, pH 7.4) and incubated for 2 h on ice in medium containing 0.3 nM ¹²⁵I-labeled anti-CD4 mAb (Leu3a or Q4120) or 0.5 nM ¹²⁵I-Fab' of Leu3a. Unbound Ab or Fab' was washed away in three changes of medium and two rinses of PBS, before cells were harvested by dissolving in 0.2 M NaOH for γ-counting.

Internalization of CD4 was measured as described (27). Briefly, adherent cells grown in 16-mm tissue culture wells were labeled with radioiodinated anti-CD4 Abs or Fab' fragments, as detailed above, and warmed to 37°C to allow endocytosis of the Ab tracer. At various times cells were cooled and either harvested directly, or cell surface ¹²⁵I-label was removed by washing in cold BM buffered to pH 2 or 3 with 10 mM morpholinoethanesulfonic acid (MES) and HCl for Ab or Fab' fragments, respectively. For the suspension cell line SupT1, the assay was adapted as described (28). The proportion of acid resistant to total cell counts was calculated for each time point and plotted. For recycling studies, cells were labeled as above, incubated in BM at 37°C for 30 min, cooled, surface stripped in cold medium at pH 3 and returned to BM at 37°C for various times before analysis as described above. To study Ab degradation, all warm media from the endocytosis and recycling studies were collected, and aliquots analyzed by γ-counting before and after precipitation with 20% TCA for 1 h on ice.

To inhibit endocytosis through coated pits, cells were preincubated for 5 min at 0–4°C in hypertonic medium (0.45 M sucrose in RPMI 1640 medium lacking bicarbonate, supplemented with 0.2% BSA, 20 mM MES, and 20 mM succinic acid, pH 5.7) and the endocytosis assay was performed in the presence of hypertonic medium.

Fluid phase endocytosis of HRP was assayed as described (30).

Electron Microscopic Localization of CD4. The distribution of CD4 at the cell surface and during endocytosis was determined as described (28, 30). Briefly, HeLa-CD4 cells grown on 22-mm² glass coverslips were labeled with 8 nM Leu3a and 9 nm protein A gold (provided by Dr. Gareth Griffiths, EMBL, Heidelberg, Germany; 28) and warmed to 37°C for 1–4 min in the presence or absence of 100 ng/ml PMA. Cells were cooled, fixed, and embedded as described (28, 30) and ultrathin sections were examined with an electron microscope (model CM12; Philips Analytical, Cambridge, UK). For quantitative analysis, cells were examined systematically, noting the location of every gold particle encountered.

Immunofluorescence Endocytosis Assay. To follow CD4 endocytosis, HeLa-CD4 cells were grown on glass coverslips, and labeled at 0–4°C with 8 nM Leu3a or rhodamine-conjugated Q4120 for 2 h. The cells were washed extensively and then warmed to 37°C for various times to allow endocytosis of the Ab-labeled CD4 mol-

¹ Abbreviations used in this paper: BM, binding medium; CD4^{ΔCT}, CD4 molecules from which the cytoplasmic domain has been deleted; CI-MPR, cation independent mannose 6-phosphate receptor; HRP, horseradish peroxidase; MES, morpholinoethanesulfonic acid; TfR, transferrin receptor; TRITC, tetramethylrhodamine isothiocyanate.

ecules. After warming, cells on some of the coverslips were cooled on ice and washed in medium adjusted to pH 2 to remove cell surface mAb. Subsequently, all cells were fixed in 3% paraformaldehyde in PBS for 30 min on ice and quenched with 50 mM NH_4Cl . Some samples were permeabilized with 0.1% Triton X-100 to reveal internalized Ab. To detect the Leu3a Ab, cells were stained with rhodamine-labeled goat anti-mouse diluted 1:2,000. Cells on some coverslips were counter stained in rabbit anti-CI-MPR at 1:200 followed by FITC-conjugated goat anti-rabbit diluted 1:1,000, whereas the TfR was detected using FITC-conjugated L01.1 diluted 1:100. Cells were washed and mounted in Moviol, and observed by confocal microscopy (model MRC 600; Bio-Rad Laboratories, Hemel Hempstead, Herts, UK).

Immunoprecipitation and Immunoblotting. M22 cells were washed once in $\text{Ca}^{2+}/\text{Mg}^{2+}$ -free PBS and harvested by scraping into PBS. The cells were centrifuged at 1,500 rpm for 5 min at 4°C, and resuspended in 20 mM Tris-HCl lysis buffer, pH 8.0, containing 3% NP-40, 150 mM NaCl, 2 mM EDTA, and protease inhibitors (1 mM PMSF and 10 $\mu\text{g}/\text{ml}$ each of chymostatin, leupeptin, antipain, and pepstatin) for 10 min on ice. Detergent-insoluble material was removed by centrifugation at 4°C for 30 min at full speed in a benchtop microfuge. The supernatants were collected and aliquots taken for protein determination using the bicinchoninic acid assay (34), immunoprecipitation, and immunoblotting.

To precipitate CD4 and CD4/p56^{lck} complexes, aliquots of each lysate containing equal amounts of cell protein were precleared by incubation for 30 min at 4°C with 50 μl packed, prewashed protein A-Sepharose (Sigma Chemical Co.). Q4120 covalently coupled to protein A-Sepharose (20 μl of a 50% slurry) was then added and the lysate incubated for 2 h at 4°C. The beads were collected by centrifugation (1 min at 1,000 rpm) and washed three times with lysis buffer and twice with 25 mM Hepes, pH 7.2, containing 0.1% NP-40, resuspended in 20 μl SDS-PAGE sample buffer without reducing agents, and run on 10% SDS-PAGE minigels. Aliquots of the lysate before immunoprecipitation were mixed 4:1 with a 5 \times concentrated sample buffer, and run on identical minigels.

After electrophoresis, cellular proteins were transferred to nitrocellulose. The blots were blocked using 10% dried skimmed milk powder (Marvel) in PBS at 4°C overnight, and then incubated in primary Ab. The affinity-purified anti-p56^{lck} (RNGS) and anti-p56^{lck} (KERP) were used at dilutions of 1:1,000 and 1:500, respectively, whereas Q4120 was used at 1.6 $\mu\text{g}/\text{ml}$. After incubation with Ab and washing, the blots were probed with peroxidase-conjugated goat anti-rabbit or goat anti-mouse Abs and developed using an enhanced chemiluminescence detection system (Amersham International, Amersham, Bucks, UK) according to the manufacturer's instructions.

Results

Downregulation of CD4 on Transfected Nonlymphocytic Cells. Phorbol esters such as PMA have been shown to cause rapid downmodulation of CD4 from the surface of human PBL and thymocytes, as well as a number of lymphocytic or myeloid cell lines (9, 14, 22, 35). In addition, PMA can downregulate CD4 expressed on nonlymphoid HeLa cells after transfection (24, 33, 36). Using a binding assay with a radioiodinated anti-CD4 mAb, we determined the concentration dependence of CD4 downregulation by PMA on 3-d-old HeLa-CD4 cells. Half-maximal downregulation (ED_{50}) was observed with 0.5 ng/ml PMA (0.8 nM). Thus, the potency of PMA on HeLa-CD4 cells is similar to that reported for PBL (22, 37, 38).

As already described for lymphocytic cells (9, 14, 22), PMA (100 ng/ml) induced rapid CD4 downregulation on HeLa-CD4 cells, with the majority of the CD4 molecules being removed from the cell surface in 1 h (36). Cell surface CD4 expression remained at a low level (20–30% of that on untreated cells) for up to 8–10 h, but subsequently the amount of cell surface CD4 increased again, recovering to near the original levels after 24–48 h of continuous treatment with phorbol ester. This recovery of CD4 expression was not due to inactivation of the phorbol ester, since PMA-containing medium taken from cells after 24 h was still able to induce CD4 downregulation in fresh HeLa-CD4 cells. Studies with

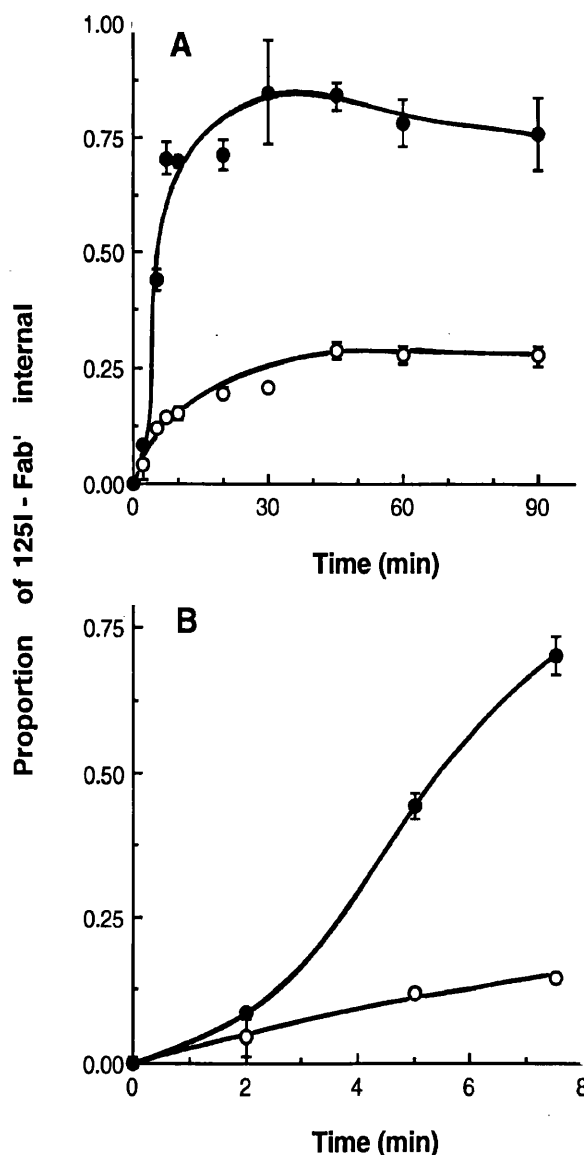


Figure 1. Effect of PMA on CD4 endocytosis in HeLa-CD4 cells. (A) Time course of internalization of CD4 on 3-d-old HeLa-CD4 cells in the presence (●) or absence (○) of 100 ng/ml PMA. CD4 endocytosis was traced with ¹²⁵I-labeled Fab' fragments of Leu3a. The plot shows the ratios of acid-resistant ¹²⁵I-Fab' to the total cell-associated label after various times at 37°C. The initial portion of the graph (0–8 min) is expanded (B).

Table 1. *Effect of PMA on CD4 Endocytosis*

Cell line	Tracer used	Control		Plus PMA		No. of experiments
		Endocytosis rate	Percent internal at 60 min	Endocytosis rate	Percent internal at 60 min	
		%/min		%/min		
HeLa-CD4 (3-d-old)	¹²⁵ I-Fab'	2.0	28	11.3	78	1*
	¹²⁵ I-Leu3a	1.8 ± 0.9	37 ± 1	8.4 ± 3.3	62 ± 14	7
HeLa-CD4 (2-d-old)	¹²⁵ I-Q4120	2.6 ± 0.2	46 ± 7	6.4 ± 0.2	79 ± 11	2
NIH-3T3-CD4	¹²⁵ I-Leu3a	3.9 ± 1.2	41 ± 10†	12.9 ± 2.8	88	2

* Data from multiple experiments are expressed as mean ± SD.

† Internal at 30–60 min.

cycloheximide indicated that the recovery requires protein synthesis (data not shown), and may involve the PMA-induced downregulation of protein kinase C (39, 40), as well as effects of the phorbol ester on CD4 transcription and translation (41). This has not been examined further in the present study.

Downregulation was dependent on the presence of the CD4 cytoplasmic domain, and was not observed in HeLa cells transfected with a mutant CD4 lacking the cytoplasmic domain (HeLa-CD4^{cyt-}; 33, 36, 42).

Like the HeLa-CD4 cells, NIH-3T3 cells transfected with CD4 (NIH-3T3-CD4) downregulated their cell surface CD4 in response to phorbol ester. The amount of CD4 downregulation on NIH-3T3-CD4 cells was consistently greater than that observed on HeLa-CD4 cells, with >70% of the CD4 being removed from the cell surface during the first 30 min of PMA treatment.

Thus, CD4 can be downregulated from the cell surface of lymphoid and nonlymphoid cells by similar concentrations of phorbol esters. This indicates that CD4 downregulation is not T cell dependent and does not require the presence of p56^{lck}. As CD4 downregulation is believed to occur by endocytosis, and CD4 endocytosis is influenced by p56^{lck} expression, we first sought to understand the mechanisms of downregulation in the p56^{lck}-negative nonlymphoid cells.

Effects of Phorbol Esters on CD4 Endocytosis. The CD4 molecules expressed in HeLa-CD4 and NIH-3T3-CD4 cells are constitutively internalized and recycled (27, 29). To study the effects of phorbol ester on this constitutive CD4 endocytosis, cells were surface labeled at 0–4°C with ¹²⁵I-labeled anti-CD4 mAb or Fab' fragments. After 2 h, the cells were washed and warmed to 37°C in the presence or absence of 100 ng/ml PMA. At various times, the level of internalized ¹²⁵I tracer was detected by acid washing as described in Materials and Methods. The result of a typical CD4 endocytosis experiment is shown in Fig. 1. PMA increased the rate of CD4 endocytosis on 3-d-old HeLa-CD4 cells by four to sixfold.

This increase was observed after a brief lag of about 2 min (Fig. 1 B). Comparable results were obtained when CD4 endocytosis was measured using Fab' fragments or intact anti-CD4 mAb (Table 1). Similar effects were seen on 2-d-old HeLa-CD4 or on NIH-3T3-CD4 cells, although the increase in CD4 endocytosis was less striking, possibly because these cells had somewhat higher CD4 endocytosis rates in the absence of phorbol ester. In addition to its effect on the rate of CD4 endocytosis, PMA increased the steady state distribution of CD4 in the cells from 40 to about 80% (Table 1). This effect was generally more pronounced on 2-d-old HeLa-CD4 and on the NIH-3T3-CD4 cells.

To investigate whether the internalized Ab ligands were degraded, the media in which the cells had been warmed for endocytosis were precipitated with TCA. The level of TCA-soluble ¹²⁵I (representing degraded Ab ligand), when calculated as a proportion of the amount of ¹²⁵I-ligand initially bound to the cells, was proportional to the amount of internalized mAb, regardless of the presence of PMA. When levels of TCA-soluble ¹²⁵I were calculated as a proportion of the endocytosed plus degraded counts (i.e., as a proportion of all the activity that was or had been inside the cells), significant increases in TCA-soluble counts (30–40%) were only apparent in cells treated with PMA for 2 h or longer. At these long time points, significant dissociation of the mAb from CD4 could have occurred, especially since CD4 and mAb would have entered acidic organelles. The appearance of degraded activity may not, therefore, reflect the fate of CD4.

These data indicated that the one important effect of phorbol ester is to increase the rate of CD4 endocytosis in HeLa-CD4 or NIH-3T3-CD4 cells. This shifts the steady state distribution of CD4 so that more than 80% is intracellular, with a concomitant decrease in cell surface CD4.

The Specificity of the Phorbol Ester Effect on CD4 Endocytosis. Previous experiments have indicated that phorbol ester-induced downregulation of CD4 is dependent on the

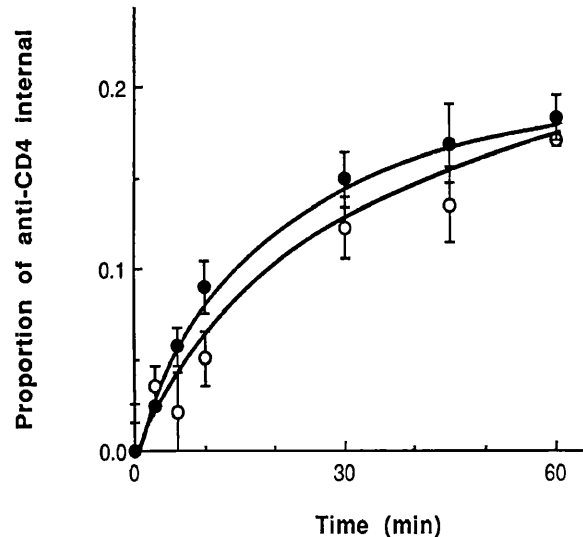


Figure 2. Time course of internalization of ^{125}I -labeled Leu3a in HeLa-CD4^{cyt-} cells that express CD4 molecules from which the cytoplasmic domain has been deleted. The plot shows the ratios of acid-resistant ^{125}I -Leu3a to the total cell-associated label on cells warmed in the presence (●) or absence (○) of 100 ng/ml of PMA.

presence of the cytoplasmic domain (33, 36, 42). We have shown that CD4^{cyt-} molecules can be internalized by bulk flow transport through coated pits in both HeLa and lymphoid cell lines (28). To determine whether phorbol ester treatment also affected the internalization of CD4^{cyt-}, we measured endocytosis on HeLa-CD4^{cyt-} cells. Virtually identical CD4 endocytosis curves were obtained in the presence or absence of PMA (Fig. 2). This observation suggests that the PMA-induced enhancement of CD4 endocytosis described above was specific for full-length CD4 molecules, and not due to a general stimulation of bulk flow endocytosis by phorbol ester, as has been described for example, for macrophages (43, 44). To demonstrate directly that phorbol esters do not stimulate the basal endocytic capacity in HeLa-CD4 cells, we measured the rates of fluid phase endocytosis using HRP. PMA did not affect the initial rate of fluid uptake measured over the first 10 min in HRP medium (fluid uptake occurred at 6×10^{-4} nl/min/ μg of cell protein). However, cells incubated with PMA for longer periods (>1 h) accumulated 20–25% more fluid than control cells, suggesting that PMA-treated cells may retain more of the internalized marker than untreated cells.

Together these results indicate that in these HeLa-CD4 cells, phorbol esters do not have a significant effect on the vesicular traffic from the cell surface, and hence that the phorbol ester-induced increase in CD4 uptake is not due to a general stimulation of endocytosis.

Phorbol Esters Increase CD4 Endocytosis Through Coated Pits. In HeLa and NIH-3T3 cells, CD4 is internalized through clathrin-coated pits and vesicles (28, 30), suggesting that it contains sequences in its cytoplasmic domain that allow it to cluster into coated pits. To examine whether the increased uptake of CD4 observed in the presence of phorbol ester also

occurs by this pathway, we used hypertonic media (45) to inhibit the formation of clathrin-coated vesicles (46). In our hands, incubation in media containing 0.45 M sucrose gave a more complete, yet reversible, inhibition of CD4 internalization than methods of acidifying the cytosol (cf. 47, 48), although long-term cell viability was improved when the hypertonic medium was slightly acidified (Pelchen-Matthews, A., and M. Marsh, manuscript in preparation). Treatment of HeLa-CD4 cells for 1 h with PMA in the presence of medium containing 0.45 M sucrose and adjusted to pH 5.7

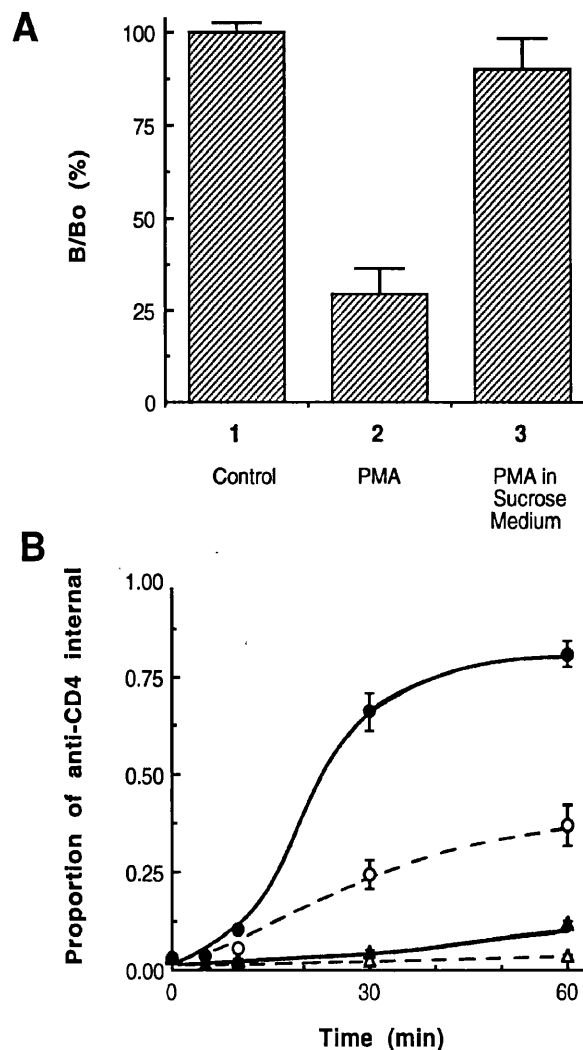


Figure 3. The effect of hypertonic medium on CD4 downregulation and endocytosis on 3-d-old HeLa-CD4 cells. (A) Cell surface expression of CD4 on HeLa-CD4 cells pretreated for 1 h in binding medium (1), medium containing 100 ng/ml PMA (2), or in hypertonic medium containing 100 ng/ml PMA (3). After incubation, cells were cooled and levels of CD4 remaining on the cell surface determined using 0.3 nM ^{125}I -labeled Q4120. The plot shows binding of ^{125}I -Q4120 compared to the untreated cells (B/B_0) after correction for cellular protein content. (B) Time courses of internalization of CD4 in the presence (filled symbols) or absence (open symbols) of 100 ng/ml PMA in normal (circles, solid lines) or hypertonic medium (triangles, dashed lines). CD4 endocytosis was traced with 0.3 nM ^{125}I -Q4120. The plot shows the ratios of acid-resistant ^{125}I -Q4120 to the total cell-associated label after various times at 37°C.

Table 2. *Effect of PMA on the Distribution of Gold-labeled CD4 on HeLa-CD4 Cells*

Time at 37°C	Total No. of particles counted	Particles over noncoated plasma membrane	Particles over coated pits and vesicles	Internalized particles	Unclassified
		%	%	%	
A: Control					
0	511	475 (93.0)	21* (4.1)	0 (0.0)	15
1 min	349	310 (88.8)	18 (5.2)	18 (5.2)	3
2 min	346	314 (90.8)	18 (5.2)	10 (2.9)	4
3 min	416	330 (79.3)	23 (5.5)	56 (13.5)	7
4 min	316	252 (79.7)	8 (2.5)	48 (15.2)	8
B: Plus PMA					
1 min	378	325 (86.0)	27 (7.1)	25 (6.6)	1
2 min	329	253 (76.9)	34 (10.3)	29 (8.8)	13
3 min	372	275 (73.9)	33 (8.9)	52 (14.0)	12
4 min	289	185 (64.0)	15 (5.2)	82 (28.4)	7

Distribution of Leu3a/protein A-gold particles were analyzed as detailed in the text and in reference 28.

* Only particles observed immediately juxtaposed to the clathrin coat were counted in this category.

almost completely inhibited CD4 downregulation (Fig. 3 A). When CD4 internalization was assayed directly, the hypertonic medium inhibited CD4 endocytosis by more than 90%. The increased CD4 endocytosis observed in the presence of PMA was also inhibited to a similar extent (Fig. 3 B), suggesting that both constitutive and PMA-induced uptake of CD4 occurred through coated pits and vesicles.

The findings that PMA does not stimulate vesicular traffic from the surface of HeLa-CD4 cells and that inhibition of coated vesicle-mediated endocytosis inhibits phorbol ester-induced downregulation suggested that the increased rate of CD4 endocytosis may be due to increased association of CD4 with clathrin-coated pits. This was demonstrated directly by immunolabeling electron microscopy. 2-d-old HeLa-CD4 cells were labeled on ice with Leu3a and protein A-gold. After washing to remove any free gold conjugate, cells were warmed to 37°C in the presence or absence of PMA, fixed, and prepared for electron microscopy. Control experiments in which the kinetics of ¹²⁵I-Leu3a uptake were examined after incubation with protein A-gold showed that internalization of the mAb was not affected by the gold probe (28). In the absence of phorbol ester, 4.0–5.5% of the gold particles at the cell surface were found in close apposition to coated plasma membrane (Table 2), in agreement with our previous study (28). In samples treated with PMA, gold particles were also observed in coated pits and vesicles (Fig. 4). When the distribution of labeled CD4 was determined at increasing times after warming in PMA medium, there was a transient increase in the number of gold particles seen in coated pits or vesicles, peaking with more than 10% of all gold particles (or 12% of the gold at the cell surface) adjacent to coated plasma membrane. This represents a threefold increase over the basal coated pit association of CD4, and can account for

the increase in the rate of CD4 endocytosis observed (cf. Table 1). Significantly, the increased association of CD4 with coated pits is observed just before the enhanced endocytosis of CD4 as measured biochemically (the lag shown in Fig. 1 B). Since ligand located in coated pits at the cell surface is still accessible to acid washing in the biochemical experiments, and the lifetime of a coated pit at the cell surface is believed to be about 1–2 min (49–51), the increased association of CD4 with coated pits can completely explain the phorbol ester-induced enhancement of CD4 uptake.

Effects of Phorbol Esters on CD4 Recycling. To investigate whether PMA also affects the recycling of internalized CD4, 3-d old HeLa-CD4 cells were loaded with ¹²⁵I-labeled anti-CD4 Fab' fragments by warming in the presence or absence of 100 ng/ml PMA. The cells were then briefly treated with acid medium at 4°C to remove any Fab' remaining on the cell surface, and reincubated at 37°C. Subsequently, the cells were subjected to a second acid wash and recycling detected as a decrease in the level of acid-resistant ¹²⁵I-Fab' tracer associated with the cells, and a loss of the previously internalized tracer intact (i.e., TCA precipitable) into the medium. In the absence of PMA, the recycling of CD4 observed was similar to our previous results (27). In contrast, very little recycling was observed in cells that had been loaded in the presence of PMA (Fig. 5). Identical results were observed when CD4 recycling was monitored using intact ¹²⁵I-labeled Ab. Furthermore, there was very little recycling of internalized tracer when cells were loaded with the ¹²⁵I-mAb in the absence of phorbol ester, and PMA only added to the recycling medium (data not shown). As in the endocytosis experiments, the level of anti-CD4 tracer found inside the cells at steady state was increased from about 40% in the absence of phorbol ester to about 80% with PMA.

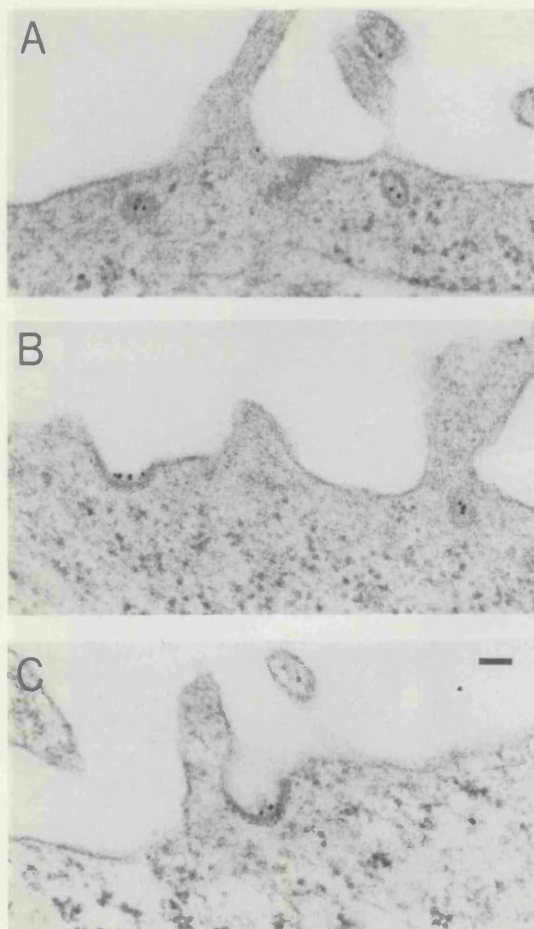


Figure 4. Electron microscopic localization of CD4 in PMA-treated HeLa-CD4 cells. 2-d-old HeLa-CD4 cells were labeled on ice with 8 nM Leu3a followed by protein A-gold, washed, and warmed to 37°C in the presence of 100 ng/ml PMA for 2 min (A and B) or 3 min (C). Scale bar, 100 nm.

Modeling of CD4 Endocytosis. The studies described above have demonstrated that one of the main effects of phorbol ester is to increase CD4 endocytosis through coated pits. To determine if this increase in CD4 internalization is alone sufficient to explain CD4 downregulation, we designed a simple mathematical model of CD4 endocytosis. The experimentally determined CD4 internalization and recycling rates were used to calculate surface and internal CD4 levels and the proportion of internalized molecules at different times using an iterative routine. Thus, for 3-d-old HeLa-CD4 cells, the model was set with 60% of the CD4 molecules at the cell surface, 40% in the endosome compartment, internalization at a rate of 2% per min, and recycling back to the cell surface at 3% of the internal level per min (27, 28), thereby maintaining a steady state. To model our endocytosis experiments, only the pool of molecules initially at the cell surface was considered labeled. This yielded a CD4 uptake curve that corresponded closely to the actual data (open circles in Fig. 6 A). Similarly, when only molecules initially internal were considered labeled, the resulting curve (Fig. 6 B) resembled

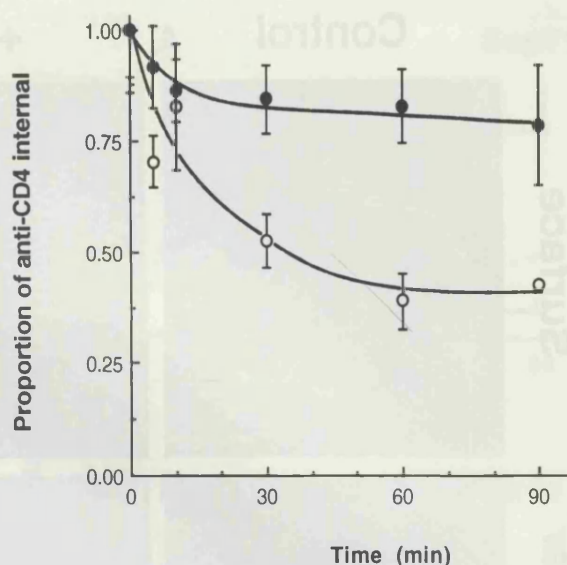


Figure 5. Effect of PMA on recycling of CD4. 3-d-old cultures of HeLa-CD4 cells were surface labeled with 125 I-labeled Fab' fragments of Leu3a, and then warmed for 30 min to 37°C in the presence (●) or absence (○) of 100 ng/ml PMA to allow the tracer to be internalized. Cells were then cooled and all 125 I-Fab' removed from the cell surface by acid washing. The time course of 125 I-Fab' recycling was then determined by rewarming the cells to 37°C for the times indicated. Cells were returned to ice and the acid-resistant activity determined after a second acid wash. The plot shows the ratios of acid-resistant 125 I-Fab' to the total cell-associated label.

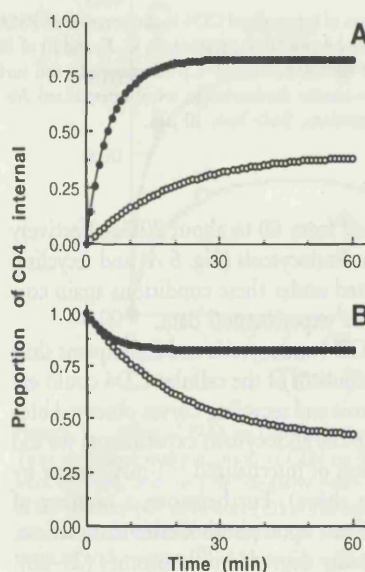


Figure 6. Mathematical modeling of CD4 endocytosis (A) and recycling (B) during endocytosis at 2% per min (○) or 14% per min (●). For details, see text.

the CD4 recycling plot determined experimentally (Fig. 5). To imitate the effect of the phorbol ester, the endocytosis rate in the model was increased to 10–14% per min, whereas all other parameters were maintained. This altered the steady state distribution of CD4 so that the proportion of CD4 at

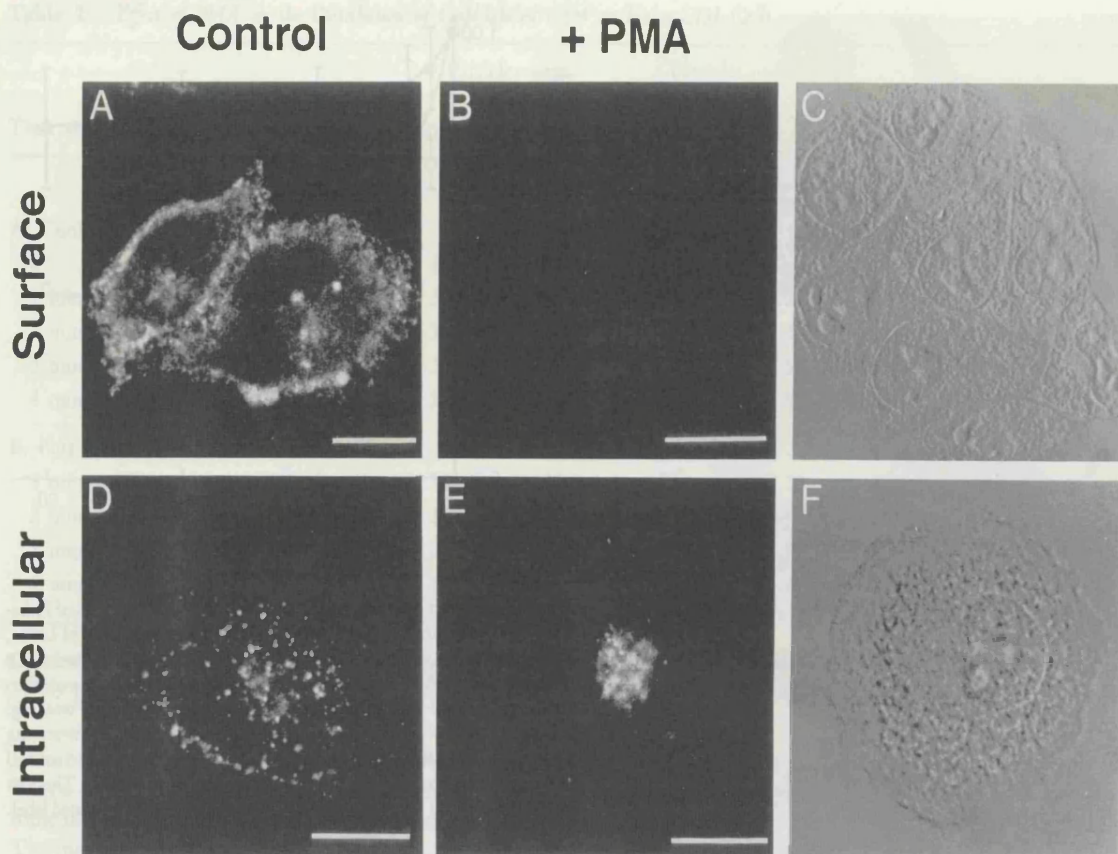


Figure 7. The distribution of internalized CD4 in the presence of PMA. 2-d-old HeLa-CD4 cells were labeled with Leu3a at 4°C and then incubated at 37°C for 1 h in the absence (A and D) or presence (B, C, E, and F) of 100 ng/ml PMA. Cells were then fixed and stained with anti-mouse rhodamine second Ab to reveal CD4 at the cell surface (A–C). Alternatively, cell surface mAb was removed by acid washing before the cells were fixed, permeabilized, and stained with anti-mouse rhodamine to reveal internalized Ab (D–F). (C and F) Phase contrast views of B and E, respectively. All images are of 2- μ m thick optical sections. Scale bars, 10 μ m.

the cell surface decreased from 60 to about 20%, effectively giving downregulation. Endocytosis (Fig. 6 A) and recycling plots (Fig. 6 B) calculated under these conditions again corresponded closely to the experimental data.

Thus, an increase in CD4 endocytosis and consequent shift in the steady state distribution of the cellular CD4 could explain the CD4 endocytosis and recycling curves observed biochemically. However, in the endocytosis experiments we did observe some degradation of internalized 125 I-mAb tracer by TCA precipitation (see above). Furthermore, a number of reports have suggested that, upon phorbol ester stimulation, internalized CD4 is rapidly degraded in lysosomes (23–26). We previously showed by immunofluorescent staining that in NIH-3T3-CD4 cells CD4 is internalized into vesicles distributed throughout the cytoplasm and resembling early endosomes (52). If phorbol ester treatment simply alters the steady state between CD4 internalization and recycling, then a similar distribution of internalized CD4 should be observed in the presence of PMA, although the quantity of CD4 in the intracellular compartment would be increased. To test this, we followed the fate of internalized CD4 by immunofluorescent staining.

Phorbol Esters Alter the Distribution of Internalized CD4. As in the biochemical endocytosis experiments, 2-d-old HeLa-CD4 cells were labeled with anti-CD4 mAb at 4°C and then incubated at 37°C in the presence or absence of PMA, before processing to reveal cell surface or internalized mAb (Fig. 7). In unstimulated cells, this revealed CD4 at the cell surface (Fig. 7 A), and in intracellular vesicular structures located throughout the cytoplasm (Fig. 7 D). Early after the addition of phorbol ester (5 and 10 min), the internalized CD4–anti-CD4 complexes were observed in a similar distribution. At later times (30 min–1 h), cell surface CD4 had become largely undetectable (Fig. 7 B), whereas the internalized anti-CD4 mAb was located in clusters of vesicles in the juxta-nuclear region of the cells (Fig. 7 E). To identify the intracellular compartments further, we performed double-staining studies, using the TfR and the CI-MPR as markers for early and late endosomes, respectively (53). In unstimulated cells which had internalized a TRITC-labeled anti-CD4 mAb for 1 h, counter-staining with a FITC-conjugated anti-TfR mAb, revealed that most of the CD4-containing vesicles were also stained for the TfR (Fig. 8, A and B), and are therefore likely to be early endosomes. In contrast, CD4 internal-

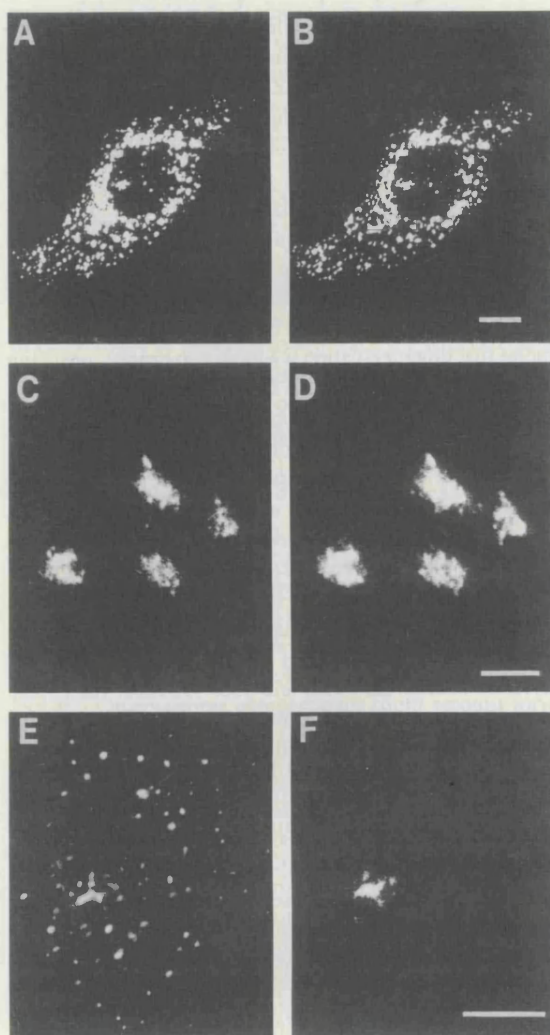


Figure 8. Colocalization of internalized CD4 with the Tfr or CI-MPR. 2-d-old HeLa-CD4 cells were labeled with TRITC-Q4120 (A and B) or Leu3a (C–F) at 4°C and then incubated at 37°C for 1 h in the presence (C and D) or absence (A, B, E, and F) of 100 ng/ml PMA, and internalized anti-CD4 was detected as described in Fig. 7. In the absence of PMA, CD4-containing vesicles (A) could be costained with FITC-labeled anti-Tfr mAb (B), whereas in the presence of PMA, CD4 (C) colocalized with the CI-MPR (D). In the absence of PMA, CD4 (E) remained in vesicles similar to those observed in A and B, which did not costain with the CI-MPR (F). The figure shows optical sections of thickness $\sim 3 \mu\text{m}$ (A and B) or $1 \mu\text{m}$ (C–F). Scale bars, 10 μm .

ized for 1 h in the presence of PMA accumulated in the juxta-nuclear region in structures that could be costained with Abs to the CI-MPR (Fig. 8, C and D). No significant colocalization with the CI-MPR was observed in cells that had internalized CD4 in the absence of PMA (Fig. 8, E and F). Together these data indicate that CD4 internalized into early endosomes is, in the presence of PMA, diverted from the recycling pathway to a CI-MPR-containing late endosome compartment. Thus, in addition to its effect on CD4 endocytosis, PMA also altered the trafficking of internalized CD4 inside the cells.

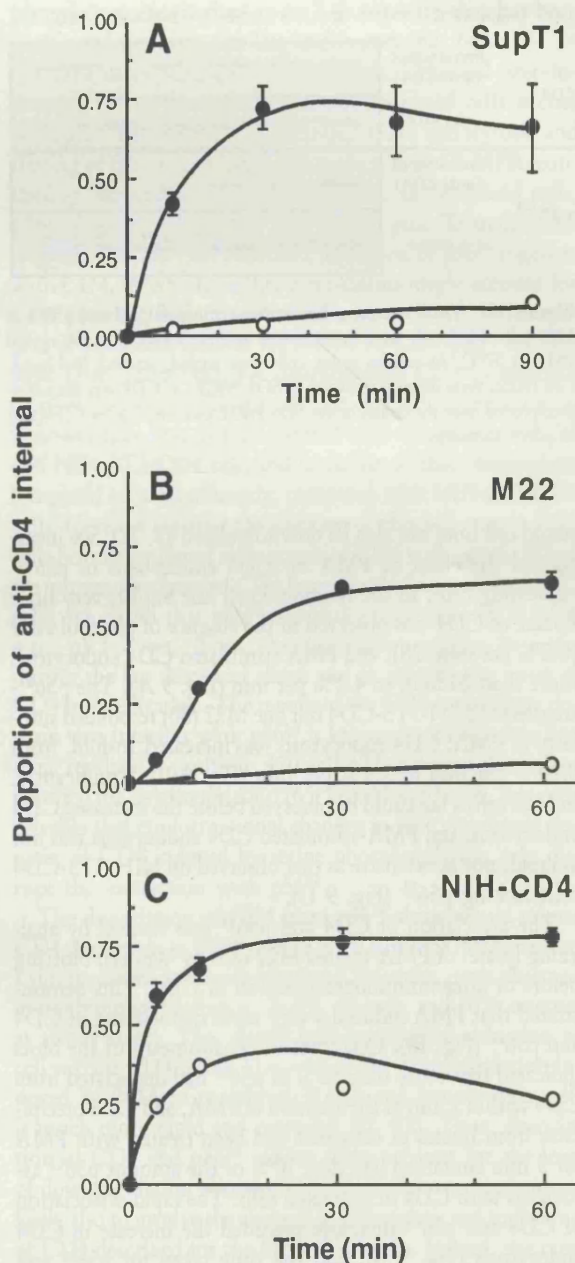


Figure 9. Effect of PMA on CD4 endocytosis in $p56^{\text{lck}}$ -expressing cells. Time courses of internalization of CD4 on SupT1 (A), $p56^{\text{lck}}$ transfected M22 cells (B), and the $p56^{\text{lck}}$ -negative parental NIH-3T3-CD4 cells (C) in the presence (●) or absence (○) of 100 ng/ml PMA. CD4 endocytosis was traced with ^{125}I -labeled anti-CD4 mAb Q4120. The plots show the ratios of acid-resistant ^{125}I -mAb to the total cell-associated label after various times at 37°C.

The Role of $p56^{\text{lck}}$ in Phorbol Ester-Induced CD4 Downregulation. As demonstrated above, in $p56^{\text{lck}}$ -negative cells expressing CD4 after transfection, PMA increases the rate of CD4 internalization and reroutes the internalized CD4 molecules to later compartments of the endocytic pathway. Since $p56^{\text{lck}}$ has been shown to regulate CD4 endocytosis (30), and since the CD4 expressed on T cells, thymocytes, and lym-

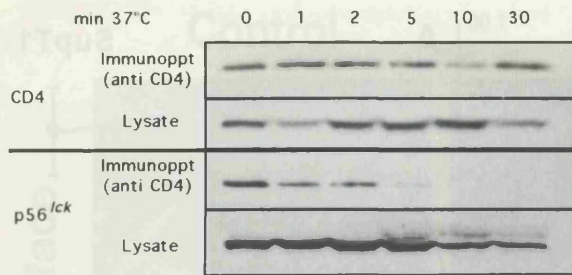


Figure 10. PMA treatment causes dissociation of CD4 and p56^{lck} in M22 cells. M22 cells were incubated in medium containing 100 ng/ml PMA at 37°C. At various times, cells were cooled, washed, and lysed. Cell lysates were directly analyzed by SDS-PAGE, or CD4 was immunoprecipitated from the lysates before SDS-PAGE and blotting for CD4 (*top*) or p56^{lck} (*bottom*).

phoid cell lines can also be downregulated (9, 22), we investigated the effect of PMA on CD4 endocytosis in p56^{lck}-expressing cells. In the lymphoid cell line SupT1, very little uptake of CD4 was observed in the absence of phorbol ester (0.2% per min; 28), and PMA stimulated CD4 endocytosis more than 20-fold, to 4.2% per min (Fig. 9 A). The p56^{lck}-transfected NIH-3T3-CD4 cell line M22 (30) responded similarly to PMA: CD4 endocytosis was increased 16-fold, from 0.24% per min to 3.8% per min (Fig. 9 B). Significantly, in M22 cells a lag could be observed before the increased CD4 endocytosis, and PMA-stimulated CD4 endocytosis was not as rapid, nor as extensive as that observed on NIH-3T3-CD4 cells lacking p56^{lck} (Fig. 9 C).

The association of CD4 and p56^{lck} was studied by analyzing lysates of PMA-treated M22 cells by Western blotting before or after immunoprecipitation of CD4. This demonstrated that PMA induced a very rapid dissociation of CD4 and p56^{lck} (Fig. 10). Quantitative densitometry of the blots indicated that more than 50% of p56^{lck} had dissociated from CD4 within 2 min of the addition of PMA, and CD4 precipitates from lysates of cells that had been treated with PMA for 5 min contained less than 10% of the amount p56^{lck} as associated with CD4 in untreated cells. The rapid dissociation of CD4 and p56^{lck} therefore preceded the increase in CD4 endocytosis (Fig. 9 B), and the time taken for p56^{lck} and CD4 to dissociate may explain the lag in the increase of CD4 endocytosis observed in these cells. The level of CD4 or p56^{lck} detectable in the lysates did not vary significantly over the time course examined. Hence, in p56^{lck}-expressing cells, the increase in CD4 endocytosis is preceded by the dissociation of CD4 from p56^{lck}, thereby allowing CD4 to interact with coated pits.

Discussion

The observation that CD4 is downmodulated when T cells are stimulated by APCs or through cross-linking with Abs suggests that the control of plasma membrane CD4 levels is important in T cell physiology and function. Antigen-induced CD4 downregulation can be mimicked by treatment

of cells with phorbol esters, allowing biochemical and morphological analysis of the mechanisms involved. Downregulation occurs by endocytosis (21–23) and appears to require phosphorylation of serine residues in the cytoplasmic domain of the molecule, in particular of Ser408 (33, 36). In T cells, phorbol ester treatment leads to the dissociation of p56^{lck} and CD4 (54), and recent data indicates that p56^{lck} dissociates before CD4 downregulation (55, 56). Internalized CD4 is believed to be directed to lysosomes and there degraded (23–26). Here we have examined the cellular mechanisms of CD4 downregulation induced by phorbol ester. Our studies indicate that downregulation is a multistep process, involving both increased CD4 endocytosis and altered endosomal sorting. In addition, the downregulation in p56^{lck}-containing cells involves an initial dissociation of the CD4–p56^{lck} complex.

Phorbol Ester-induced Endocytosis of CD4. Under normal conditions, the CD4 expressed in HeLa-CD4 and NIH-3T3-CD4 cells is constitutively internalized through coated pits and vesicles. Here we demonstrated that within minutes of the addition of phorbol ester, there was a three- to fivefold increase in the rate of CD4 internalization. Control experiments indicated that PMA does not modulate fluid phase endocytosis in HeLa-CD4 cells and does not affect the uptake and cycling properties of CD4^{wt} molecules. Thus, the increased uptake of CD4 induced by phorbol ester is not due to general effects on vesicular traffic from the cell surface, but must be due to an increased association of CD4 with endocytic coated pits. This was confirmed in studies with hypertonic media, which inhibit coated vesicle formation, and by electron microscope observation of the association of CD4 with coated pits and vesicles.

Recently, several motifs have been identified that allow plasma membrane receptors to interact with components of clathrin-coated pits and lead to rapid endocytosis of these molecules. Most of these motifs consist of four to six amino acids with flanking aromatic or large hydrophobic residues (e.g., sequences of the form ar-x-x-ar or ar-x-x-x-x-ar), where one of the aromatic residues is frequently a tyrosine (57, 58). Where information is available, these structures show a strong tendency to form β turns, and the substitution of amino acids which would disrupt the β turn has been shown to reduce the efficacy of these endocytosis signals. The cytoplasmic domain of CD4 does not contain such a motif. Nonetheless, the fact that we observe endocytosis of CD4 and clustering into coated pits indicates that an alternative signal(s) must exist (59). Recently, Letourneur and Klausner (60) suggested that a pair of leucine residues forms part of the signal responsible for the endocytosis and lysosomal targeting of the γ and δ subunits of CD3. A di-leucine sequence is found in CD4 (Leu413 and Leu414), and Shin et al. (24) have reported that these leucine residues, as well as other hydrophobic amino acids (Met407 and Ile410) are required for CD4 downregulation. Hence the di-leucine in CD4 may be a component of the endocytosis signal.

Previously it has been demonstrated that phorbol esters induce a rapid transient phosphorylation of serine residues in the cytoplasmic domain of CD4 (9, 21, 36), and that mu-

tation of these serines to alanine reduces the efficiency of downregulation (33, 36, 42). The serine at position 408 is believed to be the most important of the three cytoplasmic serine residues in this respect (36). Although the effects of these residues on phorbol ester-induced downregulation have been recorded, their role in CD4 endocytosis has not been evaluated, and it is unclear why phosphorylation of Ser408 should increase the efficiency of CD4 endocytosis. In contrast to many serine phosphorylation sites that are located at the tip of β turn structures (61), the residues surrounding Ser408 show a strong tendency to form an α helix (24). Phosphorylation of CD4 might be expected to influence the structure of this helix and thereby alter the disposition of sequences involved in endocytosis. The role of phosphorylation in coated vesicle-mediated endocytosis has been controversial (58). However, our studies indicate that PMA directly increases the association of CD4 with coated pits and hence the rate of CD4 endocytosis, and that this may be one situation in which phosphorylation does create or enhance an endocytosis signal.

Phorbol Ester-induced Endosomal Sorting of CD4. Modeling of CD4 endocytosis suggests that the PMA-induced increase in the rate of CD4 endocytosis and the consequent alteration of the steady state distribution of CD4 between the cell surface and the endosome compartment could account for the observed downregulation of CD4. However, several previous studies suggested that CD4 internalized in the presence of PMA may be diverted from the endosome compartment and degraded in lysosomes. We used immunofluorescence microscopy to demonstrate directly that PMA affects the distribution of the CD4-anti-CD4 mAb complexes internalized from the cell surface. Thus, in unstimulated cells, internalized mAb was located in vesicular organelles throughout the cytoplasm which costained with Abs to the Tfr and correspond to early endosomes. After PMA treatment, the distribution of CD4 was altered, so that the bulk of the internalized anti-CD4 mAb was seen clustered in a perinuclear region of the cell. In contrast to the early endosomes, these perinuclear clusters could be costained with Abs to the CI-MPR and may represent components of the late endosome compartment. Thus CD4 internalized into early endosomes in the presence of phorbol ester is diverted from the constitutive recycling pathway to the late endosome/lysosome pathway, and as a consequence, there is a reduction in the recycling of internalized CD4.

These observations imply that, in addition to the effects on endocytosis, the phorbol ester-induced phosphorylation of CD4 may also generate a signal that targets internalized CD4 to late endosomes and lysosomes. As with the endocytosis signal, the precise nature of this sorting signal is unclear. However, as truncation experiments (24) suggest that downregulation requires the membrane proximal half of the cytoplasmic domain of CD4, this signal may also involve, or overlap with, the L-L sequence. Significantly, it has recently been reported that phosphorylation of the cytoplasmic domain of the CI-MPR and of the polymeric Ig receptor may be involved in the endosomal sorting or targeting of these molecules (62, 63). For the CI-MPR one of the phos-

phorylation sites is close to an L-L sequence that has been implicated in sorting to late endosomes (62, 64).

CD4 Downregulation in Lymphoid Cells. Phorbol ester-induced CD4 downregulation in nonlymphoid cells occurs through a combination of increased CD4 endocytosis and sorting of the internalized CD4 molecules to CI-MPR-containing late endosomes and lysosomes. In lymphoid cells, p56^{lck} prevents CD4 entry into coated pits. To understand whether phorbol ester induces a relocation of p56^{lck} together with CD4, or whether other mechanisms might account for CD4 downregulation in these cells, we analyzed the interaction of p56^{lck} and CD4 in the NIH-3T3-CD4/p56^{lck} cell line M22 (30). These cells also downregulate CD4 in response to phorbol ester, although the rate of CD4 internalization is slower than that seen in phorbol ester-treated HeLa-CD4 and NIH-3T3-CD4 cells and is similar to that observed on lymphoid cells. Significantly, compared with NIH-3T3-CD4 cells, there is a lag after the addition of phorbol ester to M22 cells before significant endocytosis of CD4 is observed. When we immunoprecipitated CD4 from phorbol ester-treated M22 cells, we found that p56^{lck} was dissociated from CD4 with a $t_{1/2}$ of 1–2 min. Thus, the dissociation appears to occur during the lag described above and to precede the onset of CD4 internalization. The region of the CD4 cytoplasmic domain that interacts with p56^{lck} is known to involve two cysteine residues at positions 420 and 422, a region that is not required for downregulation (65, 66). Nevertheless, it is conceivable that conformational changes in the cytoplasmic domain of CD4 induced by serine phosphorylation may disrupt the interaction with p56^{lck}.

The dissociation of CD4 from p56^{lck} alone would release CD4 and result in CD4 uptake with similar kinetics and to a similar extent as the constitutive CD4 endocytosis observed in nonlymphoid cells (i.e., 2–3% per min, and 40% internal at steady state). This would lead to a partial reduction of cell surface CD4 levels. However, CD4 downregulation induced by PMA in peripheral T cells and lymphocytic cells is much more rapid and extensive (21, 22). Thus, dissociation of CD4 and p56^{lck} cannot alone account for the level of downregulation observed (55, 56) and downregulation is likely also to involve the changes in endocytosis and trafficking of CD4 described for the HeLa-CD4 cells. Indeed, the rates of CD4 endocytosis observed in PMA-treated lymphocytic cell lines are increased more than 20-fold (e.g., to 4.2% per min in SupT1 cells, see above) and exceed the rates of constitutive CD4 endocytosis in nonlymphocytic cells (cf. Table 1). The effect of PMA on CD4 endocytosis is likely to be greater than this, as asynchronous and/or incomplete dissociation of p56^{lck} and CD4 will cause an underestimate in the observed rate of PMA-stimulated CD4 endocytosis in p56^{lck}-expressing cells. Thus PMA must also significantly increase CD4 internalization in lymphocytic cells.

In conclusion, we have demonstrated that phorbol ester-induced CD4 downregulation involves a series of sequential changes in the trafficking properties of CD4. First, in p56^{lck}-containing CD4⁺ cells, phorbol ester stimulates dissociation of CD4 and p56^{lck}. The released CD4 is then able to interact

with endocytic coated pits and vesicles. Second, phorbol esters increase the clustering of CD4 into coated pits and thereby increase the rate of CD4 endocytosis. Finally, phorbol esters induce the redistribution of internalized CD4 from the constitutive recycling pathway to degradative pathways, leading

to delivery of CD4 to CI-MPR-containing late endosomes and lysosomes. Although these events have been observed in this study after stimulation with phorbol ester, it is likely that other stimuli, such as ligation of the TCR by antigen, would lead to CD4 downregulation by similar mechanisms.

We thank Christopher Hermon for technical assistance and Adele Gibson for help with the electron microscopy. We also thank our colleagues Debbie Wheeler, and Drs. Pamela Reid, Dan Cutler, and Colin Hopkins (Medical Research Council Laboratory for Molecular Cell Biology), and Dr. John Tite (Wellcome Foundation Laboratories, Beckenham, Kent, UK) for many helpful discussions and comments on the manuscript.

This work was supported by grants from the Medical Research Council AIDS-directed Programme and the Leukemia Research Fund.

Address correspondence to Dr. Mark Marsh, MRC Laboratory for Molecular Cell Biology, University College London, Gower Street, London WC1E 6BT, UK.

Received for publication 24 March 1993 and in revised form 1 June 1993.

References

1. Parnes, J.R. 1989. Molecular biology and function of CD4 and CD8. *Adv. Immunol.* 44:265.
2. Robey, E., and R. Axel. 1990. CD4: collaborator in immune recognition and HIV infection. *Cell.* 60:697.
3. Zúñiga-Pflücker, J.C., L.A. Jones, L.T. Chin, and A.M. Kruisbeek. 1991. CD4 and CD8 act as co-receptors during thymic selection of the T cell repertoire. *Semin. Immunol.* 3:167.
4. Miceli, M.C., and J.R. Parnes. 1991. The roles of CD4 and CD8 in T cell activation. *Semin. Immunol.* 3:133.
5. Sattentau, Q.J., and R.A. Weiss. 1988. The CD4 antigen: physiological ligand and HIV receptor. *Cell.* 52:631.
6. Lamarre, D., D.J. Capon, D.R. Karp, T. Gregory, E.O. Long, and R.-P. Sékaly. 1989. Class II MHC molecules and the HIV gp120 envelope protein interact with functionally distinct regions of the CD4 molecule. *EMBO (Eur. Mol. Biol. Organ.) J.* 8:3271.
7. Fleury, S., D. Lamarre, S. Meloche, S.-E. Ryu, C. Cantin, W.A. Hendrickson, and R.-P. Sékaly. 1991. Mutational analysis of the interaction between CD4 and class II MHC: class II antigens contact CD4 on a surface opposite the gp120 binding site. *Cell.* 66:1037.
8. Veillette, A., N. Abraham, L. Caron, and D. Davidson. 1991. The lymphocyte-specific tyrosine protein kinase p56^{lck}. *Semin. Immunol.* 3:143.
9. Acres, B.R., P.J. Conlon, D.Y. Mochizuki, and B. Gallis. 1986. Rapid phosphorylation and modulation of the T4 antigen on cloned helper T cells induced by phorbol myristate acetate or antigen. *J. Biol. Chem.* 261:16210.
10. Weyand, C.M., J. Goronzy, and C.G. Fathman. 1987. Modulation of CD4 by antigenic activation. *J. Immunol.* 138:1351.
11. Rivas, A., S. Takada, J. Koide, G. Sonderstrup-McDevitt, and E.G. Engleman. 1988. CD4 molecules are associated with the antigen receptor complex on activated but not resting T cells. *J. Immunol.* 140:2912.
12. Cole, J.A., S.A. McCarthy, M.A. Rees, S.O. Sharrow, and A. Singer. 1989. Cell surface comodulation of CD4 and T cell receptor by anti-CD4 monoclonal antibody. *J. Immunol.* 143:397.
13. Thuillier, L., F. Selz, P. Métézeau, and J.-L. Pérignon. 1990. The activation of protein kinase C is not necessary for the monoclonal antibody-induced modulation of CD3 and CD4 antigens. *Eur. J. Immunol.* 20:1197.
14. Blue, M.-L., J.F. Daley, H. Levine, K.R. Branton, and S.F. Schlossman. 1989. Regulation of CD4 and CD8 surface expression on human thymocyte subpopulations by triggering through CD2 and CD3-T cell receptor. *J. Immunol.* 142:374.
15. Hoxie, J.A., J.D. Alpers, J.L. Rackowski, K. Huebner, B.S. Haggarty, A.J. Cedarbaum, and J.C. Reed. 1986. Alterations in T4 (CD4) protein and mRNA synthesis in cells infected with HIV. *Science (Wash. DC)*. 234:1123.
16. Juszczak, R.J., H. Turchin, A. Truneh, J. Culp, and S. Kassis. 1991. Effect of human immunodeficiency virus gp120 glycoprotein on the association of the protein tyrosine kinase p56^{lck} with CD4 in human T lymphocytes. *J. Biol. Chem.* 266:11176.
17. Cefai, D., M. Ferrer, N. Serpente, T. Idziorek, A. Dautry-Varsat, P. Debre, and G. Bismuth. 1992. Internalization of HIV glycoprotein gp120 is associated with down-modulation of membrane CD4 and p56^{lck} together with impairment of T cell activation. *J. Immunol.* 149:285.
18. Offner, H., T. Thieme, and A.A. Vandenbark. 1987. Gangliosides induce selective modulation of CD4 from helper T lymphocytes. *J. Immunol.* 139:3295.
19. Saggioro, D., C. Sorio, F. Calderazzo, L. Callegaro, M. Panozzo, G. Berton, and L. Chieco-Bianchi. 1993. Mechanism of action of the monosialoganglioside G_{M1} as a modulator of CD4 expression: evidence that G_{M1}-CD4 interaction triggers dissociation of p56^{lck} from CD4, and CD4 internalization and degradation. *J. Biol. Chem.* 268:1368.
20. Blue, M.-L., D.A. Hafler, K.A. Craig, H. Levine, and S.F. Schlossman. 1987. Phosphorylation of CD4 and CD8 molecules following T cell triggering. *J. Immunol.* 139:3949.
21. Hoxie, J.A., J.L. Rackowski, B.S. Haggarty, and G.N. Gaulton.

1988. T4 endocytosis and phosphorylation induced by phorbol esters but not by mitogen or HIV infection. *J. Immunol.* 140:786.
22. Hoxie, J.A., D.M. Matthews, K.J. Callahan, D.L. Cassel, and R.A. Cooper. 1986. Transient modulation and internalization of T4 antigen induced by phorbol esters. *J. Immunol.* 137:1194.
23. Petersen, C.M., E.I. Christensen, B.S. Andresen, and B.K. Møller. 1992. Internalization, lysosomal degradation and new synthesis of surface membrane CD4 in phorbol ester-activated T-lymphocytes and U937 cells. *Exp. Cell Res.* 201:160.
24. Shin, J., R.L. Dunbrack, S. Lee, and J.L. Strominger. 1991. Phosphorylation-dependent down-modulation of CD4 requires a specific structure within the cytoplasmic domain of CD4. *J. Biol. Chem.* 266:10658.
25. Baenziger, J.W., A. Okamoto, E. Hall, S. Verma, and C.G. Davis. 1991. The tail of CD4 targets chimeric molecules to a degradative pathway. *New Biologist.* 3:1233.
26. Ruegg, C.L., S. Rajasekar, B.S. Stein, and E.G. Engleman. 1992. Degradation of CD4 following phorbol-induced internalization in human T lymphocytes. *J. Biol. Chem.* 267:18837.
27. Pelchen-Matthews, A., J.E. Armes, and M. Marsh. 1989. Internalization and recycling of CD4 transfected into HeLa and NIH3T3 cells. *EMBO (Eur. Mol. Biol. Organ.) J.* 8:3641.
28. Pelchen-Matthews, A., J.E. Armes, G. Griffiths, and M. Marsh. 1991. Differential endocytosis of CD4 in lymphocytic and non-lymphocytic cells. *J. Exp. Med.* 173:575.
29. Marsh, M., J.E. Armes, and A. Pelchen-Matthews. 1990. Endocytosis and recycling of CD4. *Biochem. Soc. Trans.* 18:139.
30. Pelchen-Matthews, A., I. Boulet, D.R. Littman, R. Fagard, and M. Marsh. 1992. The protein tyrosine kinase p56^{lck} inhibits CD4 endocytosis by preventing entry of CD4 into coated pits. *J. Cell Biol.* 117:279.
31. Healey, D., L. Dianda, J.P. Moore, J.S. McDougal, M.J. Moore, P. Estess, D. Buck, P.D. Kwong, P.C.L. Beverley, and Q.J. Satntau. 1990. Novel anti-CD4 monoclonal antibodies separate human immunodeficiency virus infection and fusion of CD4⁺ cells from virus binding. *J. Exp. Med.* 172:1233.
32. Brown, W.J., and M.G. Farquhar. 1987. The distribution of 215-kilodalton mannose 6-phosphate receptors within cis (heavy) and trans (light) Golgi subfractions varies in different cell types. *Proc. Natl. Acad. Sci. USA.* 84:9001.
33. Maddon, P.J., J.S. McDougal, P.R. Clapham, A.G. Dalgleish, S. Jamal, R.A. Weiss, and R. Axel. 1988. HIV infection does not require endocytosis of its receptor, CD4. *Cell.* 54:865.
34. Smith, P.K. R.I., Krohn, G.T. Hermanson, A.K. Mallia, F.H. Gartner, M.D. Provenzano, E.K. Fujimoto, N.M. Goeke, B.J. Olson, and D.C. Klenk. 1985. Measurement of protein using bicinchoninic acid. *Anal. Biochem.* 150:76.
35. Clapham, P.R., R.A. Weiss, A.G. Dalgleish, M. Exley, D. Whitby, and N. Hogg. 1987. Human immunodeficiency virus infection of monocytic and T-lymphocytic cells: receptor modulation and differentiation induced by phorbol ester. *Virology.* 158:44.
36. Shin, J., C. Doyle, Z. Yang, D. Kappes, and J.L. Strominger. 1990. Structural features of the cytoplasmic region of CD4 required for internalization. *EMBO (Eur. Mol. Biol. Organ.) J.* 9:425.
37. Favero, J., J.F.P. Dixon, P.C. Bishop, R. Languier, and J.W. Parker. 1990. Lymphocyte mitogenesis and CD4 modulation induced by different phorbol esters: comparative studies. *Int. J. Immunopharmacol.* 12:769.
38. Møller, B.K., B.S. Andresen, E.I. Christensen, and C.M. Petersen. 1990. Surface membrane CD4 turnover in phorbol ester stimulated T-lymphocytes. *FEBS (Fed. Eur. Biochem. Soc.) Lett.* 276:59.
39. Collins, M.K.L., and E. Rozengurt. 1982. Binding of phorbol esters to high affinity sites on murine fibroblastic cells elicits a mitogenic response. *J. Cell. Physiol.* 112:42.
40. Young, S., P.J. Parker, A. Ullrich, and S. Stabel. 1987. Down-regulation of protein kinase C is due to an increased rate of degradation. *Biochem. J.* 244:775.
41. Neudorf, S., M. Jones, S. Parker, R. Papes, and D. Lattier. 1991. Phorbol esters down-regulate transcription and translation of the CD4 gene. *J. Immunol.* 146:2836.
42. Bedinger, P., A. Moriarty, R.C. von Borstel II, N.J. Donovan, K.S. Steimer, and D.R. Littman. 1988. Internalization of the human immunodeficiency virus does not require the cytoplasmic domain of CD4. *Nature (Lond.)* 334:162.
43. Swanson, J.A., B.D. Yirinec, and S.C. Silverstein. 1985. Phorbol esters and horseradish peroxidase stimulate pinocytosis and redirect the flow of pinocytosed fluid in macrophages. *J. Cell Biol.* 100:851.
44. Phaire-Washington, L., E. Wang, and S.C. Silverstein. 1980. Phorbol myristate acetate stimulates pinocytosis and membrane spreading in mouse peritoneal macrophages. *J. Cell Biol.* 86:634.
45. Daukas, G., and S.H. Zigmond. 1985. Inhibition of receptor-mediated but not fluid phase endocytosis in polymorphonuclear leukocytes. *J. Cell Biol.* 101:1673.
46. Heuser, J.E., and R.G.W. Anderson. 1989. Hypertonic media inhibit receptor-mediated endocytosis by blocking clathrin-coated pit formation. *J. Cell Biol.* 108:389.
47. Davoust, J., J. Gruenberg, and K.E. Howell. 1987. Two threshold values of low pH block endocytosis at different stages. *EMBO (Eur. Mol. Biol. Organ.) J.* 6:3601.
48. Sandvig, K., S. Olsnes, O.W. Petersen, and B. van Deurs. 1987. Acidification of the cytosol inhibits endocytosis from coated pits. *J. Cell Biol.* 105:679.
49. Anderson, R.G.W., M.S. Brown, and J.L. Goldstein. 1977. Role of the coated endocytic vesicle in the uptake of receptor-bound low density lipoprotein in human fibroblasts. *Cell.* 10:351.
50. Marsh, M., and A. Helenius. 1980. Adsorptive endocytosis of Semliki Forest virus. *J. Mol. Biol.* 142:439.
51. Griffiths, G., R. Back, and M. Marsh. 1989. A quantitative analysis of the endocytic pathway in baby hamster kidney cells. *J. Cell Biol.* 109:2703.
52. Marsh, M., P. Reid, I. Parsons, C. Hermon, and A. Pelchen-Matthews. 1992. Morphological analysis of the regulation of CD4 endocytosis by p56^{lck}. *Biochem. Soc. Trans.* 20:719.
53. Griffiths, G., B. Hoffack, K. Simons, I. Mellman, and S. Kornfeld. 1988. The mannose 6-phosphate receptor and the biogenesis of lysosomes. *Cell.* 52:329.
54. Hurley, T.R., K. Luo, and B.M. Sefton. 1989. Activators of protein kinase C induce dissociation of CD4, but not CD8, from p56^{lck}. *Science (Wash. DC).* 245:407.
55. Sleckman, B.P., J. Shin, V.E. Igras, T.L. Collins, and J.L. Strominger. 1992. Disruption of the CD4-p56^{lck} complex is required for rapid internalization of CD4. *Proc. Natl. Acad. Sci. USA.* 89:7566.
56. Yoshida, H., Y. Koga, K. Nakamura, G. Kimura, and K. Nomoto. 1992. A lymphocyte-specific protein tyrosine kinase, p56^{lck}, regulates the PMA-induced internalization of CD4. *Biochem. Biophys. Acta.* 1137:321.
57. Vaux, D. 1992. The structure of an endocytosis signal. *Trends Cell Biol.* 2:189.
58. Trowbridge, I.S., J.F. Collawn, and C.R. Hopkins. 1993.

Signal-dependent membrane protein trafficking in the endocytic pathway. *Annu. Rev. Cell Biol.* In press.

59. Miettinen, H.M., K. Matter, W. Hunziker, J.K. Rose, and I. Mellman. 1992. Fc receptor endocytosis is controlled by a cytoplasmic domain determinant that actively prevents coated pit localization. *J. Cell Biol.* 116:875.
60. Letourneur, F., and R.D. Klausner. 1992. A novel di-leucine motif and a tyrosine-based motif independently mediate lysosomal targeting and endocytosis of CD3 chains. *Cell.* 69:1143.
61. Kennelly, P.J., and E.G. Krebs. 1991. Consensus sequences as substrate specificity determinants for protein kinases and protein phosphatases. *J. Biol. Chem.* 266:15555.
62. Méresse, S., and B. Hoflack. 1993. Phosphorylation of the cation-independent mannose 6-phosphate receptor is closely associated with its exit from the *trans*-Golgi network. *J. Cell Biol.* 120:67.
63. Casanova, J.E., P.P. Breitfeld, S.A. Ross, and K.E. Mostov. 1990. Phosphorylation of the polymeric immunoglobulin receptor required for its efficient transcytosis. *Science (Wash. DC)*. 248:742.
64. Johnson, K.F., and S. Kornfeld. 1992. The cytoplasmic tail of the mannose 6-phosphate/insulin-like growth factor-II receptor has two signals for lysosomal enzyme sorting in the Golgi. *J. Cell Biol.* 119:249.
65. Turner, J.M., M.H. Brodsky, B.A. Irving, S.D. Levin, R.M. Perlmutter, and D.R. Littman. 1990. Interaction of the unique N-terminal region of tyrosine kinase p56^{lck} with cytoplasmic domains of CD4 and CD8 is mediated by cysteine motifs. *Cell.* 60:755.
66. Shaw, A.S., J. Chalupny, J.A. Whitney, C. Hammond, K.E. Amrein, P. Kavathas, B.M. Sefton, and J.K. Rose. 1990. Short related sequences in the cytoplasmic domains of CD4 and CD8 mediate binding to the amino-terminal domain of the p56^{lck} tyrosine protein kinase. *Mol. Cell. Biol.* 10:1853.